ANALYSIS AND PREDICTION OF CONSERVATIVE MASS TRANSPORT IN IMPOUNDMENTS

by

Alfred J. D'Arezzo
and
Frank D. Masch

submitted under
Grant 5 ROI WP00705
Federal Water Quality Administration

HYDRAULIC ENGINEERING LABORATORY
Center for Research in Water Resources
Department of Civil Engineering
THE UNIVERSITY OF TEXAS AT AUSTIN

Tech. Rep. HYD 10-7004
CRWR-73

December 1970

PREFACE

This final report is submitted to the Federal Water Pollution Control Administration under Grant 5 RO1 WP00705. The report presents a useful engineering approach to analyze and predict the movement and distribution of conservative mass substances in water impoundments. The approach represents a practical synthesis of the major hydrodynamical, hydrometeorological and hydrothermal concepts of mixing, dispersion and transport phenomena in water impoundments. Special consideration has been given to the findings of the preceding technical reports (HYD 10-6701, HYD 10-6902, and HYD 10-6903) prepared earlier pursuant to this study grant. These earlier reports focused on special aspects of mixing and dispersion in impoundments including field investigations using dye-tracing techniques, laboratory model analysis of micro-scale turbulence created by wind-induced wave spectra, and an evaluation of the major mathematical methods for the computerized and algorithmic solution of the equation governing the convective-dispersive transport of conservative mass substance in a two-dimensional field. In addition to these previous reports, a broad-scale review and evaluation was made of the relevant work and studies of others. Thus, the physical, analytical and mathematical conceptualizations developed in this report for the impoundment hydrodynamic system and for the behavior of mass transport in that system were shaped by the numerous practical

constraints which were encountered and resolved to varying degrees by others. Finally, the approach presented in this report has been governed by the realistic axiom that system models and simulations must be harmonized at every practical step with the realities of the prototype.

It is apropos to identify clearly the engineering utility and orientation of the studies and the final report made pursuant to this grant. From the outset, the studies have been governed by the vital assumption that the natural assimilative or dilutive capacity of a water body is a fundamental factor in water treatment and an important part of water quality management. This assumption is nurtured by the belief that if water quality management is to be conducted pursuant to the principle of conservation of resources in its truest economic sense, it is essential that water be regarded as a renewable resource, and that the process of management permit the maximum sustained use or yield of the water resource. While it is true that dilution alone is not the answer to pollution, it is evident that treatment and dilution are inseparable elements of water pollution control. An understanding of natural mixing, dispersion and transport mechanisms is essential for the effective use of natural dilution capabilities of water courses and impoundments. Related to natural dilution is the matter of low flow augmentation which has assumed renewed importance in comprehensive water resources planning and in water quality management plans.

In the study of the literature on water impoundments, certain facts emerged which influenced greatly the conceptualizations and assumptions adopted in this report: (1) The aging of impoundments is a natural condition which may can accelerate or retard. (2) The typical impoundment is a stratified fluid system consisting of an "upper lake", or stratum, of warmer water floating or gliding on top of a "middle lake", or zone, containing progressively colder water with increasing depth. And, below these two strata there is a "bottom lake" of cold water in contact with the bed of the impoundment. The surface of the "upper lake" generally is in stress resulting from two powerful kinetic states, i.e., a hyperactive aerodynamic state at the air-water interface, and a turbulent hydrodynamic state extending throughout the so-called "baroclinic layer". (3) Turbulence created in one of two, thermally- or density-stabilized strata, which initially are at rest, does not invade the non-turbulent stratum, nor is a "buffer zone" necessarily created between the temperature or density discontinuities. Indications are that fluid is entrained from the interface of the non-turbulent stratum and dispersed in the turbulent stratum.

The high kinetic activity prevailing in a near surface layer of the "upper lake" provides strong support for the decision to analyze the transport phenomena in impoundments in terms of the two-dimensional field represented by the fully-mixed, surface layer of a stratified impoundment. The "macro" approach presented in this report is considered a realistic

synthesis of theory and practice, and a useful, rapid and economical strategy or technique for the analysis and prediction of conservative mass transport and distribution within water impoundments. The computerized, algorithmic solution of the partial differential equations of the impoundment transport model using the so-called Alternating-Direction Implicit Method, demonstrates excellent versatility to receive hydrodynamic input from interfacing impoundment hydrodynamic, transport and channel models as modules for the build-up and the simulation of complex impoundment systems is illustrated by use of Lake Bastrop, Texas as the prototype system.

Special acknowledgement and appreciation are expressed for the cooperation extended by the Lower Colorado River Authority in connection with dye tracer field tests conducted at Lake Bastrop. Grateful acknowledgement and appreciation also is expressed to Mr. Robert J. Brandes for his invaluable guidance in computer programming, to Mr. Ed Bruce and Mr. A. C. Radhakrishnan for their contributions in field work, and to Mrs. Joyce N. Crum for outstanding stenographic and administrative services. The partial support of the Center for Research in Water Resources at The University of Texas at Austin in the preparation of this report is gratefully acknowledged.

The authors have sought to recognize, credit and acknowledge the relevant work and studies of the many dedicated researchers who have been, and continue to be, engaged in the multi-disciplinary research assault on water pollution control in the particular field of this report. Any oversight is unintentional.

ABSTRACT

A numerical model is developed which enables making extensive simulations and analyses of near-surface hydrodynamic and transport phenomena of water impoundments. The model was developed after a careful review of the major hydrodynamical, hydrothermal and hydrometeorological factors involved in the mixing, dispersion, and transport of conservative substances in impoundments, including the effects of thermal stratification and wind-induced currents. The numerical model algorithm developed and solved by computer program is for the parabolic differential equation representing the convective-dispersion transport phenomena in a two-dimensional, fully-mixed surface layer of a water impoundment. The approximated, stepwise solution of this equation under steady state conditions is obtained by using a finite difference technique known as the Alternating-Direction Implicit Method. Two subsidiary models have been adapted to interface with the impoundment transport model: an impoundment hydrodynamic model adapted from the Masch Hydrodynamic Model for shallow, well-mixed estuaries and, an open channel transport model having as its algorithm the Taylor solution for the convective-dispersion equation for a one-dimensional, open channel flow. These three interfacing models are regarded as discretizations of a complex physical system. They possess sufficient flexibility to be used in

combinations to depict a wide variety of water impoundment types and regimes. These complementary numerical models were applied using Lake Bastrop, Texas as the prototype. The study demonstrates the use of numerical models to analyze the impacts of hydrodynamic and hydrometeorological variables on mixing, dispersion and transport of conservative substances, and to simulate a wide range of possible combinations of circulation and transport patterns. Analysis of field observations and verification tests using Rhodamine B dye tracer brought out the realistic adjustments necessary to be made in the experimental numerical model to reconcile computed and observed values. Since wind effects have the preponderant influence on dispersive and transport phenomena, it appears compelling to obtain continuous wind data and the correlative water-surface velocities, currents and stratification patterns. A continuous record of these specific field data would facilitate both the determination of realistic adjustments to experimental numerical models and the rational reconciliation of computed and observed data. Evaluation of relevant mathematical model and scale model technology indicates the common, vital requirement of experimental readjustments, harmonized with prototype observations and measurements, in order to reproduce reasonably the natural phenomena under study. This study demonstrated and confirmed the foregoing evaluation.

TABLE OF CONTENTS

Page

Page

Page

Page

LIST OF TABLES

LIST OF ILLUSTRATIONS

CHAPTER I

INTRODUCTION

Objectives

Origins and Justifications. This study is part of a comprehensive program which has been in progress since 1965 at The University of Texas, encompassing research on mixing, dispersion and transport phenomena in lakes and reservoirs. The scope of this program is: (1) To study the effects of wind-induced currents, waves, seasonal mass transfer and other natural mixing processes on the disposition of contaminants entering reservoirs or lakes. (2) To study the effects of temperature and density gradients on the stability of the receiving water. (3) To study and field-analyze the phenomena of horizontal and vertical mixing and dispersion in reservoirs. The objective of the total program is to obtain a better insight, or to find new insights, interrelating data on the mixing, dispersion and transport phenomena in lakes and reservoirs in order to develop more efficient and accurate numerical models or conceptual schemes for the study, prediction and control of convective-dispersion processes in large, surface water impoundments.

Implicit in the development of numerical models or conceptual schemes is the concept of test. Hence, the program provides inherently

for verification of models or conceptual schemes and, in fact, the development of a new method of verification may itself be a significant advance in mathematical model or scale model technology.

The comprehensive program, results of which will be described later, has been governed by the following research plan. Initially, studies would be made of the effects of currents, turbulent wave action, and periodic overturning on the disposition of wastes or contaminants discharged into reservoirs or lakes, and to investigate the stability effects of temperature and density gradients within the receiving waters on the mixing of these wastes. Then dispersion studies would be conducted in deep and shallow reservoirs to define the important mixing and convective mechanisms that affect the disposition of wastes in each type of reservoir. These initial studies would then be used to develop a mathematical model which would be useful for analyzing waste movement in reservoirs. The model would be verified first in the laboratory in a functional model reservoir by investigating systematically those mixing mechanisms that can be reproduced in the laboratory and determining, if possible, the scale effects for those mechanisms which cannot be completely reproduced in the laboratory. Finally, more extensive field studies of dispersion would be performed in actual reservoirs under more varied field conditions. The results of these field studies would not only serve to verify the mathematical model and the laboratory model reservoir results, but also provide much needed field data on actual reservoir dispersion and dispersion coefficients.

Specific Objective and Scope. The objective of this study is to investigate whether certain key parameters of "near-surface" hydrodynamics can be utilized in a computerized numerical model to analyze, simulate and predict conservative mass transport patterns in lakes and reservoirs.

Pursuant to this objective, the scope will be:

a. To develop a numerical impoundment transport model to solve the partial differential equation representing the convective-dispersion transport phenomena in a horizontal, two-dimensional plane, under steady state conditions. The boundary and initial conditions, will be assumed to be those inherent in a homogeneous, isotropically-turbulent stratum. The solution will use a finite difference approximation technique.

b. To use a previously designed numerical model for the simulation of tidal hydrodynamics in shallow, irregular estuaries (Masch, et al, 1969) for use as a numerical impoundment hydrodynamic model to generate averaged, steady state velocities needed as input data for the computerized numerical impoundment transport model.

c. To develop a numerical open-channel transport model having as its algorithm the Taylor solution for the convective-dispersion equation for a one-dimensional, open-channel flow, having a uniform cross-section and using a mean velocity. This model will be used to simulate and predict near-Gaussian, well-mixed concentration distribution inputs into the excitation cell of the computerized numerical impoundment transport model.

d. To use the numerical impoundment transport model to predict concentrations of conservative dispersants in the fully-mixed surface stratum of the impoundment, given certain initial and boundary conditions governing concentration, concentration gradients, dispersion coefficients, surface stratum velocities and, the relative thickness of the fully-mixed surface stratum with and without wind shear at the water-atmosphere interface.

e. To use the numerical impoundment transport model to analyze and predict the time and path of travel of the concentration peaks of conservative dispersant clouds, and also the time-of-travel relationships between the peak-concentrations and the cloud leading-edge concentration.

f. To analyze the sensitivity of the impoundment transport model to changes in dispersion coefficients, wind effects, flow rates and values of initial concentration peak.

g. To conduct special, preliminary tests prior to model verification tests in order to validate the reasonableness of assumptions and accuracy of constants used initially in the model. These include: random measurement of depths, measurement of velocity and concentration profiles in a vertical plane, and dye tracer measurements to enable computation of longitudinal dispersion coefficients by the method of variances.

h. To apply the numerical impoundment transport model, and the two interfacing, subsidiary models, i.e., impoundment hydrodynamic model and open channel transport model to a local lake or reservoir of sufficient complexity, verifying the predictions by on-site field explorations and controlled tracer dye tests.

The eight basic actions enumerated above are developed and described in Chapters IV through VII.

Assumptions and Stipulations. The objective and scope stated earlier will be governed by the following assumptions and stipulations:

a. The design of the numerical models in this study will be strongly influenced by the pragmatic engineering requirement to conceptualize impoundments in macroscopic terms, using the natural, near-surface, observable and measureable properties of the impoundments as the framework of parameters around which the models are designed.

b. As a logical sequence to the first condition, attention will be focused on the fully-mixed, "near-surface" stratum. Generally, the depth of this stratum is to the thermocline, or even to a lesser depth in some special cases such as where heated water is first discharged into a colder, stagnant body of water. However, in shallow areas the depth of this stratum may be tantamount to the full depth of the lake.

c. Shear forces at the water-atmosphere interface and the depth of effective turbulence penetration will be assumed to be caused by steady winds only.

d. The study will be restricted to conservative mass transport of dissolved, conservative dispersant material. Rhodamine-B dye tracer will be used as the prototype material in field tests.

e. The numerical models will be applied to Lake Bastrop, Texas as the prototype hydrodynamic system. Both historical and contemporaneously-measured hydrodynamic and flow data of this lake will be used as input data to the lake numerical models. The lake is considered to be of sufficient complexity to afford a complete evaluation of the numerical models.

The rationale for adopting the above assumptions and conditions is based on practical considerations and on findings of other investigators, whose work will be reviewed in this study.

Relation to Water Resources Engineering

Importance of Water Impoundments. There continues to be a strong impetus for more detailed research and study of the hydrodynamics in lakes and reservoirs. This concern is generated by the trend in all developed or developing regions to plan for the conversion of all major,

natural water courses and other surface water resources into regional series of optimally-operated, inter-dependent, slack water impoundments. Most comprehensive water resource development plans are formulated on this strategy.

The need for regulation of more streams will result in the construction of more impoundments to enhance the existing reservoir systems, with special attention focused on water quality standards. The effects of increased impoundments on water quality presents one of the most complex problems ever faced by modern technology.

Krenkel (1969) viewing this situation states:

> ". . .Because the fate of all rivers seems to be development, it is important to decide if the present users of the waste assimilative capacities of the streams are to be compensated for the loss of this capacity due to this development."

At times, the man-made impoundments or "run-of-the river" reservoirs, will exist in a relatively quiescent state, serving virtually as "evaporating basins" or "detention pools" - subject to minimal, natural hydrodynamic and other forces. At other times, the impoundments will be subjected to agitation and virtually converted to "mixing chambers", in which the physical transfer of materials at the water-sediment interface is increased. This, in turn, increases the conservative mass loading and stimulates exchange reactions which further affect concentration rates, the levels of reactive substances, and the distribution patterns by mass transport. (Lee, 1970)

Increased hydrodynamic action within impoundments due to intense usages such as commercial navigation, and industrial process cooling water will proliferate. Present planning envisages that most natural surface water resources impoundments will be harnessed for multi-uses, and that there will be a significant increase in the construction of artificial impoundments designed for intensive technological, industrial and economic uses, involving special treatment (e.g., aeration) and recycling, (e.g., pumped storage reservoirs).

The artifical impoundment is a man-made modification of a larger system which McGaughey (1968) terms "a link in the natural interchange of quantity and quality". A better insight of hydrodynamic actions and reactions within impoundments in receiving, distributing and transporting inputs of conservative and non-conservative reactive substances including sediments or other pollutants, and the properties of these substances, is vitally needed for the efficient management of water resources.

Importance of Transport Phenomena. The mixing processes are related to the overall assimilative or purificative efficiencies and capacities of an impoundment. Many pollution problems involve diffusion processes. Cost constraints preclude the complete removal of all pollutants from water; hence, there will always be an engineering and economic requirement for the rational use of the natural assimilative capacities of lakes and reservoirs. The design of many water and waste water treatment processes and of various treatment facilities depends upon the efficient utilization of

natural mixing processes in receiving bodies of water. Knowledge of the mixing phenomena are vital to the control of waste heat inputs into water impoundments from industrial processes and from the cooling systems of fueled electric power plants. The rigorous engineering design criteria gradually being established in water and waste water engineering are predicated on an efficient and accurate understanding and application of hydrodynamic and transport phenomena in receiving bodies of water.

In addition, a realistic knowledge and appreciation of the hydrodynamical and transport characteristics of specific reservoirs is indispensable for the optimal operation and management of the reservoirs. Experience shows that specialized reservoir concepts of various types, e.g., optimized, discrete, operational, quality and economic, taken individually, have proved inadequate for efficient, economical management of reservoirs unless these specialized models are synthesized with the hydrodynamic and transport models of the reservoirs involved. For example, the mathematical modeling studies by Thomann (1963), Thomann and Marks (1966) and by Graves, et al, (1968) pertaining to water quality management of the Delaware River estuary, are cogent illustrations of both the need for and, the technical feasibility of synthesizing various relevant models: hydrodynamic, optimal, operational, quality and economic. This synthesis of models revealed the engineering and economic options urgently needed by water resource management and planning agencies.

Thrust of Past Research on Impoundments. The main thrust of research up to the present time, insofar as inland impoundments are concerned, has been on the investigation of diffusion of thermal energy, and on the determination of "effective diffusivity" coefficients. This emphasis has produced many types of temperature prediction models. This emphasis is understandable considering the anticipated increasing heat loads to be applied to surface waters. In general, from the viewpoint of energy transport, the distribution of all substances in a reservoir could be considered to be dependent upon the distribution of heat in the reservoir. Therefore, it is not surprising that the bulk of previous major research effort in reservoir hydrodynamic and transport prediction modeling has centered around temperature distribution analyses. However, the impetus of anti-pollution research efforts now compels urgent examination of hydrodynamic and transport phenomena in terms of the behavior of conservative and non-conservative reactive contaminants, as well as the thermal, biological and chemical properties of these substances.

Conservative Versus Non-Conservative Substance. Models for predicting the distribution of water properties in reservoirs is in the early stages of development. And, generally, past research has not differentiated rigorously between conservative and non-conservative substances; the distinction was useful to explore and to describe transport-phenomena and hydrodynamic system processes. Water quality considerations now have emphasized the need for special distinction between

conservative and non-conservative substances. Gloyna (1968) in discussing stream prediction models for oxygen depletion distinguishes between conservative and non-conservative pollutants as follows:

> ". . . Pollutants that affect streams are either conservative or non-conservative. In the case of conservative (non-biodegradable) wastes the assimilative capacity of the stream is largely due to dilution although accumulation of certain wastes of this type in bottom sediments greatly influences the transport and consequent dilution. Conversely, in the case of non-conservative (biodegradable) wastes, the concentration levels become a function of time and distance."

For example, conservative pollutants, such as chlorides are those whose total amount of chemical composition are not affected by internal system processes; only transport phenomena are regarded capable of changing their concentrations. In contrast, non-conservative pollutants are materials whose amount or composition is changed in a significant fashion by the system's internal processes. A review of literature indicates that prediction of the behavior of non-conservative substances in the internal processes of a system is considerably more difficult than for conservative substances. Efforts to correlate or differentiate the behaviors of conservative and non-conservative pollutants and their respective properties is the major research area in water resources engineering. It is the crux of the pollution problem.

CHAPTER II

ANALYSIS OF MAJOR DEVELOPMENTS PERTAINING TO RESERVOIR HYDRODYNAMIC AND TRANSPORT MODELING

Recent Local Work

It was indicated earlier that this work is part of a larger research effort to study the effects of currents, wind-induced waves, and seasonal overturnings on the behavior of contaminants in water impoundments. Pursuant to this comprehensive research effort several vital studies have been made.

Field Investigations, Lake Travis, Texas. Wilson and Masch (1967) conducted tracer investigations at Lake Travis (Austin, Texas). This is a deep impoundment where the predominant mechanism for dispersion is wind-induced surface activity. The objectives were to experiment with dye tracing techniques, to measure and analyze velocity profiles, to analyze tracer dilution rates,[1] to determine empirical dispersion coefficients, and to determine possible correlations between dispersion coefficients, surface velocity, and wave conditions. Relevant findings were:

1. Under ambient conditions, characterized by a continuous dominance of wind-induced surface currents, the near-

[1] Dilution rate - the rate of diminution of the peak concentration in a dispersing cloud.

surface velocity gradient was found to be very steep near the reservoir surface, decreasing rapidly with depth. Near-surface velocities appeared to be represented reasonably well by the relationship:

$$\left[1 - \frac{u}{U_s}\right] \sim d^{1/7} \qquad (2\text{-}1)$$

where:

u = flow velocity at some depth.
U_s = flow velocity at the surface.
d = depth.

2. Under a wide assortment of ambient field conditions, it was concluded tentatively that the relative peak concentration in a cloud of conservative dispersant was governed by the relationship:

$$\frac{C}{C_0} = a\,t^{-2.5} \qquad (2\text{-}2)$$

where:

C = tracer concentration at some point and time.
C_0 = initial concentration.
a = dilution coefficient where $a \sim K_c\, U_s^{-3}$.
K_c = empirical factor for surface conditions, unique to Lake Travis, where:

$K_c = 0.78$ (no "whitecaps")
$K_c = 1.00$ ("whitecaps")

t = time.
C/C_0 = relative concentration.

3. Under steady-wind conditions, the surface current was found to be related to the wave energy spectrum, the turbulent diffusivity, the lateral dispersion coefficient, and the dilution factor. Under unsteady-wind and breaking-wave conditions, the surface current may be corrected by an empirical factor.

4. The vertical dispersion coefficient appeared to be correlated to wave height.

5. The longitudinal dispersion coefficient was found to be from five to ten times greater than the lateral coefficient, and this was attributed to shear flow mixing or convective displacement. The following table gives an "order of magnitude" comparison of the coefficients computed.

Table 2-1. Dispersion Coefficients under Various Wind-Wave Conditions

Surface Condition	Dispersion Coefficients (ft^2/sec)		
	Longitudinal (D_x)	Lateral (D_y)	Vertical (D_z)
Ripples	3	0.06	0.0004
Wave Height, 6"	2	0.11	0.0035
Wave Height, 10"	-	0.13	0.0720

It was noted that the vertical and lateral coefficients of dispersion increase with the energy in the wave spectrum, so that

$$D_y \sim D_z^{0.15} \tag{2-3}$$

and the following basic relationships were suggested:

a. $D_x > D_y$ because of shear flow mixing.

b. D_x decreases and D_y increases because of shear flow mixing.

c. D_z is relatively constant until the wave height reaches about three inches; then, increases rapidly with wave height.

6. A dye tracer cloud elongation reached its maximum length and width when wave heights $<$ 3 inches.

7. The following conditional points were made in presenting findings:

a. There is need for more accurate measurement of velocity distribution.

b. While d and U_s appear to be highly-correlated, further confirmation of the velocity relation is needed.

c. Observation for dilution times should be extended beyond 6 hours. Further tests are needed to confirm the tentative relation:

$$\frac{C}{C_0} = at^{-2.5}$$

d. In the investigation the equation selected for computing the eddy diffusivity coefficient was

$$D = 1.56\, w r^{1.2} \qquad (2\text{-}4)$$

where:

w = a diffusivity parameter with dimensions of $(ft)^{4/5}/sec.$

r = distance from center of mass of tracer cloud.

Further tests are needed to confirm the validity of the $r^{1.2}$ component.

The investigations demonstrated the considerable difficulties and efforts entailed in analyzing hydrodynamic phenomena by field data alone, and to try linking major hydrodynamic and hydrometeorological parameters by a series of empiricized relationships. The pressing need for modeling became evident after analyzing the Lake Travis field investigations.

Wind-Wave Macro-Turbulence Flume Tests. The work of wind-induced waves and currents in producing an apparent, near-surface, macro-scale turbulence was observed during the Wilson and Masch (1967)

field tests. The macro-scale turbulence and dispersion phenomena warranted investigation under laboratory controls. Therefore, as a sequel to the Wilson and Masch (1967) reservoir field explorations, Lee and Masch (1969) conducted wind-wave flume tests to examine wind-induced wave turbulence.

The general findings were:

1. The depth of penetration of turbulence due to wind-induced waves increases rapidly up to a certain wind velocity, beyond which the penetration rate decreases. And, there appears to be a limiting depth of penetration below which surface induced turbulence does not extend even at increasing wind velocities.

2. The depth of penetration of turbulence increases as the wave height and wave length increases, however at the same time the resistance to penetration also increases.

3. At small wave-steepnesses the depth of turbulent penetration increases; as the steepness increases the turbulent penetration rate decreases. However, if the wave-steepness is very large, the penetration depth decreases.

4. Turbulent fluctuation frequencies equal to or greater than ambient surface wave frequencies are generally confined to the zone of turbulent penetration. But, vortices and other turbulence effects can penetrate below the usual turbulent zone, quickly degenerating into small scale eddies.

Mathematical Investigation of Solutions for the Two-Dimensional Convective-Dispersion Equation. Gebhard and Masch (1969) evaluated several numerical models for near-surface dispersion and convection in reservoirs. The need to explore the potentialities of numerical models

became evident after considering the large expenditure of time and effort involved in major field, statistical or physical model investigations. The following evaluations were made of various finite difference methods to solve the two-dimensional convection dispersion equation:

1. Computer programs are feasible for the solution of the convective dispersion equation using finite difference methods.

2. The "method of characteristics" appears the most useful of three types examined, having broader, practical applicability than either the explicit or implicit methods.

3. No solution was found to be universally applicable to all water bodies. The choice of method depends on the combination of given flow and boundary conditions and, in any case, the solution is basically an approximate simulation, useful for preliminary analyses.

4. The finite difference methods of solution accomplish numerically what Taylor (1954) and Elder (1959) accomplished analytically.

5. The numerical algorithms enable efficient, economical, rapid exploration of mixing and dispersion phenomena in water impoundments.

In summary, the deep reservoir tests of Wilson and Masch (1967) demonstrated cogently the difficulties and the large amount of time that would be involved in obtaining the field data necessary to make a rigorous evaluation of the dispersive and transport phenomena in large bodies of water. It was evident that large quantities of observed field data would be needed to derive empirical expressions describing tentatively the relations between various hydrodynamic parameters.

The Gebhard and Masch (1969) analysis of the various methods for solving the convective dispersion equation indicated both the practical and engineering necessity of developing appropriate numerical models which serve to reduce the heavy dependence on large quantities of measured field data and on physical measurements from scale models.

Current Local Work

Formulation of Mathematical Models of Reservoir Hydrodynamical Phenomena. As a result of the Wilson and Masch (1967), Lee and Masch (1969) and Gebhard and Masch (1969) studies just described, follow-on studies were started in 1969 at The University of Texas to develop comprehensive mathematical models of hydrodynamic dispersive and transport behavior in reservoirs. Three macro-transport models are sought:

1. The first is a one-dimensional model for the depth variation of temperature which would: (a) describe the history of the thermocline, (b) provide insight into stratification and mixing coefficients and (c) define the circulation available for convective transport.

2. The second model sought is for the transport of conservative substances in a vertically, well-mixed reservoir. (The specific objective of this report.)

3. The third modeling effort is to develop a two-dimensional, time-dependent solution of the Navier-Stokes and continuity equations applicable to a stratified impoundment. The two coordinates directions would be the vertical and horizontal directions in the plane containing the characteristic length of the reservoir or, the vertical plane containing the direction of convective transport.

Evaluation of Reservoir Selective Withdrawal Models. Fruh (1970) made preliminary, general evaluations of various analytical and empirical models for the selective withdrawals of water from reservoirs. Two hydrodynamic models for the prediction of the velocity profile under stratified reservoir conditions were studied for detailed evaluation. Lake Livingston, Texas,was selected for specific verification and simulation purposes. The two models used were: the empirical, curve-fitting approach of Bohan and Grace and the analytic approach of Koh and Debler. Initially, these numerical models were tested using available input data from Lake Roosevelt, Lake Fontana and Lake Cherokee of the Tennessee Valley Authority and, Lake Travis of the Lower Colorado River Authority. Further model verification tests are planned, and efforts will be made to remedy deficiencies encountered in the preliminary tests involving boundary layer aspects and hydraulic continuity. In addition, changes in outflow water properties, other than temperature, will be measured. Ultimately, field tests will be made in Lake Livingston to determine the validity of the Koh-Debler and Bohan-Grace models for reservoir multiple outlet discharges, and other operational purposes. The need for the development of a hydrodynamic model of velocity profile in a stratified reservoir has been recognized as a prerequisite task in the formulation of a reservoir operational plan which provides for optimal selective withdrawal of waters from reservoir storage.

Analysis of Relevant Findings of Vital Studies and Investigations

Taylor on Dispersion of Matter in Turbulent Flow. In studies on accelerated diffusion and turbulent shear flow in a circular pipe, Taylor (1954) found that mixing is produced by mean velocity differences existing in a given pipe cross-section. At the center, the pipe flow is greater than average and carries a tracer fluid ahead of the bulk motion. Turbulent perturbations disperse the tracer over the whole pipe cross section. Near the pipe walls, at first, the fluid flow is retarded; subsequently, the fluid is spread out by turbulence. Taylor's findings developed as extensions of Reynolds' work, form the basis for the bulk of the theoretical, practical formulations for hydrodynamic dispersion and transport phenomena in water bodies. As stated by Schlichting (1961), the Reynolds similarity principle provides that "with flow of different fluids about geometrically similar bodies, the streamline patterns are similar if the dimensionless Reynolds number has the same value for each flow". Basically, the "Reynolds number may be interpreted physically as the ratio of inertial forces to viscous forces in the flow".

Elder on Open Channels. Elder (1959) extended Taylor's work to open channel flow. The essentials of his analysis apply to parallel flow regimens in other problems, including atmospheric steady winds and steady ocean currents without lateral flows.

Orlob on Eddy Diffusion in Homogeneous Turbulence. Orlob (1959) presented the fundamental logic underlying eddy diffusion incident to his analysis of eddy diffusion in homogeneous turbulence and his laboratory verification of the Kolmogoroff similarity principle which interrelates eddy diffusion, the rate of energy dissipation, and the Lagrangian eddy scale. His research provides an excellent analysis of the foregoing factors and their physical significance. Orlob (1959) presented as confirmation for his findings Pearson's comprehensive synthesis of investigation results concerning the relationship between the coefficient of eddy diffusion and the scale of diffusion phenomena, merging his own observations with those of many independent investigators.

Orlob's (1959) work presents a comprehensive summary of reported investigations, showing that a line of 4/3 slope fairly well establishes the trend of data from scales of 0.1 foot to over 1,000 feet. The following equation represents the relationship in over 100 investigations involving turbulence conditions:

$$D_z(\infty) = 0.013 E^{1/3} L_a^{4/3} \qquad (2-5)$$

where:

D_z = coefficient of lateral eddy diffusion.

E = rate of energy dissipation per unit mass.

L_a = Lagrangian eddy size.

Orlob's (1959) work shows the significance of the concept of a limiting diffusion coefficient. This matter will emerge again later in the discussion of Okubo's work.

When a point source discharges into the surface of a receiving body of water, the pattern of dispersion at first increases rapidly, fanning outward as the flow diffuses laterally while being carried away by the current. Near the source, the Kolmogoroff similarity principle applies with the dispersion coefficient D_z proportional to the eddy size. But, through an intermediate range of eddy sizes, the similarity principle does not apply. Further on in the spectrum of eddy scale, the dispersion coefficient continues to be affected by eddy size, but to a lesser degree. Eventually, the maximum eddy size becomes involved in the dispersion pattern and the eddy coefficient reaches a point where it stops increasing, and, attains a constant value.

Parker on Radioactive Tracer Diffusion Rates and Eddy Diffusion Coefficients. Parker (1961) of the Atomic Energy Commission reported on tests conducted on various reaches of the Metropolitan District Commission Reservoir No. 2 at Framingham, Massachusetts to determine radioactive tracer diffusion rates and eddy diffusion coefficients. The model envisaged by Parker was an idealized reservoir assumed to be of "infinite expanse and constant depth". The model was energized, supposedly, by a slug release of radioisotope tracer, which was assumed to be mixed rapidly and isotropically throughout the full depth of the reservoir, forming

an "instantaneous line source of constant strength". The model further envisages that the isotope tracer undergoes two processes: (1) radial diffusion from the origin and, (2) disintegration and losses.

A brief analysis of this important basic model will serve to bring out fundamental elements of reservoir modeling. Figure (2-1) shows an element of volume (r dr dθ dz) in the plane of diffusion, where:

c = tracer concentration.

r = radius from the source, o.

dθ = angular width of element.

dz = height of element.

The entering rate of tracer diffusion is:

$$-a^2 r\, d\theta\, dz\, \frac{\partial c}{\partial r} \tag{2-6}$$

The tracer diffusion leaving rate and die-away is:

$$-a^2(r+dr)\, d\theta\, dz\, \frac{\partial}{\partial r}\left(c + \frac{\partial c}{\partial r}\, dr\right) + k r\, dr\, d\theta\, dz\, c \tag{2-7}$$

where:

a^2 = eddy diffusion coefficient, indicating the degree of mixing, (length^2/time).[2]

k = effective decay constant of the radioisotope tracer.

c = tracer concentration.

---

[2] Prandtl's "mixing length" is implied here, which Rouse (1938) and Parker (1961) interpret as "the average distance a small mass of fluid will travel before it loses its increment of momentum to the region in which it comes."

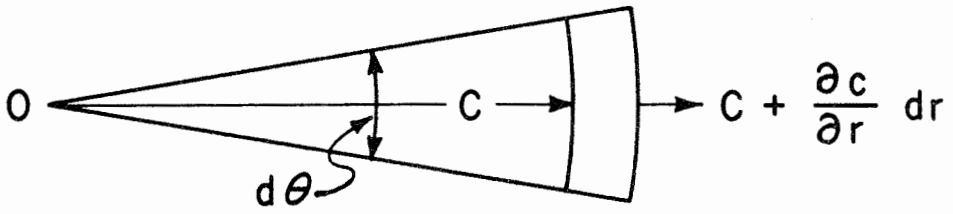

Figure 2-1. Element

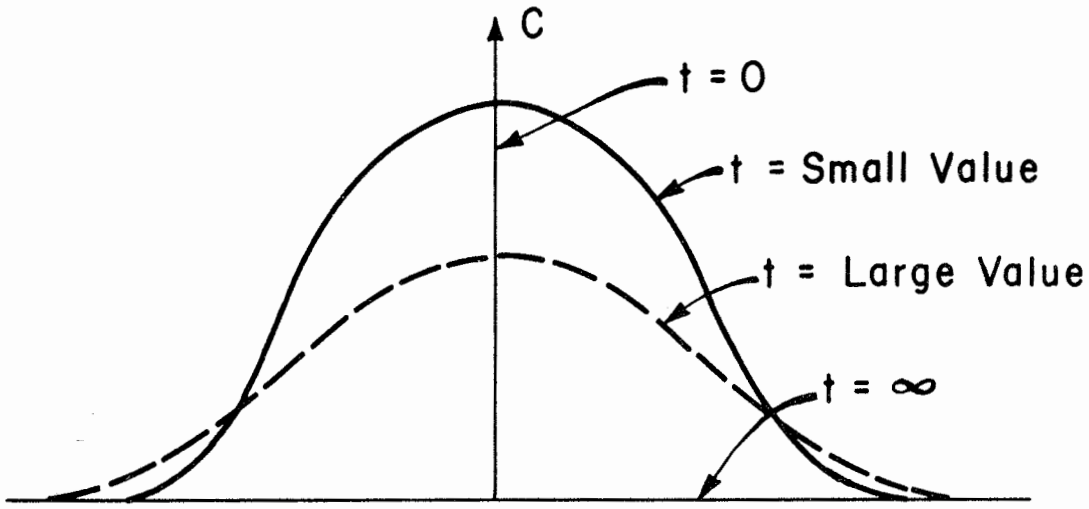

Figure 2-2. Diffusion from an Instantaneous Source (After Parker, 1961)

Equating the difference of the entering, and leaving tracer diffusion rates i.e., [Equations (2-6) and (2-7)] to the tracer build-up in the unit element [Figure (2-1)] the following balance equation is obtained:

$$\frac{\partial^2 c}{\partial r^2} + \frac{1}{r}\frac{\partial c}{\partial r} - \frac{k}{a^2}c = \frac{1}{a^2}\frac{\partial c}{\partial t} \quad . \tag{2-8}$$

The solution of the foregoing equation is given as:

$$c = \frac{N}{4\pi a^2 t} \exp\left(-\frac{r^2}{4a^2 t} - kt\right) \tag{2-9}$$

where:

c = concentration at any radius, r, and any time, t, after the tracer is discharged.

N = initial amount of radioactive tracer material added per foot of depth.

The general quantitative relationship between the parameters: c, and t is depicted schematically in Figure (2-2). The concentration frequency distribution is Gaussian; the concentration contours are circular.

The relationships between c, r and N are worthy of note. Solving Equation (2-9) for r, and let r = r' the radius of a circle having a given critical concentration, c', we obtain:

$$r' = 2\sqrt{a^2 t}\sqrt{\ln \frac{N}{4a^2 t c'} - kt} \quad . \tag{2-10}$$

Note that increasing N to N x 10^1 or even N x 10^2 has an insignificant effect on r'.

Using extensive diffusivity data, including that of other investigators, Parker (1961) derived the following empirical equation for the eddy diffusion coefficient:

$$a^2 = 7.5 \times 10^{-4} \times r^{1.47} \qquad (ft^2/sec) \tag{2-11}$$

This formula is in close accord with Richardson's law of "neighbor diffusivity" expressed by:

$$F(L) = \epsilon L^{4/3} \sim 3.03\, a^2 \tag{2-12}$$

where:

L = distance between particles.

ϵ = a constant.

a^2 = eddy diffusion coefficient.

Bowden on Horizontal and Vertical Diffusivity. Bowden (1965) applied the Taylor (1954) theory to various velocity profiles observed in ocean drift and tidal currents. He suggested that the combined effects of vertical velocity gradients and turbulent mixing in shear flows produce an "effective" horizontal dispersion. He suggested also that the effective coefficient of horizontal dispersion is inversely proportional to the coefficient of vertical eddy diffusion. Thorough vertical mixing in a flow, tends to counteract the shear effect on a tracer cloud; but, if vertical mixing is insignificant, horizontal transport is heavily influenced by the differential effects of the vertical velocity profile. The vertical transport of material

caused by vertical diffusion decreases the amount of horizontally-transported material. Thus, it is likely that if a reservoir has a stable density gradient pattern which strongly inhibits vertical mixing, the values of effective horizontal mixing and diffusion will be high.

Csanady on Tracer Diffusivity in Lakes. Csanady (1966), in tracer diffusion experiments on Lake Huron, confirmed that when the magnitude and direction of the horizontal mean velocity changes with depth, the horizontal diffusivity increases more rapidly than horizontal diffusivity under uniform flow conditions. And, if other temporal changes are imposed on the complex flow pattern, the dispersal characteristics are further greatly modified. Csanady (1966) examined horizontal diffusion in currents of complex patterns by three methods:

1. by considering the kinematics of skewed, unsteady currents;
2. by calculating effective lateral and longitudinal diffusivities using a method developed by G. I. Taylor (1954); and
3. by calculating first and second moments of the concentration distribution in shear flow using the diffusion equation.

Csanady (1966) concluded that a low eddy diffusivity tends to produce a high effective horizontal diffusivity due to acceleration of diffusion by the greater complexity of currents. The net dilution rates vary less than expected.

Finally, the shear effects noted earlier by Taylor (1954), Elder (1959) and Bowden (1965) were applicable in: (1) a longitudinal

direction in a parallel lake current with a non-uniform vertical velocity profile, and (2) a lateral direction in a skewed current.

Foxworthy on Multi-Dimensional Statistical Models of Turbulent Eddy Diffusion. Foxworthy, et al (1966) conducted diffusion experiments off the Southern California coast during 1963-1965, with the following apparent objectives:

1. To investigate the feasibility of applying statistical models of turbulent eddy diffusion to the specific case of a continous release of conservative dye tracer from point and volume sources.

2. To determine the effects of wind and of water-column stability on the dispersion process, particularly vertical eddy diffusion.

3. To verify the experimentally-determined empirical dispersion relationships in an actual coastal waste field.

Foxworthy, et al (1966) prefaced their work with two important clarifications:

1. Statistical models for the distribution of material in a plume released from a continuous, fixed point source in the atmosphere assume that the turbulent field is isotropic, homogeneous, stationary, and extends over infinite space. These assumptions imply that the statistical characteristics of turbulence in a given area are not affected by any arbitrary rotation (isotropy) and translation (homogeneity) of the selected coordinate axes. The term "stationary" means that the statistical characteristics are independent of time.

2. There are two basic types of steady-plume models:

   a. The model is assumed to be composed of a large number of overlapping patches of material as shown in Figure (2-3A).

b. If diffusion in the direction of the mean current is neglected, the model is assumed to be composed of vertical "disk elements" of material (proposed by Frenkiel (1953)) as shown in Figure (2-3 B).

Gifford on Dynamic Plume-Models. Foxworthy, et al (1966), cite Gifford's (1955) findings that the composition and behavior of a plume in the atmosphere is more complicated than described in the preceeding section. An individual plume element undergoes two motions, (See Figure (2-4)):

1. A spreading motion within the plume, resulting from turbulent eddies equal or smaller than the plume.

2. A meandering motion of the center of the element caused by large-scale eddies.

Gifford (1955) proposed a series of two-dimensional models incorporating both the spreading and meandering motions of the plume.

The models assumed a Gaussian material distribution within the disk-elements and a Gaussian-type frequency function for the variance of the tracer cloud center about the fixed axis. Gifford (1955) expressed the instantaneous concentration at a point in the plume as:

$$C(x,y,z) = \frac{Q}{2\pi\bar{\sigma}^2\bar{U}} \exp -\left(\frac{(y-D_y)^2 + (z-D_z)^2}{2\bar{\sigma}^2}\right) \qquad (2\text{-}13)$$

where:

Q = steady rate of discharge of material from a point source.

$\bar{U}$ = mean current velocity.

$\bar{\sigma}^2$ = variance of the material distribution within individual plume elements and is a function of time or distance.

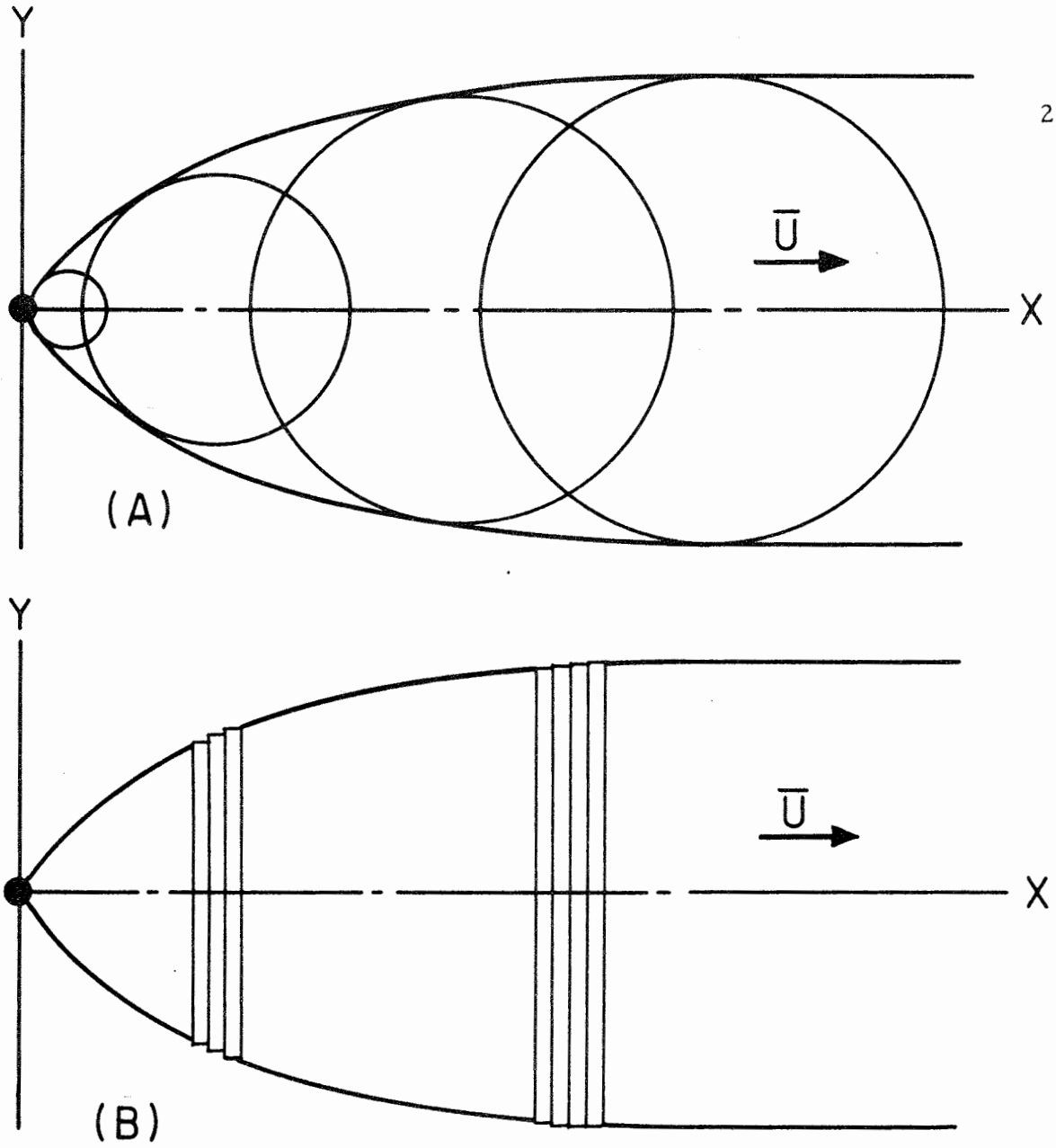

Figure 2-3. Plume Models

A. Plume Showing Superposition of Gaussian Puffs in Isotropic Turbulent Flow.

B. Plume Showing One-Dimensional Disk-Element.

(After Foxworthy, et al, 1966)

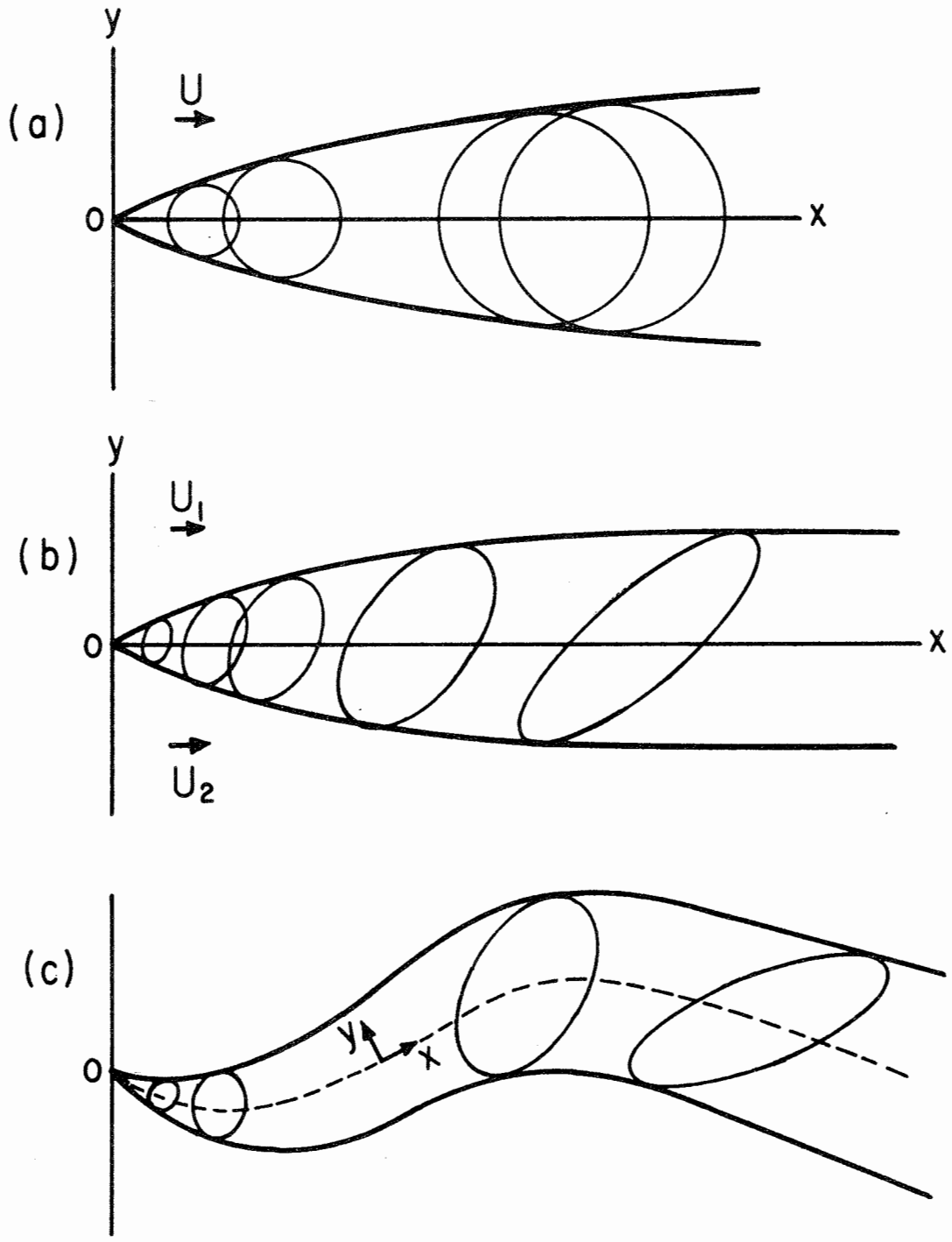

Figure 2-4. Continuous Release Plume Models

a. Ideal Plume in a Uniform Flow.

b. Ideal Plume in Shear Flow.

c. Meandering Single Plume. (An Extension of b using an Intrinsic Coordinate System along a Fluctuating Center Line.)

(After Okubo and Karweit, 1968)

x, y, z = the coordinates axes; x being the direction of the mean current.

D_y, D_z = distances of the center of gravity of a disk element from fixed axes at any given time.

In deriving Equation (2-13), Gifford (1955) made no assumption regarding the relationship between the variance, $\bar{\sigma}^2$ and the diffusion time or distance. He did assume a Gaussian material concentration distribution in the individual plume elements.

Gifford (1965) expressed the mean concentration at any point within the plume as:

$$C(x,y,z) = \frac{Q}{2\pi(\bar{\sigma}^2+\bar{D}^2)\bar{u}} \exp -\left\{\frac{r^2}{2(\bar{\sigma}^2 + \bar{D}^2)}\right\} \qquad (2\text{-}14)$$

where:

$r^2 = y^2 + z^2$

$\bar{D}^2$ = average variance of the frequency function for the variability of the center of the plume element.

In the derivation of Equation (2-14), Gifford (1955) assumed isotropic diffusion in both x-and z-directions.

Gifford (1955) also proposed a two-dimensional model where diffusion is anisotropic in two coordinate directions. The instantaneous concentration at a point for the two-dimensional anisotropic condition is:

$$C(x,y,z) = \frac{Q}{2\pi(\bar{\sigma}_y^2\bar{\sigma}_z^2)^{0.5}\bar{u}} \exp -\left\{\frac{(y-D_y)^2}{2\bar{\sigma}_y^2} + \frac{(z-D_z)^2}{2\bar{\sigma}_z^2}\right\} \qquad (2\text{-}15)$$

And, the mean concentration for the two-dimensional anisotropic conditions at any point within the plume is:

$$C(x,y,z) = \frac{Q}{2\pi(\bar{\sigma}_y^2 + \bar{D}_y^2)^{0.5}(\bar{\sigma}_z^2 + \bar{D}_z^2)^{0.5}\bar{U}} \exp -\left\{\frac{y^2}{(2\bar{\sigma}_y^2 + \bar{D}_y^2)} + \frac{z^2}{(2\bar{\sigma}_z^2 + \bar{D}_z^2)}\right\}$$

(2-16)

The following findings and conclusions from the studies and experiments of Foxworthy, et al, (1966) are relevant to this study:

1. The Gifford two-dimensional point-source model, which describes the maximum concentration-distance relationship along the center line of a steady plume in a homogeneous, stationary turbulent field of infinite extent was found to be applicable to the results of continuous point release experiments.

2. Vertical diffusion under conditions of high wind-speeds and low water-column stability, increases the dilution in a steady-release dye plume.

3. Results of full-scale experiments, in which an effluent field of a coastal outfall was tagged, showed that diffusion models of the point-source type cannot predict accurately the observed diffusion process at all distances from the source. This deficiency was attributed to the fact that the waste field at the boil did not resemble the idealized point source. This points out a major difficulty in modeling and verification. Namely, the difficulty of simulating actual initial conditions in a numerical model and, conversely, the equally difficult task of creating desired initial conditions in the field.

4. Data for experiments indicated that lateral variance of concentration distribution was a function of distance, raised to a power ranging from 0.92 to 2.24, indicating that Richardson's (1926) "4/3 law" relating the lateral coefficient of diffusion and the eddy scale, does not apply to the given oceanographic conditions. Richardson's Law of "neighbor diffusivity," Equation (2-5),

provides that the diffusion coefficient K is related to the distance L between two diffusing particles, as follows:

$$K(L) \propto L^{4/3} . \qquad (2\text{-}17)$$

Okubo on Oceanic Surface Diffusion.

1. Conceptual Basis of Surface Diffusion Diagrams. Okubo's (1962 A) oceanic surface diffusion studies indicated that contrary evidence was found regarding the validity of assuming a Gaussian concentration distribution as suggested by Gifford in his mathematical diffusion equation. Instead, Okubo indicated that Schönfeld's (1959) general equation of the superposable type, [See Figure (2-3) and (2-4)], was a more realistic representation of the spatial distribution of a diffusing substance. Schönfeld's proposed equation for the mean concentration based on horizontal diffusion from a continuous fixed source is:

$$\bar{C}(x,y) = \frac{Q\, w\,(x/\bar{u})}{\upsilon\, w^2 (x/\bar{u})^2} \qquad (2\text{-}18)$$

where:

Q, x, y, $\bar{u}$ are previously described.

w = mean diffusion velocity (assumed to be constant in time and space).

$x/\bar{u}$ replaces the dispersion time, t.

The maximum theoretical concentration along the center line of the plume is obtained by setting y = 0 in Equation (2-18). Thus,

$$C_{MAX} = \frac{Q}{\pi \bar{u} w} . \qquad (2\text{-}19)$$

2. Nature and Scope of Diffusion Tests Analyzed. Okubo (1968) investigated further certain empirical relations between diffusion characteristics by the use of carefully examined data from numerous dye release experiments made in the surface layer of the sea. The experimental data involves diffusion time scales ranging from one hour to one month and a length scale from 100 meters to 100 kilometers.

He prepared two types of "oceanic diffusion diagrams": (1) horizontal variance versus scale of diffusion, and (2) apparent diffusivity versus the scale of diffusion. He found that the behavior of horizontal variances and apparent diffusivity do not conform to the similarity theory of turbulence, except to a limited extent, locally in time-scale or length-scale. However, the Okubo (1968) diffusion diagrams provide a practical means to predict both the rate of horizontal spread of substance introduced from an instantaneous point-source and also the apparent diffusivity as a function of the size of the diffusion patch. Okubo (1968) based his studies on evaluation of data pertaining to twenty sets of diffusion experiments made by several investigators under a wide variety of hydrometeorological conditions. It is essential to consider Okubo's findings very carefully even though they pertain basically to oceanic surface diffusion, because they contain certain common experience of direct relevance to an understanding of mixing and dispersion in any major water impoundments.

As have other investigators, Okubo (1968) found that of various types of tracers used in experimental studies of oceanic diffusion, fluorescent dyes, especially Rhodamine B,have proved to be the most practical. Okubo confirmed earlier findings by Carpenter (1960) and Okubo (1957) that Rhodamine B was the most practical of all the fluorescent dyes. Pritchard and Carpenter (1960) introduced the special field technique for the direct, continuous observation of the fluorescent concentration using a fluorometer, and this technique has enabled the acquisition of considerable test data pertaining to oceanic diffusion.

The tests analyzed by Okubo (1968) cover a very wide range of length and time scales of diffusion ranging up to 100 km and one month,as were involved in the international cooperative "Operation RHENO" in the North Sea. Diffusion scales of about 30 meters were involved in tests off the coast of Southern California. And, a large amount of test data has been developed which pertains to diffusion scales ranging from 1 to 10 kilometers. Okubo (1968) found that bulk of the data pertain to tests made in the surface layers. No appropriate available data was found for dye tests at great depths.

3. Criteria for Evaluating the Suitability of Diffusion Test Results. The major criteria and considerations governing Okubo's selection, evaluation and adjustment of data of extensive previous tests for his comprehensive oceanic surface diffusion studies were:

   a. The dye should be released instantaneously from a point source.

   b. The duration of the dye release and the initial, horizontal size of the dye patch must be known. For a known initial size or a known initial variance, there is a critical time after which diffusion may be assumed to result from a point source release. This critical time can be computed from the Joseph and Sendner (1958) equation,

$$\sigma_0^2 = 6 P^2 t_0^2 \qquad (2\text{-}20)$$

   where:

   σ_0^2 = variance of the concentration in the initial dye patch.

   P = a diffusion velocity.

   t_0 = a characteristic time of diffusion of patch associated with the initial size, σ_0.

   The critical time, t_c must be $> t_0$, and it was empirically established at being $t_c >> 10\ t_0$. Diffusion data prior to the critical time are either disregarded or corrected, if feasible, by adding the critical time to the actual diffusion time.

   c. The dye patch should be located sufficiently distant from vertical boundaries so that the field of diffusion may be assumed to extend to infinity in the horizontal direction. Cognizance must be taken of all detectable boundary effects so that diffusion can be classified as two-or-three-dimensional. A sharp thermocline is regarded as a boundary. (Note: Constraints to diffusion in the vertical direction do not create drastic changes in horizontal diffusion but do have an important effect on the time behavior of the cloud peak concentration.)

d. The horizontal distribution of the dye concentration should be observed and measured in such a manner to enable the subsequent computation of the horizontal variance of the dye distribution. The use of aerial photos of dye patches is not entirely practical for these purposes. Some progress has been made in determining the concentration distribution from photos according to studies by Ichiye and Plutchak (1966). Gifford (1957) proposed a method of estimating the variance in atmospheric diffusion based on photographic observations of time changes in patches. However, Ichiye (1959) and Okubo (1962) both reported that results of applying the Gifford method to horizontal dye diffusion in the ocean were inconclusive.

e. The concentration should satisfy a mass or material balance. Pritchard and Carpenter (1960) in their Chesapeake Bay diffusion studies found that mass balances ranging from 80 to 90% were realized using rhodamine B tracer. However, Okubo (1968) finds that "mass balances as low as 50% or as high as 150% are permissible, especially in open ocean experiments and in the later stages of diffusion characterized by very low concentrations of dye within a patch". Okubo finds that in most tests he analyzed, the mass balance is neither reported nor computable due to lack of data on vertical distribution of the dye. Under these circumstances, Okubo (1968) suggests that on the basis of some indirect information, e.g., the stratification of the water column, an appropriate value of the mixed layer be adopted within which the dye is assumed to be distributed uniformly. Then, the amount of dye in the patch is computed by multiplying the horizontal distribution of the dye by the depth of the mixed layer. The mass balance also may be determined by the following indirect method. Note the observed horizontal distribution of the dye and compute the depth of mixed layer within which 100% of the material is supposedly contained, - considering the vertical diffusion in the sea, the stratification of the water column, and the total depth of water. The foregoing approaches which have been underlined, will be given special attention in this study. The approaches have a realistic, practical

relevance to the horizontal, two-dimensional numerical modeling objectives of this study.

4. Discussion on the Calculation of Diffusion Parameters. The following discussion of Okubo's (1968) comprehensive analysis of present methods of computing diffusion parameters is considered vital to this study. The most desirable parameters for computing the diffusion are the variance of the horizontal distribution of material versus the diffusion time, i.e., the time elapsed since the introduction of material. Okubo excludes the "maximum concentration" as the useful measure of diffusion "not only because the observation of the maximum concentration involves a great deal of uncertainty but also because the peak concentration is very sensitive to the presence or absence of a horizontal boundary."

The "release time" is best defined as the mid-point of the time of release; and, the "diffusion time" is best defined as the difference between the mid-point of time spent in observing the concentration and the "release time".

The variance of the horizontal distribution is a suitable measure for the spread of the dye. Okubo emphasizes that:

> "Horizontal diffusion in the sea cannot be described adequately by Fickian diffusion with a constant coefficient of diffusion. Thus, the theory of oceanic diffusion has been directed toward non-Fickian diffusion; as a matter of fact, apparent diffusivity increases with the diffusion time or with the size of the diffusive substance."

In order to estimate the variance directly, it is essential to know the horizontal concentration distribution at a certain depth. Examples of such a concentration distribution are shown in the Figures (2-5A) and (2-5B) from Okubo (1968). The figures show the ship courses along which continuous measurements of dye concentrations were made. Since the horizontal distribution of a substance is usually asymmetric, having a characteristic length larger in one direction or another, it is necessary

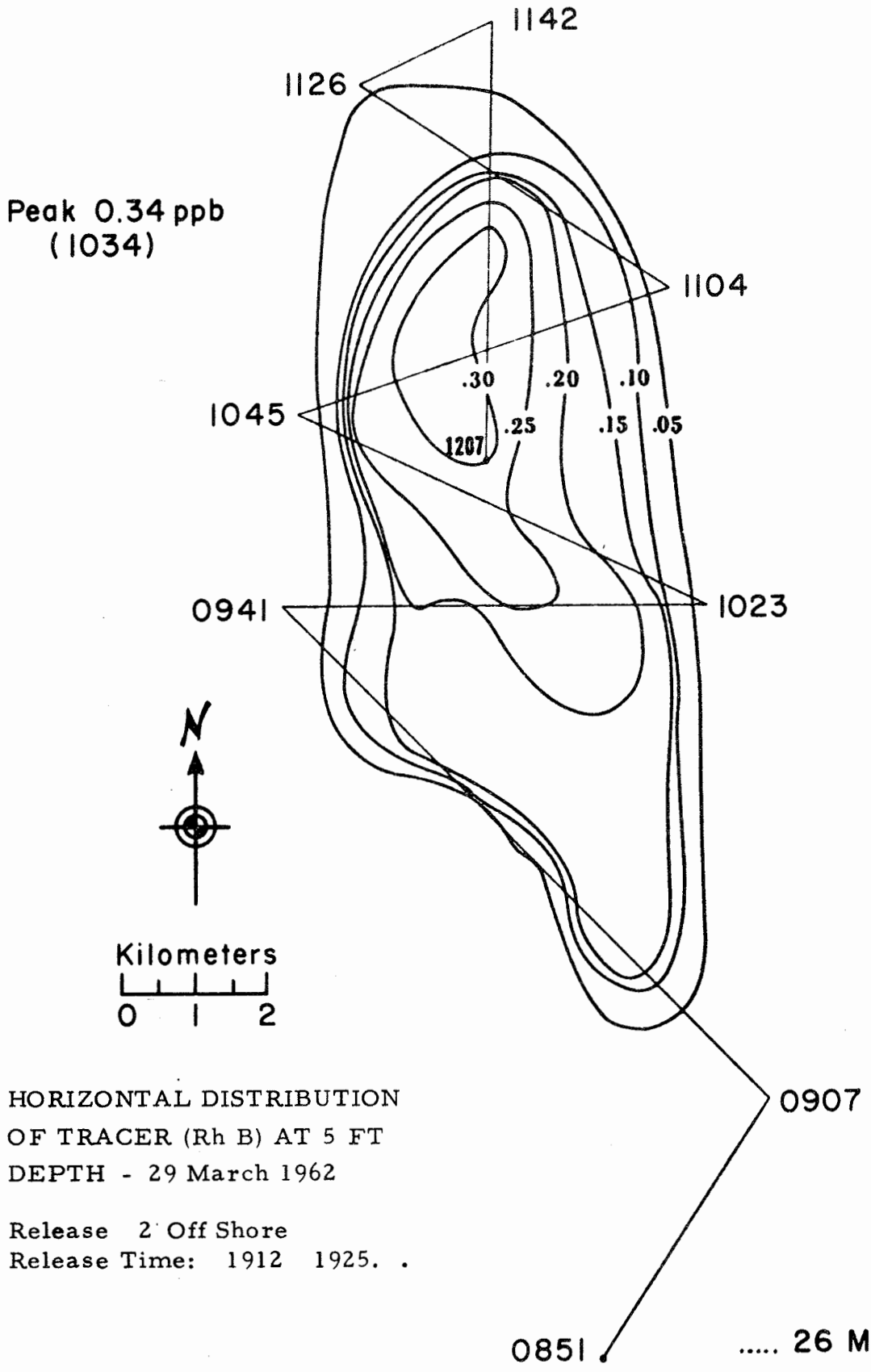

HORIZONTAL DISTRIBUTION
OF TRACER (Rh B) AT 5 FT
DEPTH - 29 March 1962

Release 2 Off Shore
Release Time: 1912 1925. .

Figure 2-5A. Horizontal Distribution of Rhodamine B at 5 Ft Depth for Release #2 (Off Cape Kennedy).

(After Okubo, 1968)

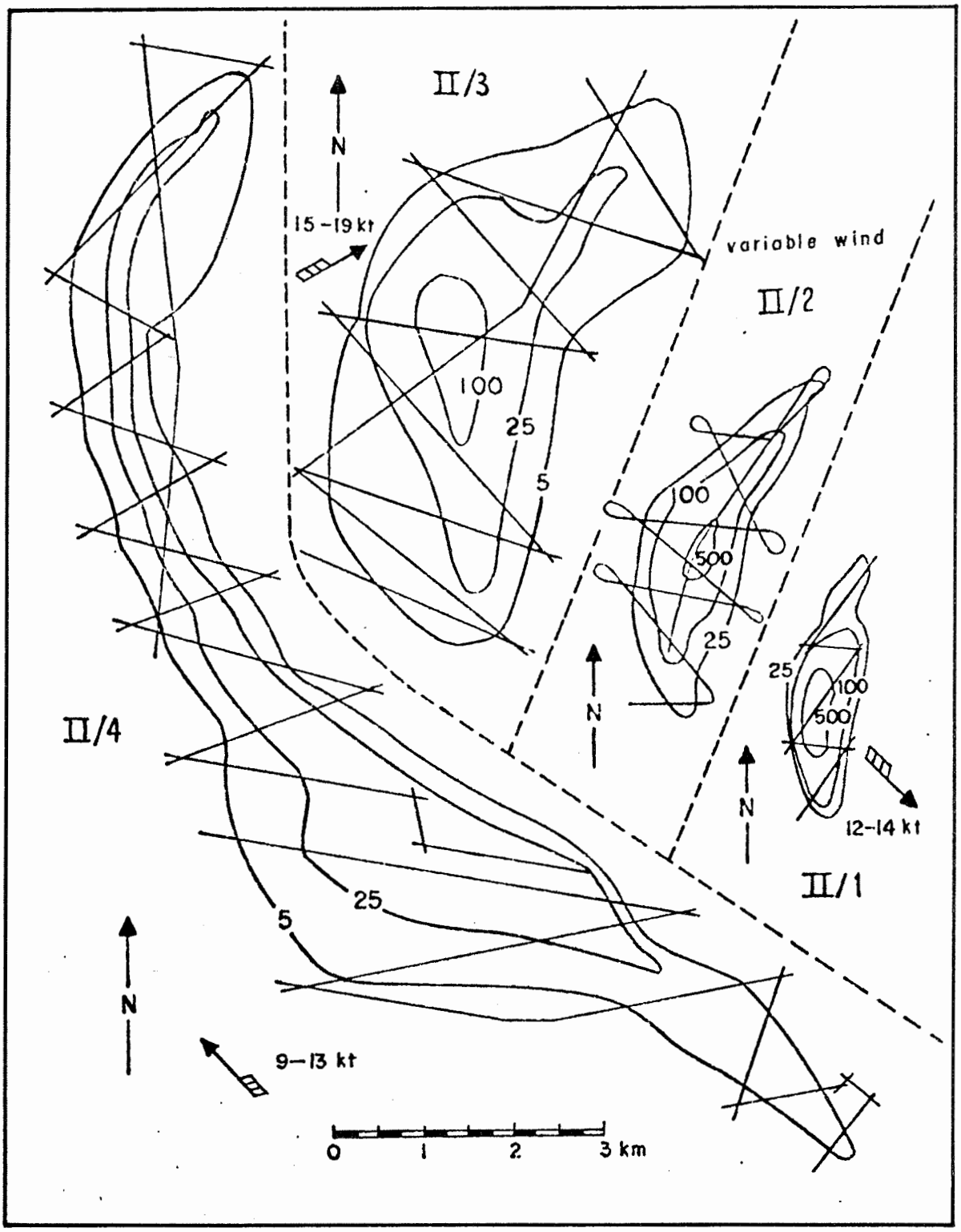

Figure 2-5B. Patterns of Dye Patch on a Horizontal Plane. The Wind Speed and Direction are also shown (from Joseph, Sendner, and Weidemann, 1964) (After Okubo, 1968)

to measure two variances along the long and short axes, respectively, in order to specify the dispersion characteristics.

Okubo (1968) also found that conversion to a "radially symmetric equivalent distribution" has been widely accepted in reporting the results of dye diffusion tests. The concept of the "radially symmetric equivalent" patch is as follows: At a diffusion time, t, the shape of the area enclosed by isolines of a concentration in any individual case will be irregular. See Figures (2-5 A) and (2-5 B); the tracer dye cloud generally is of elongated shape. Visualize making an infinite number of consecutively similar releases under the same oceanographic conditions, releasing the same amount of dye each time. Visualize taking an infinite number of such concentration distributions, each observed at the same diffusion time, and then assume that the distributions are superimposed on each other in such a way that the centers of mass of each distribution coincide. Further, visualize averaging all the superposed distributions. From this hypothetical superpositioning and averaging of the distributions obtain a radially-symmetric distribution of substance extending about the common center of mass, provided that the oceanic conditions, especially shears in the mean current, are isotropic.

5. Development and Analysis of the Two-Dimensional, Radially Symmetric Concentration Distribution Concept. Identical oceanic conditions do not necessarily insure rotational symmetry in the mean current shears. Along shores, the shears in the mean flow are likely to predominate in one direction; the dye cloud tends to elongate parallel to the shoreline. Thus, in near-shore water areas, the composite average of distributions can be expected to be of elongated shape rather than radially-symmetrical. However, since a radially symmetric distribution is one of the simplest "mathematical models" to deal with, Okubo (1968) uses this model by developing an eccentricity factor relationship between the variances of a radially symmetric distribution and a two-dimensional elliptically symmetric distribution which is a reasonably realistic mathematical model for an elongated dye cloud. The relationship is based on a practical measure of shape eccentricity.

Okubo (1968) found that the area enclosed by an iso-concentration line was approximately the same for all identical releases, regardless of the random, irregular distribution of concentration in individual dye releases. As a measure of the area enclosed by a given iso-concentration contour in an irregular patch, Okubo suggested using the radius, r_e of a circle having an area equal to the irregularly-shaped patch. A radially symmetric distribution, $S(t, r_e)$, characterized by the equivalent radius r_e and the diffusion time t would represent closely the composite radially symmetric concentration distribution previously described. Following is an exposition of Okubo's mathematical reasoning and formulations for the characteristics of dispersion associated with a two-dimensional, radially-symmetric distribution.

A two-dimensional distribution, S, of concentration from an instantaneous release of a unit amount can be expressed as:

$$S = S(t,x,y): \int_{-\infty}^{\infty}\int S\,dx\,dy = 1 \quad , t \geq 0 . \tag{2-21}$$

The mean value of any property f(x, y, t) related to S can be expressed as:

$$\bar{f} \equiv \int_{-\infty}^{\infty}\int f(S)\,dx\,dy . \tag{2-22}$$

If the origin of the orthogonal coordinate system (x, y) is given an arbitrary orientation, and is taken at the center of mass of the distribution, S, so that $\bar{x} = \bar{y} = 0$, then the mean square distance from the center of mass (i.e., the variance) can be expressed as:

$$\sigma_r^2 \equiv \bar{r}^2 = \int_{-\infty}^{\infty}\int (x^2+y^2) S\,dx\,dy . \tag{2-23}$$

Further, the value σ_r^2 can be expressed as the sum of the mean square distances (i.e., variances) from the center of mass along the two orthogonal axes:

$$\sigma_r^2 = \sigma_x^2 + \sigma_y^2 \tag{2-24}$$

The mean square separation between a pair of substance particles in a dye patch, $\overline{l}^2$ can be expressed as:

$$\overline{l}^2 = \iint \left| \underset{\sim}{r}_2 - \underset{\sim}{r}_1 \right|^2 F\left(t, \underset{\sim}{r}_1, \underset{\sim}{r}_2\right) d\underset{\sim}{r}_1 \, d\underset{\sim}{r}_2 \qquad (2\text{-}25)$$

where $\underset{\sim}{r}_1$ and $\underset{\sim}{r}_2$ are position vectors from the origin (center of mass) to two particles, respectively; $\underset{\sim}{l} = \underset{\sim}{r}_2 - \underset{\sim}{r}_1$; and, $F(t, \underset{\sim}{r}_1, \underset{\sim}{r}_2)$ is the joint probability density function for the two particles. See Figure (2-6).[3]

Okubo (1968) expressed a two-dimensional Gaussian distribution by:

$$S(t,x,y) = \frac{1}{2\pi \sigma_1(t)\, \sigma_2(t) \left(1-\lambda^2(t)\right)^2} \exp\left[A\right]$$

where:

$$\left[A\right] = \left(- \frac{1}{1-\lambda^2} \left(\frac{x^2}{2\sigma_1^2} - \frac{\lambda}{\sigma_1 \sigma_2} xy + \frac{\overline{xy}}{2\sigma_2^2} \right) \right). \qquad (2\text{-}26)$$

$\sigma_1^2(t)$ and $\sigma_2^2(t)$ are the variances in the x and y directions, respectively.

$$\lambda = \text{a coefficient of correlation} \equiv \frac{\overline{xy}}{\sigma_1 \sigma_2}. \qquad (2\text{-}27)$$

Equation (2-26) indicates that the concentration contours are a set of ellipses about the center of mass.

Rotating the orthogonal axes, (x, y), by a certain angle, the value of S can be expressed in terms of the principal axes (X, Y) as follows:

---

[3] Okubo (1969) found "that the mean square separations between a pair of particles in a dye patch is equal to twice the mean square distances of a particle from the center of mass to the patch".

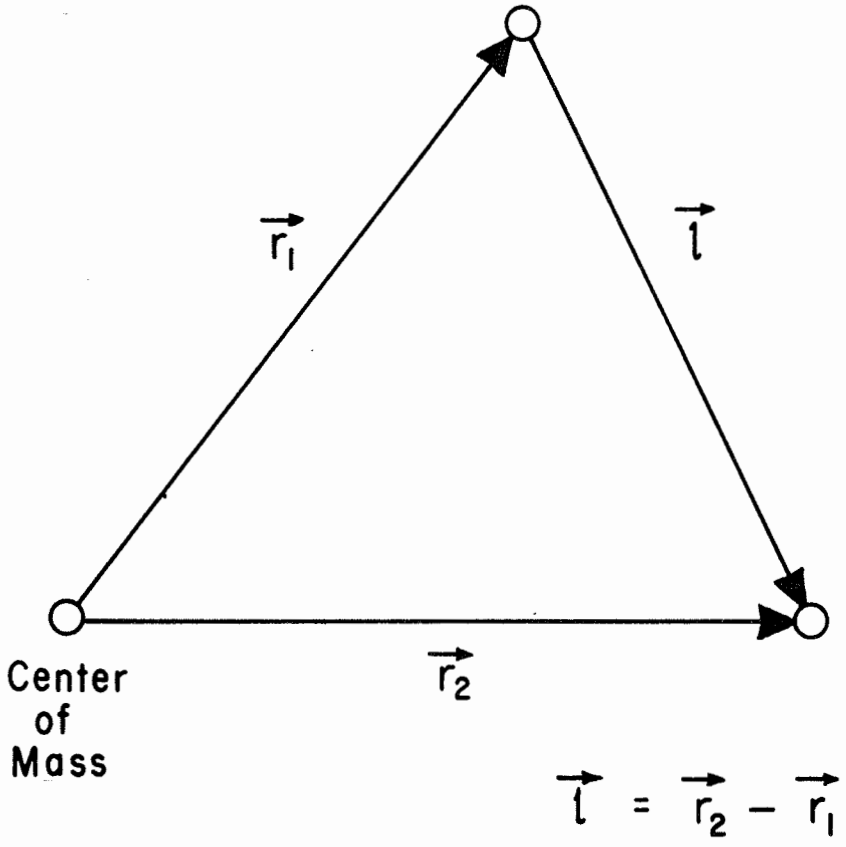

Figure 2-6. Position and Separation Vectors

$$S(t,X,Y) = \frac{1}{2\pi\sigma_x\sigma_y} \exp\left(-\left(\frac{X^2}{2\sigma_x^2} + \frac{Y^2}{2\sigma_y^2}\right)\right) \tag{2-28}$$

where:

σ_x^2 and σ_y^2 are variances in the major and minor elliptical, principal axes, respectively.

By previous Equation (2-24) we know:

$$\sigma_r^2 = \sigma_x^2 + \sigma_y^2 . \tag{2-29}$$

Converting the asymmetric distribution, Equation (2-28), into a "radially symmetric distribution" using the "equivalent radius concept," which is based on the assumption that the area enclosed by a given iso-concentration line is equal for both distributions, we have:

$$r_e^2 = \left(\frac{\sigma_y^2}{\sigma_x\sigma_y}\right)X^2 + \left(\frac{\sigma_x^2}{\sigma_x\sigma_y}\right)Y^2 =$$

$$= \left(\frac{X^2}{2\sigma_x^2} + \frac{Y^2}{2\sigma_y^2}\right) 2\sigma_x\sigma_y . \tag{2-30}$$

Therefore, Equation (2-28) reduces to:

$$S(t, r_e) = \frac{1}{2\pi\sigma_x\sigma_y} \exp\left(-\frac{r_e^2}{2\sigma_x\sigma_y}\right). \tag{2-31}$$

Defining the variance for the radially symmetric distribution by:

$$\sigma_{rc}^2 \equiv \int_0^\infty r_e^2 S(t, r_e) 2\pi r_e \, dr_e \quad , \tag{2-32}$$

we get:

$$\sigma_{rc}^2 = 2\sigma_x \sigma_y \quad . \tag{2-33}$$

Therefore

$$S(t, r_e) = \frac{1}{\pi \sigma_{rc}^2(t)} \exp\left(-\frac{r_e^2}{\sigma_{rc}^2(t)}\right) . \tag{2-34}$$

Thus, Okubo (1968) shows that the variance for the radially symmetric distribution is equal to twice the geometric average of the one-dimensional variances in the principal axes for the original two-dimensional Gaussian distribution. Generally,

$$\sigma_{rc} \neq 2\sigma_x \sigma_y \tag{2-35}$$

where x and y are orthogonal coordinates in an arbitrary orientation with respect to an elliptical patch of substance.

Okubo (1968) shows that the variance for an elliptical distribution is never less than that of the corresponding radially symmetric distribution, i.e.,

$$\sigma_r^2 - \sigma_{rc}^2 = \sigma_X^2 + \sigma_Y^2 - 2\sigma_X \sigma_Y = \left(\sigma_X - \sigma_Y\right)^2 \geq 0 . \tag{2-36}$$

Then, defining the degree of patch elongation by the approximation

$$\rho \equiv \sigma_Y / \sigma_X \quad , \tag{2-37}$$

Okubo (1968) eliminates σ_y and σ_x from Equations (2-29), (2-33) and (2-37) to obtain the following important relationship between variances and elongations:

$$\sigma_r^2/\sigma_{rc}^2 = 1 + \frac{(1-\rho)^2}{2\rho}. \qquad (2\text{-}38)$$

Finally, Okubo (1968) gives the expressions for calculating the relative amount of substance contained between r = 0 and $r = n\sigma_{rc}$ for $n > 0$, for radially symmetric, Gaussian type distributions. He proves that 95% of a substance stays within a diameter of $3\sigma_{rc}$ for all values of time, t.

6. Detailed Analysis of Oceanic Diffusion Tests. With the foregoing basic mathematical formulations, Equations (2-21) to (2-38) inclusive, as the basis for analytic criteria, Okubo analyzed a large number of oceanic diffusion tests. Okubo's formulations, the data he amassed, and his analytical observations are vital to the attainment of a clearer understanding of diffusion and dispersion studies and tests in water impoundments.

Certain additional realistic considerations emerge from the Okubo analyses. The sampling of concentrations for dispersion tests in a small dye patch is difficult and is very sensitive to surface disturbances. In order to minimize these disturbances during fluorometer samplings, Foxworthy, et al (1966) made only single crossings whenever dye patches were less than 30 meters in areal dimension. The crossings were made in the direction of the longer axis of the dye plume and then along the lateral or perpendicular direction. This procedure enabled calculation of variances along the principal axes of the concentration distribution. The observed concentration distributions were fitted to a Gaussian curve to compute the variances and in most cases the fit was satisfactory. Since the transits along the principal axes were not made simultaneously, empirical relationships were developed between the estimated variance and diffusion time for each axis. Thus, the following relations were developed from a log-log plot of the variance versus time for the variances along the principal axes:

$$\sigma_x^2 = k_x t^n$$
$$\sigma_y^2 = k_y t^m . \qquad (2\text{-}39)$$

From these values we can compute the variance for the radially symmetrical distribution:

$$\sigma_{rc}^2 = 2\sigma_x\sigma_y \qquad (2\text{-}40)$$

Okubo's (1968) evaluations elucidate two major points: The nature of variance and the nature of apparent diffusivity. Generally, Okubo (1968) noted that the variance σ_{rc} increases as a power of t, and that horizontal-diffusion is a process in which the apparent-diffusivity increases with the time-of-diffusion or the scale-of-diffusion.

a. The Nature of Variance. Figure (2-7) shows a linear fit applied to a plot of recent vintage data amassed by Okubo (1968) which gives the following empirical relationship between variance and time-of-diffusion:

$$\sigma_{rc}^2 = 0.018\, t^{2.34} \quad ;\sigma_{rc}^2 : \overline{cm}^2, t : sec. \qquad (2\text{-}41)$$

And, using field data obtained before 1961, Okubo (1962) derived:

$$\sigma_{rc}^2 = 0.006\, t^{2.5} \quad ;\sigma_{rc}^2 : \overline{cm}^2, t : sec. \qquad (2\text{-}42)$$

According to the similarity theory of turbulence, the variance was to increase with time to the power 3.0. Okubo's formulations (1968) show that while some of the data may be fitted locally in time to the power 3.0, the overall slope of the line of log σ_{rc}^2 versus log t in Figure (2-7) is somewhat less than 3.0. Figure (2-8) shows a plot of all data amassed by Okubo, including pre-1961 vintage. Observed variances at particular diffusion times vary as much as one order of magnitude. Major fluctuations and extreme values of variance occur during short diffusion times. In contrast, at longer diffusion times, the diffusion behavior undergoes an "averaging" process due to a variety of reasons such as changing winds and surface currents. Thus, most experiments involving long diffusion times, approach a statistical equilibrium in the σ_{rc}^2 vs. t relationship.

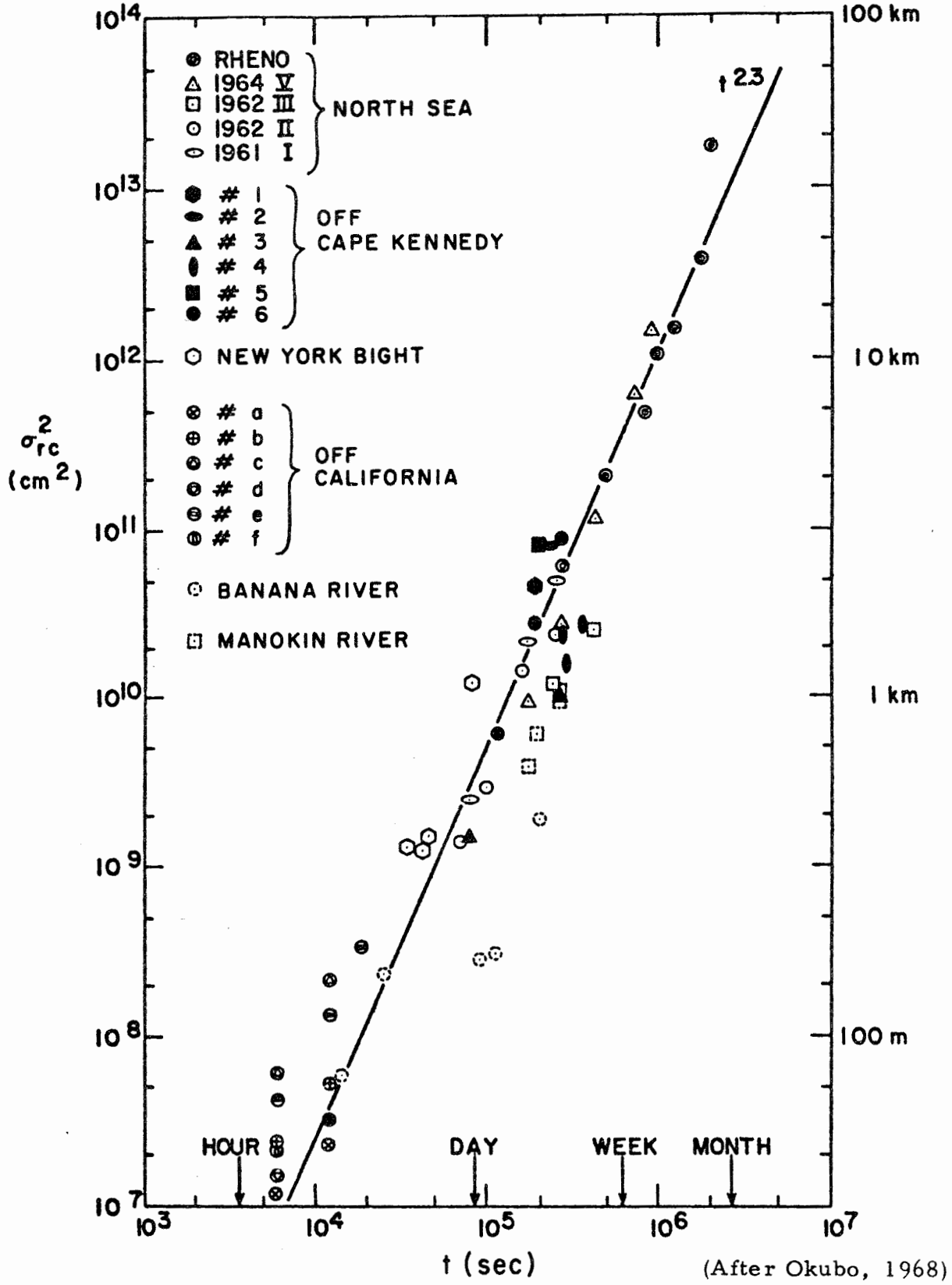

Figure 2-7. Variance, σ_{rc}^2, vs. Diffusion Time. (New Data)

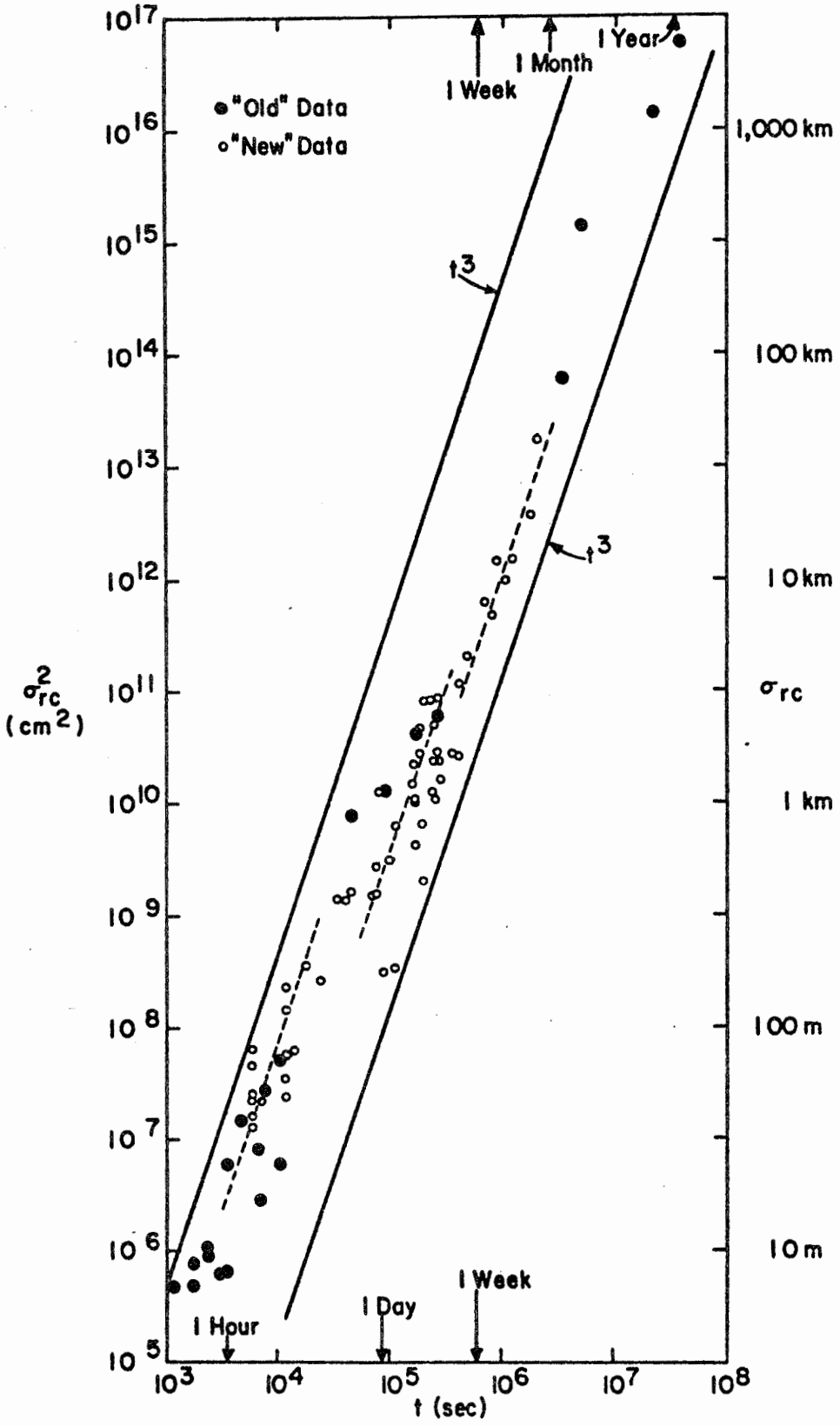

Figure 2-8. Variance vs. Diffusion Time (Old and New Data): Fit of the t^3 Relation Locally. - (After Okubo, 1968).

b. The Nature of Apparent Diffusivity. Based on linear fit to new data amassed by Okubo (1968) as shown in Figure (2-9) the following empirical relationship was developed:

$$K_a = 0.0103 \ell^{1.15} \quad ; K_a : \overline{cm}^2/sec, \ell : cm. \tag{2-43}$$

Based on earlier data, Okubo (1962) derived

$$K_r \propto \ell^{1.19} \tag{2-44}$$

where

$$K_r = \frac{1}{2} \frac{d\sigma_{rc}}{dt} \tag{2-45}$$

and,

$$\ell \equiv 4\sigma_{rc} \tag{2-46}$$

It appears from Figure (2-9) that insofar as dye diffusion experiments in oceanic regimes are concerned, apparent diffusivity does not conform to the "4/3 law".

Figure (2-10) is a plot of σ_{rc}^2 versus t, using all data showing the discontinuities of local scales.

7. Major Findings and Conclusions.

a. Regardless of oceanographic conditions prevailing during a test, the horizontal diffusion phenomena exhibits certain trends. A principal one is that the variance increases with diffusion time to a power between 2 and 3.

b. Only relatively few dye studies have been conducted in which the horizontal migration and distribution of substance is related to environmental factors, such as the stability of water column as considered by Foxworthy, et al (1966).

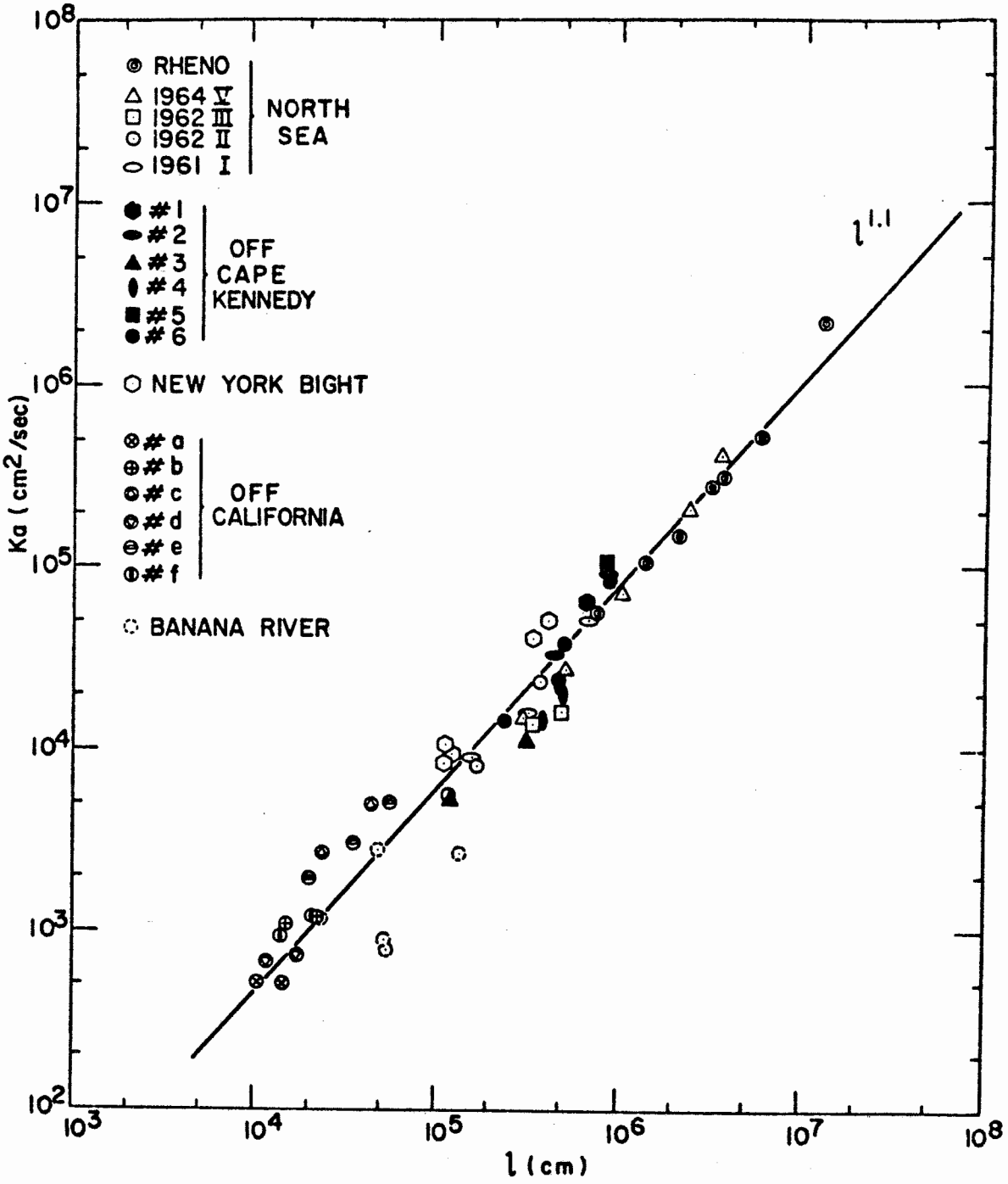

Figure 2-9. Apparent Diffusivity, K_a vs. Scale of Diffusion, $\ell \equiv 3\sigma_{rc}$, (New Data). - (After Okubo, 1968).

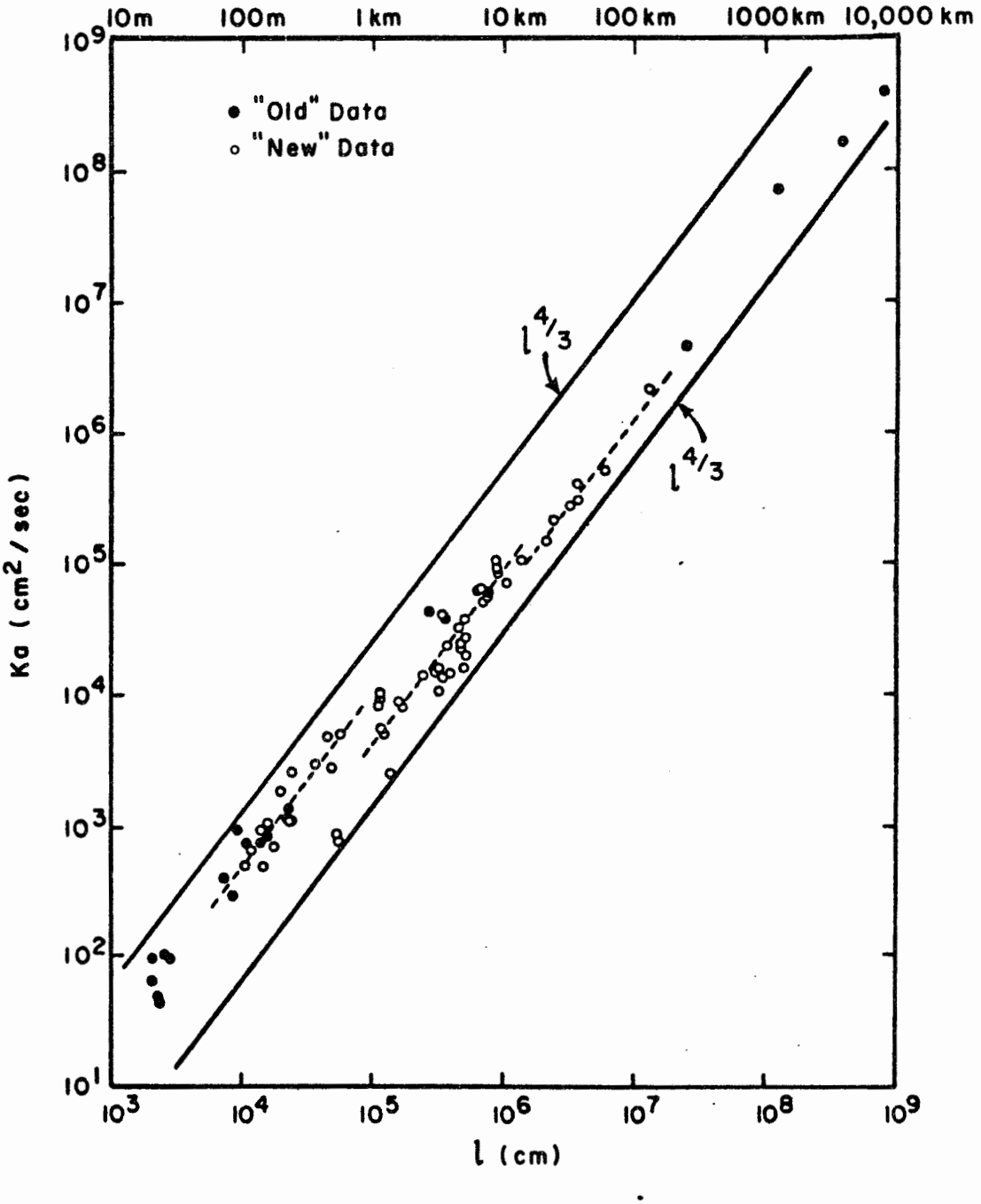

Figure 2-10. Apparent Diffusivity vs. Scale of Diffusion (Old and New Data): Fit of the $l^{4/3}$ Law Locally. (After Okubo, 1968).

Foxworthy, et al (1966) studied the effect of water column stability and wind speed on the variances in the directions of the principal axes of a diffusing dye cloud and their studies brought out some additional diffusion trends. They found that at any average wind speed between 2 and 14 knots, lower values of dilution are associated with higher values of average stability. In other words, increased stability suppresses vertical diffusion, but the effect of stability on horizontal diffusion is indeterminate. For example, in the range of 2 to 8 knot winds, an increase in variance σ_x^2 accompanied by a decreasing stability might prove to be a predictable relationship but there is insufficient data to support this expectation. It should be noted also, that under similar conditions of decreasing stability there appears to be no definite effect on σ_y^2.

c. Plots of variances vs. wind velocities indicate a general trend to increased σ_x^2 with increasing wind velocities, but no conclusive correlation between σ_y^2 and wind velocity. (Wind velocity may be considered as a measure of a characteristic current speed in the water column within which diffusion takes place.) Velocity shear can be a major influence in the horizontal spread of contaminant material in the ocean surface. Current shear produces an effective longitudinal dispersion by the combination of the gradient of the mean velocity and turbulent mixing in the same direction. If a uniform vertical shear exists in the horizontal current, the variances σ_x^2 and σ_y^2 were expressed by Carter and Okubo (1965) as:

$$\sigma_x^2 = \frac{1}{6}\Omega_z^2 A_z t^3 \qquad (2\text{-}47)$$

$$\sigma_y^2 = 2A_y t \qquad (2\text{-}48)$$

where:

Ω_z = constant vertical shear.

A_z = vertical eddy diffusivity.

A_y = lateral eddy diffusivity.

From an analysis of the above equations, it can be speculated that:

i. Lateral eddy diffusivity would be affected slightly by stability; that is, σ_y^2 is uncorrelated to stability.

ii. Horizontal eddy diffusivity, σ_x^2, would be increased by increasing wind velocity (i.e., increasing vertical shear Ω_z). Also, σ_x^2 would decrease with increasing stability due to the suppression of A_z by the increasing stability. The foregoing equations, which constitute a simple shear-diffusion model interprets qualitatively the experimental results of Foxworthy, et al (1966).

iii. A radially symmetrical distribution may not properly represent the actual pattern of oceanic diffusion. Generally, the converted radially symmetrical horizontal variance is always smaller than the actual variance. The correction factor is:

$$\frac{\sigma_r^2}{\sigma_{rc}^2} \qquad (2\text{-}49)$$

where:

σ_r^2 = mean variance.

σ_{rc}^2 = for radially symmetrical distribution.

The factor depends on the degree of elongation of the dye plume; the more elongated the dye plume the larger the correction factor. Often, the elongation of the plume increases with time. Figure (2-11) shows a plot of σ_r^2 versus t, suggesting the local validity of the "t^3 law".

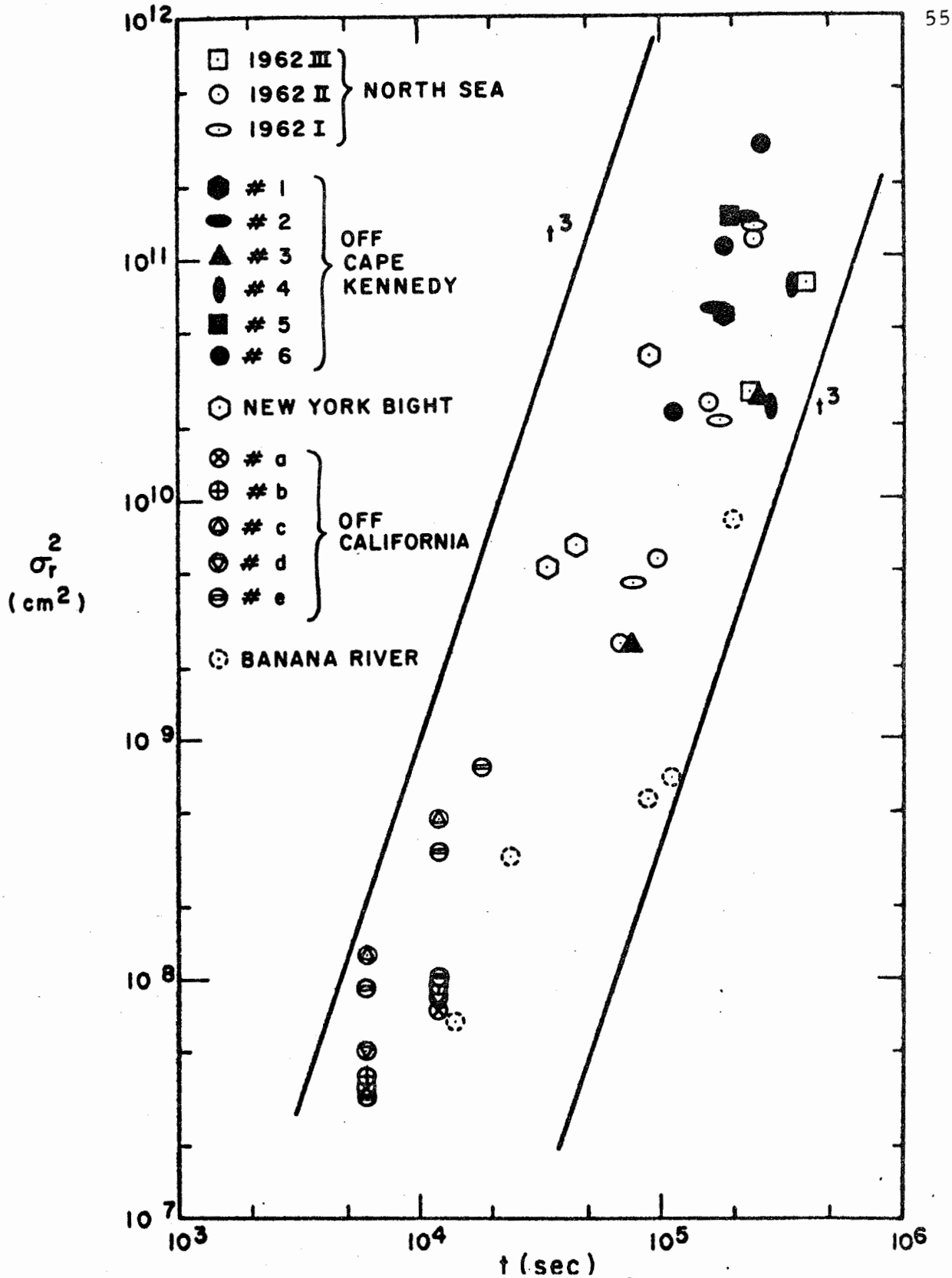

Figure 2-11. Mean Variance, σ_r^2, vs. Diffusion Time. (After Okubo, 1968).

d. The turbulent diffusion of a dye cloud is a problem of relative diffusion. Dispersion is a fluid motion relative to the mean velocity of water; advection is motion with the mean velocity of water. Turbulent diffusion is the basic mechanism for dispersion. Okubo (1968) shows that the apparent diffusivity increases as the 4/3 power of patch size:

$$K_d \propto E^{1/3} \sigma_r^{4/3} \qquad (2\text{-}50)$$

where E = the rate of energy dissipation per unit mass through turbulence.

Levich on Turbulent Diffusion. Equation (2-50) which is Richardson's "law of relative diffusion", is based on the physical theory that regards relative diffusion as an accelerating process. The rate of diffusion increases with the size of the dye cloud. The scale of eddies responsible for the horizontal dispersion of a conservative substance lie in what Kolmogoroff, (1941) termed the "inertial sub-range". In order to better understand the practical limitations of the foregoing empirical concepts, let us examine more closely the theoretical concepts of the general nature of turbulent motion of a fluid when $Re >> Re_{cr}$. (Note: Re is the Reynolds number and Re_{cr}, the critical value at "developed turbulence", (Levich 1962). Under this condition, eddy velocities of varied magnitudes are added to U, the average fluid velocity. Turbulence eddies are characterized by their velocities and the distances over which these velocities undergo a large change. The distances are known as the "scale of motion". The most rapid eddy motion has the largest scale of motion. The velocities U', of the most rapid eddies can be approximated by:

$$U' \approx \Delta U \qquad (2\text{-}51)$$

where ΔU is the change in the average fluid velocity over a distance equal to the scale of eddy motion, ℓ.

For example, for turbulent motion in a pipe, the largest scale of motion, ℓ, of turbulence eddies approximates the diameter of the pipe, and the eddy velocities vary within the range of average velocity over a longitudinal distance equal to the pipe diameter. That is, the eddy velocities in the pipe approach the maximum velocity at the center of the pipe. Large scales of eddy motion account for most of the kinetic energy inherent in turbulent motion.

The Reynolds number[4] of the motion produced by large scale eddies have values equal to the Reynolds number of the stream, as a whole. But, in addition to these large scale eddies, turbulent flow also includes eddies of the smaller scale, λ with smaller velocities V_λ. And, it is emphasized in the present turbulence concepts, that while the number of small scale eddies may be very large, they provide only a small portion of the total kinetic energy of the stream. However, the small eddies have a vital effect on turbulent flow.

---

[4] Reynolds Number $= \dfrac{\Delta U \ell}{\upsilon}$ (2-52)

In order to clarify the effect of small scale eddies, let us examine the Reynolds number that corresponds to an eddy of small scale λ , that is,

$$Re_{\lambda} = \frac{V_{\lambda}\lambda}{\upsilon} . \tag{2-53}$$

The smaller the value of λ and the related velocity V_{λ} , the smaller is Re_{λ} .

For large scale eddies the Reynolds number is very large. Therefore, in a fluid motion with a scale $\lambda \doteq 1$, the viscous forces actually have no effect and, motion takes place without energy dissipation. However, the addition of large scale eddies on each other produces small scale eddies whose Reynolds numbers decrease rapidly with decreasing λ .

At a certain value of $\lambda = \lambda_o$ the Reynolds number for the motion is $Re_{\lambda_o} = \frac{V_{\lambda_o}\lambda_o}{\nu}$. (2-54)

This means that in the region of λ_0, the viscous forces begin to affect fluid motion; and, eddy motion of scale λ_0 is accompanied by a loss of energy. Stated in another way, "micro-scale of turbulence" is related to the size of the smallest eddies in the turbulence field which become dissipated due to viscosity effects. In the THERMO-SYSTEMS INC. manual on the theory and application of hot-film and hot-wire anemometry, the micro-scale of turbulence is expressed numerically as:

$$\lambda = \bar{U}\tau u'/y \tag{2-55}$$

where:

U = instantaneous velocity.

$\bar{U}$ = average (mean) velocity.

τ = time constant.

U' = root mean square (rms) average of the fluctuating velocity turbulence.

u = fluctuating portion of velocity.

$y = \tau \sqrt{\left(\frac{du}{dt}\right)^2}$

With a large quantity of small scale motion, there is a large loss of energy, which is converted to heat. The energy is continually drawn by small scale motions from large scale motions, so that one might visualize the flow of a continuous transfer of energy from large scale eddies to progressively smaller eddies, until in eddies of scale λ_0 the energy is converted to heat. Therefore, small-scale eddies serve as transitional media by which kinetic energy of large-scale motions is transformed into thermal energy. For steady state fluid flow, the process of energy transfer is also steady in nature. That is, eddies of a given scale receive as much energy from larger-scale eddies as they in turn pass on to smaller-scale eddies. Thus, their properties depend only upon the rate of energy transfer which must be equal to the rate of energy dissipation if the energy of the eddies remains constant, (Levich 1962).

However, in natural hydrological or hydrodynamic systems, it is likely that additional energy sources such as wind and wave systems

are added sporadically or steadily to the idealized turbulent fluid energy system just described, and the resulting eddies from this "energy mix" cannot be strictly regarded as belonging in the so-called "inertial subrange" of the natural spectrum of eddy sizes. Therefore, the results derived from the turbulence concept upon which both Richardson's Law of Relative Diffusion and Kolmogoroff's Theory of Similarity are based cannot be regarded as universally applicable to describe the behavior of diffusion and dispersion in oceanic, estuarine or impoundment regimes. These facts were confirmed by the comprehensive studies of Okubo, discussed in the preceding section.

Okubo (1968) noted that as the scale of diffusion increases, the smaller is the rate of turbulence due to energy transfer, because the local supplies of energy tend to be transferred through the irregular, non-linear, interactions from the larger eddies to the smaller eddies. As a result, the overall rate of growth of the variances with time would be slower than that derived from the cube power law (Batchelor 1952):

$$\sigma_r^2 = C E t^3 \qquad (2\text{-}56)$$

where:

C = constant of order unity.

E = rate of energy dissipation per unit mass through turbulence.

t = time of diffusion.

And, the overall growth rate of apparent diffusivity with the eddy scale should be smaller than derived by the 4/3 law, Equation (2-50).

Special Dye Tracer Tests and Investigations

This study involves dye tracer measurements to verify mathematical hydrodynamic and transport models for a lake. Following are the germane results of a review made of dye-tracing tests, measurements and techniques.

1. Use of Rhodamine B. The problems of using Rhodamine B dye, including the effects of physical adsorption, photochemical decay, water temperature and pH, were investigated by Feuerstein and Selleck (1963). Foxworthy and Kneeling (1969) found that most of the problems encountered in using Rhodamine B in tracer tests in estuarine water carrying highly-diluted waste fields were of minor importance, however, the effect of water temperature on fluorescence was significant.

2. Temperature Correction for Fluorescence Measurements. A satisfactory method of correcting for the temperature effects on Rhodamine B, used by Pritchard and Carpenter (1960) and others, is to monitor continuously the water temperature and apply a correction factor to measured fluorescence levels. Another method, used by Foxworthy, et al (1966), is to measure fluorescence with a fluorometer, enabling rapid field calibration, using standard solutions of dye and local ocean water as a diluent.

3. Dye Plume Behavior and Dye Concentrations. Foxworthy and Kneeling (1969) found that the time behavior of dye concentrations at a given point in the leading segments, along the longitudinal axis of waste field plumes in marine waters varied considerably. This wide variation was attributed to unsteady conditions caused by advection and three-dimensional diffusion throughout the forward part of the plume. Elsewhere on the plume axis, the time

behavior of dye concentration at a point remained nearly constant, indicating virtual steady-state conditions and essentially two-dimensional diffusion laterally and vertically.

Foxworthy and Kneeling (1969) and Csanady (1966) have shown that in dye fields created by continuous point-releases, the mean concentration distributions both laterally and vertically were virtually Gaussian.

Foxworthy and Kneeling (1969) specified formulas for computing the "effective" diffusivity coefficients, based on tracer measurements, for unsteady and steady flows,

$$\text{Unsteady:} \quad D = \frac{1}{2}\frac{d\,S^2}{d\,t}; \quad S^2 = f\ (\text{time}) \tag{2-57}$$

$$\text{Steady:} \quad D = \frac{U}{2}\frac{d\,S^2}{d\,x}; \; S^2 = f\ (\text{distance}) \tag{2-58}$$

where:

D = coefficient of effective diffusivity.

S^2 = point source variance in a given coordinate direction.

U = average current velocity.

These coefficients are variable unless the asymptotic or linear diffusion phase is reached, that is,

$$S^2 \propto X\ (\text{or } t) \tag{2-59}$$

$$D = \frac{1}{2}\frac{d\,S^2}{dt} \quad \text{and,} \quad D = \frac{U}{2}\frac{d\,S^2}{d\,x} \tag{2-60}$$

Integrating Equation (2-60) between appropriate limits we obtain:

$$D = \int_0^1 dx \doteq \frac{U}{2} \int_0^1 dS^2$$

$$D' = \frac{U}{2} \left(\frac{S_1 - S_0}{x_1 - x_0} \right)$$

(2-61)

and since $S_0^2 \longrightarrow$ zero for a point source, Equation (2-61) reduces to

$$D \doteq \frac{US^2}{2x} \quad .$$

(2-62)

For a larger plume,

$$D \doteq \frac{U}{2} \left(\frac{\sigma_1 - \sigma_0}{x_1 - x_0} \right)$$

(2-63)

where

σ = computed standard deviation of the mean distribution.

σ_0^2 = mean coordinate variance of concentration distribution at the origin of a large-scale plume.

x, y, z = orthogonal coordinate directions; x is along the longitudinal axis of the plume; y is laterally perpendicular to x; z is vertically perpendicular to the x and y.

U = average current velocity.

In the deterministic models, the variances S^2 of lateral and vertical dye concentration distributions are known to vary linearly with distance. Hence, the spread of dye in these coordinate directions can be described by Fickian-type equations involving a constant diffusivity.

4. Density Effects on Initial Plume Sizes and Subsequent Dilution Rates. Vital experience concerning dispersive and transport phenomena has stemmed from coastal waste outfall studies. Foxworthy and Kneeling (1969) in reviewing Harremoës (1967) extensive report on density effects in marine disposal, point out that in some cases, buoyancy may have a great initial effect on the lateral spread of a waste plume. Coastal tests showed that maximum dye and bacterial concentrations were usually found at or very near the water surface.

The effects of buoyancy transport and waste plume formation from large volume, submarine, off-shore waste outfall facilities have relevance to this study because it is within the purview of this work to consider the movement of conservative material after it has "surfaced" from a submerged outfall, theoretically creating in the process, a fully-mixed surface layer.

Foxworthy and Kneeling (1969) found that the waste plume dilution rate is affected greatly by the initial size of the plume at the origin. Generally, the smaller the initial plume size, the higher the initial dilution rate. This does not infer that the dilution rate at a point downstream in the plume surface will be greater for surface plumes of relatively smaller size. This is true because the lateral diffusion rate which has a great effect on the net dilution, is dependent on the initial size of the plume. Foxworthy (1969) concluded that the wider the initial plume, the higher the lateral diffusion rate. And, that in the process of "surfacing", the wider-plume undergoes a higher initial dilution. This is the reason why subsequent dilution rates appear low, at first, in wide plumes after surfacing. Special consideration has been given to the above findings concerning the behavior of subsurface discharges after surfacing. They indicate the impracticality of assuming a constant depth for the fully-mixed, near-surface stratum of an impoundment. There is a general important similarity between the case of a submarine outfall discharging buoyant substance in a body of water through a diffuser and, an open-channel discharging a fully-mixed flow having a radically different density than the receiving body. Thus, at first, the fully-mixed stratum extends to the full depth. After "surfacing", the

mass transport stratum can have a highly variable thickness. The special assumptions and stipulations in the preceding chapter, and the special stratification correction factor developed in Chapter VII, stem from these outfall studies.

Mathematical Hydrodynamic, Hydrological or Transport Modeling for Inland Water Impoundments

Origins. McEwen (1929) made the first major attempt to devise a rigorous mathematical treatment for the physics of a reservoir thermal system.

Hutchinson (1957) computed heat transfer coefficients from assumed temperature profiles in lakes. This, and earlier efforts, characterized the thermocline as the limiting mechanism of energy transfer into the impoundment.

Munk and Anderson (1948), applying Richardson's Theory of Stability for dynamic air masses, found that changes in the mixing properties of ocean masses could be made direct functions of fluid density, and in turn, density could be correlated to thermal energy.

Ertel (1954) made a temporal and spatial diffusion model of thermocline development based on constant coefficient of diffusivity.

Throughout the period of the initial efforts typified above, there was a continual recognition of the need to balance the hydrometeorological forces governing the regime of energy at the surface of water bodies with the internal hydrodynamical processes of fluid masses. For

example, energy budget computations pertaining to Lake Hefner were basically mass balances.

Lake Hefner Studies. The comprehensive Lake Hefner, Oklahoma studies by the U. S. Geological Survey and other government agencies, (1954) had the objectives of developing "an improved method or methods for the determination, and if possible the prediction from climatological and limnological data, of water losses by evaporation using mass-energy and energy-budget theory". This study proved that the classical energy-budget equation needed modification. The relevant findings were:

1. The water-budget control method met the requirement that errors in the computed water budget not exceed 5 percent of the monthly evaporation.

2. Evaporation computed using the budget equation showed that:

   a. For periods of less than seven days, errors were excessive because changes in energy storage could not be measured with sufficient accuracy.

   b. For periods of seven days or more, evaporation could be determined with an accuracy of $\pm$ 5%, if all terms in the energy-budget equation were carefully calculated.

   Of considerable importance in the Lake Hefner studies was the exhaustive investigation on evaporative losses due to wind-wave action. Two types of mass-transfer equations were examined: One type involved the Prandtl "mixing length" concept; another type involved the "continuous mixing" concept. Relevant results were:

   a. No deviation from the logarithmic wind law could be detected between 2 and 8 meters, regardless of stability conditions, over periods of 3 hours or longer.

b. The lake surface was aerodynamically rough at all times with no evidence of a critical wind speed for water-air boundary processes. The roughness length varied from 0.55 to 1.15 cm, increasing with wind-speed. Taken as a whole, the evidence indicated that flow conditions very near the surface are critically important in predicting evaporation.

c. Of all the mass-transport equations tested, only those of the form developed by Sutton and Sverdrup (1937) proved amenable to the use of field data within the measurement capabilities of current instruments.

Sauer and Masch (1969) reported that as a result of the Lake Hefner and other studies, the Harbeck quasi-empirical mass transfer equation for predicting evaporation, developed in 1962, has gained acceptance. The "mass transfer coefficient", which is the crux in most mass transfer equations, represents a combination of many variables, including:

a. manner of variation of wind with height

b. size of the lake

c. roughness of water surface

d. atmospheric stability

e. barometric pressure

f. density and kinematic viscosity of air.

Sauer and Masch, (1969) point out that the Harbeck equation is relatively simple, requiring only:

a. water surface temperature

b. air temperature

c. relative humidity

d. wind movement.

And, they conclude that:

> "Observations of climatic factors at nearby weather stations may be used for estimating purposes."

Velz and Gannon (1960) in their study of impoundment temperature prediction techniques, demonstrated the practicality, economy and, necessity of statistical analysis of local meteorological record data, including air temperature, wind velocity, and vapor pressure. They emphasized the importance of long-term meteorological data.

The studies by Velz and Gannon (1960) and, by Sauer and Masch (1969), bring out a matter of special relevance to this numerical modeling investigation. This relevance was expressed by Velz and Gannon (1960) as follows:

> "With a rational method for forecasting expected water temperature conditions, based on the probability of occurrence of the controlling meteorologic and hydrologic variables, it is possible to evaluate temperature effects before construction of facilities. This provides an advance in stream sanitation evaluation dealing with an increasing variety of waste heat problems. . ."

In short, the synthesis of a numerical model with key, real-time variables of a given physical system is indispensable.

The Raphael Model Concept. Raphael (1962) demonstrated a practical procedure of making temperature forecasts using unified energy relationships to impoundments on specific reservoirs and rivers in California and Washington. The Raphael concept (1963) envisaged a reservoir as being made up of a series of horizontal layers each having the average

temperature of the temperature gradient in that layer. Heat moves in and out of the layer chiefly by means of water transported in and out of the layer. Some heat is transferred between layers by conduction (molecular diffusion). This concept is based on making subjective judgments, and arbitrary assumptions regarding internal mixing processes and the effects of advected and withdrawn flows.

The Wunderlich-Elder Graphical Temperature Prediction Model.

1. Introduction. Wunderlich and Elder (1968) reported that as a first step in the search for a mathematical model which could simulate the influence of reservoir (or impoundment) hydrodynamics on stream water quality and, eventually also predict water quality in a reservoir and its discharge, the Tennessee Valley Authority (TVA) decided to develop a preliminary, broad-scale method of analyzing and predicting essential hydrodynamic effects and tendencies in thermally-stratified reservoirs. While the TVA recognized that water quality in reservoirs is dependent on many factors, the Authority recognized the general scientific consensus to focus on thermal or density stratification since the effects of these phenomena have pronounced spatial and temporal influences on water movement and water quality in impoundments. It appears that the studies conducted on TVA's Fontana Reservoir, were made to investigate the hydrodynamics of a large, density-stratified reservoir; to evaluate the observed data for possible correlations between essential parameters; and, to use the data for conceptualization of a stratified reservoir numerical model.

   However, for expedited interim purposes, TVA conceived a simplified reservoir temperature prediction model which would consider some of the major factors involved in thermal stratification as a result of temperature differences caused specifically by heat advection of inflows

and outflows. Wunderlich and Elder (1968) used the temperature model to show the complex interrelationships between such factors as reservoir geometry, outlet works design, reservoir operation, hydrology of the drainage basin, optical properties of the impounded waters and the climate of the environment. The successful, macro-scale approximations afforded by the model in two cases, one involving temperature prediction and another dissolved oxygen predictions, initially gave some weight to the belief that the interim model had indeed encompassed a large number of major factors of the reservoir hydrodynamic system. This matter will be discussed later, incident to modeling efforts for selective withdrawal operations of reservoir waters.

2. Basic Concepts and Assumptions Regarding the Temperature Prediction Model. The Wunderlich and Elder (1968) reservoir temperature prediction model provided important insights into the major factors of a reservoir hydrodynamic system even though many aspects, of necessity, have been treated by intuitive and approximate methods, pressed by the need to obtain practical,immediate information. (Wing 1962, p. ix)

The assumptions made in the temperature prediction model are:

a. Density changes are due to temperature changes only.

b. A 10-ft. surface layer only is involved in the heat exchange process between reservoir and atmosphere. This layer is established mainly by solar energy. The layer insulates the rest of the reservoir from surface heating. Downward transfer of heat by molecular conduction and turbulent diffusion from the layer is neglected.

c. The temperature of the 10-ft. surface layer is taken as the equilibrium temperature of the impoundment and is computed from the heat budget equation.

d. Inflow temperatures are based on observed records, determined from appraisal of upstream conditions, or computed from heat budget equations.

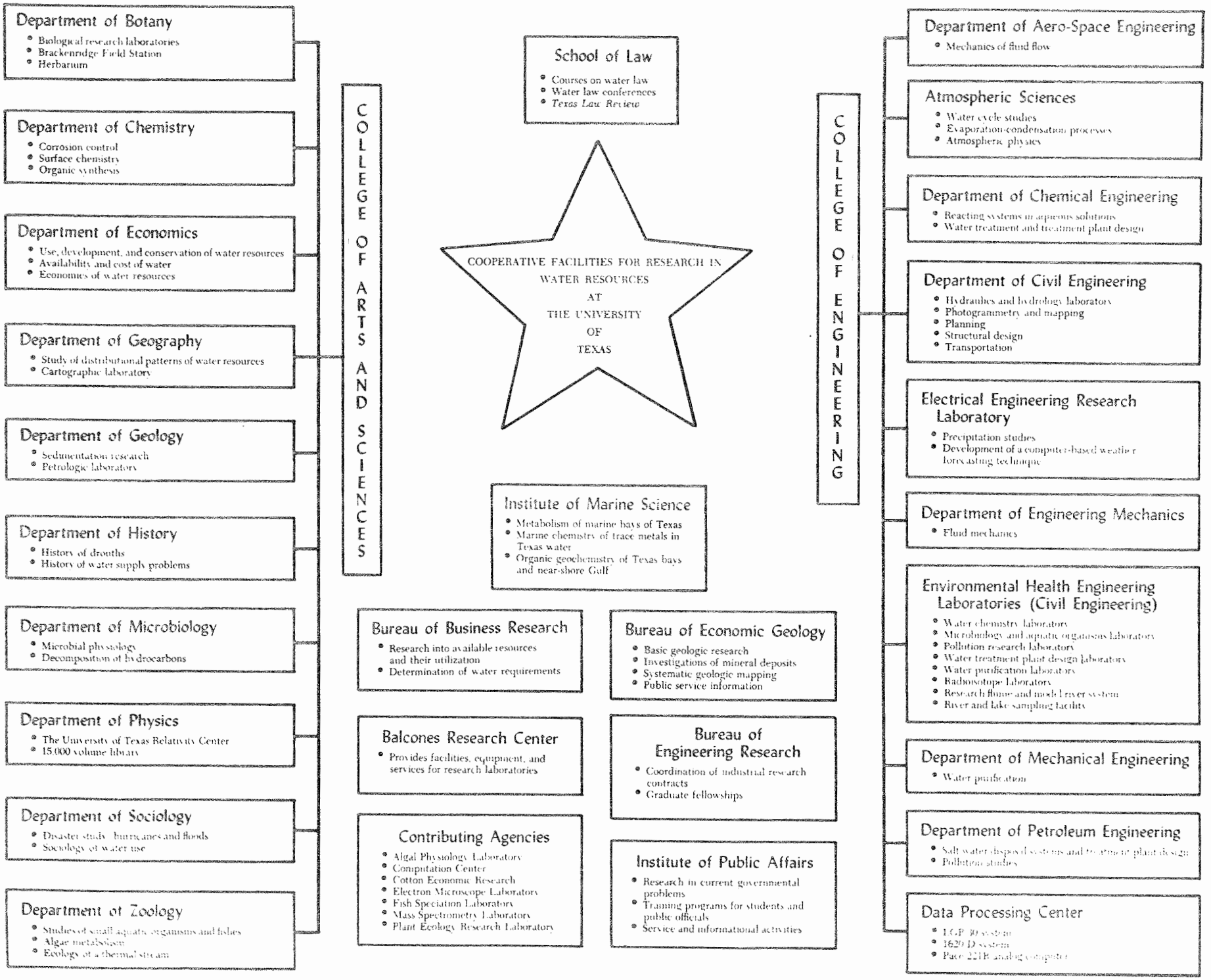
COOPERATIVE FACILITIES FOR RESEARCH IN WATER RESOURCES AT THE UNIVERSITY OF TEXAS
COLLEGE OF ARTS AND SCIENCES
COLLEGE OF ENGINEERING
Department of Botany
Biological research laboratories
Brackenridge Field Station
Herbarium
Department of Chemistry
Corrosion control
Surface chemistry
Organic synthesis
Department of Economics
Use, development, and conservation of water resources
Availability and cost of water
Economics of water resources
Department of Geography
Study of distributional patterns of water resources
Cartographic laboratory
Department of Geology
Sedimentation research
Petrologic laboratory
Department of History
History of droughts
History of water supply problems
Department of Microbiology
Microbial physiology
Decomposition of hydrocarbons
Department of Physics
The University of Texas Relativity Center
15,000 volume library
Department of Sociology
Disaster study - hurricanes and floods
Sociology of water use
Department of Zoology
Studies of small aquatic organisms and fishes
Algae metabolism
Ecology of a thermal stream
School of Law
Courses on water law
Water law conferences
Texas Law Review
Institute of Marine Science
Metabolism of marine bays of Texas
Marine chemistry of trace metals in Texas water
Organic geochemistry of Texas bays and near-shore Gulf
Bureau of Business Research
Research into available resources and their utilization
Determination of water requirements
Balcones Research Center
Provides facilities, equipment, and services for research laboratories
Contributing Agencies
Algal Physiology Laboratory
Computation Center
Cotton Economic Research
Electron Microscope Laboratory
Fish Speciation Laboratory
Mass Spectrometry Laboratory
Plant Ecology Research Laboratory
Bureau of Economic Geology
Basic geologic research
Investigations of mineral deposits
Systematic geologic mapping
Public service information
Bureau of Engineering Research
Coordination of industrial research contracts
Graduate fellowships
Institute of Public Affairs
Research in current governmental problems
Training programs for students and public officials
Service and informational activities
Department of Aero-Space Engineering
Mechanics of fluid flow
Atmospheric Sciences
Water cycle studies
Evaporation-condensation processes
Atmospheric physics
Department of Chemical Engineering
Reacting systems in aqueous solutions
Water treatment and treatment plant design
Department of Civil Engineering
Hydraulics and hydrology laboratory
Photogrammetry and mapping
Planning
Structural design
Transportation
Electrical Engineering Research Laboratory
Precipitation studies
Development of a computer-based weather forecasting technique
Department of Engineering Mechanics
Fluid mechanics
Environmental Health Engineering Laboratories (Civil Engineering)
Water chemistry laboratory
Microbiology and aquatic organisms laboratory
Pollution research laboratory
Water treatment plant design laboratory
Water purification laboratory
Radioisotope laboratory
Research flume and model river system
River and lake sampling facility
Department of Mechanical Engineering
Water purification
Department of Petroleum Engineering
Salt water disposal systems and treatment plant design
Pollution studies
Data Processing Center
I.C.P. 30 system
1620 II system
Pace 221R analog computer

e. Reservoir inflow spreads uniformly over the horizontal area of the corresponding temperature stratum.

f. Below the 10-ft. layer, water remains at its original inflow temperature for the duration of the reservoir stratification period and no temperature change takes place during migration to its level. Thus, no mixing occurs between inflow-water and reservoir-water.

g. Water withdrawal affects only a layer defined by the top and bottom of the withdrawal, below this there are stagnant zones.

h. Water is withdrawn from the horizontal layer extending over the entire reservoir stratum area at intake level. Water from upper strata sink gradually as whole layers to the withdrawal level.

i. After mid-summer and, as the inflow temperatures drop, the inflows will enter the reservoir at greater depths as the cold season approaches, thus lifting the upper layers.

j. As the surface temperature declines, the reservoir assumes a homogeneous temperature. Convective cooling mixes the reservoir downward from the surface to the isotherm corresponding to the surface temperature. Hence, the fall isotherms are assumed to be vertical lines connecting the water surface and the isotherm equal to the surface temperature.

3. Analysis of Graphical Temperature Prediction Model. At the beginning of the year, the reservoir is assumed to have a homogeneous temperature. Inflows early in the year are assumed to mix with the reservoir water. Later as the inflows warm, they will spread out uniformly over the cold surface layer of the reservoir. Subsequently this layer is topped by additional, slightly-warmer layers until a 10-ft. warm surface layer is incrementally developed. Thereafter, the inflows spread out beneath the 10-ft. surface layer and will remain at its original inflow temperature.

The outflow temperature corresponds to the value of the isotherm at the withdrawal center line. The model indicated that high inflows tend to spread out the temperature gradient in a vertical direction, while low inflows crowd the isotherms near the 10-ft. surface layer, thus indicating the formation of a strong temperature gradient below the homogeneous surface layer.

In dry years, characterized by low inflows and outflows, the low temperatures at great depths may persist longer than in a wet year with high inflows and outflows.

Dry years are characterized by strong temperature gradients below the surface layer and by cool outflow temperatures; wet years are characterized by gradual temperature gradients and warmer outflow temperatures.

In summary, the idealized, graphical temperature prediction model revealed useful insights into the effects of stratification caused by: (1) variations in intake location, (2) variation in inflow-outflow operations, and (3) reservoir size.

The model provided data for estimating: (1) the general type of thermal system which might develop, (2) the possible outflow temperature pattern, and (3) an idea of the possible impacts of creating impoundments on streams.

The Wunderlich and Elder (1968) Mathematical Reservoir Temperature Prediction Model.

1. Concepts and Assumptions.

a. In contrast to the graphic model, the mathematical model does not assume that diffusion of heat is negligible, nor does it assume that the bulk of advected heat comes from inflows and outflows.

b. The mathematical model assumes that while horizontal velocities are small, they are effective over long periods of time in eliminating horizontal temperature gradients caused by large inflows, wind and other natural causes. This condition implies, that

only "long-time mean temperature" can be predicted from this model because long periods of times would be needed to break down horizontal temperature gradients. The model is one-dimensional, in which only the vertical density or temperature gradients are considered. No gradients are assumed in a horizontal plane.

c. The mathematical model involves the simultaneous solution of the heat and mass conservation equations. The heat conservation equation for a layer of thickness dz between elevation z and (z + dz) is:

$$E_{in} + E_{out} + E_{vert} + E_{sol} + E_{dif} + E_{bot} + E_c = 0 \qquad (2\text{-}64)$$

where:

E_{in} = heat inflow rate due to advection.

E_{out} = heat outflow rate due to advection.

E_{vert} = heat flow rate due to vertical water movement.

E_{sol} = heat flow rate due to solar radiation.

E_{dif} = net heat flow rate due to vertical diffusion.

E_{bot} = heat flow rate due to vertical diffusion.

E_c = change of heat content of considered layer, (heat/time).

The mass conservation equation for the same layer is:

$$Q'_{vert} - Q_{in} + Q_{out} = 0 \qquad (2\text{-}65)$$

where:

Q'_{vert} = variation of vertical water flow with elevation (volume/time/unit of depth).

Q_{in} = water flow rate entering laterally into the layer (volume/time/unit of depth).

Q_{out} = water flow rate exiting laterally out of layer (volume/time/unit of depth).

d. All terms of Equations (2-64) and (2-65) are functions of depth and time. Introducing the proper partial differentials or analytical expressions for these terms, and combining the two equations, leads to the differential equation of heat transfer in the water column. If the heat transfer component, E_{bot} is neglected, it is found that E_{dif} is the only term which cannot be readily determined. According to Fick's First Law, the diffusive heat flux can be assumed to be proportional to the product of a diffusivity, A,and a temperature gradient $\partial\theta/\partial z$. The diffusivity, A,is assumed to consist of three components:

i. molecular thermal conductivity, A_m.

ii. free convective, A_f.

iii. forced convective, A_t.

Only A_m has been established numerically, (5.2×10^{-4} sq. m./hr. at 20° C.). A_t and A_f may act simultaneously or separately during certain time periods, for example, A_t as wind-induced turbulent diffusion and, A_f as convective night-cooling.

The diffusivity, A, can be evaluated from the differential equation of heat transfer obtained from Equations (2-64) and (2-65). Orlob and Selna (1967) computed values of A as functions of time and depth, using Fontana Reservoir field data. With proper assumptions for A, and the boundary conditions at the water surface, and at the reservoir walls, the temperature distribution with depth and time can be obtained by the numerical integration of the heat transfer equation. [Wunderlich and Elder (1968) citing Orlob and Selna (1967)].

2. Evaluation of Mathematical Reservoir Temperature Prediction Model. If large inflows and outflows are involved, the assumption of homogeneous horizontal spreading in a one-dimensional model will be erratic; a refined two-dimensional model would be necessary but many of the simplified assumptions used previously for the one-dimensional model would be impractical.

3. Wunderlich-Elder Temperature Prediction Model and Selective Withdrawal. It was noted earlier that the graphical temperature prediction method, using many simplifying assumptions, consisted essentially of a graphical representation of an annual, cyclical mass balance inventory of the reservoir, with special emphasis on accounting for storage of water masses and their temperatures during the stratification phase. The important simplifying assumptions governing this model were discussed earlier.

Wunderlich and Elder (1969) judged that the simplifying assumptions regarding heat diffusion and inflow-outflow distribution within the reservoir were acceptable only if mean flows and temperatures are used.

Evaluating the results of applying the prediction model, Wunderlich and Elder concluded that further study was needed on:

a. Determination of the thickness of the reservoir withdrawal layer.

b. The unsteadiness of inflow and withdrawal.

c. The spread of inflow.

d. The diffusion of heat and matter in reservoirs.

They also concluded that a concurrent consideration of all the aforementioned critical factors increases the complexity of the temperature prediction model such that recourse to numerical methods (where again one is faced with having to assume considerable simplifications) appears to afford the best chances for a solution to the temperature distribution prediction problem.

Water Resources Engineers, Inc. (WRE). Water Resources Engineers, Inc., (1968) made a rigorous, viable, physical conceptual representation for describing the complex exchanges and transport of heat

energy within a deep, fresh-water impoundment and also the hydrodynamics of the water mass. The complexity was noted by the recognition that fluid flows can be functions of all or combinations of the following factors: boundary conditions, the irregular three-dimensionality of the impoundment, the extent of density and temperature stratification caused by reservoir inflows or outflows, energy transfers through the surface, and internal mixing.

The primary objective of the WRE model was to provide a capability for simulating the thermal behavior of reservoir-channel systems. WRE decided to structure separate models for two classes of problems and then couple them ultimately to form a cohesive simulation package. Separately, one model would be capable of representing a "turbulent stream or a fully-mixed, short-detention time reservoir". The other would represent a more complicated problem of energy distribution in a deep lake or reservoir in which temperature density stratification would occur seasonally. Linked together through common boundary conditions, the models can be combined to provide capability for simulation of a system of reservoirs which tend to become thermally stratified, river channels and canals operating under steady flow conditions, and combined systems of reservoirs and discharge channels.

Specifically the WRE model was designed to:

a. Execute a water balance computation under either steady or non-steady conditions.

b. Receive solar energy inputs and accommodate energy losses through the reservoir surface or flowing streams.

c. Distribute energy by advective and diffusional mechanisms along the principal axis of flow (the vertical in case of reservoir).

d. Be capable of being discretized into any desired number of horizontal segments to specify desired spatial variations in thermal energy or reservoir geometry.

e. Provide for temporal description of thermal energy changes throughout water body over seasonal or operational cycles at any desired time interval.

f. Describe the development or decay of a thermal profile, including identification of the thermocline subject to hydromechanical, hydrologic or operational changes.

The WRE model was verified using the Fontana Reservoir data. Results indicate "generally good agreement" between model and prototype in some features such as isothermal contours. However, the model still has limitations insofar as (1) the mathematical structure and (2) the quantity and quality of data needed for simulation and verification. Also, the model is essentially one-dimensional in a mathematical sense, permitting transfer to occur only along a single axis. Therefore, in a stream it is tacitly assumed that no vertical stratification occurs and that the turbulence of flow keeps the properties of the fluid uniform at all points in a cross section taken normal to the flow. For a reservoir, transport or transfer is assumed to occur along the vertical axis and properties are assumed to be uniform

throughout a horizontal plane. While there are rigidities and oversimplifications in the model, it has demonstrated through the techniques of sensitivity analysis, its obvious potential for comprehensive system analysis and data analysis. The WRE model constitutes a major break through in numerical modeling technology.

The Chen Ecologic Model. Using the previously described WRE model concepts of the segmented-stream system and the horizontally-layered reservoir system, Chen (1970) has expanded and adapted the WRE mathematical model so as to encompass the basic ecologic processes, including photosynthesis, respiration, planktonic activity, sedimentation, nutrient recycling and others. He has demonstrated that the mathematical functions representing essential physical, chemical and biological processes of an ecosystem can be solved by computerized algorithms or semi-algorithms. The Chen ecologic numerical model includes a hydrodynamic program which solves equations or motion and continuity simultaneously for discretized systems in order to define transport properties of these systems. In addition, the model includes a reservoir temperature program to simulate density-dependent temperature and flow regimes in an impoundment and to predict thermal stratification and seasonal overturn. The chemical and biological programs of the model involve the simultaneous integration by a Runge-Kutta method, the differential equations which "express the rate of change of each chemical or biological constituent as

a function of the other variables and coefficients describing the ecologic process." Chen concludes that:

> "Preliminary tests of the ecological model indicate the reasonableness of the technique. It is concluded that model development and application will aid greatly in the development of a more fundamental understanding of eutrophication processes and their control."

The functional test of the Chen model consisted of computed concentrations at hourly intervals on a hypothetical, uni-directional stream, using input data, coefficients and constants assumed or deduced from a broad review of relevant literature. Bella (1970), in his mathematical model of lake dissolved oxygen incorporated the basic elements of the Chen ecologic model focusing, however, on hypolimnetic dissolved oxygen estimates in stratified lakes. Based on his evaluation of data pertaining to Lake Sammamish, Washington, Bella concluded that:

> "An investigator must determine the acceptability of the model for each application of the model. In other words, one does not verify a model but rather one justifies the use of a particular model for each situation in which it is used. The acceptability of the model in one situation does not guarantee its acceptability in other situations."

Bella emphasizes some practical difficulties of applying assumption of one-dimensional variations with space and the importance of considering the time scale of variations over a horizontal area.

> "Modification of the basic lake DO model. . . might often be needed. As an example long lakes and impoundments in which DO variations with

> length are substantial might be satisfactorily modeled by dividing the length into adjacent segments with each segment containing vertical variations. Also, waters immediately adjacent to lake bottoms might be included as separate regions within the model."

These conclusions by Bella (1970), added to those of Okubo (1968) which were discussed earlier, lend further weight to the orientation of the objectives of this study to numerical modeling in a horizontal, two-dimensional, well-mixed, surface layer.

CHAPTER III

MIXING AND DISPERSION IN LAKES AND RESERVOIRS

Mechanisms of Motion and Sources of Mixing in Lakes and Reservoirs

General. Much data on diffusion and dispersion in water systems have been found to be highly empirical, and data obtained from dye tests have been largely qualitative in nature. The large number of variables involved in natural and artifical water impoundments (e.g., currents, wind, wind-induced waves, thermal effects, bottom topography, shore configurations and many others) seems to have precluded up to the present time the successful conduct of systematic, comprehensive field tests which would determine the relative importance to the mixing process of each variable, singly or in combination.

A review of the literature, some of which was presented earlier in this study, shows that a prevalent practice has been for investigators to conduct a combination of qualitative dye or tracer tests and a series of model experiments. Then, the test results are analyzed with the objective of finding a general mathematical expression which will describe some feature of the mixing process and which can be used to predict the behavior of a contaminant discharged into a given body of water. But generally, these measurements are not conclusively and clearly correlated with the true governing factors and basic kinematic

mechanisms of dispersion. Empirical data on mixing and dispersion in water has proved of limited value for prediction of the assimilative or dispersive capacities in lakes and reservoirs. Sediment and solid pollutant transport, including artifically-induced, gas-bubble pollution, is strongly affected by turbulent dispersion; but, the knowledge of the dispersion characteristics of a water molecule does not serve to describe fully the dispersion properties of such types of finite inertia particles. It appears that turbulent dispersion in water bodies is the controlling transport mechanism for sediment and other contaminants. However, in small streams, particulate pollution may be transported mainly by convective flow. In estuaries, wide rivers, and the ocean, dispersion of pollution is controlled by mean flow and turbulence.

The special cogency and relevancy of this matter was brought out by K. F. Bowden in a discussion of Masch's (1964) work in mixing and dispersion of wastes by wind and wave action. Referring to the matter of the general applicability of the $L^{4/3}$ law to the relationship of the diffusion coefficient and the scale of a dispersing dye patch[5], Bowden suggested that in diffusion problems, it may be necessary to consider different kinds of turbulence which are "not all amenable to the same statistical laws". There is, for example, a fine-structural turbulence added to the long wave-

[5]See relevant discussion pertaining to Okubo's oceanic diffusion studies and to Levich's analysis of turbulent diffusion, presented in Chapter II.

length portion of the spectrum, for which the Kolmogoroff law may be apropos. Then, there is a turbulence which is due to wave action, added by energy at a shorter wave-length scale, for which a different law may apply to the diffusion coefficient. Wind effects are further complicated because in addition to induced wave action, they also impart energy on a larger scale in a drift current. The resulting turbulence may be substantially different from that of a large-scale current. The turbulence characteristics of large natural bodies of water also are affected by meteorological conditions, flows and tidal conditions.

Therefore, it is evident that in order to apply available knowledge concerning the "laws of dispersion" first it is necessary to identify the "mechanisms" which generate and sustain motion and turbulence in a fluid system. Broadly speaking the "laws of dispersion" are the basis for transport models, while the "mechanisms" which generate and sustain motion and turbulence are the basis for hydrodynamic models. Moreover, transport and hydrodynamic models must be formulated as complementary elements of a physical system model. Hence, transport and hydrodynamic modeling of a physical system requires identification and mathematical formulation of the forces and motions governing the physical system.

In order to crystallize conditions for a specific study, first it is necessary to identify and to examine in some detail, all major forces which are involved in the mixing and dispersion phenomena for lakes and

reservoirs. The major sources of mixing and dispersion in lakes and reservoirs are: currents created by reservoir outflows; wind-induced currents; stability effects associated with density and temperature gradients; turbulent wind-wave motions; large-scale circulations resulting from periodic, seasonal overturnings of water within the reservoirs; and artifical flows resulting from water resource uses such as industrial plant recirculated cooling waters.

The degree of influence of currents, flows, and circulations varies among impoundments. For example, in shallow reservoirs, it is likely that there will be a lack of temperature and density gradients. The lack of these gradients enhances the tendency for rapid uniform vertical distribution of solutes. In deep impoundments, solutes would disperse vertically for prolonged periods of time resulting in a significant downward transport of solute concentrations and a reduction in horizontal dispersion. In strongly-stratified impoundments, downward vertical dispersion may be inhibited severely by the increasingly dense lower strata. Dense aquatic plant growth also may enhance the formation of stagnated strata.

A closer examination of the effects of temperature, density, stratification, wind, and hydrological phenomena follows:

Temperature, Density and Stratification of Lake and Reservoirs. According to Vercelli (1951), under conditions of stable equilibrium there are two possible types of thermal stratification:

1. Direct ("ana-thermal") stratification, with temperatures increasing from bottom to top, provided that the temperatures exceed 4° C, which is the temperature corresponding to maximum density.

2. Inverse ("cata-thermal") stratification, with temperatures increasing from top to bottom provided that the temperatures are below 4° C.

Vercelli (1951) credits Forel (1894, 1901) for devising a qualitative classification of various types of lakes according to thermal regimes. Thus, lakes having direct stratification were termed "tropical lakes"; those having inverse stratification were termed "polar lakes". There is a third type which are designated as "temperate lakes". The "temperate lakes" are "tropical" during the hot seasons and "polar" during the cold seasons. They have a uniform temperature in the spring and autumn.

It is possible that in an impoundment, features of the above three types could exist simultaneously. The predominant water mass could stratify according to one of the above types, while along shorelines stratification could be of a different type. For example, Lake Baikal (between 51.5° and 55.5° North Latitude) demonstrates "polar lake" stratification, having about 99% of its water volume continually under 4° C, while various isolated shoreline areas reach 16° C, demonstrating "temperate lake" thermal stratification. The large sub-Alpine lakes are "tropical", but in the coldest winters the shallow shoreline zones freeze.

Cold season convections in warm lakes evolve by virtue of certain predictable thermal effects: the cooled surface waters sink and in so doing make the temperature of the zone through which it sinks uniform down to that level that has the same minimum temperature as the overlying strata. Then this thermal convection ceases. This phenomenon is accelerated by thermal conductivity or by mechanical (physical) convection. The turbulent wind currents heat the lower strata at the expense of the overlying strata in the case of "tropical lakes", and conversely, in the case of "polar lakes". Quiescent conditions on the water surface tend to establish stable, well-defined stratification. The waters in the calm, shallow zones are particularly subject to extremely stable, thermal stratification. Inverse (cata-thermal) stratifications along the littoral zones of the "temperate lakes" remain in equilibrium with respect to the main water mass or "core" of the lake because between this core and the shoreline there develops a "wall" having a temperature of 4^{o} C; this wall acts as a thermal barrier. This barrier is a zone in which turbulent currents prevail and which transfer heat from the warmer central core of the lake to the colder water masses along the littoral. The barrier phenomenon renders possible the coexistence of two different thermal regimes in the same lake basin.

The lower strata in deep lakes and reservoirs are conducive to the development of well-defined "tropical" thermal stratification in the

warm or temperate climates, and of the "polar" type in the cold climates. A shallow lake is conducive to "temperate" thermal stratification, while in the same climate a deep lake could behave either as a "tropical" or "polar" type insofar as thermal stratification is concerned.

The freezing of surface layers, due to the poor conductivity of ice, attains a limited thickness; ice sheets of from 70 centimeters to 1 meter in thickness are attained only in climates in which ice lasts throughout a greater part of the year.

The special characteristics (morphological, climatological, hydrodynamical, and optical) of each lake determine the thermal regime and can produce widely diverse effects. In lakes, the upper stratum which is involved in the annual cyclical variations has a lesser thickness than the similar layer involved in oceanic masses. In turbid waters the layers can be only a few meters in thickness. In the lower strata, the temperatures are stationary; they vary only due to accidental causes which are independent of annual cyclical factors. At great depths the temperatures could reach to the limit corresponding to maximum density, that is, below 4° C. In "tropical lakes", the temperatures are generally above these extreme values.

This analysis of temperature, density and stratification indicates that shallow reservoirs are usually well-mixed, having minor or no vertical temperature and density gradients. Hence, the shallow reservoir

under these homogeneous conditions would be easier to model - both mathematically and experimentally. In stratified, deep reservoirs, current movements are confined generally to the more homogeneous stratum of water above the thermocline. However, the designation of the thermocline as the reference datum for this purpose is inaccurate from a strict viewpoint because stratification actually is a direct result of density differences between water strata regardless of whether the denser water is caused by dissolved solutes or by lower temperatures.

Seasonal Hydrothermal Phenomena. The following important phenomena of thermal stratification of impounded waters must be considered carefully, (Krenkel 1968):

1. After the winter months, the impoundment has a uniform quality and a low temperature. If the impoundment is quiescent and clear, solar radiation penetrates the surface and is absorbed at an exponential rate, creating an exponential temperature gradient. If the water surface is undergoing evaporative cooling and sheared by wind-induced currents, mixing will ensue which will enhance the downward transport of heat and momentum.

2. Rises in atmospheric temperature cause relative temperature increases both in impoundment surface and the inflows to the impoundment. With the temperature rise there is a decrease in water density. Three strata of water are developed: the upper stratum, or epilimnion; the lower stratum or hypolimnion; and the thermocline which is a transition zone between these two. According to Hutchinson (1957) the thermocline is the plane of maximum rate of decrease of temperature; that is,

$$\frac{d^2\theta}{dh^2}=0 \qquad (3\text{-}1)$$

where:

Θ = the temperature.

h = the depth.

Fair, et al (1968) indicate that the thermocline is conventionally regarded as consisting of the water layer in which the temperature decreases by at least 0.5 degrees F. for each foot of depth.

3. The thermocline exists generally during the period, April to November. The thermocline is 10 to 20 feet thick; the epilimnion is 30 to 50 feet thick; and the hypolimnion extends to the bottom of the impoundment.

4. During the summer months, the stratification becomes increasingly pronounced. In autumn, the impoundment begins to develop a heat deficit. As the water becomes colder and denser, the thermocline level drops and an unstable situation is created which ultimately causes complete mixing in the lake. Lakes with the hydrothermal behavior just described are called monomictic lakes.

5. In regions where the water temperature may go below 4^{o} C (which is the temperature of maximum water density), the onset of surface heating (say up to 4^{o} C) may cause the surface water to again become more dense than the lower layers, resulting in unstable stratification and causing another turnover of the lake waters. Lakes with the hydrothermal behavior just described are called dimictic lakes.

6. Circulation due to hydrothermal gradients may vary depending on the extent of density strata. Some impounded waters circulate completely; these are called holomictic impoundments. Some impounded water circulate only partially; these are called meromictic impoundments. The apparent stability of the extreme, lower layers of an impoundment may be caused by dissolved or suspended solids that impart virtually a "permanent increase" in density.

> Fair, et al (1968) summarized in effect the seasonal, hydrothermal phenomena in lakes as follows: In the circulation or epilimnetic zone the water is of substantially uniform temperature and density, and therefore, "is easily moved along horizontally by wind-induced currents and vertically by convective currents". The transitional or mesolimnetic zone is a relatively thin stratum in which the temperature changes at the rate of at least 0.5 degrees F. per vertical foot of depth. In the lowermost zone, - the stagnation or hypolimnetic zone, "horizontal movements are very slight" and, "vertical ones are almost absent".

The effect of dissolved substances on impoundment stability phenomena warrants detailed attention. This will be taken up next.

Stability Phenomena. We have seen that if density stratification were a function of temperature only, the temperature profile and the inflow temperature would suffice to indicate which stratum the inflow will enter. However, most natural waters will contain varying amounts and types of dissolved substances. These substances may affect fluid density to such an extent that they will govern the stratification process in the impoundment. However, Brooks and Koh (1969) suggested that:

> "In lakes and reservoirs, stable density stratification is caused primarily by the temperature variation with depth, and secondarily by a variable concentration of dissolved and suspended solids."

In addition, Harleman (1961) has indicated that since it is realistic to consider stratified fluids as virtually incompressible because of the inherently small magnitude of the velocities involved, it follows that:

> "The density differences are therefore due to temperature gradients and variations in solute concentrations or variations in suspended solid concentration and are independent of the pressure intensity and the elastic properties of the fluid."

According to Krenkel (1968), the National Bureau of Standards states that:

> "A density current is the movement, without loss of identity by turbulent mixing at the bounding surface, of a stream of fluid, under, through or over a body of fluid, with which it is miscible and the density of which varies from that current, the density differences being a function of the differences in temperature, salt content and/or silt content of the two fluids."

Krenkel (1968) shows that the condition leading to a stratified flow is represented by the relation:

$$\frac{\Delta \rho}{\rho} = 0.0005 \qquad (3\text{-}2)$$

where:

ρ = the fluid density of the upper layer; and

$\Delta \rho$ = the density differential between the fluid layers.

Expressing this criteria in terms of temperature differential, it can be shown that the density difference between water at 31° C and 32.5° C may be sufficient to cause stratification in which case the relation is:

$$\frac{\Delta \rho}{\rho} = 0.000503 \qquad (3\text{-}3)$$

If the density of an inflow into an impoundment is greatly affected due to its dissolved substance load, it would migrate to its corresponding density stratum, a stratum which might have a lower temperature than the inflow temperature. This situation is depicted in Figure (3-1). Thus, the inflow water with temperature, θ, and density, ρ, would be at the "proper" density stratum but with a fictitious temperature, say θ_f. This temperature is defined by the following relationship:

$$\rho_i(\theta) = \rho_p(\theta_f) \tag{3-4}$$

where:

$\rho_i(\theta)$ = density of inflow water at temperature, θ.

$\rho_p(\theta_f)$ = density of pure water at temperature, θ_f.

It is to be noted that $\rho_p(\theta_f)$ cannot be $>$ 0.999973 g./cc., which is the maximum density at 4° C.

Referring again to Figure (3-1), note that for the situation represented, the various temperatures and densities shown have the following relationships:

$$\left.\begin{aligned} \theta_2 < \theta_1 < \theta \\ \rho_1 < \rho < \rho_2 \end{aligned}\right\} \tag{3-5}$$

The inflow water with density, ρ, and temperature, θ, has moved into a density layer which does not correspond to its temperature layer. Thus, the upper boundary of the inflow stratum borders on the layer with θ_1 and

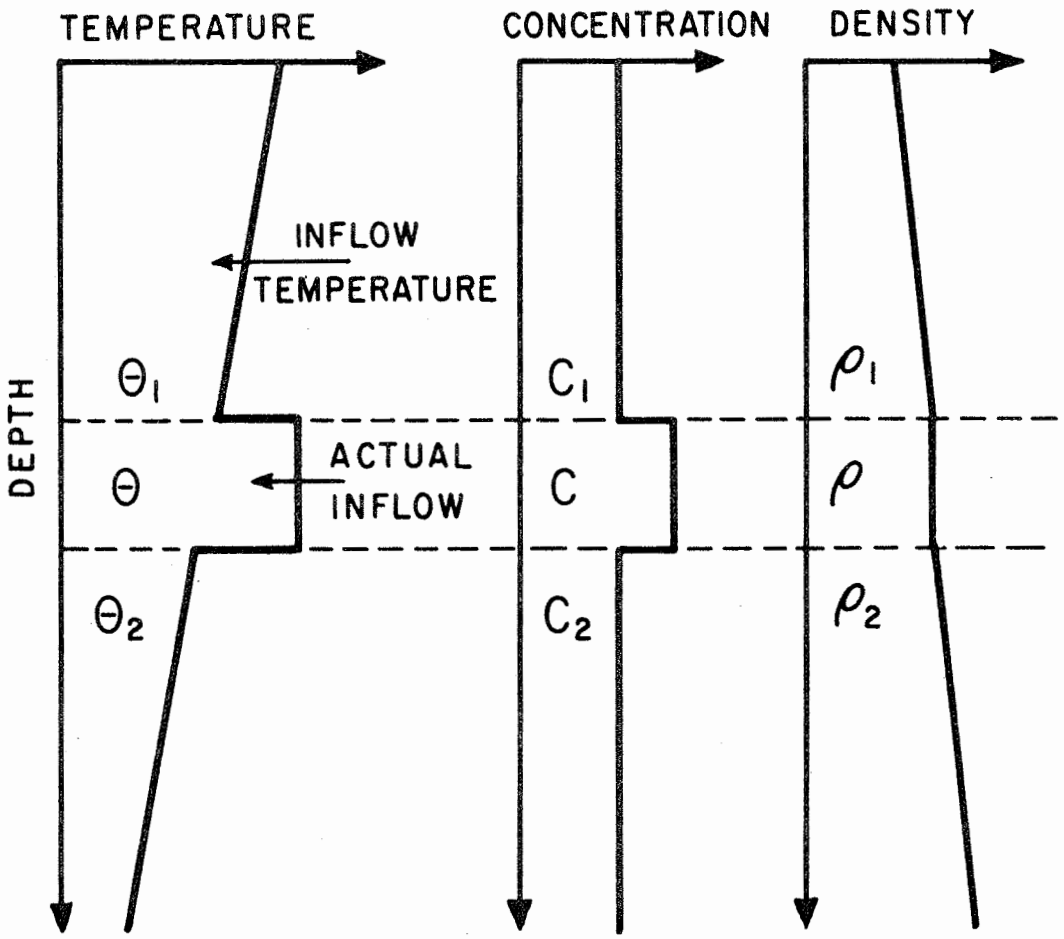

Figure 3-1. Disturbance of Thermal Stratification by Polluted Inflow. (After Wunderlich and Elder, 1968).

ρ_1; the lower boundary border on the layer with θ_2 and ρ_2. Hence, cooling of the inflow will take place along both its upper and lower boundaries. At the upper boundary, heating of the overlying water will make it less dense, while cooling of the inflow will make it denser. Thus, buoyancy and gravity forces tend to move water particles at the upper boundary, therefore little interchange will occur between the two layers. But cooling of the top of the inflow layer and heating of the bottom of the overlying layer, will induce vertical mixing in the inflow and overlying layers.

Cooling of the lower interface of the inflow layer will increase its density; heating of underlying layer boundary will decrease its density. Mixing will normally occur across this lower interface with a consequent rapid exchange of temperature and solute concentration. The temperature and concentration exchange has a great propensity for downward diffusion, increasing the diffusive component of heat transfer. On the other hand, density undercurrents along the bottom of an impoundment will become "overstabilized" by the presence of dissolved substances, and little or no mixing with overlying strata takes place.

Harleman (1961) said that one of the most interesting aspects of the motion in a fluid having a vertical density gradient is the condition necessary for the maintenance of vertical turbulence. The change of potential energy due to vertical mixing must be balanced by a change in the

kinetic energy of the motion producing the mixing. If it is assumed that the kinetic energy of the turbulence remains constant, then the energy must be supplied from the mean horizontal motion, U . Introducing the coefficient of eddy diffusion for the vertical direction, E_Z ft^2/sec, then "the time rate of increase of potential energy per unit volume" is:

$$g E_z \cdot \frac{\partial \rho}{\partial Z} \tag{3-6}$$

where:

$$E_z = \frac{-\overline{w'\rho'}}{\partial \rho / \partial Z} \cdot \tag{3-7}$$

On the other hand, "the time rate at which kinetic energy is lost from the mean motion per unit volume", in terms of the eddy coefficient, ϵ_z is:

$$\rho \epsilon_z \left(\frac{\partial U}{\partial z}\right)^2 \tag{3-8}$$

where:

$$\epsilon_z = \frac{-\overline{\rho U' w'}}{\rho \partial U / \partial z} \cdot \tag{3-9}$$

The conditions under which turbulent mixing may occur will now be developed from another approach. According to Prandtl, the order of magnitude of a turbulent vertical disturbance velocity w' can be expressed approximately as:

$$w' \doteq \ell \cdot \frac{\partial U}{\partial z} \tag{3-10}$$

where:

ℓ = mixing length.

$\partial u / \partial z$ = the velocity gradient in the vertical direction.

The kinetic energy available for the vertical movement of a liquid element of volume, V, is:

$$E = \rho V \frac{w'^2}{2} = \frac{1}{2} \rho V \ell^2 \left(\frac{\partial u}{\partial z}\right)^2 , \qquad (3\text{-}11)$$

i.e., Energy = 1/2 (Mass x Velocity^2)

Equation (3-11), derived by Wunderlich and Elder (1968) is analagous to Equation (3-8), the expression derived by Harleman (1961) and, was referred to earlier as "the time rate at which kinetic energy is lost from the mean motion per unit volume".

Refer again to Figure (3-1) and suppose that a water parcel of density, ρ at depth, z is forced upward into water of density, ρ_1 at depth z_1, where $\rho > \rho_1$. Under these conditions, the upward acting force must exceed the downward directed gravitational force; the latter can be expressed as:

$$F = gV(\rho - \rho_1) = gV \frac{d\rho}{dz}(z - z_1) \quad , \qquad (3\text{-}12)$$

(i.e., Force = Mass x Acceleration).

Where all symbols, except g, represent parameters previously described; g is the gravitational acceleration.

The work necessary to move the unit parcel of water upward against the force of gravity to the new depth, $z_1 = (z - \ell)$ can be expressed as:

$$W = -gV\frac{d\rho}{dz}\int_{z}^{z-\ell}(z-z_1)\,dz = \frac{1}{2}gV\ell^2\frac{d\rho}{dz}\ , \tag{3-13}$$

(i.e., Work = Force x Distance).

Equation (3-13) derived by Wunderlich and Elder (1968) is analagous to Equation (3-6) derived by Harleman (1961) and was referred to earlier as "the time rate of increase of potential energy per unit volume".

The criterion for the maintenance of vertical turbulence is given by the ratio of the above quantities, W/E.

That is, the equilibrium between the above expression for work, W, and the available kinetic energy, E, yields a minimum value which the energy must exceed if turbulent mixing can occur. The ratio W/E is called the local Richardson number:

$$Ri = \frac{W}{E} = \frac{g\,d\rho/dz}{\rho(du/dz)^2}\ . \tag{3-14}$$

The Richardson number may be defined as the dimensionless ratio of the shear forces to the buoyant forces acting on a portion of stratified fluid.

Theoretically, the following conditions of motion may exist:

1. Ri = 1 or, W = E, (Equilibrium exists; turbulence dies out).
2. Ri $>$ 1 or, W $>$ E, (Turbulence cannot develop).
3. Ri = 0, (Neutrality exists, as would prevail in the absence of density).
4. Ri $<$ 1 or, W $<$ E, (Turbulence can develop).

and,

$$F' = \frac{\Delta U}{\sqrt{\frac{\Delta \rho}{\rho} \cdot g \, \Delta z}} \qquad (3\text{-}17)$$

we can obtain a further insight into the physical significance of the Richardson number. Harleman (1961), in his treatise on stratified flows, indicates that the Froude number remains as the primary similitude parameter for subsurface flows. In its generalized form, the densimetric Froude number may be written as

$$F' = \frac{U}{\sqrt{g' z}} \quad , \qquad (3\text{-}18A)$$

where:

$$g' = \frac{\Delta \rho}{\rho} \cdot g \quad , \qquad (3\text{-}18B)$$

which is the gravitational acceleration, reduced by the factor $\frac{\Delta \rho}{\rho}$.

However, it is of interest to review also how Wunderlich and Elder (1968) derived the relationship between the local Richardson number and the densimetric Froude number:

Let:

$$U = \Delta U$$
$$g' = (\Delta \rho / \rho) \cdot g$$
$$z = \Delta z$$

Substituting the above values in the equation for the densimetric Froude number,

$$F' = \frac{U}{\sqrt{g' z}} \quad , \qquad (3\text{-}19A)$$

we obtain:

$$F' = \frac{\Delta U}{\sqrt{(\Delta\rho/\rho)\cdot g\,\Delta z}} \cdot \tag{3-19B}$$

Squaring Equation (3-19 B), we obtain:

$$(F')^2 = \frac{(\Delta U)^2}{(\Delta\rho/\rho)\cdot g\,\Delta z} \cdot \tag{3-19C}$$

Taking the reciprocal of Equation (3-19 C), we obtain:

$$\frac{(\Delta\rho/\rho)\cdot g\cdot\Delta z)}{(\Delta U)^2} = \frac{1}{(F')^2} \cdot \tag{3-20}$$

Thus, the Richardson number is equal to the reciprocal of the square of the densimetric Froude number:

$$Ri = \frac{1}{(F')^2} \tag{3-21}$$

There is a basis for belief that the local Richardson number is not an adequate criterion for defining the relative propensities of turbulence in a hydrodynamic regime. The following so-called "flux form" of the Richardson number (R_f) may be more meaningful:

$$R_f = \frac{K_H}{K_M}\left\{\frac{g\cdot\frac{d\rho}{dz}}{\left(\frac{dU}{dz}\right)^2}\right\} = \frac{K_H}{K_M}(Ri) \tag{3-22}$$

where:

K_H = eddy diffusivity for heat.

K_M = eddy diffusivity for momentum.

However, meager analytical or experimental information has been found about the ratio K_H/K_M. Tentative indications are that for the neutral

condition, the ratio varies from 1.0 ~ 2.0; for large values of Ri, the ratio K_H/K_M assumes values $\ll 1.0$. For example, for Ri = 4 to 10, the value of $K_H/K_M \approx 0.4$ and $R_f \equiv< 1$. Yet, turbulent exchange may prevail even while the values of Ri are large. Wunderlich and Elder (1969) concluded that greater knowledge of the significance of R_f values must be determined to enhance chances for major advance in reservoir water quality modeling.

The foregoing analysis of stratification by Wunderlich and Elder (1969) represents a synthesis of two concepts: the multi-layered systems and continuous-density gradients. Harleman (1961) cites Yih (1957) as the one who established the link between flows with a continuous-density variation and those with a large number of discrete layers. Harleman states:

> "It has been shown that the continuous-density variation can be analyzed as the limiting case of the multi-layered system."

Diffusion Phenomena. The hydrodynamical analysis of stratified flow can be subdivided into 3 phases:

1. Patterns of flow in well-defined layers.
2. Stability of layered flow.
3. Advanced stages of mixing beyond the point of instability.

The previous section discussed phases 1 and 2 above. Now the third phase will be discussed.[6] This phase involves the basic question:

---

[6]See discussion on analysis by Levich, in Chapter II.

"What is turbulent diffusion in a stratified flow?"

Rouse and Dodu (1955) investigated experimentally the mechanism of vertical diffusion across a horizontal interface between liquids of slightly different density. Turbulence produced mechanically in the upper layer did not penetrate extensively into the lower layer, but produced interboundary cusps from which streamers were projected into and, diffused through, the upper layer. This is contrary to the concept of the formation of a buffer layer of intermediate density, as in the case of breaking interfacial waves, between parallel streams. It is reasonable to conclude that the formation of an intermediate density layer is a characteristic of shear-generated turbulence.

The equation expressing turbulent mixing of incompressible fluids containing at least one property in varying amounts is called the convection-diffusion equation. It is a mass conservation expression and is not to be confused with a dynamical equation of motion. The general convection-diffusion equation is:

$$\frac{\partial c}{\partial t} + u\frac{\partial c}{\partial x} + v\frac{\partial c}{\partial y} + w\frac{\partial c}{\partial z} = \frac{\partial}{\partial x}\left(E_x\frac{\partial c}{\partial x}\right) + \frac{\partial}{\partial y}\left(E_y\frac{\partial c}{\partial y}\right) + \frac{\partial}{\partial z}\left(E_z\frac{\partial c}{\partial z}\right), \tag{3-23}$$

where:

c = the concentration of a conservative property.

u, v, w = mean velocity components in the x, y and z directions.

E_x, E_y, E_z = coefficients of eddy diffusivity in the x, y and z directions.

And, if E is constant due to homogeneous turbulence, the equation can be written as

$$\frac{\partial c}{\partial t} + U \cdot \text{grad}\, c = E \nabla^2 c \,. \tag{3-24}$$

Note that the transport of concentration due to the mean current, (u, v, w), is independent of transport due to turbulence, (E_x, E_y, E_z).

Numerous solutions of simplified modifications of the above general convection-diffusion equation have been suggested. As an introduction to the subject, Harleman (1961) illustrates the case of the unsteady, one-dimensional diffusion. If the mean motion of the fluid is zero (u = v = w = 0) and, the concentration gradients in the Y and Z directions are small compared to that in the X direction, the general convection-diffusion equation reduces to:

$$\frac{\partial c}{\partial t} = \frac{\partial}{\partial x}\left(E_x \frac{\partial c}{\partial x}\right) . \tag{3-25}$$

And, if homogeneous turbulence is present, E_x = a constant; then the above equation becomes:

$$\frac{\partial c}{\partial t} = E_x \left(\frac{\partial^2 c}{\partial x^2}\right) . \tag{3-26}$$

The solution of the foregoing equation for a semi-infinite medium extending in the X direction with a constant concentration C_0

maintained at the boundary, $x = 0$ is

$$\frac{c}{c_0} = 1 - \text{erf}\left(\frac{x}{2\sqrt{E_x t}}\right) \tag{3-27}$$

Various theories of turbulent diffusion show that

$$E_x = (\text{constant})\ (G^{1/3})\ (\ell^{4/3}) \tag{3-28}$$

where:

G = mean rate of energy dissipation per unit mass of fluid.

ℓ = the measure of the scale of turbulence, or "mean eddy size".

The above relation was verified by Orlob (1959) and by Harleman and Ippen (1960).

In a stratified fluid, when there is a considerable density difference between a diffusant and the surrounding fluid (as in the case of saltwater intrusion in freshwater), mixing ensues as a result of turbulence and gravitational convective currents due to density difference. Hence, the problem is no longer a one-dimensional one since, u, w, and $\frac{\partial c}{\partial z} \neq 0$ everywhere. A rigorous solution is hopelessly complex. The mass transfer due to gravitational convection (due to density difference) and transfer due to turbulence may be combined and considered as a one-dimensional problem if the eddy diffusivity E_x is replaced by:

$$E'_x = E_x + \Delta E_x \tag{3-29}$$

where ΔE_x is a function of the dissipation rate and the density difference between the diffusant and receiving fluid. This consolidation is justified

on the basis that gravitational convection currents result in a net circulation or eddy formation which is physically larger and, from a mixing standpoint, is similar to turbulent eddies. As a comparative illustration for low-turbulence, the value of ΔE_x is approximately an order of magnitude larger than the value of E_x corresponding to a density difference of about 1%. For increasing turbulence levels, the vertical gradients become smaller under the action of intense turbulent mixing and $\Delta E_x \longrightarrow 0$ for the truly one-dimensional case.

Types of Impoundments

Lakes and impoundments can be classified according to their use, their geometry and their biological and chemical development. However, a review of the various phenomena which take place in impoundments, shows the difficulties of permanently type-classifying a given body of water.

The lake or reservoir is a variable system whose surface area expands and contracts as the water rises and falls. Closer observation reveals that these oscillations have seasonal trends, and operate between variable extremes.

The degree to which an impoundment may be controlled depends largely on physical conditions such as the surrounding topography, the presence of outlets, the size of the contributing watershed, and the inflow of water. The water flowing into the impoundment will determine largely the amounts of water that must be regulated to gain control.

Not all problems stem from a need for control or stabilization, some may arise from an engineering need to increase or decrease the surface area, or raise or lower the average level. Whatever the purpose, the solution will involve a change in some physical feature connected with the impoundment, and some manipulation that will tend to counteract the normal process of nature: precipitation, evaporation, transpiration, productivity, change of temperature, surface runoff, and underground inflow and outflow. Physical features frequently may be changed, and the changes made quite permanent, but usually it is practical to obtain only a limited control over the natural processes. With this multiplicity of processes the study of impoundments becomes a study in hydrology. Engineering considerations require knowledge of the development of a given impoundment, the factors that tend eventually to obliterate it, the annual cycle of water temperature, the theory of temperature changes within the body of the impoundment, evaporation problems involved in attempting to stabilize lake levels, and the natural processes that effect the behavior of all impoundments. Kittrell (1959) in analyzing impoundments from the viewpoint of dissolved oxygen resources and the problem of location of intakes in dams, classified reservoirs into two basic types: storage and main-stream reservoirs. The storage reservoir stores water when surface run-off is high for release when run-off is low; its surface level varies greatly from 60 to 80 feet. The typical main-stream reservoir generally

changes the configuration of the stream less than the storage reservoir; much of the impounded water is restricted to the original channel; the increase in surface area is small compared to the storage reservoir; flow velocities are less than in the original stream; the retention period of water is from a few days to a few weeks; uses often include navigation, power and others which involve a reasonably constant surface level, within 2 to 3 feet. Kittrell (1959) indicates that each of the two types of reservoirs exhibits its individual type of stratification. Hutchinson (1957) has amassed a large amount of vital data on natural lakes. Churchill (1957) also has analyzed a vast amount of data on artifical storage reservoirs of the Tennessee Valley Authority. Thermal stratification in both natural lakes and artifical storage reservoirs is similar in many ways.

From the viewpoint of aquatic biology, the convenient concept of a lake or impoundment as a "closed community" affords a basis for classification of lakes according to their "productivity". A combination of physical, chemical and biotic elements affects the "nutrient levels" for the "productivity". Fair, et al (1968) suggest that based on productivity levels, lakes and impoundments can be classified as: (1) oligotropic, (2) eutrophic, and (3) dystrophic - - signifying little, well and poorly-nourished conditions, respectively. The cited authors further indicate that in time, an evolution process takes place as a result of natural and cultural pollution which changes oligotrophic lakes into eutrophic lakes and the latter ultimately into dystrophic bodies of water.

Difficulties in Formulating Mathematical Hydrodynamical Models for Reservoirs

General. Throughout the entire course of practical, experimental work runs the common experience that it is rare to encounter a steady current in natural impoundments. Invariably, anomalies intrude into the system. The direction and magnitude of the current changes gradually; variations occur in the observed lateral diffusivities and in the observed behavior of maximum concentration along diffusing dye plumes. For example, Csanady (1966) concluded in his lake experiments that the major cause of the day-to-day changes in observed horizontal diffusivity values were due not to changes in the horizontal eddy structure, but rather changes in the structure of the mean current, such as the introduction of a strongly skewed velocity profile or the onset of a rapid change in the direction of the current.

A careful consideration must be made of the main kinematic factors involved in a reservoir hydrodynamics. The subject can be subdivided into two parts: (1) spatial and (2) temporal. These will be discussed in detail. Table (3-1) lists symbols and notations used in Csanady's mathematical formulations, and are tabulated to facilitate reference in the discussion which follows in this chapter.

Spatial Considerations. Spatial non-uniformity seems to be the "normal" state of natural impoundments. For example, Csanady (1966) noted that the top layers of the Great Lakes were not characterized by steady

Table 3-1. Symbols and Notations Used in Csanady's Formulations

$U(z)$	= mean velocity component along X-axis, as a function of depth, z.
$V(z)$	= mean velocity component along Y-axis, as a function of depth, z.
Z	= depth.
Z_1, Z_2	= depth at levels 1 and 2, respectively.
S_y	= standard deviation in the direction of the y-axis.
a	= angle between the velocity vectors at any two levels Z_1 and Z_2.
x	= distance from the point of release in a suitable intermediate direction between the two current vectors.
V, U	= current velocity components.
U_0, a, b, c	are constants.
t	= time (also t_1, t_0).
x, y	= are coordinates.
r	= radius.
K_e	= effective diffusivity for turbulent diffusion.
h	= the depth of a diffusion layer.
v	= root mean square turbulent velocity in the lateral direction.
V_d	= diffusion velocity.

parallel currents but rather by a velocity structure of three-dimensional boundary layers, which may be described by two, more or less, independent velocity profiles as shown in the upper portion of Figure (3-2). The lower portion of the figure shows the hodograph[7] of hypothetical velocity vectors at various depths.

Realistically, both the direction and magnitude of the current velocity change with depth. Mathematically, the situation should be described by U(z) and V(z), the mean velocity components as functions of depth along two horizontal axes. Refer to the hodograph in Figure (3-2) and consider the kinematics of the mean motion of the fluid at different levels. For example, a fluid particle at the surface and a particle at some depth may have divergent paths. Thus, a tracer dye plume forming in the wake of a fixed, continuous dye source would have a skewed cross-section, and because of vertical mixing the width of the dye plume at any depth would be larger than if the current flowed at all levels. This widening effect on the plume is what Csanady (1966) referred to as an "acceleration of diffusion in the lateral direction". Csanady's approximation of this "acceleration"

---

[7]Hodograph - If the velocity vectors of a moving particle are laid off from a fixed point, the extremities of these vectors trace out a curve called the hodograph of the moving particle. If $\vec{v} = \vec{f(t)}$ is the vector equation of the path of the particle, then $\vec{dv/dt} = \vec{f(t)}$ is the equation of the hodograph.

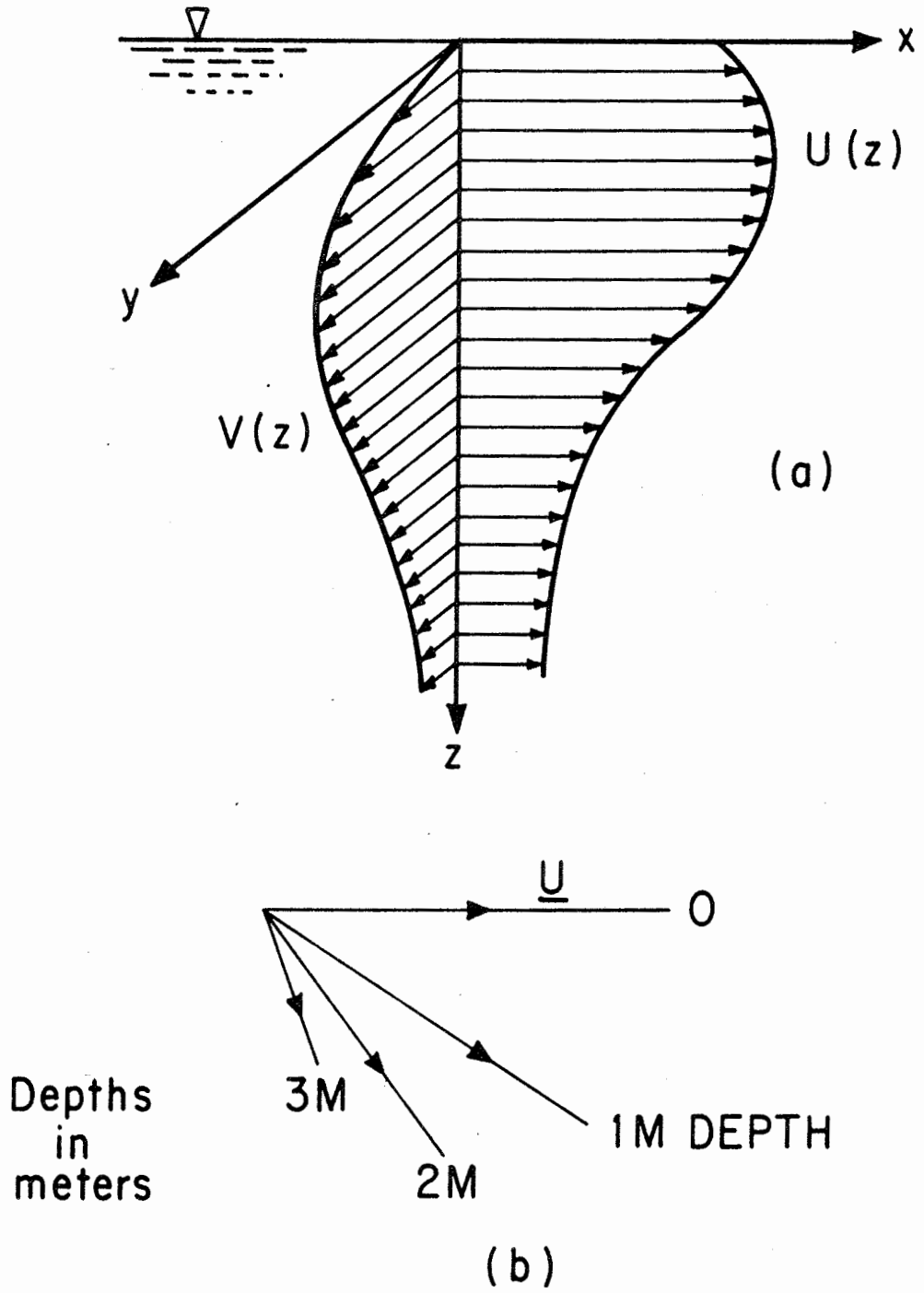

Figure 3-2. Velocity Distribution in Typical Lake Currents:

a. Velocity Profiles.

b. Hodograph.

(After Csanady, 1966).

effect on the lateral diffusion in a 3-dimensional field was based on the relation that the width of the dye plume is proportional to the tangent of the half-angle between velocity vectors at the two levels Z_1 and Z_2 containing the bulk of the marked fluid. That is:

$$S_y = \frac{x}{2} \tan\left(\frac{a}{2}\right) \tag{3-30}$$

where:

$$a = \left[\tan^{-1} \frac{V}{U}\right]_{Z_1} - \left[\tan^{-1} \frac{V}{U}\right]_{Z_2} \tag{3-31}$$

S_y = the standard deviation in the direction of the Y-axis, used as the approximate measure of the 1/4 plume width.

x = the distance from the point of release in a suitable intermediate direction between the two current vectors.

See also Table 3-1, for notations.

The foregoing mathematical expressions are based on two major assumptions: (1) efficient mixing occurs between levels Z_1 and Z_2 so as to produce a wide plume rather than one with a sheared cross-section; (2) the depth range Z_1 to Z_2 is small compared with the vertical scale of eddies.

Temporal Considerations. Let us now consider the temporal factor in reservoir hydrodynamics. We have seen already, that in reality, we are confronted with non-uniformity in the spatial relationships of

reservoir hydrodynamics, and that idealizations must be adopted in order to proceed with the study. For the temporal factor, investigators generally have adopted the idealization of a steadily-changing current having a constant angular velocity and a constant velocity magnitude at a given level. This idealization assumes that the velocity direction only is changing at a fixed level and at a constant rate, although differences in velocity magnitude and direction between different levels may exist. Mathematically such a current was described by Csanady (1966) as follows:

$$U = (U_0 - bz) \cos [a (t - cz)] \tag{3-32}$$

$$V = (U_0 - bz) \sin [a (t - cz)] \cdot \tag{3-33}$$

See Table 3-1, for notations.

Note carefully that in the above equations, the velocity components, U and V, do not depend on the horizontal space coordinates x and y since current changes happen simultaneously in the diffusion area of interest. Equations (3-32) and (3-33) are based on the following simplifying assumptions:

1. The vertical velocity gradient is linear.
2. The angular velocity is constant.
3. There is a linear dependence of phase lag on depth.

Integrating the Equations (3-32) and (3-33) with respect to time, yields the set of equations for particle trajectories as follows:

$$\left.\begin{aligned} x &= \int_{t_1}^{t} u\,dt = \frac{U_0}{a}\left[\sin a(t-t_0) - \sin a(t_1-t_0)\right] \\ y &= \int_{t_1}^{t} v\,dt = \frac{V_0}{a}\left[\cos a(t_1-t_0) - \cos a(t-t_0)\right] \end{aligned}\right\} \qquad (3\text{-}34)$$

The release time t_1 may be regarded as a parameter in obtaining the instantaneous shape of a dye plume. Allowing t_1 to assume all values from zero to t we find, at a fixed time t, the position of all particles released before t_0. Eliminating t_1 from Equation (3-34), we obtain:

$$[(ax/U_0) - \sin a\ (t - t_0)]^2 + [(ay/U_0) + \cos a\ (t - t_0)]^2 = 1 \qquad (3\text{-}35)$$

Hence, the instantaneous shape of a tracer plume can be considered as an arc of a circle centered at coordinates:

$$x = \frac{U_0}{a} \sin a\ (t - t_0) \quad \text{and,}$$

$$y = \frac{-U_0}{a} \cos a\ (t - t_0) \qquad (3\text{-}36)$$

and having a radius of $r = U_0/a$.

Particle trajectories are also circles, as is evident from Equation (3-34). For the trajectories, t is the parameter and t_1 is fixed (a certain particle may be identified by its release time.) After eliminating the parameter we have:

$$\left[(ax/U_0) + \sin a(t_1 - t_0)\right]^2 + \left[(ay/U_0 - \cos a(t_1 - t_0)\right]^2 = 1 \qquad (3\text{-}37)$$

Again, this is an arc of a circle of radius $r = U_0/a$, centered at coordinates

$$x = \frac{-U_0}{a}\sin a(t_1 - t_0) \quad ; \quad y = \frac{U_0}{a}\cos a(t_1 - t_0). \tag{3-38}$$

Figure (3-3) denotes that particle trajectories and plume shapes are circular arcs of equal radius but opposite curvature. And, from the hodograph of Figure (3-2) it can be surmised that if the radius of curvature of the plume shape decreases with depth there will result a lateral stretching of the cross-section of the plume.

Figure (3-3) also illustrates the diffusive effects of particle and plume motions which result if parallel currents existed at all depths. The dye plume starts off parallel from the source at the surface and at a given depth Z. Then, after a point in the flow is reached representing a 90^o change in the direction of the curving plume current, it will be noted that the curving particle trajectories are exactly perpendicular to their corresponding plume element in which they are entrained. At this important temporal junction, a shear effect is created as a result of the intersecting directions of the plume current and the particle trajectory. The increase in the effective diffusivity will be in the direction perpendicular to the direction of the plume current.

In this case, which assumes a steadily-changing parallel current, the increase in effective lateral diffusivity at various points along a dye plume can be approximated by resolving particle velocities into components which are parallel and perpendicular to the plume element.

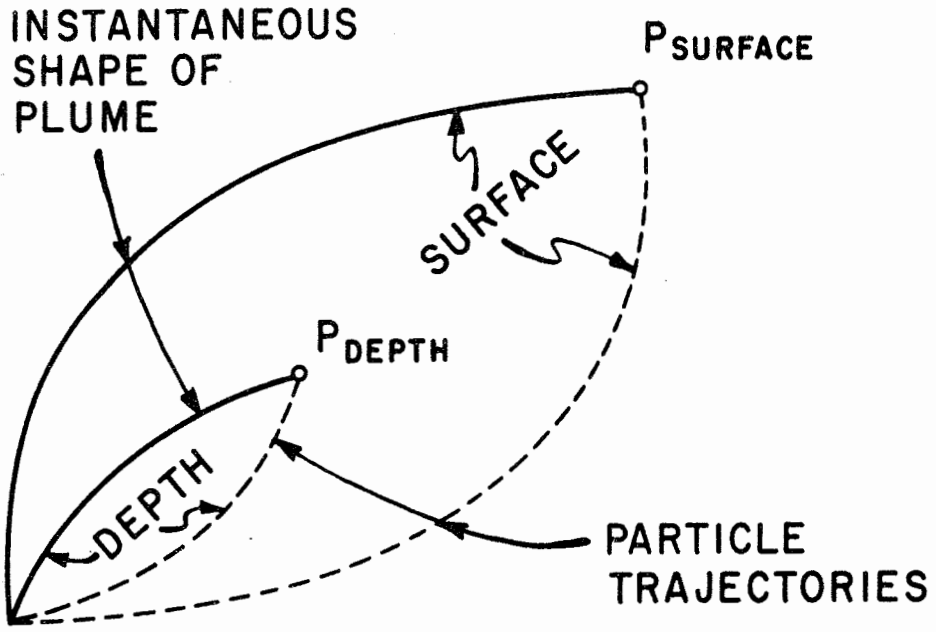

P_{DEPTH} and $P_{SURFACE}$ are the Simultaneous Positions of Two Particles Released at Time T = 0.

Figure 3-3. Instananeous Plume Shape and Particle Trajectories in Steadily Changing Plume at Surface and at a Constant Depth. (After Csanady, 1966).

The plume element, once released, maintains its direction. But, the particle velocity changes its direction according to the set of Equations (3-32) and (3-33). The perpendicular velocity component can be derived from Equations (3-32) and (3-33) by setting c = 0 for parallel current conditions:

$$V = (U_0 - bz) \sin a\ t \tag{3-39}$$

Equation (3-39) may be used in conjunction with the following equation for the ratio of two diffusivities, (Csanady 1966), to estimate the effective diffusivity K_e:

$$\frac{K_e}{K_y} = \left[\frac{h^2}{16v^2}\right] \cdot \left[\frac{dV}{dx}\right]^2 = \frac{V_d^2}{16v^2} \tag{3-40}$$

The Three-Dimensional Character of Dispersion. The preceding section included a discussion of the general spatial non-uniformity of flow prevalent in impoundments. This feature was discussed earlier for the purpose of conveying the overall complexity encountered by other investigators in attempting to model a comprehensive hydrodynamic regimen of a reservoir. The previous section included a general mathematical expression for calculating values of dye plume widths. At this point, it is essential to examine more closely the three-dimensional aspects of dispersion. Csanady (1966) analyzed the basic differences in dispersion phenomena when the field of dispersion is vertically bounded and when the field is unbounded.

First, consider the case in which the field of dispersion is vertically-bounded, such as when a well-defined thermocline, acting as a "diffusion floor", exists in the impoundment. The diffusing substance is constrained within a relatively thin surface stratum. Refer to the hodograph in Figure (3-2), and assume, for example, that the thermocline is at a shallow depth of two meters. When a diffusing substance has reached the thermocline, the angle, a, between velocity vectors [see Equation (3-31)] remains constant; and, as an approximation only, the plume width increases linearly with distance in accordance with Equation (3-30). However, mixing will reduce the rate of plume spreading. And, for very large distances the applicability of Equation (3-30) is doubtful.

To overcome this defect, Csanady (1966) proposed the following expression for effective eddy diffusivity for turbulent diffusion:

$$K_e = \frac{U}{2} \cdot \frac{d\,(Sy^2)}{dx} \quad , \tag{3-41}$$

where U is a mean velocity between any two desired levels, and Sy is the standard deviation in the y-direction. Equation (3-41) gives:

$$K_e = U \cdot x \cdot \tan^2 (\alpha/2)/4. \tag{3-42}$$

A diffusivity which increases linearly with x also characterizes turbulent diffusion in a homogeneous current very close to the dye source and can be represented by the following expression:

$$K_y = v \cdot x \cdot (v / U) \quad , \tag{3-43}$$

where v is the root mean square turbulent velocity in the lateral direction. The ratio of the two diffusivities, Equations (3-42) and (3-43), is:

$$\frac{K_e}{K_y} = U^2 \tan^2 (a/2) / 4v^2 \qquad (3\text{-}44)$$

This ratio is an indicator of conditions under which shear effect on diffusion may be considered significant. That is, the effective diffusivity caused by current shear is dominant or not according to whether

$$\tan (a/2) > \frac{2v}{U} \qquad (3\text{-}45)$$

The quantity $2v/U$ is two times the lateral turbulence level, a quantity called "gustiness" in atmospheric applications. If the angular divergence of layers above a diffusion floor is greater than a few degrees, significant lateral diffusion is likely to occur.

The angle $a/2$ can be expressed in terms of mean velocity gradient, as follows:

$$\tan\left(\frac{a}{2}\right) \approx \left[\frac{1}{2U}\right] \cdot \left[\frac{dV}{dx}\right] \cdot \left[h\right], \qquad (3\text{-}46)$$

provided that dV/dz is nearly constant over the diffusion layer of depth, h, where V is the component of the mean velocity perpendicular to U. Using Equation (3-44), the ratio of the two diffusivities becomes:

$$\frac{K_e}{K_y} = \left[\frac{h^2}{16v^2}\right] \cdot \left[\frac{dV}{dz}\right]^2 = \frac{V_d^2}{16v^2}, \qquad (3\text{-}47)$$

where $V_d = h(dV/dz)$ is regarded as a diffusion velocity.

Secondly, consider the case in which the field of dispersion extends from a point source on the water surface into an hypothetically infinite fluid, i.e., where the dye cloud depth is very small compared to either the thermocline depth or the lake depth. In this case, the angle, a, may increasesteadily. It is evident that a wide variety of cloud growth rates is possible depending on the actual rate of growth of the angle, a , and the actual variation of the vertical velocity profile. For example, referring to Equation (3-30): $S_y = X/2 \tan (a/2)$, it will be seen that if the vertical spread is by micro-scale movements, such as in molecular diffusion, the depth of diffusion increases as $x^{1/2}$. For small values of angle a, and a velocity profile which varies linearly with depth, the standard deviation, $S_y \approx X^{3/2}$.

Csanady (1966) summarized his analysis of the general relationships between effective horizontal diffusivity and observed dye plume width, under conditions of skewed shear flow, as follows:

$$K_e = \frac{U}{2}\frac{dS_y^2}{dx} = U \cdot x \cdot \tan^2(a/2)/4 \qquad (3\text{-}48)$$

(Effective horizontal diffusivity)

$$K_y = v \cdot x \left(\frac{v}{U}\right) \qquad (3\text{-}49)$$

(Lateral diffusivity)

$$\frac{K_e}{K_y} = U^2 \tan^2(a/2)/4v^2 \qquad (3\text{-}50)$$

(Ratio of diffusivities)

Table 3-2. Behavior of Effective Horizontal Diffusivity and Observed Plume Width in Skewed Shear Flow

Condition	Effective Horizontal Diffusivity, K_e	Lateral Standard Deviation, S_y
If the dye plume extends over the available depth	K_e is constant and of magnitude ranging from K_y to 10^2 higher.	$S_y \approx x^{1/2}$
If plume deepens gradually along x	K_e increases as x^n; n = 1 to 2, or higher.	$S_y \approx x^{(n + 1/2)}$
If plume is circular and in a swinging current	K_e increases sharply with angle.	$S_y \approx x^m$; m = 1/2 to 3

(After Csanady, 1966)

Field Measurement of Dispersion and Mass Convective Transport

The Coefficients of Dispersion.

1. Laminar Flow. Taylor (1959) in reviewing the contemporary position on the theory of turbulent diffusion states that the dispersion of soluble matter in laminar, steady flow through a pipe is due mainly to laminar convection. The flow in the middle of the pipe is faster than it is near the wall. If diffusible material is introduced into the flow, the part at the center of the pipe gets transported into the uncontaminated fluid. This produces a "radial gradient of concentration" which causes radial transport by molecular diffusion and so prevents the contaminating substance from spreading along the pipe as fast as it would without molecular diffusion. The result of the combined convection and molecular diffusion is to cause the soluble material to disperse relative to a point

which moves with the mean velocity of flow as though it were affected by a vertical coefficient of diffusion:

$$K_L = \frac{a^2 u^2}{48 D} \qquad (3\text{-}51)$$

where:

K_L = dispersion coefficient.

a = radius of the tube.

u = mean velocity.

D = coefficient of molecular diffusion.

2. Turbulent Flow. In turbulent pipe flow, the radial transport is due mainly to turbulence, not molecular diffusion. Taylor (1954) predicted that dispersion along a pipe relative to a point moving with the mean velocity of flow would be as though it were due to a virtual coefficient of longitudinal turbulent diffusivity in the pipe. The mean coefficient of diffusion, K' due to the longitudinal components of turbulent velocity is

$$K' = 0.052\, a\, V_* \ . \qquad (3\text{-}52A)$$

The corrected value of dispersion coefficient, allowing for longitudinal diffusion is

$$K_L = (10.06 + 0.05) = (10.1)\, a\, V_* \ , \qquad (3\text{-}52B)$$

where:

K_L = dispersion coefficient.

$V_* = \sqrt{\tau/\rho}$ = the shear velocity.

τ = surface shear stress.

ρ = density.

a = pipe radius.

Taylor (1959) confirmed by tests that if a concentrated mass of some contaminant is released into a pipe flow at time t = 0, it will spread so that the concentration, c is proportional to the value indicated below:

$$c \propto t^{-1/2} \exp(-x^2/4K_L t) \ , \qquad (3\text{-}53)$$

where:

t = time since release of contaminant.

x = distance from point of release.

Malkus, in his discussion following Taylor's (1959) paper on the theory of turbulent diffusion, made the following comments on some possible limitations of Taylor's formula, Equation (3-52 B):

> ". . . one might expect that kinematic viscosity ν and molecular diffusivity D to appear in the expression for turbulent diffusivity for longitudinal diffusion in pipe flow. The apparent unanimity among available experiments on the empirical coefficient 10.1 may be attributable to the fact that all liquid cases with asymptotically large molecular Prandtl number ν/D."

Elder (1959) applied Taylor's analysis and developed the following formula for the dispersion coefficient for turbulent shear flow in a two-dimensional open channel of infinite width:

$$E_T = 5.93\, h\, u^* \ , \qquad (3\text{-}54)$$

where:

h = depth of flow.

u^* = shear velocity.

Fischer (1966) has cautioned that the application of Taylor's concept may have become over-extended. From his review of the relevant literature, he noted that whatever causes the spreading out of a pollutant has been described generally by the classical diffusion equation,

using an apparent diffusion or dispersion coefficient. And, this concept has been applied to type of flows for which it was not specifically derived, such as flows in natural streams and estuaries yet, experiments by many investigators have generated dispersion coefficient values greatly exceeding those derived from the Taylor formulae. Fischer (1966) notes that the widespread engineering practice is "to assert that a coefficient exists, but to obtain that coefficient by experiment".

Lake Measurements by Csanady. Csanady (1966) reporting on his earlier experimental data on the Great Lakes, attributed to the shear effect the fact that the longitudinal diffusion of a dye patch on Lake Huron was much faster than the lateral diffusion. He assumed the longitudinal direction along the mean current and the lateral direction perpendicular to mean current. Also, in experiments on Lake Erie and Lake Huron, he found that the effective lateral diffusivity was 2 to 4 times greater in the changing current than in a steady current. In Lake Erie, for example, the lateral diffusivity in a changing current was 2000 $\overline{cm}^2$ / sec.

Generally, variations in diffusivity are due to temporal current changes. Csanady (1966) recommends that the following equation be used to obtain a theoretical estimate for the effective diffusivity, (See Table 3-1, for notations):

$$V = (U_0 - b z) \sin a t \qquad (3\text{-}55)$$

This is obtained by letter C = 0 in Equations (3-32) and (3-33). Equation (3-55) applies point by point along a bent plume; the average over a full

90^{o} change is regarded as 1/2 maximum value. Using Equation (3-55), the effective diffusivity can be computed from:

$$K_e = U_0^2 h^2 / 30 K_z \quad \text{or} \quad K_e = AU_0^2 / 30 K_z \tag{3-56}$$

However, Csanady (1966) found that the Equation (3-56) gave values considerably less than the actual diffusivity measured. The discrepancy was attributed to the fact that the characteristic velocity difference under actual shear flow conditions is 2 to 3 times greater than the value computed by the formula.

In other tests, involving continuous concentration sampling at a small depth while travelling along what was thought to be the thickest part of the dye plume, Csanady (1966) obtained results that were not compatible with those expected under steady and uniform current theory. The rationale is as follows, using the principle of continuity to express maximum concentration:

$$C_m = (\text{constant}) \cdot Q / U S_y S_z \tag{3-57}$$

where:

C_m = maximum concentration.

Q = source strength.

U = current velocity.

S_y, S_z = standard deviations in the horizontal and vertical directions.

Near a source, in a steady and uniform flow, $C_m \approx x^{-2}$ if S_y and S_z increased linearly.

Values of C_m ranging from x^{-1} to $x^{-1/2}$ are obtained rapidly once the bottom, the thermocline, or a "diffusion floor" is reached. At greater distances, C_m can attain a value of x^{-3}. Finally, Csanady (1966) indicated that analysis of the diffusivity equation:

$$K_e = U_0^2 h^2 / 30 K_z \qquad (3\text{-}58)$$

explains important observations indicating that the lower the value of K_z the more complex the flow pattern is likely to be. Also important is the fact that the product $K_e \cdot K_z$ (which product is relevant to the determination of C_m) tends to remain more nearly constant with a changing K_z than the value of $K_e \cdot K_z$ in a parallel current. Thus, overall dilution factors are much less seriously affected by stable stratification of the top layer than might at first be expected.

Sayre - Chang Analysis of Open-Channel Dispersion Measurements. Sayre and Chang (1968) in exploring the various approaches for determining dispersion in open-channel flow, found that all known approaches could be grouped under five major categories:

1. The Fick diffusion theory.
2. The theory of diffusion by continuous movements.
3. The Kolmogoroff theory of local similarity in turbulence.
4. The theory of longitudinal dispersion by differential convection due to a velocity gradient.
5. The diffusion theory pertaining to the transport of suspended sediment.

Sayre and Chang (1968) reported the results of tests conducted in a rigid-boundary laboratory flume having an artificially roughened bed, in order to provide additional information on dispersion processes in open channels. The test series included lateral dispersion experiments with suspended silt-size particles and fluorescent dye, as well as longitudinal and lateral dispersion experiments with small polyethylene particles floating on the water surface. The results of application of several dispersion theories to open-channel flow were evaluated. The following relevant conclusions were reported regarding the determination of dispersion coefficients of a dissolved dispersant in two-dimensional turbulent flow in a rough-bed, open-channel:

1. The longitudinal dispersion process can be approximated generally well by the one-dimensional Fickian diffusion equation, except in the initial mixing stages. The Fickian equation starts to be valid and applicable at a distance downstream from the source, expressed by

$$L_m = 1.8 \frac{y_n}{\kappa} \frac{\bar{U}}{U_r} \qquad (3\text{-}59)$$

where:

L_m = length of initial increment of dispersion distance within which the one-dimensional Fickian diffusion theory does not apply.

y_n = normal depth; depth of flow in a channel with uniform flow.

κ = Von Karman turbulence coefficient.

$\bar{U}$ = Average velocity of flow in cross-section.

U_r = Shear velocity in a wide open channel, defined as $\sqrt{\tau_0/\rho}$ or $\sqrt{g y_n S}$.

2. The longitudinal dispersion coefficient can be computed with sufficient accuracy using Elder's (1959) equation,

$$K_x = \left[\frac{0.404}{\kappa^3} + \frac{\kappa}{6}\right] y_n U_r \cdot \qquad (3\text{-}60)$$

3. The lateral dispersion process for a dissolved dispersant released from a continuous point source can be closely approximated by the two-dimensional Fickian diffusion equation if the dispersant is fully-mixed in the flow. The minimum distance to obtain a uniform, fully-mixed condition, is approximately

$$L_m \approx 0.45 \frac{y_n}{\kappa} \frac{\bar{U}}{U_r} \cdot \qquad (3\text{-}61)$$

4. The lateral dispersion coefficient is about 1/30 that of the longitudinal dispersion coefficient.

5. Boundary wall effects on the lateral distribution of the dissolved dispersant can be represented by the principle of reflecting barriers.

6. Generally, if a dispersion process does not conform to Fickian diffusion, the various methods which must be used to evaluate dispersion coefficients may lead to significantly different values. To facilitate comparative analysis of the coefficients, Sayre and Chang (1968) recommend that evaluating equations should be of the type

$$K = \frac{1}{2}\left(\frac{d\sigma^2}{dt}\right) \qquad (3\text{-}62)$$

where σ^2, the variance of the concentration distribution with respect to time, is evaluated by the method of moments.

Wilson - Masch Analysis Versus Instantaneous Dye Release Methods in Field Measurements of Dispersion Coefficients. Wilson and Masch (1967), evaluated two methods of dye release in using tracer dye methods for determining dispersion coefficients and related aspects.

1. The first method is the release of the dye as a slug (i.e., an instantaneous point source). The dye cloud is then followed and at uniform time intervals, concentration measurements are made in the three coordinate directions. The dispersion coefficients are computed for the concentration profile along each of the coordinate axes by use of Equation (3-62). This confirms the conclusions reached by Sayre and Chang (1968). The dispersion coefficient can also be determined by plotting graphically σ versus $\sqrt{t}$ and then measuring the slope of the line of best fit. The slope of the line is $\sqrt{2D}$.

2. The second method is the release of dye in a continuous flow from a fixed point. It was found that the longitudinal dispersion coefficient could not be easily calculated using a continuous dye release approach. And, the lateral and vertical dispersion coefficients could be calculated only by the expedient of "instantaneous" concentration profiles taken in a plume at a known distance x from the source, using the equation

$$D = \frac{1}{2} \bar{u} \frac{d(\sigma^2)}{dt} . \qquad (3\text{-}63)$$

Considerable uncertainty surrounds the accuracy of measuring $\bar{u}$, the mean velocity of the dye plume. The Wilson and Masch (1967) tests could not adopt as valid the assumptions used in the Csanady (1963, 1966) plume measurement tests for evaluation of dispersion. Hence, in the Wilson and Masch (1967) tests no data from continuous flow releases were used to estimate the magnitude of dispersion coefficients. However, insofar as

measuring the effect of scale on diffusivity, the method of continuous release was found preferable to the instantaneous release method because for scale effect one is concerned primarily with the correlation between the relative change in diffusivity versus plume size. So, if the flow velocity is assumed constant during tests, the effects of flow velocity are precluded by examining the relative change in diffusivity.

However, for measuring relative changes in the dispersion coefficient, the continuous dye release plume is theoretically preferable to the instantaneous dye release cloud because the continuous release technique enables making more measurements at any given point and the resulting concentration profiles undergo an "averaging effect", thus reducing statistical error. In contrast, measurements in an instantaneous release cloud necessarily are made at various times and, cannot undergo comparable "averaging effects". Another advantage of the continuous release technique is the flexibility of reducing the measurement interval so that at any given point

$$\frac{\Delta\sigma^2}{\Delta x} \longrightarrow \frac{d(\sigma^2)}{dt} .$$

(3-64)

In contrast, the measurements incident to the instantaneous dye releases may involve considerable time lapses in making successive measurements.

Collings' Analysis of Site Selection Criteria for Dye-Injection and Measuring Sites for Time-of-Travel Studies. Collings' (1968) analysis of time-of-travel methods using fluorescent dyes in streams, provides practical criteria regarding the selection of sites for dye injection and measurement, as well as other practical guide-lines which should be considered in any field investigation using dye-tracers. Following are essential guide-lines of special relevance to this study:

1. Time-of-travel estimates in streams may be made either by a single injection for an entire study reach or, by separate injections for subdivisions of the reach. The injection method adopted in a given situation should be made after a field reconnaissance of channel characteristics, potential loss of dye, municipal restrictions, tributary inflow, and channel discharge. Ideally, both methods of injection should be used for a given reach. In practice, a choice of one method is made since study objectives generally can be established either as being comprehensive in nature and requiring multiple injections, or preliminary in nature and requiring a single injection only.

2. The selection of dye injection points should be governed by the objectives to minimize dye loss and to maximize recovery. Estimates should be made of the effects of sorption, chemical reaction, and photochemical decay. These processes, in addition to natural dilution, must be considered in order to determine the size of adequate dye dosages to insure reliable detectability at the most remote sampling site despite losses. The loss in most cases will not vitiate measurement. It should be borne in mind that high concentrations of sediment or organic material may reduce the peak dye concentration before reaching the sampling site, e.g., laboratory tests on 40-percent solutions of Rhodamine B dye have shown losses of up to 12-percent dye after 4-hour contact with sand and, losses of up to 28-percent dye after 2-hour contact with organic material.

3. The loss of dye by sorption and (or) chemical reaction may be remedied by use of Rhodamine W T, which is less sorbed than other dyes. Also, the dosage could be increased, or the injection points could be located at shorter intervals. If large dye losses are expected, stream samples should be collected before dosing and known dye concentrations should be prepared and tested with a fluorometer to ascertain an estimate of the magnitude of dye loss. Pre-testing is necessary also to ascertain and to correct for background fluorescence.

An excellent illustration of the practical application of the foregoing basic guide-lines is contained in Williams' (1967) field tests on the movement and dispersion of fluorescent dye in the Duwamish River Estuary, Washington.

Synthesis of Basic Diffusion - Dispersion - Convective Concepts

Introduction and Clarification of Terminology.

The dispersion process can be described rigorously in differential-equation form by the diffusion equation for turbulent flow, which is based on the principal of the conservation of mass.

Clarification of the terminology and components of this vital equation by Holley (1969) is helpful. Holley suggested that "diffusion" be applied to transport which is associated mainly with time-averaged velocity fluctuations, and "dispersion" refer to transport associated with spatially averaged velocity fluctuations.

Gebhard and Masch (1969) suggested that a better understanding of the mass balance equation would result from the clear recognition of the three primary "phenomenological" causes of mixing which are involved in

the equation namely: molecular diffusion, turbulent diffusion, and convective displacement. For consistency and clarification in their study they adopted the following criteria:

1. If a case exists where the effects of three phenomena are distinguishable, the name of the separable phenomena should be used.

2. The term "diffusion" should be used for molecular and/or turbulent diffusion, when no convective displacement effects are involved.

3. The term "dispersion" should be used for convective displacement effects regardless of other effects involved.

4. More detailed descriptions of phenomena should be used for clarity where necessary, e.g., "longitudinal turbulent diffusion", lateral dispersion, etc.

A similar terminology will be adopted for this study. The term "diffusion" will be used for pure molecular and turbulent diffusion; and, the term "dispersion" will be used for convective displacement and to all combined effects of convective displacement and diffusion.

The Generalized Mass Conservation Equation. The generalized differential equation for conservation of mass, stated in tensor form, for dispersion in a steady flow of incompressible fluid, and assuming that the fluid properties of the dispersant are identical with those of the transporting medium, was given by Sayre and Chang (1968), as follows:

$$\frac{\partial \bar{c}}{\partial t} + U_i \frac{\partial \bar{c}}{\partial x_i} = -\frac{\partial \overline{c' u_i'}}{\partial x_i} + \epsilon_M \frac{\partial^2 \bar{c}}{\partial x_i \partial x_i} \qquad (3\text{-}65)$$

where:

$C = \bar{C} + c' = C(x_1, x_2, x_3, t)$ is the local concentration of dispersant expressed as the sum of the slowly varying part, $\bar{C}$, and a rapidly fluctuating part, c'.

t = time.

$U_i = \bar{U}_i + u_i' = U_i(x_1, x_2, x_3)$ is the local velocity of flow expressed as the sum of the time-averaged velocity, $\bar{U}_i$, and the turbulent component, u_i'.

x_i = the distance and the index i = 1, 2, 3 indicates direction in a rectangular coordinate system.

ϵ_M = coefficient of molecular diffusivity.

A coefficient of turbulent diffusion, $\epsilon_{T_{ij}}(x_i, x_2, x_3)$ can be defined as

$$\epsilon_{T_{ij}} \frac{\partial \bar{C}}{\partial x_j} \equiv -\overline{c' u_i'} \quad . \tag{3-66}$$

Assuming that molecular and turbulent diffusion are independent and additive, as shown by Mickelsen (1960), the coefficients of molecular and turbulent diffusion can be expressed as

$$\epsilon_{ij}(x_1, x_2, x_3) = \epsilon_{T_{ij}} + \epsilon_M \cdot \tag{3-67}$$

Combining Equations (3-66) and (3-67) and, eliminating the average bars, permits Equations (3-65) to be transformed as follows:

$$\frac{\partial C}{\partial t} + U_i \frac{\partial C}{\partial x_i} = \frac{\partial}{\partial x_i}\left(\epsilon_{T_{ij}} \frac{\partial C}{\partial x_j}\right) + \epsilon_M \frac{\partial^2 C}{\partial x_i \partial x_j} \quad , \tag{3-68A}$$

$$\frac{\partial C}{\partial t} + U_i \frac{\partial C}{\partial x_i} = \frac{\partial}{\partial x_i}\left(\epsilon_{T_{ij}} \frac{\partial C}{\partial x_j}\right) + \frac{\partial}{\partial x_i}\left(\epsilon_M \frac{\partial C}{\partial x_j}\right),$$

(3-68B)

$$\frac{\partial C}{\partial t} + U_i \frac{\partial C}{\partial x_i} = \frac{\partial}{\partial x_i}\left[\left(\epsilon_{T_{ij}} + \epsilon_M\right) \frac{\partial C}{\partial x_j}\right].$$

(3-68C)

Synthesis of Molecular Turbulent Diffusion. Whether turbulent diffusion and molecular diffusion are truly independent continues to be a moot question. However, for most practical purposes the distinction between the two types is academic. For example, if we are dealing with open channel flows the question would be trivial since $\epsilon_T >> \epsilon_M$. Also, suppose that the coordinate axes are designated to coincide with the principal axes of the diffusion tensor then $\epsilon_{ij} = 0$ for all $i \neq j$. And, suppose we define $\epsilon_{ij} = \epsilon_i$ for $i = j$, then Equation (3-68 C) simplifies to

$$\frac{\partial C}{\partial t} + U_i \frac{\partial C}{\partial x_i} = \frac{\partial}{\partial x_i}\left[\epsilon_i \frac{\partial C}{\partial x_i}\right].$$

(3-69)

Using the convectional form expressed in Cartesian coordinates, i.e., letting

$$x_1, x_2, x_3 = x, y, z$$

$$U_1, U_2, U_3 = U, V, W$$

$$\epsilon_1, \epsilon_2, \epsilon_3 = D_x, D_y, D_z$$

(3-70A)

we obtain the generalized equation

$$\frac{\partial C}{\partial t} + u\frac{\partial C}{\partial x} + v\frac{\partial C}{\partial y} + w\frac{\partial C}{\partial z} = \frac{\partial}{\partial x}\left(D_x\frac{\partial C}{\partial x}\right) + \frac{\partial}{\partial y}\left(D_y\frac{\partial C}{\partial y}\right) + \frac{\partial}{\partial z}\left(D_z\frac{\partial C}{\partial z}\right). \qquad (3\text{-}70B)$$

Harleman (1966) is more explicit in his development of the conservation of mass equation for a substance introduced into a fluid medium. Neglecting molecular diffusion relative to macroscopic turbulence, he elucidates the physical significance of the equation considerably by introducing the basic concept of mass flux into the generalized equation. Harleman's rigorous derivation of the foregoing equation synthesizes all the major dispersion and diffusion concepts.

CHAPTER IV

FORMULATION OF A TWO-DIMENSIONSAL CONSERVATIVE TRANSPORT MATHEMATICAL MODEL

General

A mathematical model is a functional representation of the physical behavior of a system or process, and is expressed in a form amenable to economical solution. The mathematical formulation of a process consists of an input, a transfer function and an output. The output is related to the input,or some function of the input, by the transfer function. Mathematical models generally permit discretizing a larger problem or system into segments which are easier to analyze and more tractable to mathematical solution. This is especially desirable in systems where boundary conditions are numerous and varied. Discretization involves subdivision of a complex prototype into subsystems that can be expressed by feasible mathematical formulations and solved. Numerical methods are well-suited for application to discretized systems where the transfer functions may be regarded as "time-independent" if the intervals of time are very short. However, there are limitations inherent in the numerical process. There is an optimum size of element and time interval. Invariably a decision must be made regarding the desired accuracy of the model versus the economy of computational effort required to obtain a mathematical

solution which is stable and convergent. The concept regarding a lake or reservoir as a system composed of a hydrodynamic model and a complementary transport model, is a logical solution method of a complex fluid body. However, it must be emphasized that the attendant discretization is to facilitate the mathematical analysis and solution of the hydrodynamic and transport properties of the fluid bodies. The discretization is a practical simplification dictated by engineering expediency. However, ultimate synthesis must take place to reconstruct the fragmented system. Discretization of systems for analysis purposes without ultimate synthesis and reconstruction would be a major deficiency from the practical engineering viewpoint. The objectives of this study are oriented toward engineering utility.

The Equations

In the previous chapter the generalized form of the three-dimensional convective dispersion equation for conservative diffusants was developed, see Equation (3-70). The objectives and scope of this study require that the generalized convective dispersion equation be modified to represent dispersion, in a horizontal, two-dimensional field. This modification stems from the adoption of the following specific assumptions:

1. The molecular diffusion is deemed neglible compared to turbulent diffusion, and therefore, can be neglected.

2. The epilimnion region of the impoundment is a relatively well-defined and well-mixed layer. (However, this does not infer a constant-thickness epilimnetic layer.)

3. The circulation, transport and dispersive characteristics of the upper portions of the epilimnetic layer can be analyzed to reveal adequately the regimen of the fully-mixed surface layer.

In view of the foregoing assumptions, the velocity conditions can be expressed as

$$\bar{u} \neq \bar{v} \neq 0$$

$$\bar{w} = 0$$

and, the conditions governing the "effective" macroscopic turbulent diffusion coefficients are

$$D_x \neq D_y \neq 0$$

$$D_z = 0.$$

Thus, the modified equation becomes a second order parabolic partial differential equation as follows:

$$\frac{\partial \bar{c}}{\partial t} + \frac{\bar{u}\partial \bar{c}}{\partial x} + \frac{\bar{v}\partial \bar{c}}{\partial y} = \frac{\partial}{\partial x}\left(D_x \frac{\partial \bar{c}}{\partial x}\right) + \frac{\partial}{\partial y}\left(D_y \frac{\partial \bar{c}}{\partial y}\right). \qquad (4\text{-}1)$$

Diachishin (1963 A) and Glover (1964) derived explicit solutions to both the two-and three-dimensional convective dispersion equations. Diachishin (1963 B) stated that the three-dimensional equation had received little attention up to 1962. Furthermore, no effort had been made to measure the three dispersion coefficients simultaneously, each of which appeared to have different significant periods of time: molecular or macroscopic.

Diachishin (1963 A), emphasized the importance of noting the period of observation and the estimated significant periods of each distinct diffusion coefficient. This is important because peak concentrations decrease faster at later periods, due to the decrease in the total diffusion coefficient. As shown by Gebhard and Masch (1968), the solution for the two-dimensional equation is

$$c = \frac{c_0}{2\pi} \cdot \frac{\exp -\left[(x-\bar{u}t)^2/4E_x t\right]}{\sqrt{2E_x t}} \cdot \frac{\exp -\left[(y-\bar{v}t)^2/4E_y t\right]}{\sqrt{2E_y t}} \cdot \qquad (4\text{-}2)$$

A similar solution was presented by Diachishin (1963 B) for the three-dimensional equation. However, Gebhard and Masch (1968) found that these explicit solutions often do not describe the concentration distributions which occur in most moving fluids because only the mean velocity of the fluid-mass in motion is considered and the dispersive effects of shear flow are neglected; i.e., the convective diffusion phase of the problem is solved rather than the convective dispersion phase. Gebhard and Masch (1968) discuss the development and use of a "total dispersion coefficient" which appears to afford the best prospects for a realistic approximation of the convective dispersion distribution for most commonly occurring problems of mixing in moving fluids. However, there continues to be a high-priority need for research of three-dimensional mathematical models for determining complex hydraulic conditions on both macro and micro-scales, as recommended by Parker and Krenkel (1969), and Masch, et al (1970).

Solution by the Methods of Finite Differences

Introduction. There are three major approaches involving the solution of non-linear, partial differential equations.

1. Reduce the problem to ordinary differential equations and solve them using numerical integration techniques.
2. Reduce the equation by linearization techniques and solve them by analytical methods.
3. Reduce the equations by the method of finite differences to obtain a set of algebraic equations and solve them by either direct or iterative techniques.

The first two approaches involve excessive analytical work; also, their application is limited because of the necessity to assume steady-flow conditions. In contrast, the finite differences methods have a wider range of application, including unsteady-flow conditions and complicated boundary configuration. However, it is well to recognize that all forms and methods of practical modeling involve varying degrees of rational simplifications through linearization, boundary approximations and the use of transition and geometrical symmetries. Also, it should be appreciated at the outset insofar as hydrological and hydrometeorologic processes are concerned, experience indicates that great discrepancies can exist between observed and calculated model results under the same simulated excitation. Theoretically, the relationships between the selected variables in most hydrodynamic problems are provided by solution of the equations of momentum, energy, mass and state; but, in practice, the formulation of the equations is found to be imprecise because of:

1. Incomplete knowledge of hydrodynamic system behavior.

2. System heterogeneities and anisotropies which must be treated only intuitively or in empirical terms.

3. Time dependence relationships of parameters which must be assigned constant values merely to make numerical solution tractable.

4. Approximations which must be introduced for computational economy.

Basic Considerations in Adoption of the Implicit Finite Difference Method. Gebhard and Masch (1968) evaluated the limitations and relative advantages of three finite difference methods for the mathematical solution of the two-dimensional, convective dispersion equation, namely, the explicit, implicit and characteristic methods. Their findings on dispersion in water bodies confirmed those of Peaceman and Rachford (1955) regarding the numerical solution of parabolic and elliptic differential equations in connection with solutions of the heat flow equation in two space dimensions. Explicit difference equations are simple to solve but require an excessively large number of time steps of limited size. Implicit difference equations do not limit the time step but require at each time step the solution by iteration of many sets of simultaneous equations.

A fundamental consideration in finite difference methods and applications is the requirement of convergency of the solutions. Two important concepts are involved in convergency. These are: stability and consistency. As described by Carnahan, et al (1969), stability is the be-

havior demonstrated by a given finite difference equation as the time increment $\Delta t \rightarrow 0$. In other words, as $\Delta t \rightarrow 0$, there is an upper limit to the possible amplification of any data either existing in or introduced into the computational procedure. Stability represents the relative "boundedness" of the finite difference solution, at a given time t, as $\Delta t \rightarrow 0$. The related concept, consistency, denotes whether or not a finite difference approximation approaches the true solution of the partial differential equation under study. These two concepts govern the bulk of the design efforts involved in numerical model formulation. Underlying the problem of attaining stability and consistency are the generation of truncation errors of finite difference equations and discretization errors of the solution of these equations. Generally, discretization errors are decreased by using smaller increments, but the number of steps and hence the amount of computation required to cover a given interval are increased. When the number of steps taken are large, there is the possibility that round-off errors will accumulate significantly.

As a result of mathematical stability tests, using the gross values of dispersion coefficients expected to be encountered in inland impoundments, it was found necessary to adopt the implicit finite difference solution method to the convective dispersion equation. The cell sizes of workable hydrodynamic models were an equally vital factor in the design process. The explicit method was found to be inadequate for the solution of the two-dimensional, convection dispersion equation considering the range of

hydrodynamic factors (i.e., flows, velocities, grid intervals and coefficients of dispersion) expected to be encountered in the Lake Bastrop impoundment, where the hydrodynamic and transport models will be verified. The following three stability requirements placed undesirable restrictions on the time increment, which precluded the use of the explicit method:

$$1.\quad 0 < \frac{\Delta t}{(\Delta x)^2} \leq \frac{1}{2} . \tag{4-3}$$

$$2.\quad \Delta t \leq \frac{(\Delta x)^2 (\Delta y)^2}{2\left(E_x (\Delta y)^2 + E_y (\Delta x)^2\right)} . \tag{4-4}$$

$$3.\quad \Delta x \leq \frac{2E_x}{U_{MAX}} \quad ; \quad \Delta y \leq \frac{2E_y}{V_{MAX}} . \tag{4-5}$$

In contrast, the implicit method overcomes the stability and time interval obstacles at the expense of slightly more detailed and complicated computations procedures. Carnahan, et al (1969) concluded that the implicit method converges to the solution of the partial equation as $\Delta t \rightarrow 0$ and, as $\Delta x \rightarrow 0$, regardless of the value of the ratio $\frac{\Delta t}{(\Delta x)^2}$. However, as indicated earlier in this discussion, the sizes of the time and space increments must be constrained to insure that truncation and discretization errors are within acceptable, practical limits.

Salient Elements of the Implicit Method. Essentially, the implicit finite difference method consists in representing the value of

second order partial derivations by the finite difference form evaluated at an advance point of time t_{k+1}, instead of at time t_k, as in the explicit method. There are several methods for the approximate evaluation of partial derivative expressions. The method of central differences illustrates the fundamental theory. Figure (4-1) shows a rectangular grid with uniform spacing, h, in the x-y plane. For example, suppose that we desire to express the Laplacian operator, $\nabla^2\phi$, in terms of the function values ϕ (x, y) at the node points. For the node (y = i, x = j) we may write:

$$\left[\frac{\partial^2\phi}{\partial x^2}\right]_{i,j} = \frac{\left[\phi_{i,j-1} - 2\phi_{i,j} + \phi_{i,j+1}\right]}{h^2} \tag{4-6}$$

and also,

$$\left[\frac{\partial^2\phi}{\partial y^2}\right]_{i,j} = \frac{\left[\phi_{i-1,j} - 2\phi_{i,j} + \phi_{i+1,j}\right]}{h^2} \tag{4-7}$$

then

$$\nabla^2\phi = \left[\frac{\partial^2\phi}{\partial x^2}\right]_{i,j} + \left[\frac{\partial^2\phi}{\partial y^2}\right]_{i,j} . \tag{4-8}$$

Crank and Nicolson (1947) used a more accurate method of averaging the second order derivative approximations in terms of central differences over two time-intervals. For example, the approximation in the y-direction,

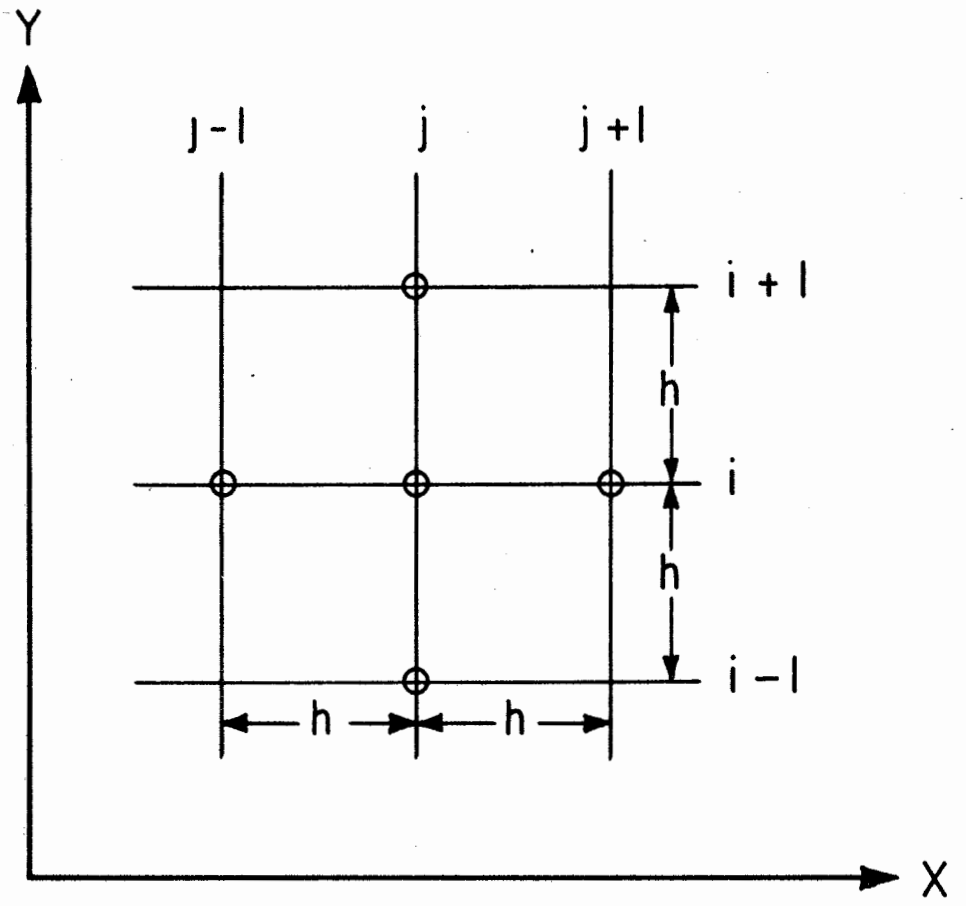

Figure 4-1. Molecule for Central Differences Method of Approximations.

$$\frac{\partial^2\phi}{\partial y^2} = \frac{1}{2}\left\{\frac{(\phi_{i+1,k} - 2\phi_{i,k} + \phi_{i-1,k})}{(\Delta y)^2} + \frac{(\phi_{i+1,k+1} - 2\phi_{i,k+1} + \phi_{i-1,k+1})}{(\Delta y)^2}\right\}. \tag{4-9}$$

Rewriting Equation (4-1), omitting the averaging bars for c, u, and v, we have the normal, two-dimensional, convective dispersion equation:

$$\frac{\partial c}{\partial t} = E_x \frac{\partial^2 c}{\partial x^2} + E_y \frac{\partial^2 c}{\partial y^2} - u\frac{\partial c}{\partial x} - v\frac{\partial c}{\partial y}. \tag{4-10}$$

Substituting in Equation (4-10) the Crank-Nicolson (1947) partial derivative approximations we obtain:

$$\frac{C_{i,j}^{K+1} - C_{i,j}^{K}}{\Delta t} =$$

$$\frac{E_x}{2}\left[\frac{(C_{i-1,j}^{K} - 2C_{i,j}^{K} + C_{i+1,j}^{K})}{(\Delta x)^2} + \frac{(C_{i-1,j}^{K+1} - 2C_{i,j}^{K+1} + C_{i+1,j}^{K+1})}{(\Delta x)^2}\right] +$$

$$\frac{E_y}{2}\left[\frac{(C_{i,j-1}^{K} - 2C_{i,j}^{K} + C_{i,j+1}^{K})}{(\Delta y)^2} + \frac{(C_{i,j-1}^{K+1} - 2C_{i,j}^{K+1} + C_{i,j+1}^{K+1})}{(\Delta y)^2}\right] +$$

$$\frac{u}{2}\left[\frac{(C_{i+1,j}^{K} - C_{i-1,j}^{K})}{(2\Delta x)} + \frac{(C_{i+1,j}^{K+1} - C_{i-1,j}^{K+1})}{(2\Delta x)}\right] +$$

$$\frac{v}{2}\left[\frac{(C_{i,j+1}^{K} - C_{i,j-1}^{K})}{(2\Delta y)} + \frac{(C_{i,j+1}^{K+1} - C_{i,j-1}^{K+1})}{(2\Delta y)}\right]. \tag{4-11}$$

See Figure (4-2) showing the space time nodal relationship of the computational molecule. It is evident from the foregoing discussion and numerical formulations of the finite difference expressions that the convective dispersion equation is time-dependent in nature, requiring given initial conditions and given time-dependent boundary conditions for its solution.

In using the finite difference technique a network of grid points must be established throughout the entire region of interest. Figure (4-3) represents a portion of such a grid network showing cellular parameters and variable locations at time k, pertaining to the convective dispersion equation. Actually, a double Eulerian mesh is involved: one for mapping the average cellular value; and one for mapping adjacent cell averages. The solid grid divides the system into cells; and the dashed line grid is used for variable placement. In this particular case, the concentration $C_{i,\ j}$ is defined at the center of the cell while the horizontal components of the velocity, $U_{i,\ j}$ and $V_{i,\ j}$, and the effective coefficients of horizontal dispersion $E_{x_{i,\ j}}$ and $E_{y_{i,\ j}}$ are defined at the sides of the cell. The gist of the problem is to approximate the partial derivatives of the original partial differential equation by use of suitable finite difference expressions involving Δ x, Δ y, Δ t and other initial functions such as $C_{i,\ j,\ k}$.

Rearranging Equation (4-11) so that all expressions of C at time k are on the left side of the equation and all expressions of C for time k + 1 are on the right side, we obtain Equation (4-12), which follows:

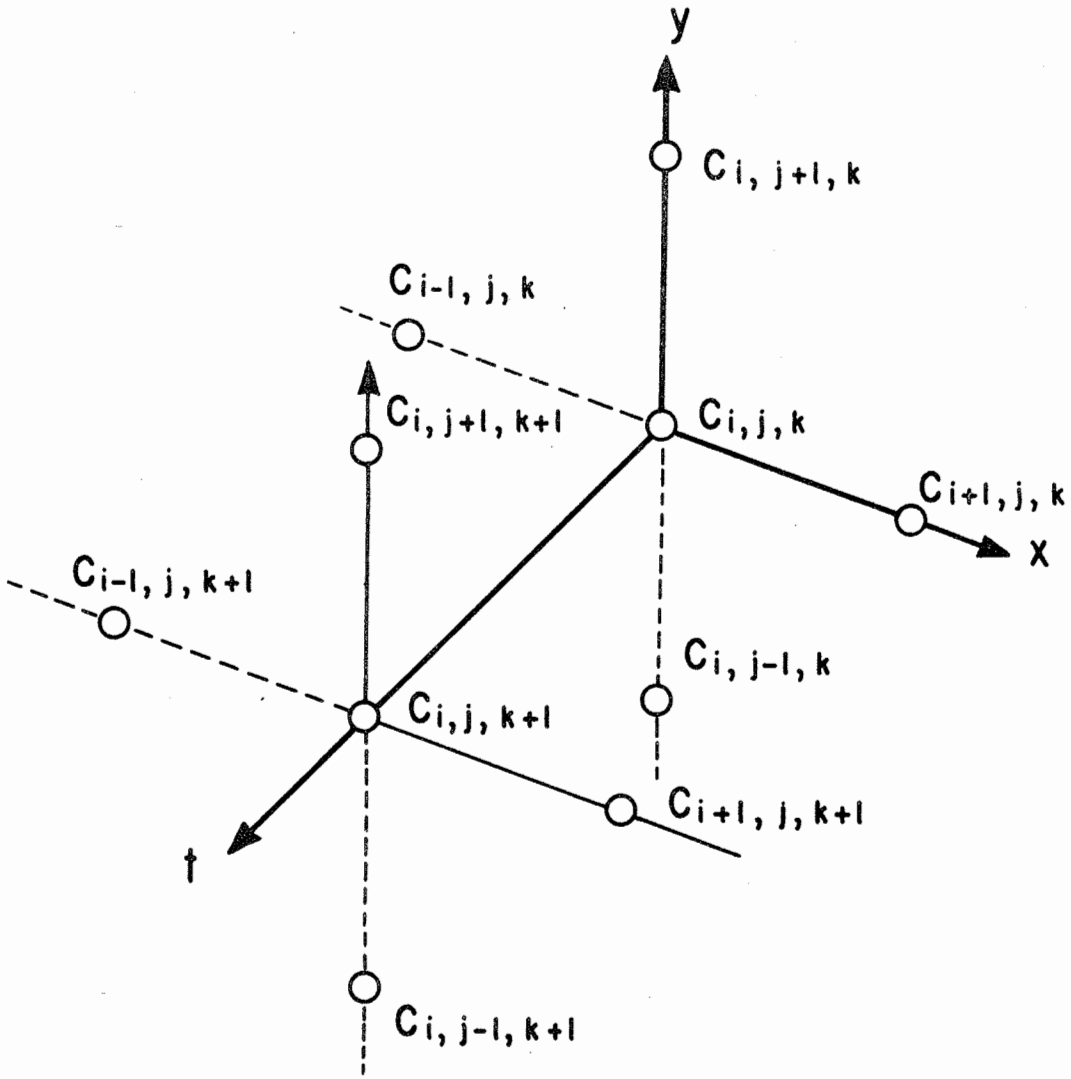

Figure 4-2. Space - Time Molecule for Use in the Implicit Finite Differences Method.

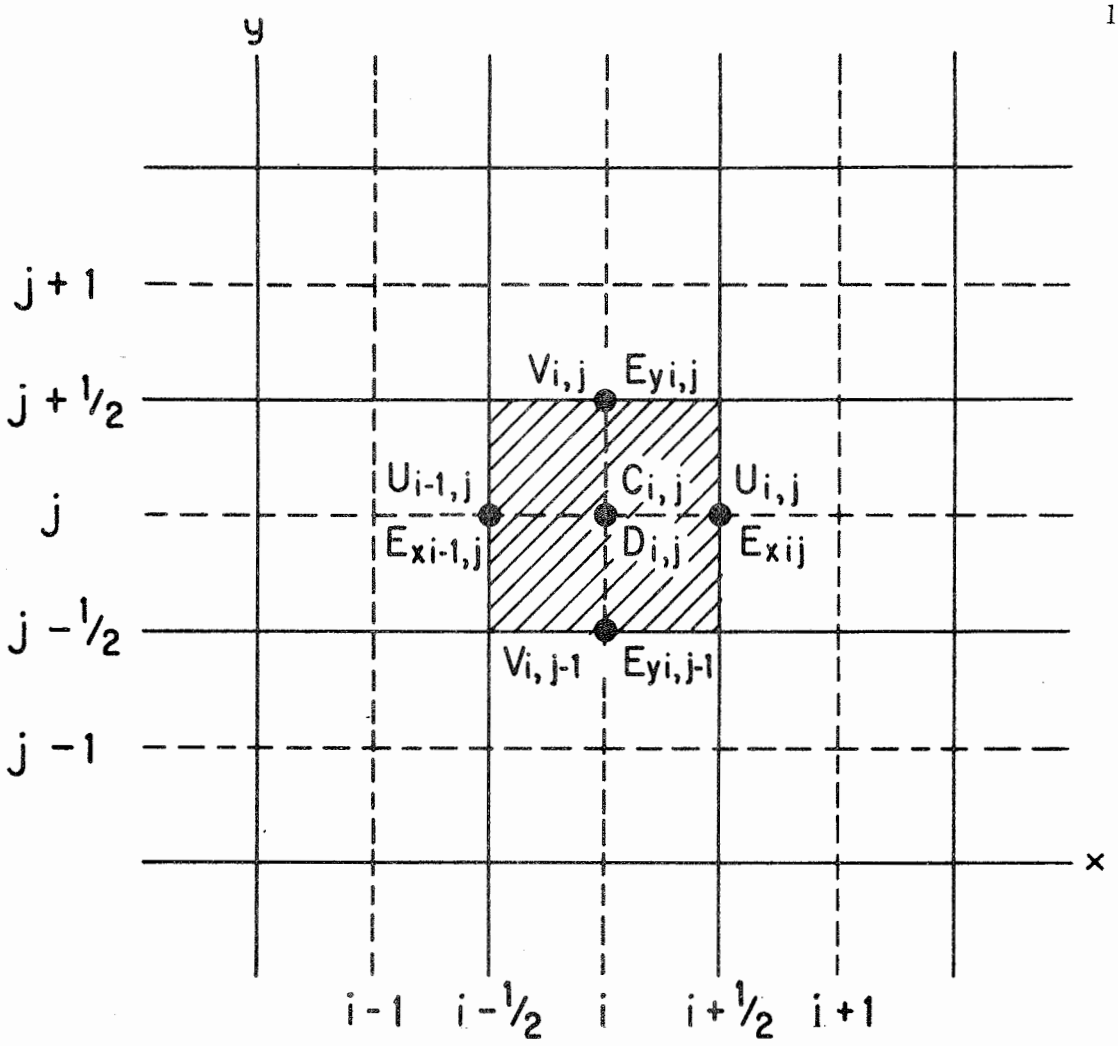

U = Velocity in x Direction
V = Velocity in y Direction
D = Depth
E = Coefficient of Dispersion

Figure 4-3. Double Eulerian Mesh
(The i j th Cell is Highlighted)

$$C_{i,j}^{k}\left[\frac{Ex(\Delta t)}{(\Delta x)^2}+\frac{Ey(\Delta t)}{(\Delta y)^2}-1\right]+C_{i-1,j}^{k}\left[-\frac{Ex(\Delta t)}{2(\Delta x)^2}+\frac{u(\Delta t)}{4(\Delta x)}\right]+$$

$$C_{i+1,j}^{k}\left[-\frac{Ex(\Delta t)}{2(\Delta x)^2}-\frac{u(\Delta t)}{4(\Delta x)}\right]+C_{i,j-1}^{k}\left[-\frac{Ey(\Delta t)}{2(\Delta y)^2}+\frac{v(\Delta t)}{4(\Delta y)}\right]+$$

$$C_{i,j+1}^{k}\left[-\frac{Ey(\Delta t)}{2(\Delta y)^2}-\frac{v(\Delta t)}{4(\Delta y)^2}\right]=$$

$$C_{i,j}^{k+1}\left[-\frac{Ex(\Delta t)}{(\Delta x)^2}-\frac{Ey(\Delta t)}{(\Delta y)^2}-1\right]+C_{i-1,j}^{k+1}\left[\frac{Ex(\Delta t)}{2(\Delta x)^2}-\frac{u(\Delta t)}{4(\Delta x)}\right]+$$

$$C_{i+1,j}^{k+1}\left[\frac{Ex(\Delta t)}{2(\Delta x)^2}+\frac{u(\Delta t)}{4(\Delta x)^2}\right]+C_{i,j-1}^{k+1}\left[\frac{Ey(\Delta t)}{2(\Delta y)^2}-\frac{v(\Delta t)}{4(\Delta y)}\right]+$$

$$C_{i,j+1}^{k+1}\left[\frac{Ey(\Delta t)}{2(\Delta y)^2}+\frac{v(\Delta t)}{4(\Delta y)}\right].$$

(4-12)

The above equation expresses five unknown values of C at time k + 1, in terms of five known values of C at time k. Three unknowns are on the x-axis and three unknowns on the y-axis. The above expression can be resolved by solving simultaneous equations for each point (i, j) at time k. The specific method selected will be described in the following section.

Adoption of the Alternating-Direction Implicit Method (ADI)

Peaceman and Rachford (1955) developed the so-called Alternating-Direction Implicit Method (hereinafter called the ADI method) for the solution of heat flow equations. The ADI method affords a practical, direct application for the solution of the two-dimensional, steady-state, convective dispersion equation. Carnahan, et al (1969) indicated that the ADI method has general application. The method was developed with the specific objective of obtaining a rate of convergence substantially greater than obtainable by other finite difference methods. Analysis of the ADI method shows that it is stable for any time-step size and requires less computational effort than other implicit methods.

The ADI method involves solving a system of equations with a tridiagonal coefficient matrix of the following basic form: Letting a, b, c be coefficients and v be variables,

$$\begin{aligned}
b_1 v_1 + c_1 v_2 &= d_1 \\
a_1 v_1 + b_2 v_2 + c_2 v_3 &= d_2 \\
a_3 v_2 + b_3 v_3 + c_3 v_4 &= d_3 \\
&\cdots \\
a_i v_{i-1} + b_i v_i + c_i v_{i+1} &= d_i \\
&\cdots \\
a_{n-1} v_{n-2} + b_{n-1} v_{n-1} + c_{n-1} v_n &= d_{n-1} \\
a_n v_{n-1} + b_n v_n &= d_n
\end{aligned} \tag{4-13}$$

Referring to the tridiagonal matrix formed by the coefficients a, b and c alone, Carnahan, et al (1969) indicated that the system of equations could be solved by using a Gaussian elimination method at the expense of a considerable amount of computation or, by using the Gauss-Seidel iterative method provided that the large number of iterations are made to achieve proper convergence. The ADI method precludes these disadvantages. Therefore, the ADI method has been adopted in this study as the basis of the numerical model algorithm for the solution of the convective dispersion equation. Essentially, the principal involved in the ADI method is to employ two difference equations which are used in turn over successive time-steps of $\frac{\Delta t}{2}$ duration. The first equation is implicit only in the x-direction and the second is implicit only in the y-direction.

Figure (4-3) depicts the grid system including the specific node locations assigned to the relevant variables at time k, applicable to the ADI method. Note the values of U and V, the velocities in the x and y directions of a horizontal plane, are assigned to nodes on the borders of a grid cell. The values of the coefficients of dispersion, D_x and D_y in the x and y directions, respectively, also are assigned to the node locations on the borders of the cell. The value of the cellular concentration, $C_{i,\,j}$, is assigned to the central node of the cell.

Rearranging Equation (4-1), in the form of Equation (4-14) which follows, illustrates the essential components which must be trans-

formed by partial derivative approximations and are designated by the circled letters: A, B, C, D and E. The values of these components at time $(t + \Delta t)$, that is, $t = (k + 1)$ are shown in the set of Equations (4-15), which also follows. By substituting the component approximations, Equation (4-15), into the basic Equation (4-14) and then combining terms, we obtain Equation (4-16), which is the first equation of the required pair of alternating-direction implicit equations. Equation (4-16) is implicit in the x-direction. Similarly, at time, $(t + 2 \Delta t)$, that is, at $t = (k + 2)$, the approximations for the five basic components of the partial differential equation are shown by the set of Equations (4-17). By substituting the component approximations, Equations (4-17), into the basic Equation (4-14) and then combining terms, we obtain Equation (4-18) which is the second equation of the required pair of equations. Equation (4-18) is implicit in the y-direction. The overall procedure for the two time steps is stable for any size of time step. The coefficients of the three C^{k+1} terms in Equation (4-16) and Equation (4-18) will be used in the tridiagonal coefficient matrix computations. (See earlier Equations (4-13) and related discussion.)

$$\frac{\partial c}{\partial t} = \underset{(A)}{\frac{\partial}{\partial x}\left(E_x \frac{\partial c}{\partial x}\right)} + \underset{(B)}{\frac{\partial}{\partial y}\left(E_y \frac{\partial c}{\partial y}\right)} - \underset{(C)}{\frac{\partial}{\partial x}(uc)} - \underset{(D)}{\frac{\partial}{\partial y}(vc)} \qquad (4\text{-}14)$$

$$(A) \rightarrow \frac{\partial c}{\partial t} = \frac{c_{i,j}^{K+1} - c_{i,j}^{K}}{\Delta t}.$$

$$(B) \rightarrow \frac{\partial}{\partial x}\left(E_x \frac{\partial c}{\partial x}\right) = \frac{E_{x_{i,j}} \frac{\partial c}{\partial x} - E_{x_{i-1,j}} \frac{\partial c}{\partial x}}{\Delta x}.$$

$$= \frac{E_{x_{i,j}}\left(\frac{c_{i+1,j} - c_{i,j}}{\Delta x}\right) - E_{x_{i-1,j}}\left(\frac{c_{i,j} - c_{i-1,j}}{\Delta x}\right)}{\Delta x}.$$

$$= \left(E_{x_{i,j}} \frac{c_{i+1,j}^{K+1}}{\Delta x^2}\right) - \left(E_{x_{i,j}} \frac{c_{i,j}^{K+1}}{\Delta x^2}\right) - \left(E_{x_{i-1,j}} \frac{c_{i,j}^{K+1}}{\Delta x^2}\right) + \left(E_{x_{i-1,j}} \frac{c_{i-1,j}^{K+1}}{\Delta x^2}\right).$$

$$(C) \rightarrow \frac{\partial}{\partial y}\left(E_y \frac{\partial c}{\partial y}\right) = \frac{E_{y_{i,j}} \frac{\partial c}{\partial y} - E_{y_{i,j-1}} \frac{\partial c}{\partial y}}{\Delta y}.$$

$$= \frac{E_{y_{i,j}}\left(\frac{c_{i,j+1} - c_{i,j}}{\Delta y}\right) - E_{y_{i,j}}\left(\frac{c_{i,j} - c_{i,j-1}}{\Delta y}\right)}{\Delta y}.$$

$$= \left(E_{y_{i,j}} \frac{c_{i,j+1}^{K}}{\Delta y^2}\right) - \left(E_{y_{i,j}} \frac{c_{i,j}^{K}}{\Delta y^2}\right) - \left(E_{y_{i,j-1}} \frac{c_{i,j}^{K}}{\Delta y^2}\right) + \left(E_{y_{i,j-1}} \frac{c_{i,j-1}^{K}}{\Delta y^2}\right).$$

(4-15)
Continued

$$(D) \rightarrow -\frac{\partial}{\partial x}(uc) = -u\frac{\partial c}{\partial x} - c\frac{\partial u}{\partial x}$$

$$= -\frac{1}{2}\left[u_{i-1,j}^{k+1}\left(\frac{c_{i,j}^{k+1} - c_{i-1,j}^{k+1}}{\Delta x}\right) + u_{i,j}^{k+1}\left(\frac{c_{i+1,j}^{k+1} - c_{i,j}^{k+1}}{\Delta x}\right)\right] - c_{i,j}^{k+1}\left(\frac{u_{i,j}^{k+1} - u_{i-1,j}^{k+1}}{\Delta x}\right)$$

$$= \left(u_{i-1,j}^{k+1}\frac{c_{i-1,j}^{k+1}}{2\Delta x}\right) - \left(u_{i-1,j}^{k+1}\frac{c_{i,j}^{k+1}}{2\Delta x}\right) + \left(u_{i,j}^{k+1}\frac{c_{i,j}^{k+1}}{2\Delta x}\right) - \left(u_{i,j}^{k+1}\frac{c_{i+1,j}^{k+1}}{2\Delta x}\right) - \left(u_{i,j}^{k+1}\frac{c_{i,j}^{k+1}}{\Delta x}\right) +$$
$$+\left(u_{i-1,j}^{k+1}\frac{c_{i,j}^{k+1}}{\Delta x}\right).$$

$$= c_{i-1,j}^{k+1}\left(\frac{u_{i-1,j}^{k+1}}{2\Delta x}\right) + c_{i,j}^{k+1}\left(-\frac{u_{i-1,j}^{k+1}}{2\Delta x} + \frac{u_{i,j}^{k+1}}{2\Delta x}\right) - c_{i+1,j}^{k+1}\left(\frac{u_{i,j}^{k+1}}{2\Delta x}\right).$$

$$(E) \rightarrow -\frac{\partial}{\partial y}(vc) = -v\frac{\partial c}{\partial y} - c\frac{\partial v}{\partial y}$$

$$= -\frac{1}{2}\left[v_{i,j-1}^{k}\left(\frac{c_{i,j}^{k} - c_{i,j-1}^{k}}{\Delta y}\right) + v_{i,j}^{k}\left(\frac{c_{i,j+1}^{k} - c_{i,j}^{k}}{\Delta y}\right)\right] - c_{i,j}^{k}\left(\frac{v_{i,j}^{k} - v_{i,j-1}^{k}}{\Delta y}\right)$$

$$= \left(v_{i,j-1}^{k}\frac{c_{i,j-1}^{k}}{2\Delta y}\right) - \left(v_{i,j-1}^{k}\frac{c_{i,j}^{k}}{2\Delta y}\right) + \left(v_{i,j}^{k}\frac{c_{i,j}^{k}}{2\Delta y}\right) - \left(v_{i,j}^{k}\frac{c_{i,j+1}^{k}}{2\Delta y}\right) - \left(v_{i,j}^{k}\frac{c_{i,j}^{k}}{\Delta y}\right) +$$
$$+\left(v_{i,j-1}\frac{c_{i,j}^{k}}{\Delta y}\right).$$

$$= c_{i,j-1}^{k}\left(\frac{v_{i,j-1}^{k}}{2\Delta y}\right) + c_{i,j}^{k}\left(-\frac{v_{i,j-1}^{k}}{2\Delta y} + \frac{v_{i,j}^{k}}{2\Delta y}\right) - c_{i,j+1}^{k}\left(\frac{v_{i,j}^{k}}{2\Delta y}\right).$$

(4-15)

End

$$C_{i-1}^{k+1} - \left[Ex_{i-1,j} \left(\frac{\Delta t}{\Delta x^2} \right) - U_{i-1,j}^{k+1} \left(\frac{\Delta t}{2\Delta x} \right) \right] +$$

$$+ C_{i,j}^{k+1} \left[1 + Ex_{i,j} \left(\frac{\Delta t}{\Delta x^2} \right) + Ex_{i-1,j} \left(\frac{\Delta t}{\Delta x^2} \right) + U_{i-1,j}^{k+1} \left(\frac{\Delta t}{2\Delta x} \right) - U_{i,j}^{k+1} \left(\frac{\Delta t}{2\Delta x} \right) \right] +$$

$$+ C_{i+1,j}^{k+1} \left[-Ex_{i,j} \left(\frac{\Delta t}{\Delta x^2} \right) + U_{i,j}^{k+1} \left(\frac{\Delta t}{2\Delta x} \right) \right] =$$

$$C_{i,j-1}^{k} \left[Ey_{i,j-1} \left(\frac{\Delta t}{\Delta y^2} \right) + V_{i,j-1}^{k} \left(\frac{\Delta t}{2\Delta y} \right) \right] +$$

$$+ C_{i,j}^{k} \left[1 - Ey_{i,j} \left(\frac{\Delta t}{\Delta y^2} \right) - Ey_{i,j-1} \left(\frac{\Delta t}{\Delta y^2} \right) - V_{i,j-1}^{k} \left(\frac{\Delta t}{2\Delta y} \right) + V_{i,j}^{k} \left(\frac{\Delta t}{2\Delta y} \right) \right] +$$

$$+ C_{i,j+1}^{k} \left[Ey_{i,j} \left(\frac{\Delta t}{\Delta y^2} \right) - V_{i,j}^{k} \left(\frac{\Delta t}{2\Delta y} \right) \right] .$$

$$(A) \rightarrow \frac{\partial c}{\partial t} = \frac{c_{i,j}^{K+1} - c_{i,j}^{K}}{\Delta t}$$

$$(B) \rightarrow \frac{\partial}{\partial x}\left(E_x \frac{\partial c}{\partial x}\right) = Ex_{i,j}\left(\frac{c_{i+1,j}^{K}}{\Delta x^2}\right) - Ex_{i,j}\left(\frac{c_{i,j}^{K}}{\Delta x^2}\right) - Ex_{i-1,j}\left(\frac{c_{i,j}^{K}}{\Delta x^2}\right) + Ex_{i-1,j}\left(\frac{c_{i-1,j}^{K}}{\Delta x^2}\right).$$

$$(C) \rightarrow \frac{\partial}{\partial y}\left(Ey \frac{\partial c}{\partial y}\right) = Ey_{i,j}\left(\frac{c_{i,j+1}^{K+1}}{\Delta y^2}\right) - Ey_{i,j}\left(\frac{c_{i,j}^{K+1}}{\Delta y^2}\right) - Ey_{i,j-1}\left(\frac{c_{i,j}^{K+1}}{\Delta y^2}\right) + Ey_{i,j-1}\left(\frac{c_{i,j-1}^{K+1}}{\Delta y^2}\right).$$

$$(D) \rightarrow -\frac{\partial}{\partial x}(uc) = c_{i-1,j}^{K}\left(\frac{u_{i-1,j}^{K}}{2\Delta x}\right) + c_{i,j}^{K}\left(-\frac{u_{i-1,j}^{K}}{2\Delta x} + \frac{u_{i,j}^{K}}{2\Delta x}\right) - c_{i+1,j}\left(\frac{u_{i,j}^{K}}{2\Delta x}\right).$$

$$(E) \rightarrow -\frac{\partial}{\partial y}(vc) = c_{i,j-1}^{K+1}\left(\frac{v_{i,j-1}^{K+1}}{2\Delta y}\right) + c_{i,j}^{K+1}\left(\frac{v_{i,j-1}^{K+1}}{2\Delta y} + \frac{v_{i,j}^{K+1}}{2\Delta y}\right) - c_{i,j+1}^{K+1}\left(\frac{v_{i,j}^{K+1}}{2\Delta y}\right).$$

(4-17)

$$c_{i,j-1}^{K+1}\left[-Ey_{i,j}\left(\frac{\Delta t}{\Delta y^2}\right) - v_{i,j-1}^{K+1}\left(\frac{\Delta t}{\Delta y^2}\right)\right] +$$

$$c_{i,j}^{K+1}\left[1 + Ey_{i,j}\left(\frac{\Delta t}{\Delta y^2}\right) + Ey_{i,j-1}\left(\frac{\Delta t}{\Delta y^2}\right) + v_{i,j-1}^{K+1}\left(\frac{\Delta t}{2\Delta y}\right) - v_{i,j}^{K+1}\left(\frac{\Delta t}{2\Delta y}\right)\right] +$$

$$c_{i,j+1}^{K+1}\left[-Ey_{i,j}\left(\frac{\Delta t}{\Delta y^2}\right) + v_{i,j}^{K+1}\left(\frac{\Delta t}{2\Delta y}\right)\right] =$$

$$c_{i-1,j}^{K}\left[Ex_{i-1,j}\left(\frac{\Delta t}{\Delta x^2}\right) + u_{i-1,j}^{K}\left(\frac{\Delta t}{2\Delta x}\right)\right] +$$

$$c_{i,j}^{K}\left[1 - Ex_{i,j}\left(\frac{\Delta t}{\Delta x^2}\right) - Ex_{i-1,j}\left(\frac{\Delta t}{\Delta x^2}\right) - u_{i-1,j}^{K}\left(\frac{\Delta t}{2\Delta x}\right) + u_{i,j}^{K}\left(\frac{\Delta t}{2\Delta x}\right)\right] +$$

$$c_{i+1,j}^{K}\left[Ex_{i,j}\left(\frac{\Delta t}{\Delta x^2}\right) - u_{i,j}^{K}\left(\frac{\Delta t}{2\Delta x}\right)\right].$$

(4-18)

Differenced Boundary Conditions

It was indicated earlier in the discussion of finite difference techniques that a double Eulerian grid network (Figure 4-3) must be established to cover the fluid region of interest. This network of cells must satisfy the following criteria:

1. Enable approximation of the land-water boundary in terms of line segments of the grid system.

2. Encompass the regions in which fluid motion exists.

3. Permit interfacing of the hydrodynamic and transport models to enable feed-in of hydrodynamic model output into the transport model. The models involve the solution of algorithms by explicit and implicit finite difference methods, respectively.

4. Enable proper "flagging" of cells in order to designate mathematically boundary conditions and other vital, averaged parameters which are unique to each cell, such as cell geometry, depth, flow resistance, dispersion coefficients, and inflow and outflow sources.

5. Enable designation of model excitation cells.

The solution of the algorithm involved in the interfacing hydrodynamic and transport models necessitates use of quantities from surrounding grid cells in order to compute values in any particular cell. In order to compute values near a land-water boundary, the boundaries are manipulated to act as "reflecting barriers". That is, a layer of image cells are constituted outside of the fluid boundary, and the values for these image cells are dependent upon the special land-water boundary conditions which exist at the junction of the actual and image cells. Sayre and Chang (1968) have validated the practicality of the reflecting barrier boundary concept

insofar as open-channel lateral distributions are concerned, based on comparisons of open-channel dye distribution curves with theoretical curves based on the Fickian model. However, due to lack of detailed vertical dispersion data, they were not able to evaluate the applicability of the concept at channel bed and at the water surface. Nevertheless, they concluded that the reflecting barrier principle was reasonably adequate for predicting the dispersion distance required for uniform mixing in the vertical direction.

The reflecting barrier concept is quite simple and can be applied to an extremely wide variety and combination of boundary conditions. The basic concept is easily illustrated by the treatment of the impermeable boundary. Assume that an impermeable boundary impedes a flow in the x-direction. Then, if $C^k_{i,\,j}$, the concentration existing in a live cell is assumed to exist symmetrically also in its image cell across the impermeable boundary, an equivalence of concentration is achieved; there is an absence of gradients and hence, no transport can occur. That is,

$$C^k_{i,\,j} = C^k_{i+1,\,j}$$

and

$$\frac{\partial C}{\partial x} = 0 \quad . \tag{4-19}$$

This is a mathematical construct representing an absence of transport and the consequent neutralization of other kinetic gradients.

After the irregularly-shaped planimetric land-water boundary has been linearized into line segments of the horizontal grid network, a flagged cell system is devised which best represents the unique physical characteristics of a given water impoundment and which will serve as the mathematical computation grid. A typical grid scheme and boundary indexing system for cells is shown in Figure (5-5), indicating the i and j rectangular coordinates which specify the cell centers. The x-axis (along which i-values are measured) is oriented in any direction of convenience. The cell sizes are selected as a compromise between the requirement of retaining the essential features of the physical system and the requirement of selecting the proper grid interval to avoid, on one hand, computational coarseness and, on the other hand, excessive fineness requiring large computer storage requirements. The complete flagged cell system includes not only the cells inside the boundaries but also the special image cells, input and output cells and others which fall outside the boundaries. Each quadrilinear cell is identified according to the unique conditions that exist at its four sides. The cell flag system used in the numerical models developed in this study, is the system designed by Masch, et al (1969) in their development of numerical models for tidal and estuarine hydrodynamics, and is illustrated schematically in the work of

Shankar (1970). Following are the salient types of flags of the cell system:

1. External Boundary Cells, i.e., cells which fall outside the impoundment system boundaries but border the system. There are two types:

   a. Flow - Indicate inflow to or discharge from the system.

   b. No flow - Indicate zero flow across the cell boundary.

2. Empty Cells, i.e., cells which fall outside the system boundary and not used, but needed to fill out the indexing matrix.

3. Internal Boundary Cells, i.e., cells which fall inside the system boundary or on internal barriers. There are three types:

   a. Flow - Indicate inflow to or discharge from the system.

   b. No flow - Indicate zero flow across the cell boundary.

   c. Barrier - Indicate a submerged or partial barrier.

4. Internal Cells, i.e., cells which fall inside the system boundary but are not adjacent to the system boundary or any internal barrier.

Algorithms

Three models are involved in this study representing the basic components of the hydrodynamic physical system:

1. A lake or reservoir hydrodynamic model.

2. An open-channel transport model.

3. A lake or reservoir transport model.

The Lake or Reservoir Hydrodynamic Model. The two-dimensional, tidal hydrodynamic model for shallow, well-mixed bays and estuaries, developed by Masch, et al (1969) was found to be easily adapted to the shallow layer in well-mixed fresh water impoundments. The cellular velocities computed from the model for any given set hydrometeorological and hydromechanical conditions approach steady state values if the computations are carried out according to its long-term model assumptions. Velocities were generated until they stabilized to an average fluctuation of 17.5%. This matter is discussed in greater detail in Chapter VI. These averaged velocities served as direct input to the transport model.

The hydrodynamic model involves the simultaneous solution of two dynamic equations of motion and the continuity equation. The motion equations are:

$$\left.\begin{aligned} \frac{\partial Q_x}{\partial t} + gD\frac{\partial H}{\partial x} &= K'V^2\cos\Psi - fQQ_xD^{-2} + \Omega Q_y \\ \frac{\partial Q_y}{\partial t} + gD\frac{\partial H}{\partial y} &= K'V^2\sin\Psi - fQQ_yD^{-2} - \Omega Q_x \end{aligned}\right\} \qquad (4\text{-}19)$$

where:

Q_x and Q_y = the mean flows per unit width in the x and y direction, respectively.

H = water surface with respect to Mean Sea Level (MSL) as datum.

D = depth of water at position x, y at time t.

$Q = (Q_x^2 + Q_y^2)^{1/2}$.

f = dimensionless bed resistance coefficient computed from the Manning's equation as $(gn^2/2.21\ D^{1/3})$ where n is Manning's roughness coefficient.

V = wind velocity at 10 meters elevation above the water surface.

Ψ = the angle between the wind velocity vector and the positive direction of the x-axis, measured in a counter-clockwise direction.

K' = a dimensionless coefficient in the Van Dorn (1953) relation for wind stress, as reported by Shankar (1970).

g = acceleration of gravity.

Ω = the Coriolis parameter, arising from the earth's rotation. The parameter is equal to $2\omega \sin\Phi$; ω is the angular velocity of the earth taken as 0.73×10^{-4} radians per second.

Φ = the latitude.

The two-dimensional continuity equation is:

$$\frac{\partial Q'_x}{\partial x} + \frac{\partial Q'_y}{\partial y} + \frac{\partial A}{\partial t} = 0 \qquad (4\text{-}20)$$

where:

Q'_x and Q'_y are the components of the volume rates of flow in the x and y directions.

A = cross-sectional area of flow.

Equations (4-19) are essentially in the form regarded by Chow (1954) as adequate to describe approximately the motion of sea water. With

further modifications they serve also to describe approximately, within the framework of comparative investigations, the hydrodynamics of large water impoundments. The transformation of the partial differential Equations (4-19) and (4-21), in terms of finite difference approximations, are contained in the work of Masch, et al (1969). The computer program (a complete description of which is not within the scope of this study), includes the solution of the foregoing equations by the explicit difference method, and is available at The University of Texas at Austin.

The Open-Channel Transport Model. The main purpose of the channel transport model is to generate inputs of fully-mixed, temporally-varying material concentrations into the excitation cell of the reservoir transport model. Two equations are used in the channel model to compute the temporally-varying inputs resulting from instantaneous, point source dosages of conservative material into the channel. For practical modeling purposes, the channel model is "energized" by a finite quantity of conservative material injected uniformly and instantaneously over the cross section of the flow at $x = 0$ and $t = 0$.

The first equation provides for computation of the longitudinal dispersion coefficient:

$$D_L = 77\, n\, V\, R^{5/6} \qquad \text{(Ippen 1966)} \qquad (4\text{-}21)$$

where:

D_L = the longitudinal dispersion coefficient.

n = Manning's coefficient of roughness.

V = the average longitudinal velocity.

R = the hydraulic radius of the channel.

The second equation is to compute the distribution of concentrations:

$$C = \frac{M}{A\rho(4\pi D_L t)^{0.5}} \exp\left[\frac{-(x-\bar{U}t)^2}{4D_L t}\right] \quad \text{(Ippen 1966)} \qquad (4\text{-}22)$$

where:

M = mass of material injected.

A = channel cross-sectional area.

ρ = density of material injected.

D_L = longitudinal dispersion coefficient.

t = time elapsed since release of the diffusant.

$\bar{U}$ = average longitudinal velocity.

Equation (4-22) is Taylor's (1954) approximate solution for Equation (4-23), below the dispersion equation in a one-dimensional, open-channel flow, having a uniform cross-section and a mean velocity, for a point source and a fixed coordinate system:

$$\frac{\partial C}{\partial t} = D_L\left[\frac{\partial^2 C}{\partial x^2}\right] - \bar{U}\frac{\partial C}{\partial x} \; . \qquad (4\text{-}23)$$

1. Major Equations Considered in Selection of the Algorithm. Equations (4-21) and (4-22) were selected after a careful consideration of open-channel dispersion and transport equations. The selected equations together constitute a practical algorithm for an open-channel transport model, which envisages the channel as a "feeder" of fully-mixed flows of any desired concentration into an impoundment. The channel transport model is a necessary adjunct to the impoundment transport model.

Following are some of the major concepts and factors considered in making the selection.

a. Hays, et al (1966) suggested that for streams, a "dead zone" model based on the use of time-averaged concentrations and velocities, is superior to and is more realistic than a dispersed flow model based on the convective-dispersion equation, Equation (4-23). The "dead zone" mathematical model conceptualizes the existence of two major transport regions of flow, an upper active region and a lower stagnant region, physically connected by a "mass transfer mechanism," which can be described by two coupled partial differential equations.

b. White and Gloyna (1970) reported that the simplified one-dimensional dispersed flow model, Equation (4-23) and the solution, Equation (4-22), served as the most practical expression of the "initial condition" in the finite difference formulation of the one-dimensional, open-channel transport model, based on instantaneous release of radioactive substance.

Following is a general assessment made by Thackston and Krenkel (1966) of the major equations for estimating dispersion coefficients in streams:

a. Taylor Equation:

$$D_L = \frac{\bar{U}^3 t_{1/2}}{4 \times \ln 2} \qquad (4\text{-}24)$$

where:

D_L = dispersion coefficient.

x = distance from tracer injection point to observation point.

$2\,t^2_{1/2}$ = time during which concentration is greater than one-half the maximum concentration.

$\bar{U}$ = average velocity of tracer cloud.

This equation yielded only rough estimates because of the assumption of normal distribution, and was considered useful only for preliminary estimates.

b. Parker Equation:

$$D_L = \frac{x^2 m_2}{2\ m_1} \qquad (4\text{-}25)$$

where:

m_1 = first moment of time-concentration curve.

m_2 = second moment of the time-concentration curve.

c. Fischer Equation:

$$D_L = \frac{\bar{u}^2 (\sigma^2_{t_2} - \sigma^2_{t_1})}{2\Delta t} \qquad (4\text{-}26)$$

where:

$\bar{u}$ = average longitudinal velocity.

$\sigma^2_{t_1}$ = variance of the time-concentration curve, Station 1.

$\sigma^2_{t_2}$ = variance of time concentration curve, Station 2.

Δt = average time of flow between stations and basically:

$$\sigma_t^2 = \frac{\Sigma c t^2}{\Sigma c} - \left[\frac{\Sigma c t}{\Sigma c}\right] \qquad (4\text{-}27)$$

where c is the concentration at time, t.

Equations (4-25) and (4-26) were found subject to errors common to solutions which involve moment functions. The errors stem from skewed concentration-time curves. Fischer (1966) emphasized the difficulties of obtaining reliable variances for high-skewed, long-tailed concentration-time curves, and recommended that values of D_L computed by the method of variances be verified by field test.

d. Levenspiel and Smith Equation:

$$D_L = \frac{\bar{u} x}{8}\left[\sqrt{8\sigma^2 + 1} - 1\right] \qquad (4\text{-}28)$$

where:

$$\sigma^2 = \frac{\sigma_t^2}{t_{ave}}$$

$$t_{ave} = \frac{x}{\bar{u}}$$

Equation (4-28) depends heavily on second moments and, therefore, subject to errors of skewed-curve tails.

e. Harris Equation:

$$\hat{D}_L = \frac{\hat{\bar{U}}(\hat{\bar{U}}\bar{t} - x)}{2} \qquad (4\text{-}29)$$

where:

$$\hat{\bar{U}} = \left[\frac{1}{n}\sum\frac{1}{t}\right]. \qquad (4\text{-}30)$$

The Harris equation was adjudged to give a better D_L estimate than the Levenspiel-Smith equation because it is dependent only on the first moment. Also, in contrast to the others, the Harris equation does not use $\bar{u} = \frac{X}{t}$ or $\frac{Q}{A}$.

2. The Significance of Average Velocity and Time-of-Travel. Thackston and Krenkel (1966) emphasized that a proper determination of "mean travel-time", or "flow-through time" was vital for computing the dispersion coefficient. Since in any basic approximation equation, $\bar{u}$, the average velocity, is really the average velocity of the tracer cloud, it must be computed from the mean travel-time, and not be the rough calculations of $\frac{X}{t}$ or $\frac{Q}{A}$. There are also misconceptions to guard against.

   a. The average flow-through time is not the same as the peak concentration because inspection of the basic equation for computing the distribution of concentrations Equation (4-22) shows that the exponential term obviously will skew the curve to the right.

   b. The use of the centroid of the time-concentration curve for determining mean travel-time is unjustifiable because it has been shown that the time from dye injection to the centroid is:

$$t_c = \left[\frac{x}{\bar{U}} + \frac{2D_L}{\bar{U}^2}\right] \qquad (4\text{-}31)$$

and the time to the peak, t_{max} is:

$$t_{max} = \frac{-D_L \pm \sqrt{D_L^2 + \bar{U}^2 x^2}}{\bar{U}^2} \quad . \tag{4-32}$$

Thus, according to Thackston and Krenkel (1966) neither the mode nor the centroid of the time-concentration curve can represent the average flow-through time; they surmise that it must have a value between the mode and the centroid. They concluded that all methods analyzed for estimating D_L and $\bar{u}$ from the time-concentration curve are not valid unless the observed curve fits the assumed mathematical model. Therefore, the practical use of any D_L equation involves a trial-and-error correction process following the initial estimate of D_L.

Yotsukura and Fiering (1964) found that solutions for turbulent flows with logarithmic velocity distribution, show that the "longitudinal distribution of solute concentration is highly skewed at intermediate time stages but gradually approaches a Gaussian normal pattern as the dispersion progresses". In this light, the Taylor solution, Equation (4-22) adopted in this study for determining concentrations is apropos since it is based on the concept that the tracer material in a uniform channel spreads out as a symmetrical Gaussian curve whose peak concentration, moving at velocity u, decreases in the positive x-direction.

At this point, it is well to reiterate that in the discussion thus far, the instantaneous manner of dye injection has been implied. However, the equation for computing the concentrations due to continuous, steady release in a given time interval, can be derived from the basic equation by integrating the following expression which represents a concentration increment, dc, due to an input dM at time, t, (Reference Harleman, 1966):

$$dc = \frac{dM}{A\rho(4\pi D_L(t-\tau))^{1/2}} \exp -\frac{(x - v(t-\tau))^{1/2}}{4D(t-\tau)} \quad . \tag{4-33}$$

Harleman (1966) solves Equation (4-33) using Riemann's integrals.

See Appendix B for the computer program (PROGRAM CONCO) which solves the open-channel transport model algorithm. Also see Appendix C for the computer program (PROGRAM TRACE) used to compute dispersion coefficients by the method of moments.

The Lake Transport Model. The lake transport model uses the Peaceman-Rachford finite difference method for the solution of the two-dimensional, convection-dispersion equation. The mathematical formulation was developed in detail earlier in this chapter. See Equations (4-13) to (4-18), inclusive. In addition, detailed descriptive data for the computerized program (PROGRAM TRACER) is contained in Appendix A.

Recall that the hydrodynamic and channel models provide inputs to the transport model, namely (a) steady-state component velocities for each cell and, (b) well-mixed, time-concentration inflows for the excitation cell.

Rationale for the Selection and Design of Two-Dimensional Lake Hydrodynamic and Transport Models.

The rationale for the selection and design of a horizontal, two-dimensional concept for the lake or reservoir hydrodynamic and transport models in lieu of one-dimensional or three-dimensional concepts warrants explanation. Obviously, the magnitude of energy associated with the two-dimensional, air-water interface of the water impoundment differs significantly from the energy associated with the entire three-dimensional

impoundment physical system. The questions arise: What is the rationale for, and what is the value of a two-dimensional concept?

To answer these questions we must first consider and clarify the matter of what is meant by the "state of the system" insofar as a lake or reservoir is concerned. In thermodynamics and electrodynamics, the concept of the "state of the system" is fundamental. In hydrodynamics, specific clarifications are needed. The classical thermodynamic, electrodynamic and mechanical concepts of "state", were based on the premise that "state" is the total of all the measurements that can be made on the system at the present time. That is, two systems were considered to be in the same "state" if all the measurements capable of being made now on the two systems, produced the same results. But this concept of "state" was shattered by the facts of irreversible thermodynamics. As a result, the old deterministic thesis of "state" now can be retained logically only if it is stated with the following stipulations:

Two systems may be considered in the same state if all measurements presently capable of being made give the same results and, if the past history back to some selected time is also the same. The important implications of this qualified concept of "state of system" require that systems can be considered in the same state only if they behave the same in the future under the same environment. Thus, "state" is "determined" in terms of present measurements and past history, because the

future is determined by these requirements. Bridgman (1959) states that in the quantum domain of physics we have been confronted with the fact that the present state of a system does not determine its future state because it is possible to have a number of systems all with the same "present state", but different future states under identical external conditions. Thus, it is no longer feasible to persist in a wholly deterministic philosophy. It is not possible in thermodynamics, nor electrodynamics; nor electrodynamics; nor is it possible in hydrodynamics. In the realization of this fact, perhaps, lies the most intrinsic value of numerical models, which enables producing "identical replicas", as Bridgman (1959) terms them, of systems and conducting on them an indefinite number of experiments.

It is concluded that in hydrodynamics, the description of the "state of system" should be in terms of operations which one can actually perform.

As was experienced in other branches of physics, it appears rational in hydrodynamical systems also, to adopt a concept of "state" based on two surface variables and one time variable since they appear to be equivalent, in effect, to the three space variables. This, precisely is the rationale of the finite differences method adopted in this study. In other words, it is reasonable to assume that the evaluation of the hydrodynamical state of the system can best be made from the point of view of a surface and its history, which has full instrumental significance, rather than from

the instrumentally meaningless specifications in terms of fields throughout three-dimensional space.

The next questions which arise are: What are all the possible measurements? How shall we be sure we have investigated all environments? The impact of this discussion, in short, is that we can in no ultimate sense separate a system from its states or a system from its environment. In order to achieve some sort of reasonable reconciliation between models and reality, Bridgman (1959) takes the view that the best we can do is:

> "Given an isolated enclosure as a function of time and all the measurements that can be made inside the enclosure as a function of time, then these measurements will be found to be correlated into some sort of pattern."

He suggests that a synthesis can be made by the "principle of essential correlation". The views of Thackston and Krenkel's (1966) on the use of numerical models and the conduct of field tests typify the Bridgman (1959) philosophy. They contend that predictions based on analytical solutions under assumed conditions must be experimentally verified; a major pitfall of experimental work being that it is often not conducted under the conditions assumed in the derivation of the models being verified. The most common gaps arise from assumptions concerning.

1. Non-uniform flow;
2. Lateral velocity profiles.

With the collapse of such assumptions in the face of actual tests, the

experiments actually neither substantiate nor refute the models investigated.

Therefore, in preparing for the field verification of the models of this study, attempts were made to conduct field operations under conditions as close as possible to a uniform, two-dimensional well-mixed stratified, flow regime.

Also, Thackston and Krenkel (1966) have cautioned on the danger of applying ideal, two-dimensional models to real three-dimensional systems. However, they support the use of the Equation (4-23), that is:

$$\frac{\partial c}{\partial t} = D_L \frac{\partial^2 c}{\partial x^2} - U \frac{\partial c}{\partial x}$$

to a three-dimensional system on the grounds that the solution to the three-dimensional equation converges asymptotically to the solution of the one-dimensional equation for long dispersion times. And, even if uniform flow does not exist, Equation (4-23) may be used if the average value of D_L within a river reach is used.

The prediction of D_L and transport in impoundments which are complicated by dead zones, sharp bends, sloughs, and sand bars and other discontinuities can and should be provided for by careful cell and boundary design. Therefore, effort has been made to prepare the transport model to provide for features which are unique to the verification zone at Lake Bastrop.

Shull and Gloyna (1968) demonstrated in a comprehensive manner the approach necessary in any attempt to make a rigorous specification of the "state" of a physical system. In their analysis of numerical models relative to radioactivity transport in water, they concluded that:

> ". . . numerical modeling techniques frequently are only applicable to certain ranges of parameters, necessitating the inspection of these parameters for the intended application of the model."

The field tests which will be described subsequently in this study will indicate the special efforts made to synthesize the analytical and actual systems by a series of actions involving simulation, prediction and verification of the various hydrodynamical phenomena involving mixing, dispersion and transport.

CHAPTER V

THE SELECTION AND USE OF LAKE BASTROP AS A GENERAL LAKE HYDRODYNAMIC SYSTEM

General Description of Lake Bastrop, Texas

Lake Bastrop, Figure 5-1, was selected as the hydrodynamic system for development of the numerical lake hydrodynamic and transport models, and for the field verification of these numerical models. Lake Bastrop is well-suited for the above purposes. A description will be given of the essential variables and parameters involved in developing and verifying the lake hydrodynamic model and lake transport model.

Lake Bastrop provides steam condensing and plant cooling water for the Sim Gideon Electric Station, operated by the Lower Colorado River Authority (LCRA). The plant has two 125,000 kilowatt units. The impoundment is created by a dam located off the Colorado River on Spicey Creek, 3-1/2 miles northeast of Bastrop, Texas. The dam is an earth-filled embankment with a concrete spillway and two tainter gates. The total length of the dam is 4,500 feet, the height at the spillway is 85 feet. The two 45-foot x 27-foot gates have a discharge capacity of 53,000 cfs with the lake at elevation 454.30 feet (MSL). The surface area is about 906 acres and the storage capacity is about 16,600 acre-feet at the normal operating level 450.00 feet (MSL), see Figure 5-2. The electric power

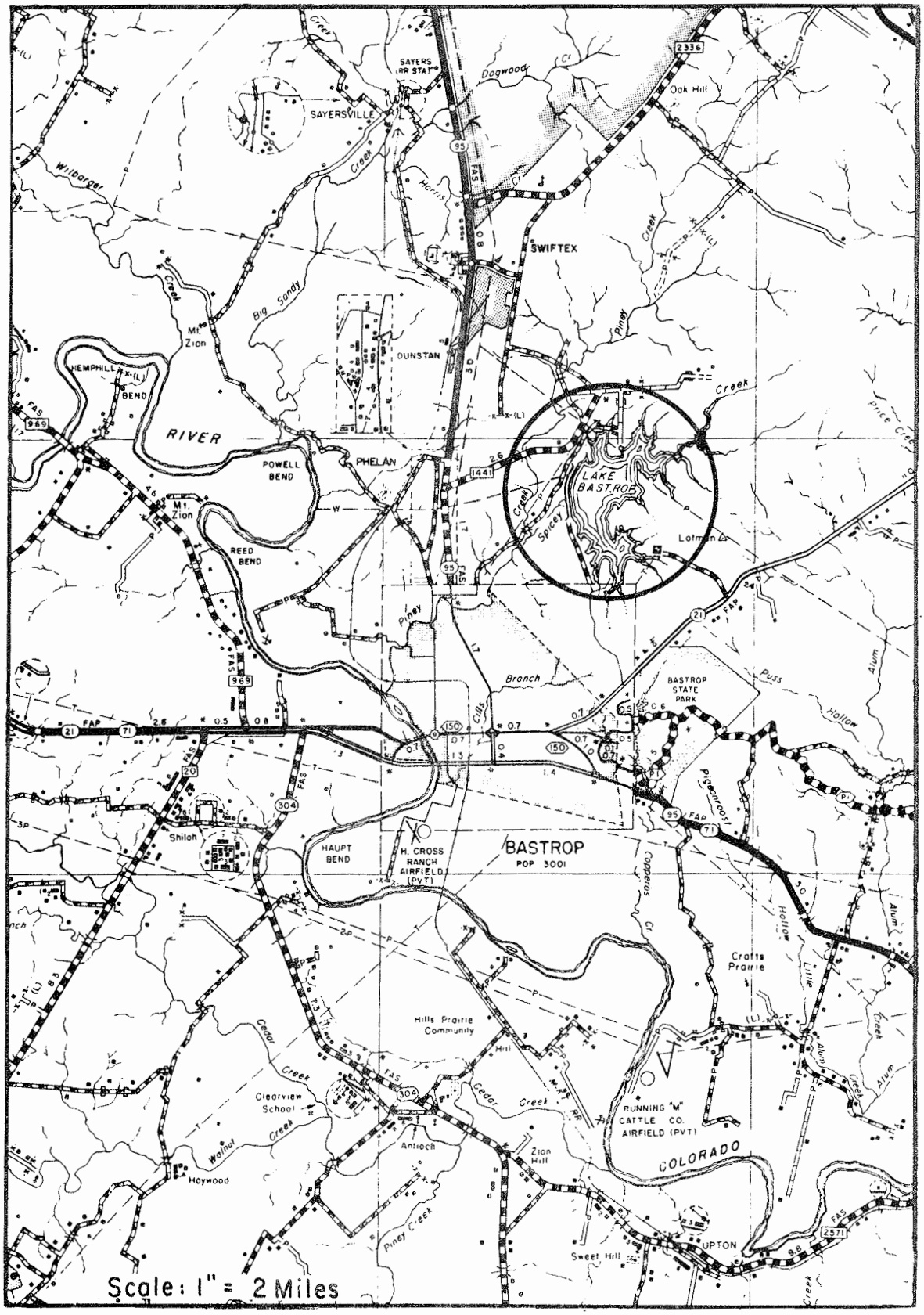

Figure 5-1. Lake Bastrop, Texas.

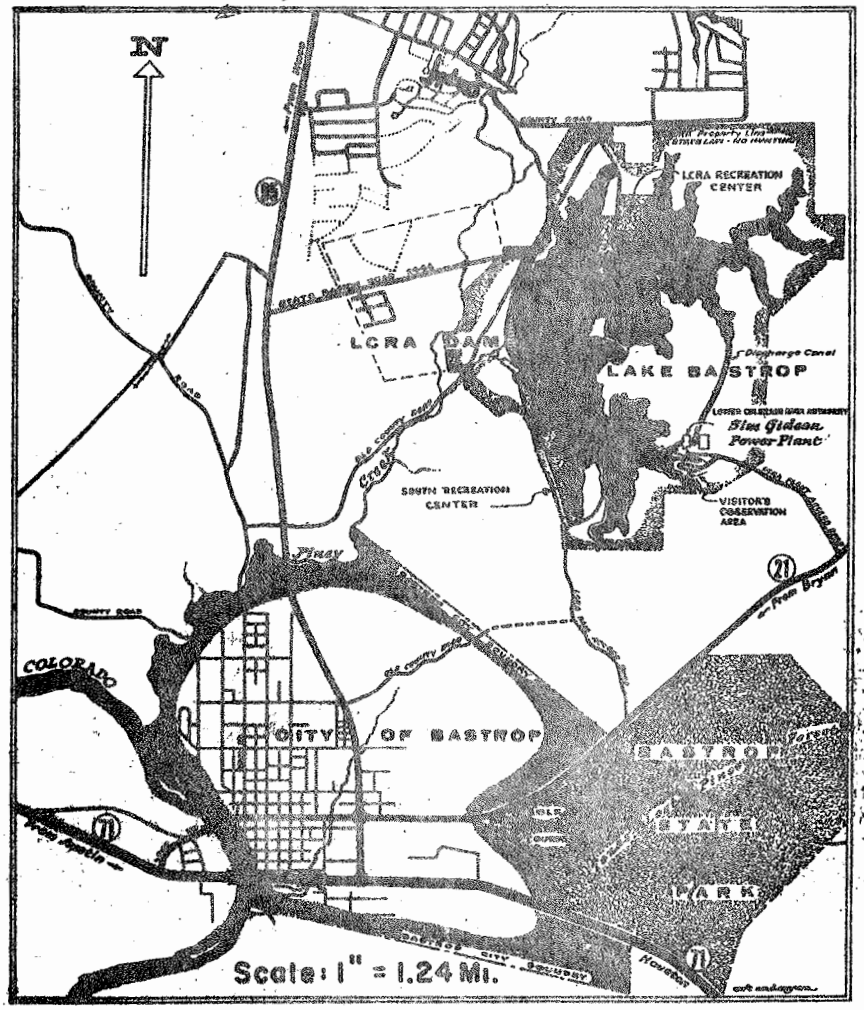

Figure 5-2. Lake Bastrop and Sim Gideon Power Plant.

plant is located near the southern end of the lake with discharge canal flowing into the northern portion of the lake, providing a mean circulation path of about 4 miles long for the normal plant flow discharge of 500 cubic feet per second or 324 million gallons per day.

The reservoir level is maintained at a constant level and replenishment of evaporation losses is made through a pumping station, on the Colorado River at Powell Bend. The pump station has three 300 HP pumps, designed to pump in parallel 15,000 gallons per minute against an approximate head of 220 feet. A 3-1/2 mile, 33-inch concrete water pipeline connects the pumping station to Lake Bastrop. The lake is virtually a closed, steady-state circulation system, involving a steady discharge of 500 cfs and a steady plant intake of 500 cfs. There are no other major inflows or outflows.

The Discharge Channel

The discharge channel, (Figure 5-3, and photos, Figures 5-4) is a concrete lined, trapezoidal channel with side slopes of 2-1/2 on 1, a length of 4,200 feet, a base width of 12 feet, a depth of 13 feet, and an average slope of 0.047%. An additional 700 feet of discharge canal has been rough-graded only and is not lined. At normal plant flow of 500 cfs the depth of water at the centerline of the channel is 10.3 feet and the average velocity is 1.3 feet per second.

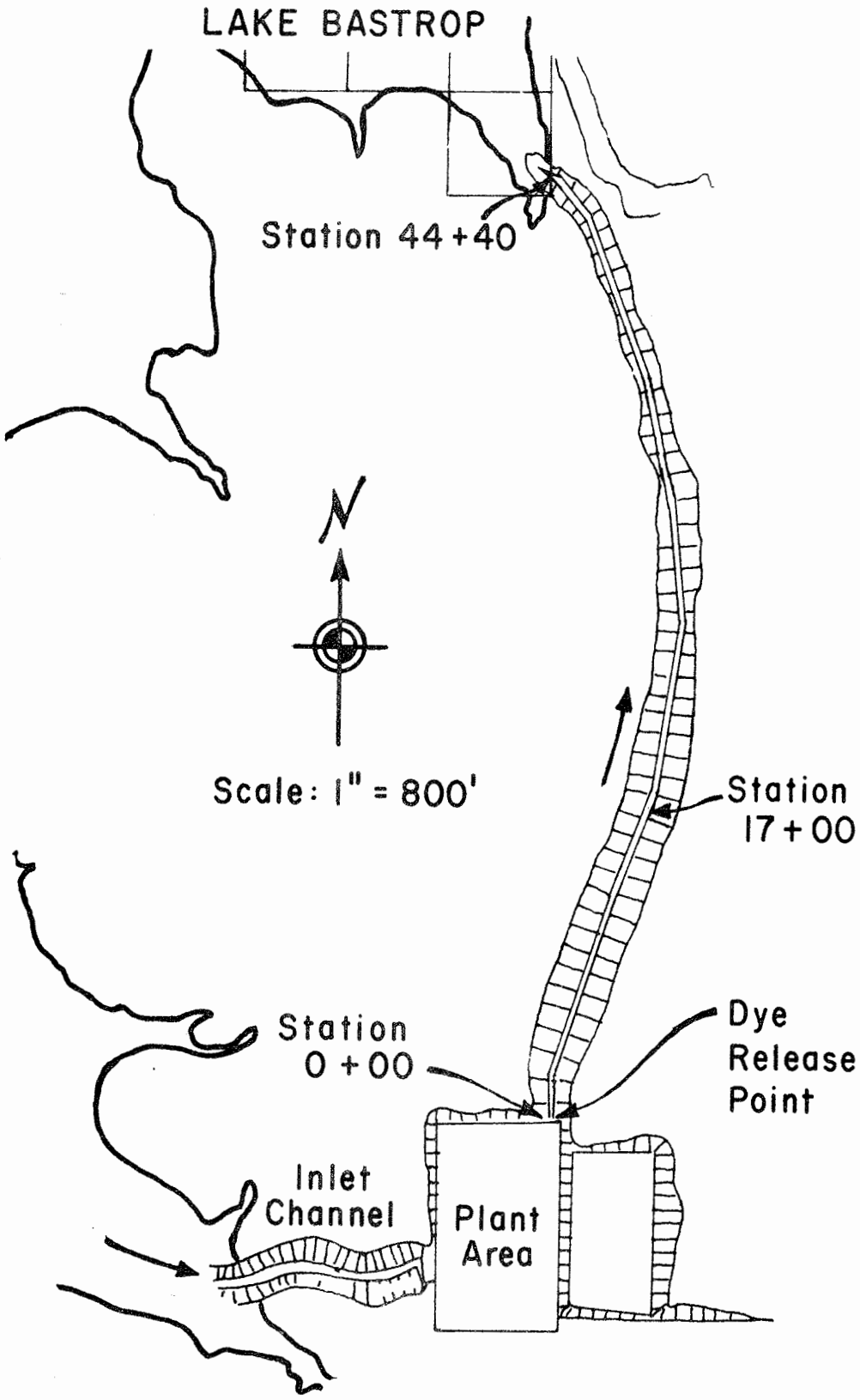

Figure 5-3. Power Plant Discharge Channel into Lake Bastrop.

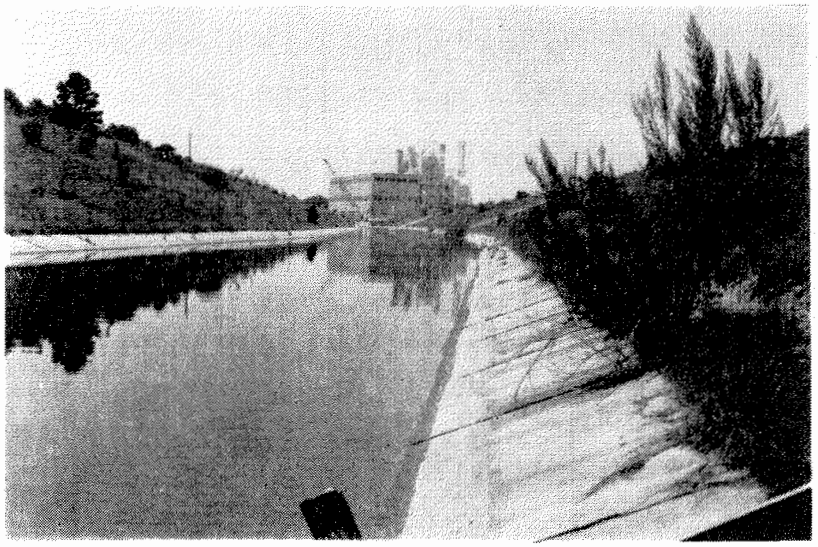

A. View to the South from Station 17 + 00 toward Power Plant.

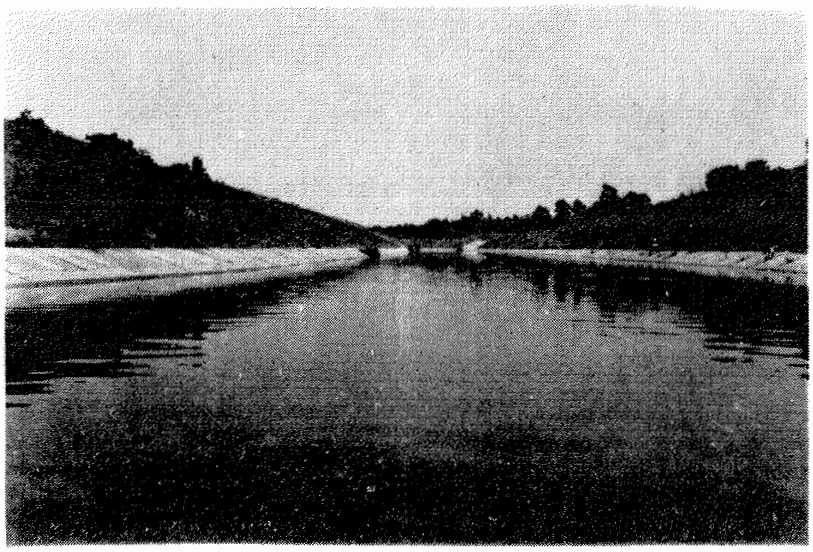

B. View to the North from Station 17 + 00.

Figure 5-4. Lake Bastrop Discharge Channel.

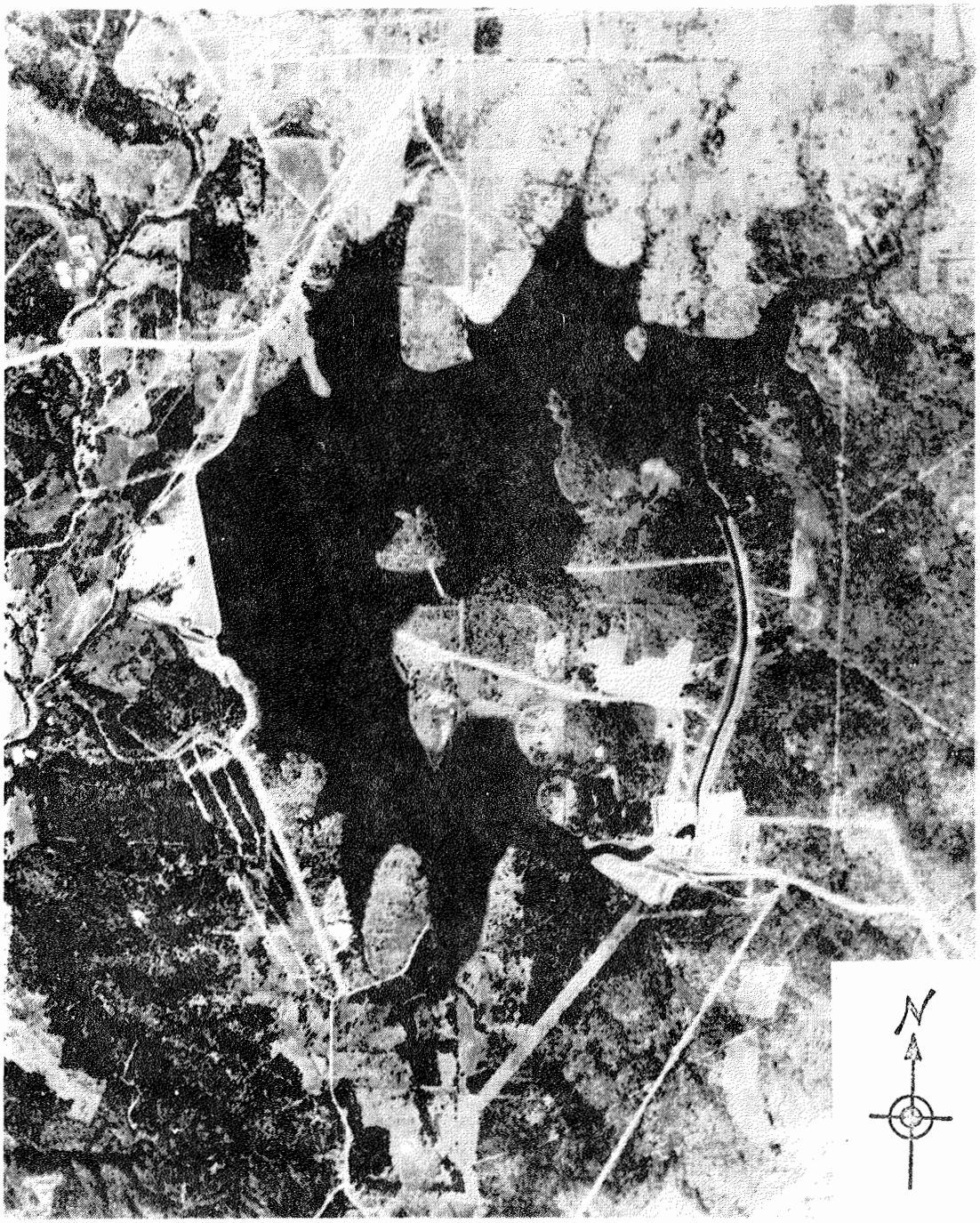

Scale: 1" = 0.62 miles

Figure 5-4 C. Vertical Aerial Photograph of Lake Bastrop, Texas. (Source: LCRA)

Essential Hydrologic Data

Figure D-1 and D-2, Appendix D, depict the typical vertical temperature profiles at the centrally-located LCRA temperature Station No. 6. Figure 5-5 shows the locations of all test cell markers and stations involved in field measurements. Station No. 6 has been used as a general indicator for the lake temperature. It will be noted from Figure D-3, that the lake has a history of stratification. During the 5-month period of interest (i.e., May - September), the upper and lower limits of the thermocline follow a characteristic pattern, and the epilimnetic stratum is 10 to 15 feet thick. The average thickness of the thermocline is greatest during the month of June.

Figures D-4 and D-5 show the maximum and minimum yearly surface temperatures at each of the LCRA temperature stations and also the contemporaneous electrical power generation loads and ambient temperatures. The variations in electrical load are due to normal demand fluctuations.

Figure D-6 depicts the average monthly temperature at the surface and at the 30 foot depth at LCRA Temperature Station No. 6 for the past 5 years. It should be noted that a variation of from 10 to 20 degrees Fahrenheit can occur during the mid-summer months.

Figure D-7 shows the average monthly surface temperatures at the power plant discharge and at the power plant intake during the past 4 years.

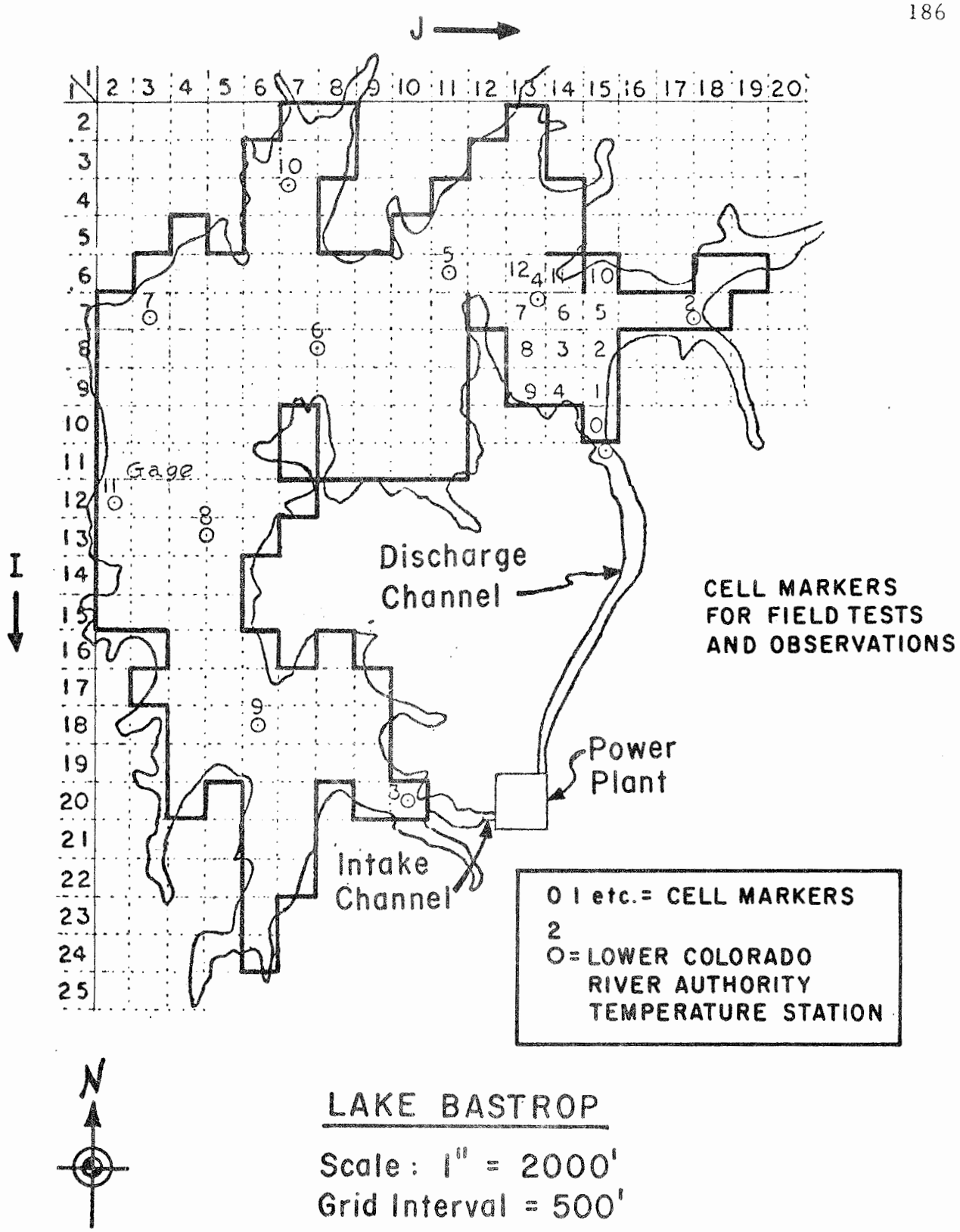

Figure 5-5. Cell Markers and Stations for Field Tests and Measurements.

Figures D-8 and D-9 show results of Lake Bastrop water quality tests, in terms of pH, chlorides, total dissolved solids and the total hardness.

The purpose of the foregoing considerations of Lake Bastrop water temperature and composition is to bring out two facts which have special relevance in the selection of Lake Bastrop for the design and verification of the Alternating-Direction Implicit Transport Model.

First, water temperature is the main factor governing density and density variation with depth in Lake Bastrop. The high quality of the Lake Bastrop water generally precludes attributing density stratification to other than temperature. This eliminates a troublesome question which arises when dealing with impoundages having water of lesser quality. For example, in analyzing the Fontana Reservoir field measurements in connection with the temperature prediction model (See Chapter II), Elder and Wunderlich (1968) reported that improved density-measuring methods would have to be developed before they could conclude that factors other than temperature caused density stratification in Fontana Reservoir. Also, Fietz and Wood (1967) attested to the difficulty of measuring three-dimensional density currents of engineering interest such as the discharge of temperature-varying, silt-laden, or chemical-bearing effluents into impoundments. They concluded that a better understanding of the behavior of non-suspended (i.e., dissolved chemical substances) density currents is necessary before study of the more complex suspension or turbidity density currents can be undertaken. The selection of Lake Bastrop permits assumption of stratification due to thermal causes and thus precludes the complexities of non-thermal stratification.

Secondly, under the present state of technology, none of the ordinary, natural constituents or properties of water are amenable to economic or reliable measurements which would afford greater insight into mixing, dispersion and transport phenomena. The use of additive tracers must be considered

> for study of these phenomena. Regarding this matter, Elder and Wunderlich (1968) reported that in the cited Fontana Reservoir Study, various data were taken on changes in water properties which occurred during storage time in the reservoir. The properties measured included temperature, electrical conductivity, light extinction, and dissolved oxygen concentration. None of the properties afforded a basis for a realistic, efficient correlation of the effects of water movements and diffusion. Chemical, biochemical and other processes intervened in the measurements and obscured the transport and mixing effects.

Thus, from a review of the Bastrop hydrologic data, it is concluded that the use of temperature-stable, fluorescent dye tracers and conventional tracing techniques are proper for hydromechanical transport analysis and measurements in Lake Bastrop. The high quality waters would introduce a minimum of background effects. However, careful adjustment of fluorescence readings for high temperature must be made by accurate fluorometer precalibrations. Another factor entailing some adjustment is the anticipated dye sorption and delayed release due to the proliferating aquatic plant, (Myriophyllum heterophyllum).

Special Hydromechanical and Morphological Aspects of Lake Bastrop

Lake Bastrop presents an excellent combination of lake and reservoir morphology for field measurements and model verification. Refer to earlier Figures (5-2) and (5-4). The lake consists essentially of a small and a large basin. The lake orientation is such that both the longest and shortest fetches of the impoundment occur in a north and south direction, the direction of prevailing winds throughout the year.

The eastern part of the lake, having the characteristic of a small discharge mixing basin, is ideal for the observation of wind effects over short fetches and also for the field analysis of hydrodynamic and transport phenomena unique to shallow lakes of between 10 to 30 feet in depth with vertically well-mixed flows restricted in a shallow surface stratum. The western part of the lake is ideal for the observation and measurement of wind effects over long fetches and other hydromechanical and hydrodynamic effects unique to deeper reservoirs. Vertical aerial photo, Figure 5-4C, clearly shows the dendritic configuration of Bastrop Lake which is typical of man-made lakes. Aerial photo interpretation shows areas that are likely to have similar limnological characteristics. For example, one can identify narrow but relatively deep arms not likely to be subject to strong wave action, deep areas where there is a strong possibility of stable or periodic thermal stratification, and shallow siltation areas subject to possible extensive floating vegetation.

Physical reconnaissances on the lake indicated that:

1. In the central portions of the lake, wind currents generally prevail; flow-through currents are not discernible. In shallow areas and along shore, the water and wind movement is synchronous. In the deeper central portions there is no apparent immediate synchronous relationship between the wind and water movements.[8]

---

[8] Zumberge and Ayers (1964) stated that "The time lag between application of the new (wind) stress and modification of the currents appears to be inversely dependent upon the ratio of new stress magnitude and existing current momentum and directly dependent upon the direction difference (up to 180°) between the new transport direction and the existing current direction."

2. Due to the different but evident peculiarities of regime which prevail in the shallow eastern and the deeper western portions of the lake, it is necessary to take these differences in consideration in the study of the hydrologic processes throughout the lake, in the application of the models, and in field tests.

In addition, the discharge channel serves as a steady "mechanism" for pre-mixing and injecting dye tracer dosages into the lake. The controlled operational flows of cooling water facilities making accurate instantaneous or continuous dye releases to obtain desired well-mixed flows into the lake. The open-channel also affords ideal anchorages to make dye-peak travel measurements. As such, the discharge channel should be regarded an integral part of the entire hydrodynamic system. Its main purpose, from the transport model point of view is to provide desired concentration inputs (either deterministic or stochastic) in the lake excitation cell. In other words, the channel transport model establishes the "initial conditions" for the lake transport model.

CHAPTER VI

NUMERICAL MODEL ANALYSIS AND SIMULATIONS

Introduction

The thrust of the study to this point has been to formulate the physical system of a reservoir or lake, and to identify the "laws" of mixing and dispersion in water impoundments with a view toward developing practical assumptions which would permit reducing the problem to sets of mathematical equations. After formulating the problem mathematically, methods were selected to obtain mathematical solutions to the sets of equations by models or algorithms solved by computer programs. In this manner, a transport model was developed and, a hydrodynamic model previously developed by others (Masch, et al, 1969) was adapted for use.

These computerized numerical models permit a wide range of simulative and investigative calculations. This study will demonstrate the versatility of the models for hydrodynamical and hydromechanical analysis of a lake or reservoir. These analyses will be seen to have relevance not only to anti-pollution control but to overall reservoir management. The two major tasks now remaining in this study are:

1. To test the mathematical efficiency, and flexibility of the models using hypothetical sets of hydromechanical and hydrometeorological conditions. The objective is to demonstrate the versatility of the models for making preliminary investigations.

2. To verify the numerical model solutions by field tests and measurements. The objectives are: (a) to demonstrate the predictive use of the models, (b) to diagnose the major discrepancies between computed and observed results and, (c) to assess the adequacy of the verification procedures.

The first task will be taken up in this chapter; the second task will be discussed in the next chapter.

Model Simulations

Scope. Pursuant to previously-stated objectives, the following model simulations have been made:

1. Using the hydrodynamic model, velocities and flow circulation patterns for Lake Bastrop under actual high and low flow rates, were computed based on assumed variations in wind.

2. Using the channel transport model, mass transport patterns, concentration distribution patterns and dispersion coefficients were computed based on actual flow rates, specified quantities of conservative material injected and assumed wind conditions.

3. Using the lake transport model, mass transport and distribution patterns of a conservative substance throughout Lake Bastrop under actual high and low flow rates, were computed based on assumed wind conditions, dispersion coefficients and, quantities of dye released.

Use of the Hydrodynamic Model to Compute Steady State Velocities and to Determine Lake Circulation Patterns. Using the horizontal grid-cell system, and average cell depths indicated in Figure 6-1, the hydrodynamic model was used to compute the steady-state velocities for each cell of the lake model, for the following combinations of steady flow and wind conditions:

1. Flow of 180 MGD (280 CFS) with
   a. no wind
   b. 10 (MPH) from south
   c. 15 (MPH) from north
2. Flow of 324 MGD (500 CFS) with
   a. no wind
   b. 10 (MPH) from south
   c. 15 (MPH) from north

The specific conditions outlined above represent actual normal power plant discharge flows and prevailing wind conditions at Lake Bastrop.

Figures 6-2 to 6-7, inclusive, show the steady-state circulation patterns for each of the 6 sets of conditions outlined above. Results confirm evidence presented by Shankar (1970) on the versatility of the Masch hydrodynamical model for application to a wide variety of shallow, vertically-mixed bodies of water.

The cell velocities computed by the hydrodynamic model assume critical importance in the algorithms contained in the transport model for computing dispersion coefficients and concentration distributions. Velocities computed by the hydrodynamic model follow a fluctuating rather than a trend or cyclical time-series pattern. For example, Figure 6-8 shows the fluctuating time-series of the Y-component of velocity in a randomly-selected test cell I = 8, J = 8 at one minute intervals after the

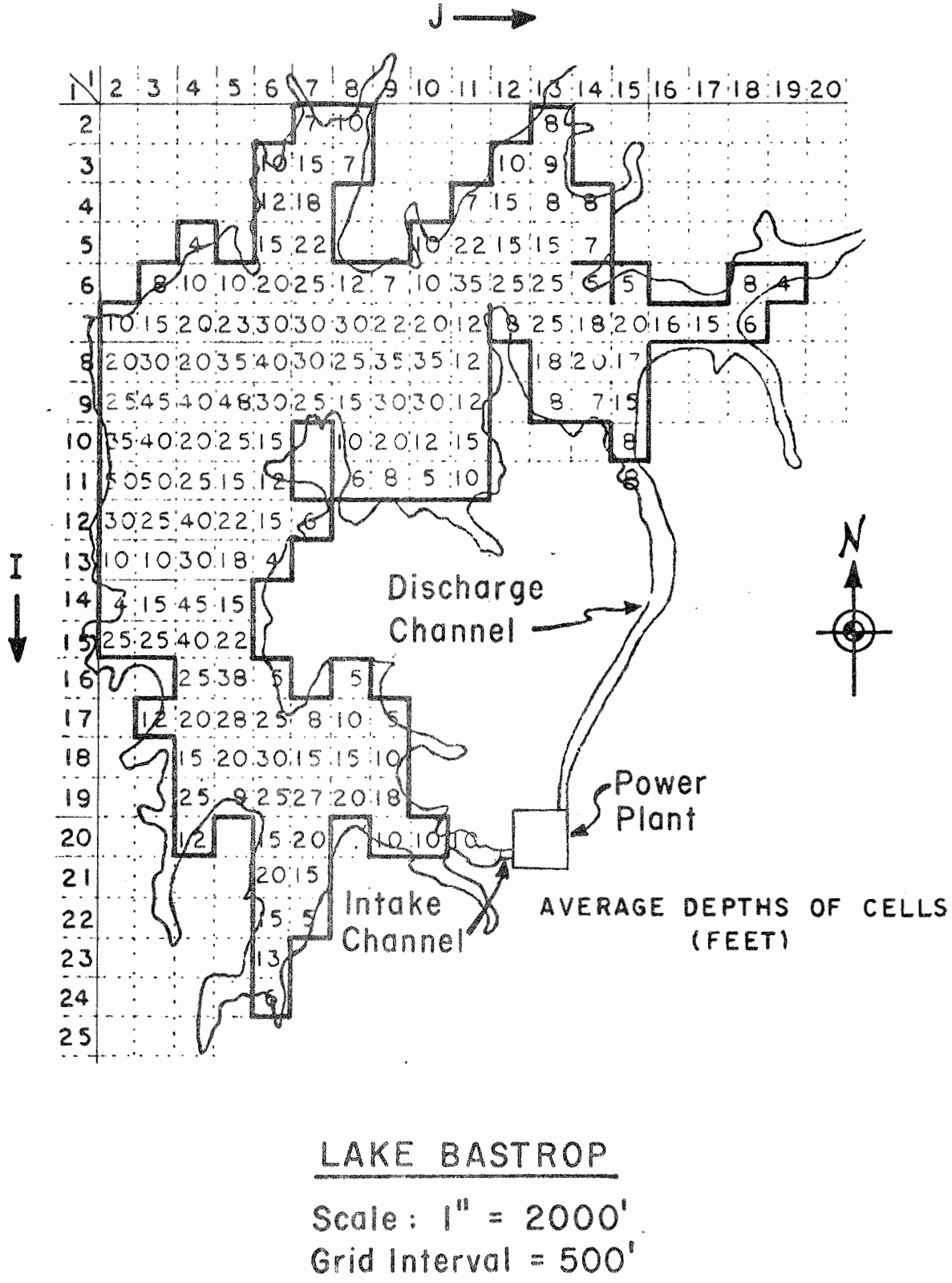

Figure 6-1. Average Cell Depths Used for Lake Bastrop Hydrodynamic and Transport Models.

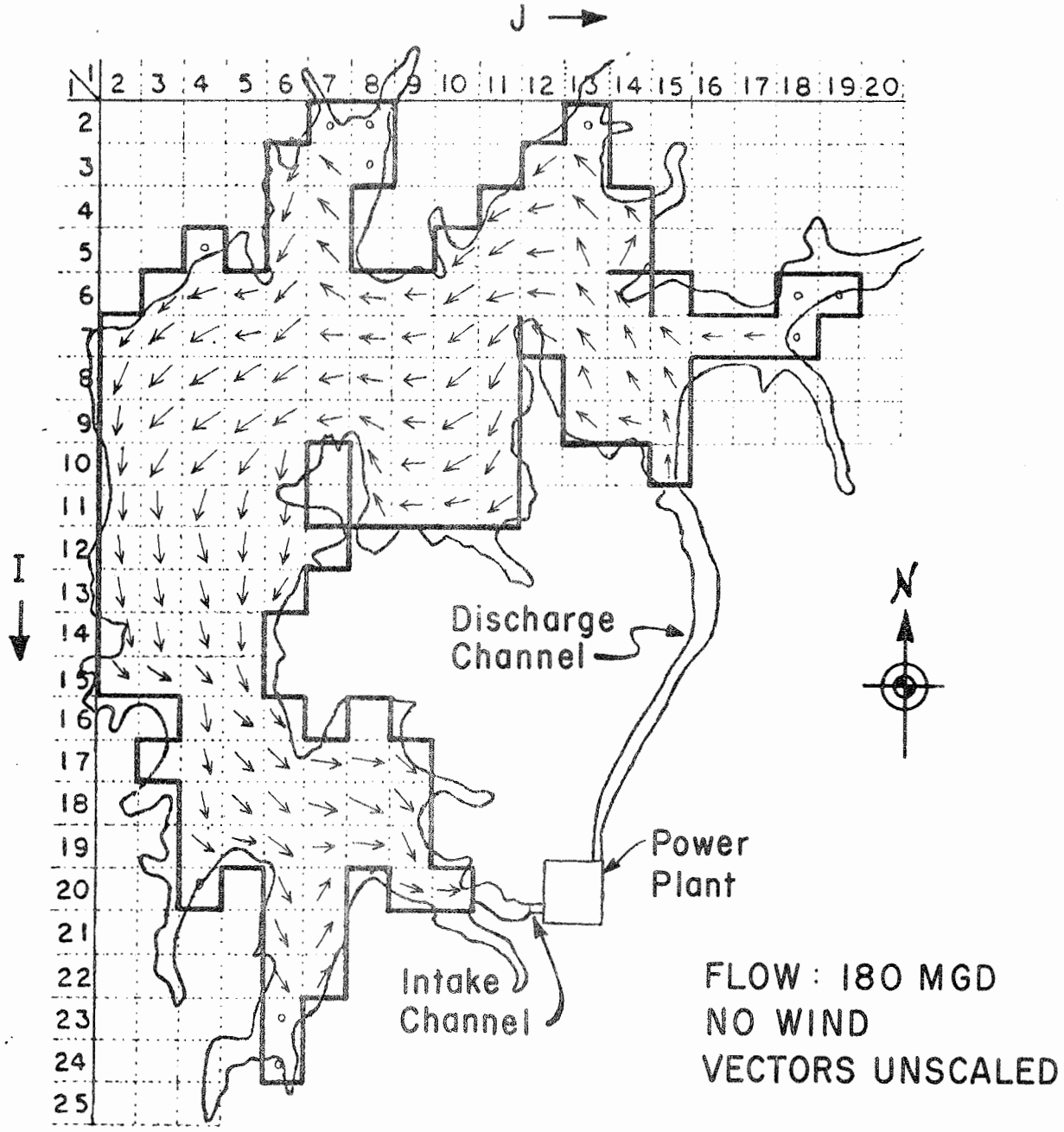

Figure 6-2. Lake Bastrop Hydrodynamic Model, Circulation Pattern.

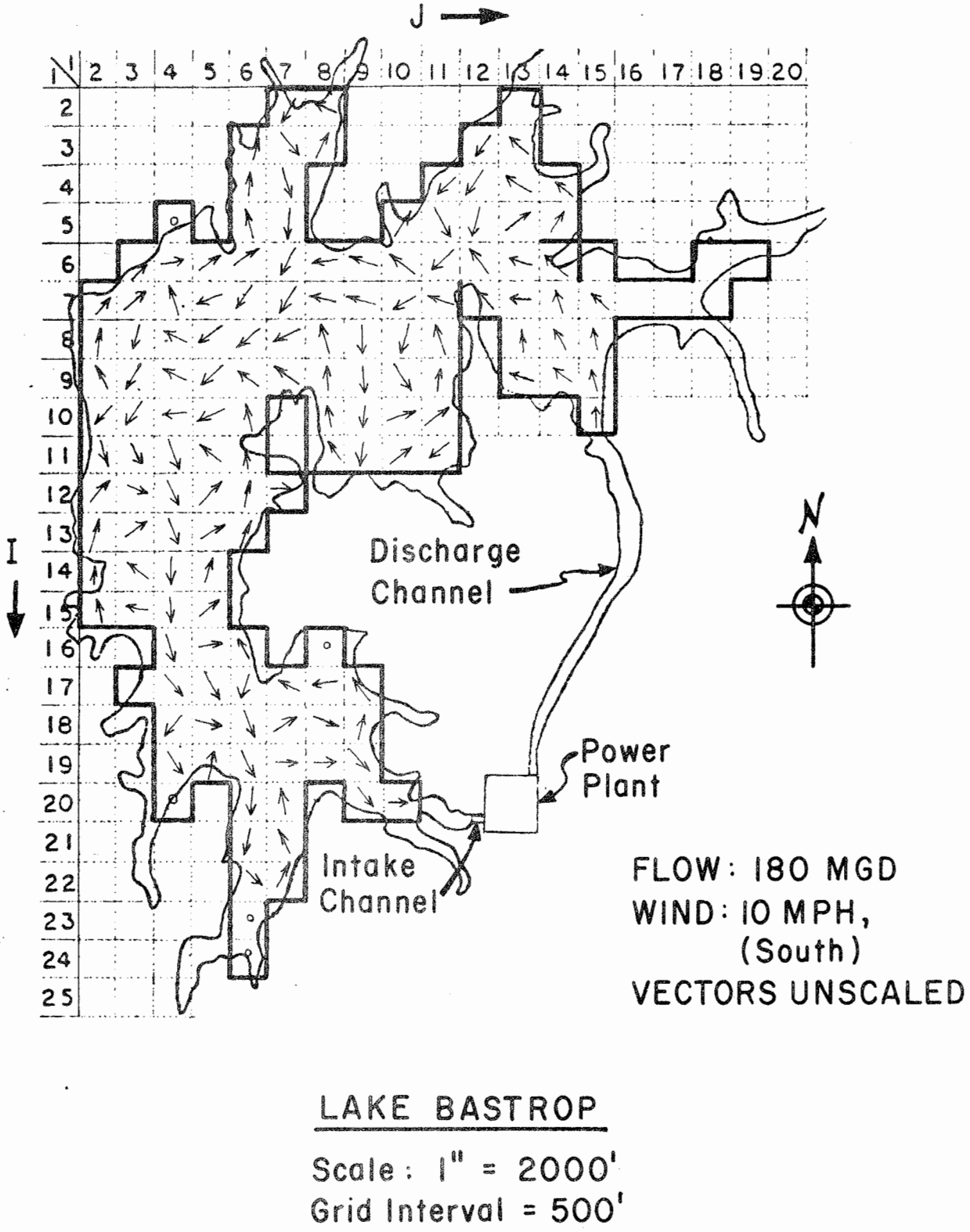

Figure 6-3. Lake Bastrop Hydrodynamic Model, Circulation Pattern.

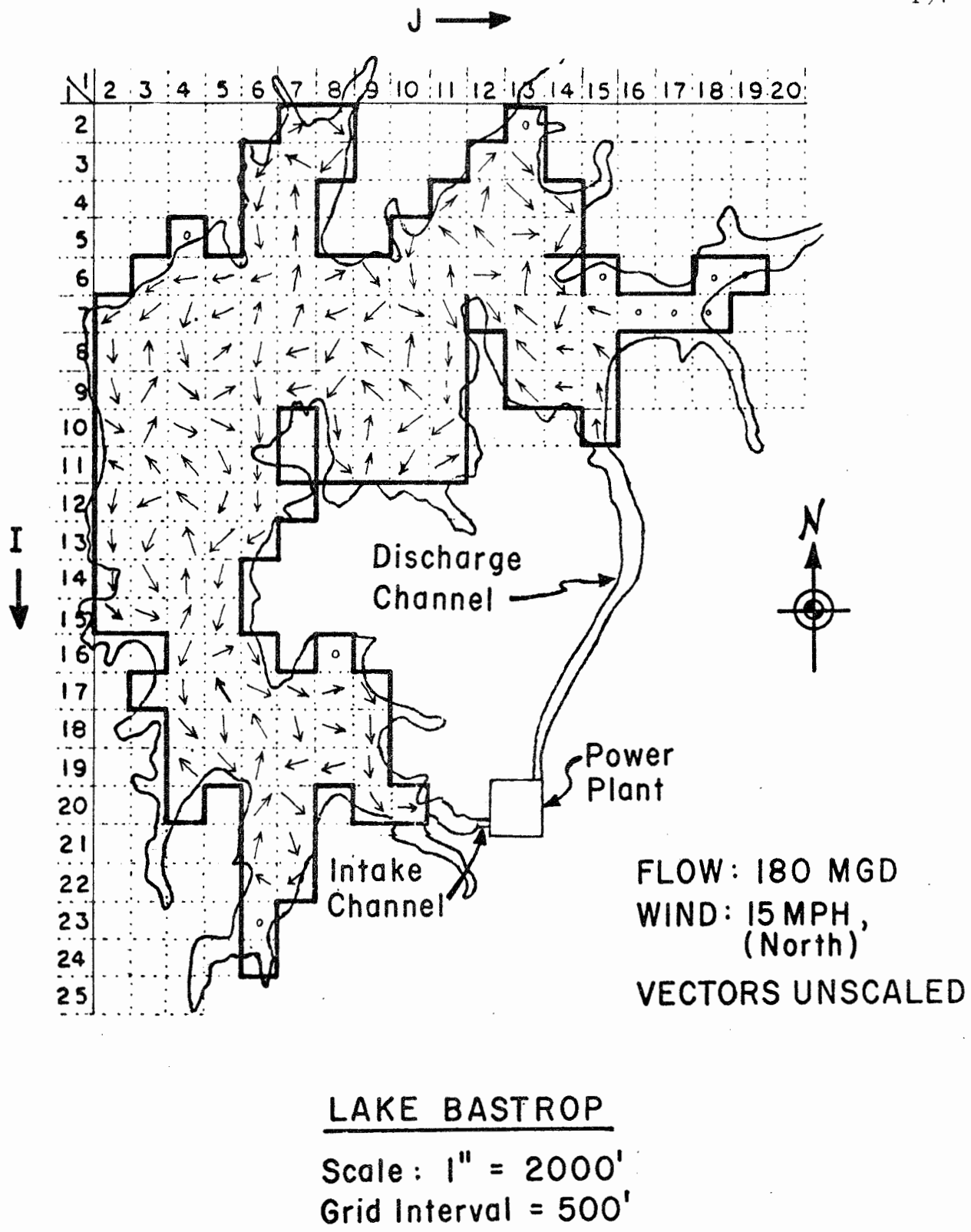

Figure 6-4. Lake Bastrop Hydrodynamic Model, Circulation Pattern.

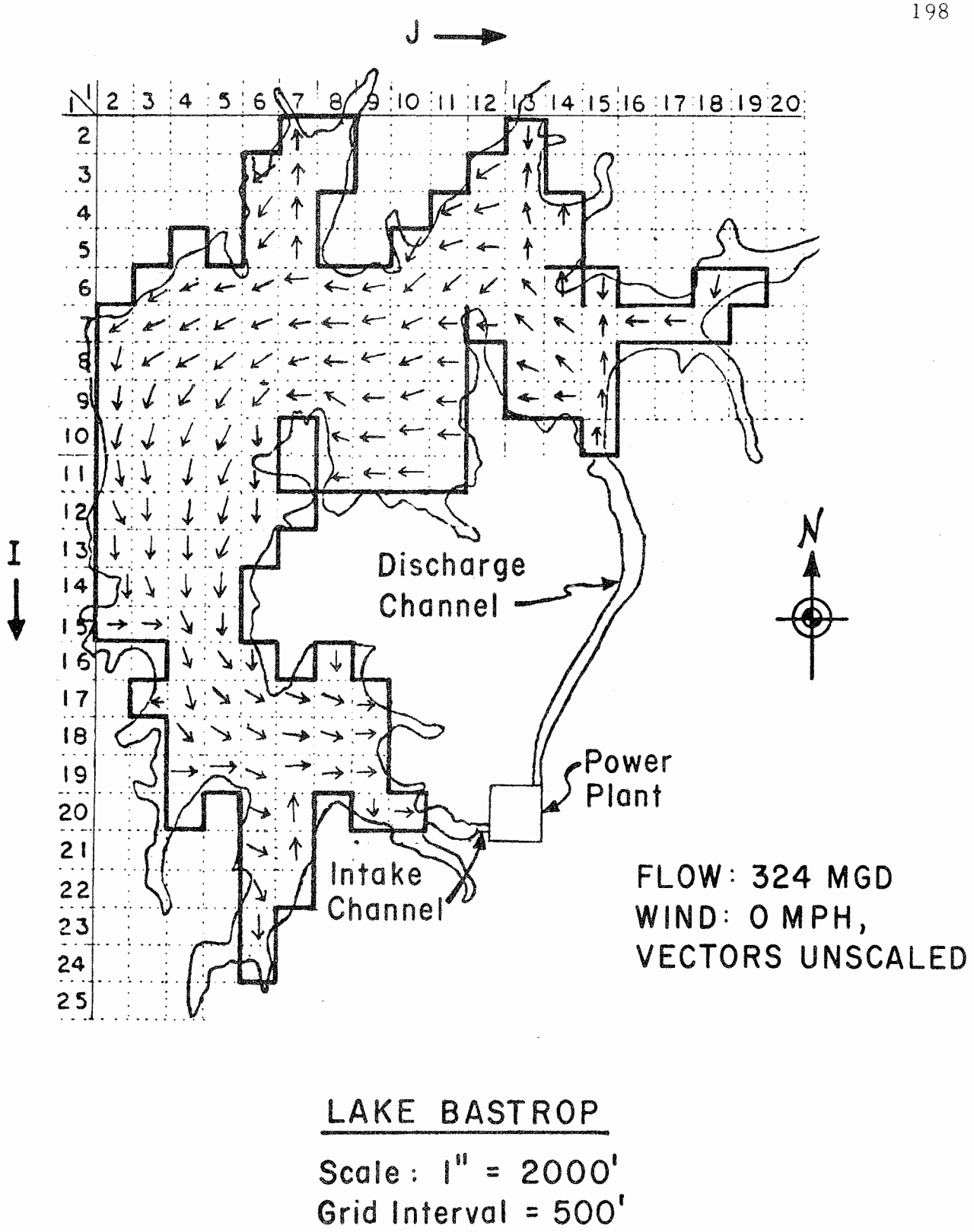

Figure 6-5. Lake Bastrop Hydrodynamic Model, Circulation Pattern.

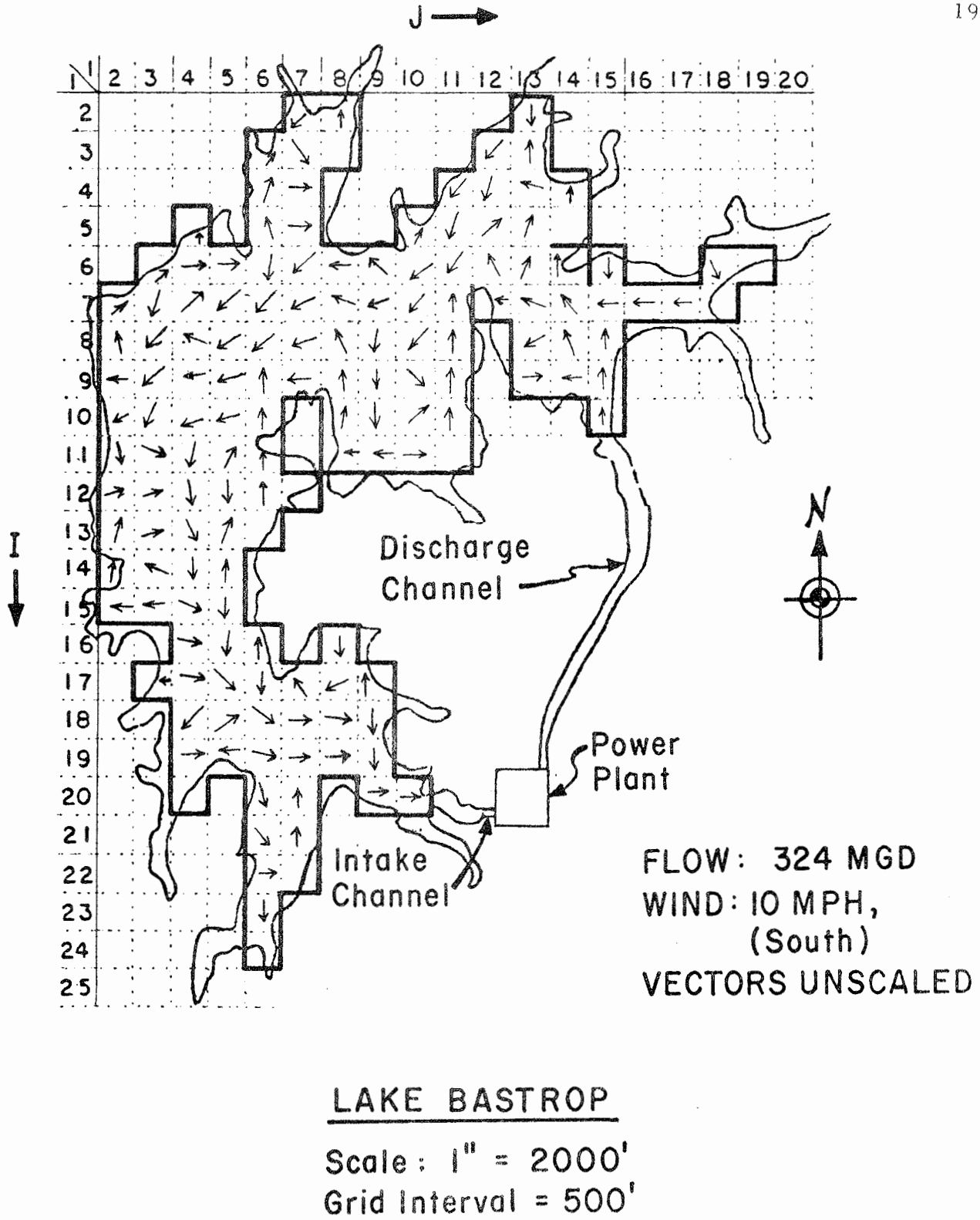

Figure 6-6. Lake Bastrop Hydrodynamic Model, Circulation Pattern.

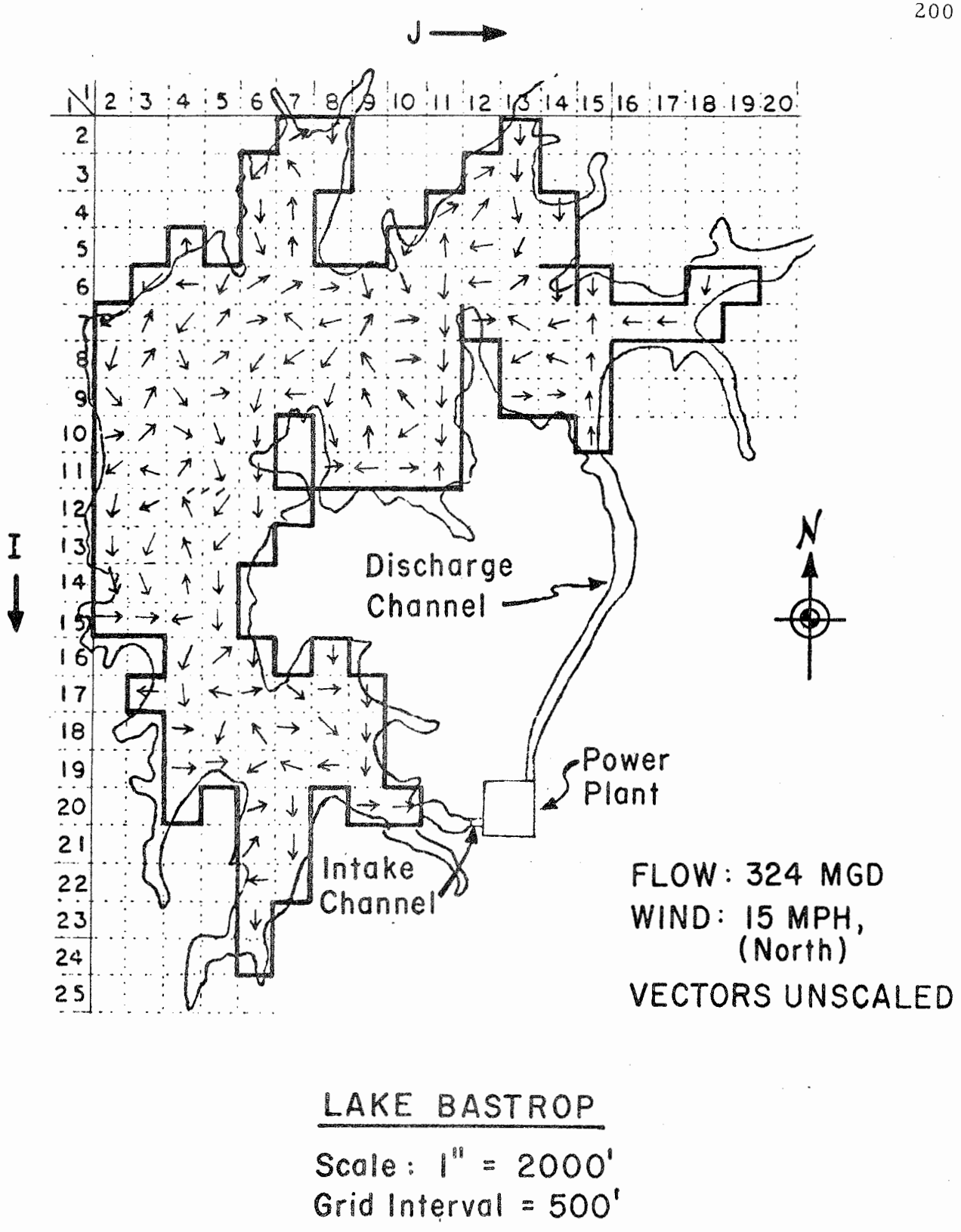

Figure 6-7. Lake Bastrop Hydrodynamic Model, Circulation Pattern.

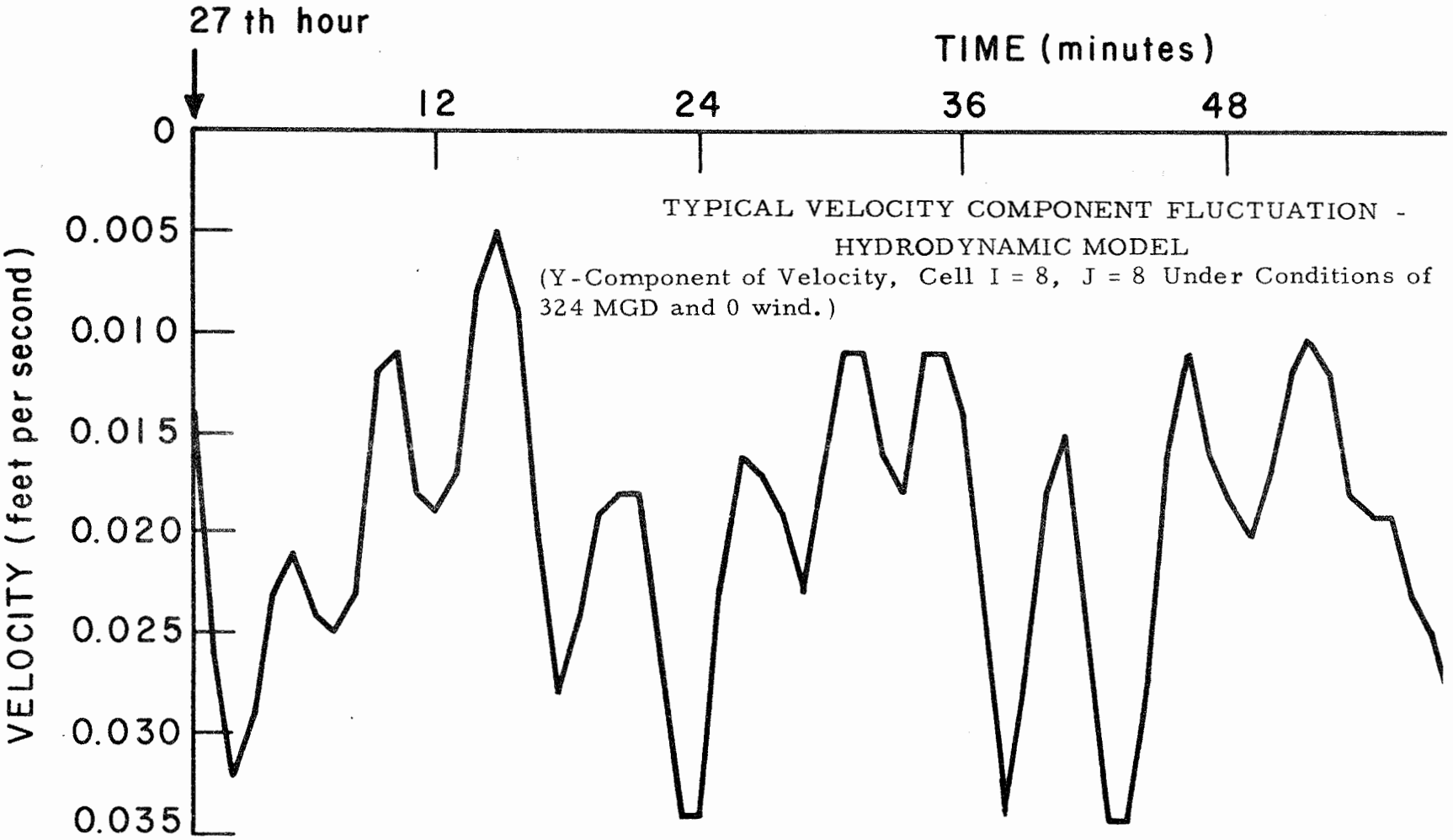

Figure 6-8. Velocity Fluctuations.

27th hour of simulated operation under zero wind conditions. This fluctuation is typical of that encountered also in 10 other test cells. Using the statistical expressions for the standard fluctuation[9] and the coefficient of fluctuation[10], as suggested by Fair, et al (1966), a stabilized, average coefficient of fluctuation of 0.175 or, 17.5% was computed for the component velocities in 10 random test cells after a simulated period of 4 hours. This coefficient of fluctuation was obtained from the computed longitudinal velocity component at one minute time intervals, for the 4-hour period ranging from the 27th to the 31st hour of model simulation.

It was decided that velocities generated by the hydrodynamic model, based on a fully-mixed lake or a fully-mixed layer, averaged over a 4 hour period would adequately serve as the "steady-state" or "quasi-equilibrium" velocities of a generalized scale and accuracy commensurate with the macro-synthetical model approach enunciated in this study. This important generalization is at the crux of the computation, preparation and analysis of the hypothetical, lake circulation patterns illustrated in Figures 6-2 to 6-7. This generalization required the consideration and practical reconciliation of the following factors:

---

[9] Standard of Fluctuation, $F = \sqrt{\Sigma(\Delta'')^2/n-2}$.

[10] Coefficient of Fluctuation, $C_F = F/\mu$, where:
n = the number of observations.
μ = the mean of observations.
Δ'' = the second difference in the magnitude of successive observations.

1. While constant inflow-outflow in a lake tends to produce a flow current, the effects of this current generally are negligible compared to lake-wide currents and circulation patterns produced by wind forces. Zumberge and Ayers (1959) indicated that this is true for most lakes. Generally, the characteristic cross-section of a lake greatly exceeds the size of the inlets or outlets and therefore, the lake cross-sectional velocities are low. Fair, et al (1968) note that water build-up on the windward shore of a reservoir generates return currents, which travel at or below the water surface, depending on shore configuration and on the vertical gradient of temperature. These two factors influence the relative thicknesses of the epilimnetic or circulation zone in which the surface currents occur, the mesolimnetic or (thermoclinal) transitional zone in which the return currents occur, and the hypolimnetic or stagnation zone. For example, in coves the return currents are displaced downward; where land juts out from shore, the return currents are deflected laterally. In addition, the greater the vertical temperature gradient, the greater is the tendency for the return currents to stratify in a surface stratum because of thermal resistance to vertical mixing. The seasonal differentiation of water strata and zones is most pronounced during the summer stagnation period. And, these effects may be heightened by functional uses of impoundments which involve the addition of head loads to the water body. All of these factors come into play by the selection of the power plant cooling water impoundment at Lake Bastrop, as the basic lake hydrodynamic model and by the decision to run verification tests during the summer. See Chapter III for a more detailed discussion of seasonal, hydrothermal phenomena in lakes.

2. Strong evidence points to the fact that the rapid drop in temperature in the thermocline during the summer season creates a resistance to mixing which is not easily broken even by wind-induced stresses. According to Fair, et al (1968), a lake is "normally two lakes, one superimposed upon the other". In addition, they point out that "diurnal temperature changes in the surface strata establish a variable micro-environment". From a theoretical viewpoint of transport, hydrothermal and hydrodynamic modeling conditions prevail within each layer. The "two-

lake" concept is analogous to the "dead zone" model for streams (which envisages a stream as being made up of two separate regions of flow), by Hays, et al (1966), discussed in the previous chapter.

3. Even though steady wind conditions were assumed in the hydrodynamic model, it appears from the circulation plots that non-periodic water currents may have been induced by boundary conditions. Zumberge and Ayers (1959) have encountered certain non-periodic currents in lakes, and described them as "irregularly variable in direction and velocity but have a propensity toward a time-mean uni-directionality that is related to a similar time-mean directionality of the prevailing wind".

The important aspects of velocities and circulation deserve further discussion, because they are at the core of both the hydrodynamic and transport models. In water under the influence of wind, the eddy viscosity is considered as a function of wind stress. Non-periodic currents form as result of energy imparted to the surface water through wind stress. Zumberge and Zyers (1959) reported general agreement among investigators that stress energy input varies with a power of wind velocity ranging from 1.8 to 3.0; and that an accepted relationship for wind shear stress is the following Equation (6-1 A), which Reynolds (1966) attributes to Ekman's (1905) study of wind-induced, water movements for high winds:

$$T = (3.2)\ (10^{-6})\ (W^2) \qquad \text{and,} \qquad (6\text{-}1A)$$

$$A_v = (4.3)\ (10^{-4})\ (W^2) \qquad (6\text{-}1B)$$

where:

T = wind shear stress in grams/cm/sec^2.

A_v = coefficient of eddy viscosity in cm^2/sec.

W = wind velocity in cm/sec.

According to Reynolds (1966), Ekman's equation for the surface velocity also is apropos:

$$V = \frac{T}{\sqrt{\Omega 2 \rho A_v \sin\phi}} \qquad (6\text{-}1C)$$

where:

V = the water surface velocity.

T and A_v (previously defined).

Ω = angular velocity of the earth's rotation, (7.29×10^{-5} sec.$^{-1}$).

ρ = density of the water.

ϕ = latitude.

A rigorous verification of these relationships has not been included in this study for reasons which will be brought out in the discussion of Liggett's (1970) circulation model studies, which follows shortly. However, the effects have been examined indirectly in terms of dye tracer time-of-travel incident to the transport model investigations. Zumberge and Ayers (1959) hypothesized that stress energy entering the water produces acceleration of water particles, causing in turn, waves and water currents. They found surface currents produced by wind having velocities between one and three

percent of the wind velocity. While the realistic determination of wind-induced, surface velocities is somewhat subdued in the hydrodynamic model due to the assumption that the lake is well-mixed over its full depth or over some finite stratum, this is not an insurmountable shortcoming. Rational adjustments can be made to bring out the surface effects which must be considered in the transport model and in field verification tests.

Here it is apropos to analyze Liggett's (1970) efforts to model wind-driven circulation in real lakes. This will serve to elucidate lake velocity and circulation effects and wind-induced surface phenomena. Also, it will show further reasons why the decision was made in this study to use velocities corresponding to an assumed fully-mixed surface stratum. Liggett (1970) encountered instabilities in finite difference calculations when certain magnitudes of horizontal eddy viscosity were combined with highly-varied, vertical eddy viscosity. The instabilities showed up as isolated areas of chaotic velocity patterns. However, these instabilities were reduced by decreasing the size of the computational increment. Liggett (1970) found that the key factors in surface circulation are the magnitudes of the horizontal and vertical eddy viscosities because velocities are highly affected by the friction. But, he adds that it is difficult to determine realistic values of eddy viscosities, noting that many seemingly-logical combinations of horizontal and vertical eddy viscosity with typical vertical distribution of eddy viscosity caused only small, detectable differences in model circulation

patterns. In earlier work on steady and unsteady lake flow circulation Liggett (1969) found it necessary for practical mathematical reasons to assume a constant eddy viscosity throughout the fluid, because the exact numerical variation of eddy viscosity with depth is not known. Liggett (1969) found that under steady-state conditions, the model surface currents were in the direction of the wind. However, in some model simulations, the velocities approached zero at a depth of only 0.1 D.

The Bastrop Hydrodynamic Model and the Liggett (1969, 1970) Lake Circulation Models are based substantially on the same tacit or implied assumptions. As expressed by Liggett (1969):

1. The lake model is shallow so that $D/L \ll 1$, in which D and L are characteristic lake depth and length, respectively.

2. $D/d \approx 1$, in which:

$$d = \pi \sqrt{2\eta/f} \, .$$

(This is the Ekman "depth of frictional influence".) (6-2)

η = vertical eddy viscosity.

f = Coriolis parameter.

3. Vertical velocities are assumed small compared to horizontal velocities.

4. Density stratification is neglected.

There is, however, an important distinction underlying these assumptions. Liggett (1969) assumed a shallow homogeneous (nonstratified)

lake. In contrast, the Bastrop Lake transport and hydrodynamic models assume a shallow, stratified lake having a fully-mixed surface layer. In his investigation of parameters for application of his circulation model to Lake Michigan and Lake Huron, Liggett (1969) appeared to deal indirectly with the stratification condition by the approach that ". . .D must be chosen so that the lake is shallow but can otherwise have a wide variation. . ."

Liggett (1969) analyzed the possible variational ranges of key parameters in lake circulation phenomena through analysis made with the Taylor's number,

$$2m^2 = \frac{f D^2}{\eta} . \qquad (6-3)$$

(Note: $\frac{1}{2m^2}$ is referred to as the Ekman number). Liggett found that the values of m may vary widely from near zero to a very large number.

1. f can range from 0 at the equator to $\pm$ 1.458 x 10^{-4} sec^{-1} at the poles.
2. D may vary sufficiently throughout portions of large lakes and thus affect the shallowness criterion.
3. η can range from 10 to 1,000 cm^2/sec.

At low m values, the η component dominates Equation (6-3) and tendencies emerge for currents to be deflected.

Liggett (1969) also found that "the lake comes reasonably close to equilibrium in approximately one day. For shallower lakes, the

equilibrium time would be shorter, whereas the equilibrium time could be considerably longer for deeper lakes."

An analysis of Liggett's (1969, 1970) lake circulation model tests and investigations provides strong justification for the adoption of the macroscopic approach underlying the development and use of Lake Bastrop hydrodynamic and transport models which compute average, macro-cell, surface-stratum circulation and distribution patterns.

This analysis of circulation models also brings out the basic analogy and similarity between the transport of vorticity or turbulence and the transport of conservative substance in fluids. The transport of turbulence involves the use of the coefficients of kinematic or eddy viscosity; the transport of substance involves the use of coefficients of diffusion and dispersion. All these coefficients except diffusion depend predominantly on the structure of the flow, and the latter is affected predominantly by resistance and shear in the fluid. While attention of this study is focused mainly on the mixing and dispersion impacts in impoundments of various hydrodynamic, hydrometeorological and hydrothermal phenomena, it should be emphasized that wind effects assume a great importance not only from the viewpoints of physical mixing and dispersion but that in many important instances, wind also assumes great limno-chemical import as the main factor in the oxygen supply of lakes. For example, Entz (1969) reporting results of extensive investigations in Volta Lake, Africa, indicated that with wind speeds of four to five meters

per second, the oxygen saturation of the epilimnion increased very rapidly, and, under unstable stratification conditions, wind effects were manifest on the deepest water layers. Specifically, Entz (1969) noted:

> " On 29 February 1968, for example, within two hours the oxygen content of a 45 m deep water mass rose from 90 g/m^2 by 74 g O_2/m^2 (80 percent increase) to 164 g/m^2 at a wind speed of 4-5 m/sec as a result of the wave action. . . From all this we come to the conclusion that at present a wind of two hours duration and of the above-mentioned speed may counterbalance all the oxygen loss caused by decomposition, within a 24-hour period. "

Use of Channel Transport Model to Compute Desired Time-Concentration Discharges. A description of the channel, Figure 5-3, was given in Chapter V and, the algorithm for the channel transport model was described in Chapter IV. Using this model, four separate simulations were made involving assumed instantaneous release of solutions containing 56.9 grams, 90 grams, 1.17 lbs, and 1.225 lbs. of Rhodamine B. Figures 6-9 and 6-10 show the computed time-concentration distributions at Stations 17 + 00 and 44 + 40, for each of the 4 releases.

The Gaussian distribution shown in these figures is characteristic of a dye tracer cloud in a fully-mixed stream flow. According to Fischer (1967), the dispersion process of a tracer cloud released from a point source into a stream undergoes two phases: (1) a convective phase during which tracer movement is under the influence of the initial convective velocity, (b) a diffusive phase during which the bulk transport of the cloud

cloud can be defined by a one-dimensional diffusion equation in the flow direction.

The "convective" phase is characterized by sharply-skewed tracer curves; the "diffusive" phase, by the decay of the initially-skewed distributions and the gradual onset of Gaussian-type distributions. During the "diffusive" phase the cloud spreading is totally defined by the mean flow velocity and the dispersion coefficient.

These hypotheses of Fischer, will be discussed in the next chapter in connection with the verification and evaluation tests of the Lake Bastrop channel model. It suffices at this point to state that the Lake Bastrop discharge channel exhibits these dispersive phases clearly. The turbulence created at the power plant outlets accelerates the formation of a fully-mixed, convective phase, and this phase prevails in the upstream reach, a distance of about 1/3 the total channel length. Then, a transitional phase prevails over about the middle third of the channel in which the skewness of distributions is attenuated. In the lower reach of the channel a diffusive phase prevails; at the end a nearly-Gaussian concentration distribution is obtained.

Lake Transport Model Simulations and Investigations.

1. Determination of Conservative Substance Transport Patterns. Using an assumed, temporally-varying input of dye tracer which produces a very high and sharp concentration peak at the excitation cell (I = 11, J = 15), and multiplying the Taylor equation for dispersion coefficient by a factor to

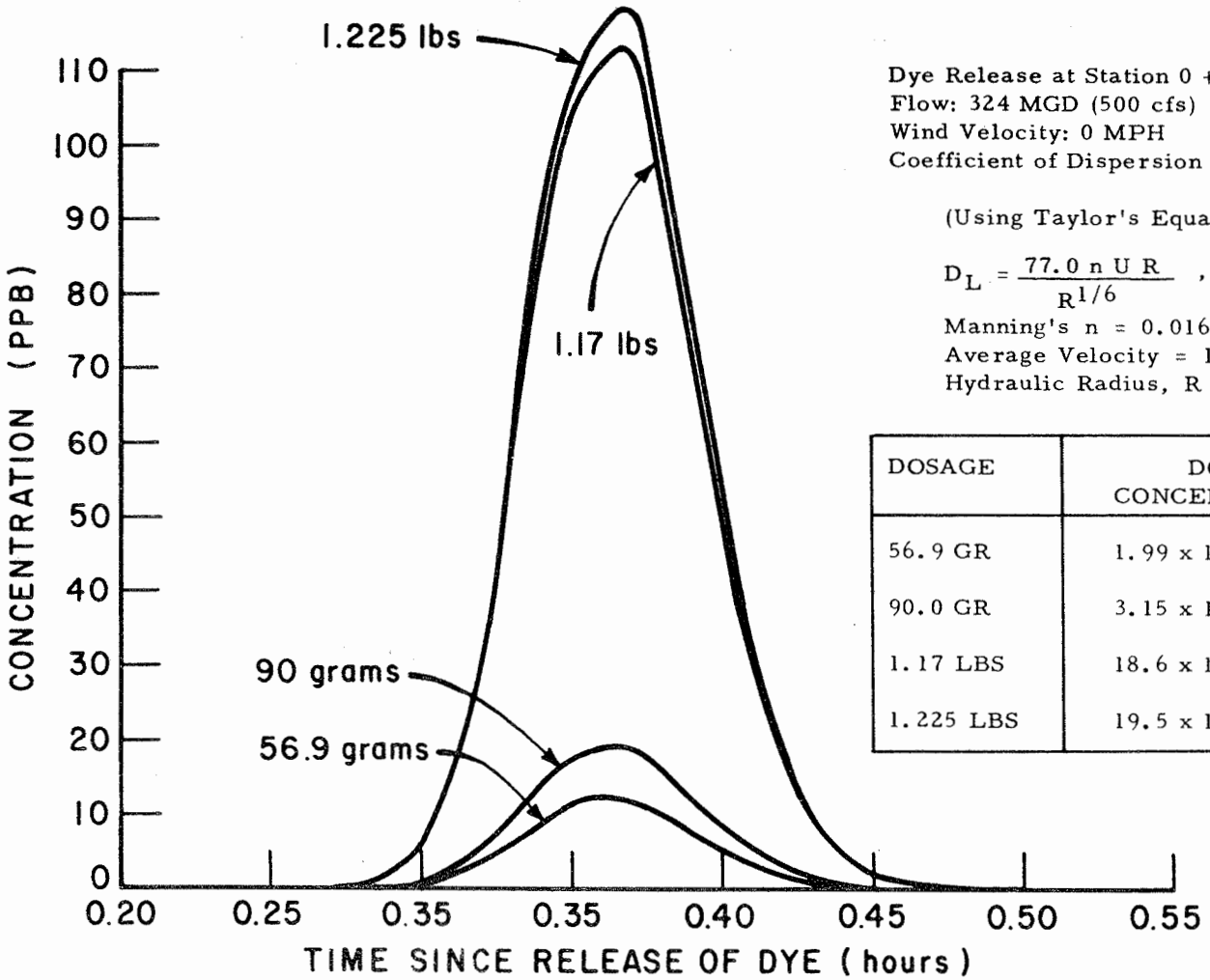

Dye Release at Station 0 + 00
Flow: 324 MGD (500 cfs)
Wind Velocity: 0 MPH
Coefficient of Dispersion D_L: 6.50 Ft^2/Sec

(Using Taylor's Equation

$$D_L = \frac{77.0\ n\ U\ R}{R^{1/6}}$$, where

Manning's n = 0.016
Average Velocity = 1.30 fps
Hydraulic Radius, R = 5.74)

DOSAGE	DOSAGE CONCENTRATION
56.9 GR	1.99×10^6 ppb
90.0 GR	3.15×10^6 ppb
1.17 LBS	18.6×10^6 ppb
1.225 LBS	19.5×10^6 ppb

Figure 6-9. Concentration vs. Time at Station 17 + 00, Discharge Channel.

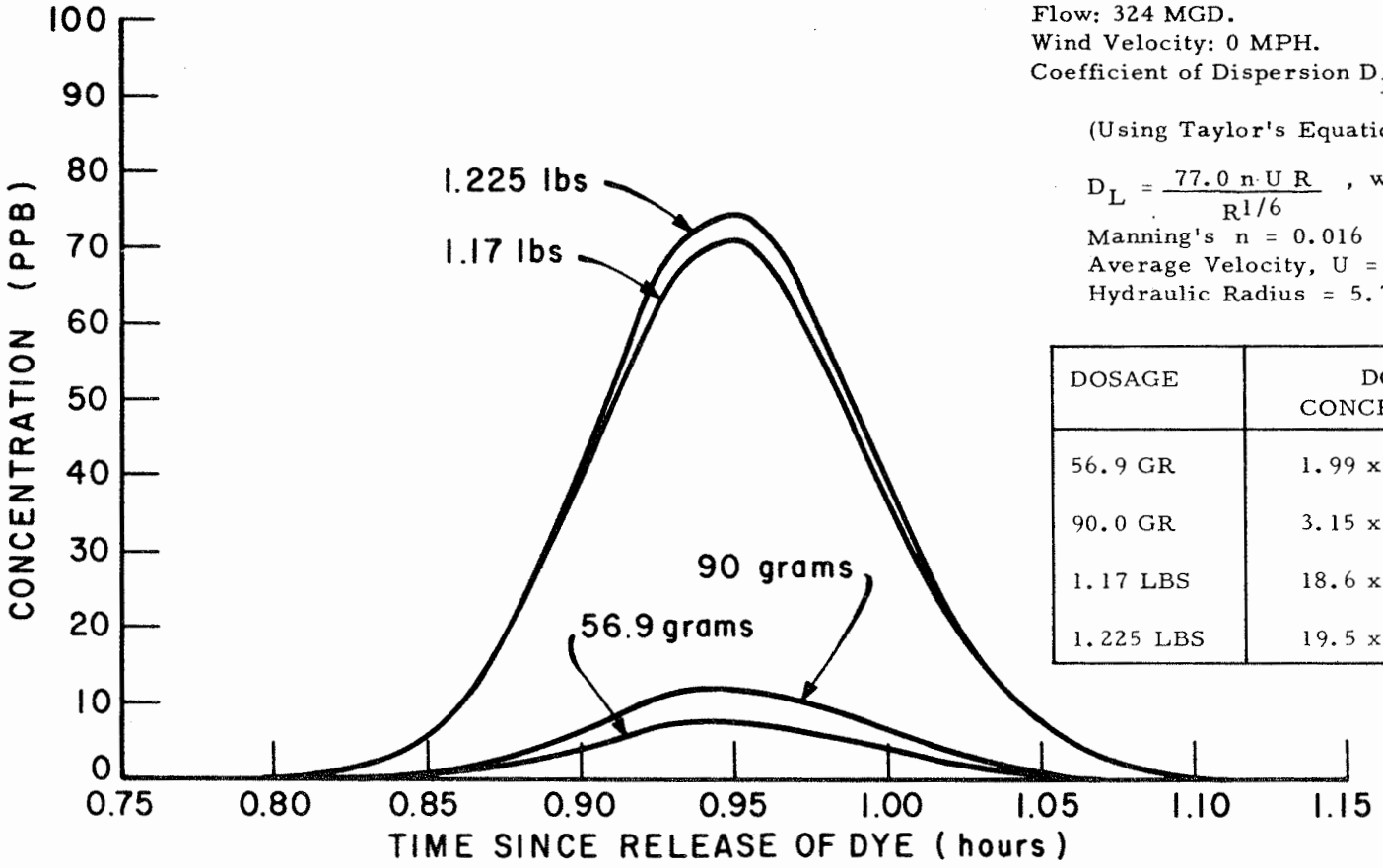

Dye Release at Station 0 + 00.
Flow: 324 MGD.
Wind Velocity: 0 MPH.
Coefficient of Dispersion D_L: 6.50 Ft^2/Sec

(Using Taylor's Equation

$D_L = \frac{77.0\ n\ U\ R}{R^{1/6}}$, where:
Manning's n = 0.016
Average Velocity, U = 1.30 fps
Hydraulic Radius = 5.74)

DOSAGE	DOSAGE CONCENTRATION
56.9 GR	1.99×10^6 ppb
90.0 GR	3.15×10^6 ppb
1.17 LBS	18.6×10^6 ppb
1.225 LBS	19.5×10^6 ppb

Figure 6-10. Concentration vs. Time at Station 44 + 40, Discharge Channel.

ten in order to simulate increased wind shear effects and to magnify slightly the low lake velocities, the transport model was used to compute concentration distributions in the lake for 10 days, assuming the following combination of conditions:

a. Steady flow of 180 MGD with the cell component velocities inputs from the hydrodynamic model for no wind.

b. Steady flow of 324 MGD with the cell component velocities inputs from the hydrodynamic model for:

   i. no wind.

   ii. 10 (MPH) from south.

   iii. 15 (MPH) from north.

These simulations had two main purposes. First, to energize the lake model strongly enough to examine theoretical transport trends within the range of flow and wind conditions expected to occur at Lake Bastrop during the on-site verification tests. Second, to obtain an estimate of time required for the tracer to migrate to all cells of the lake model. Figures 6-11 to 6-14, inclusive are sequential contour or isopleth maps of predicted 1, 2, 10 and 14-day concentrations based on the 180 MGD flow and zero wind. Figures 6-15 to 6-23 are sequential contour or isopleth maps of 1, 2 and 10-day predicted concentrations based on a 324 MGD flow for each of 3 different wind conditions (0, 10 MPH from south, 15 MPH from north).

These concentration isopleth maps bring out graphically some of the factors discussed earlier regarding the hydrodynamic model. The maps show the predominant effect of wind in the transport process, and the formation of stagnant, lagging or isolated peak areas due to boundary configurations. These maps indicate that a satisfactory grid size and computational time increment have been attained to assure a continuum of finite difference method calculations. In addition, it is apparent, that the program

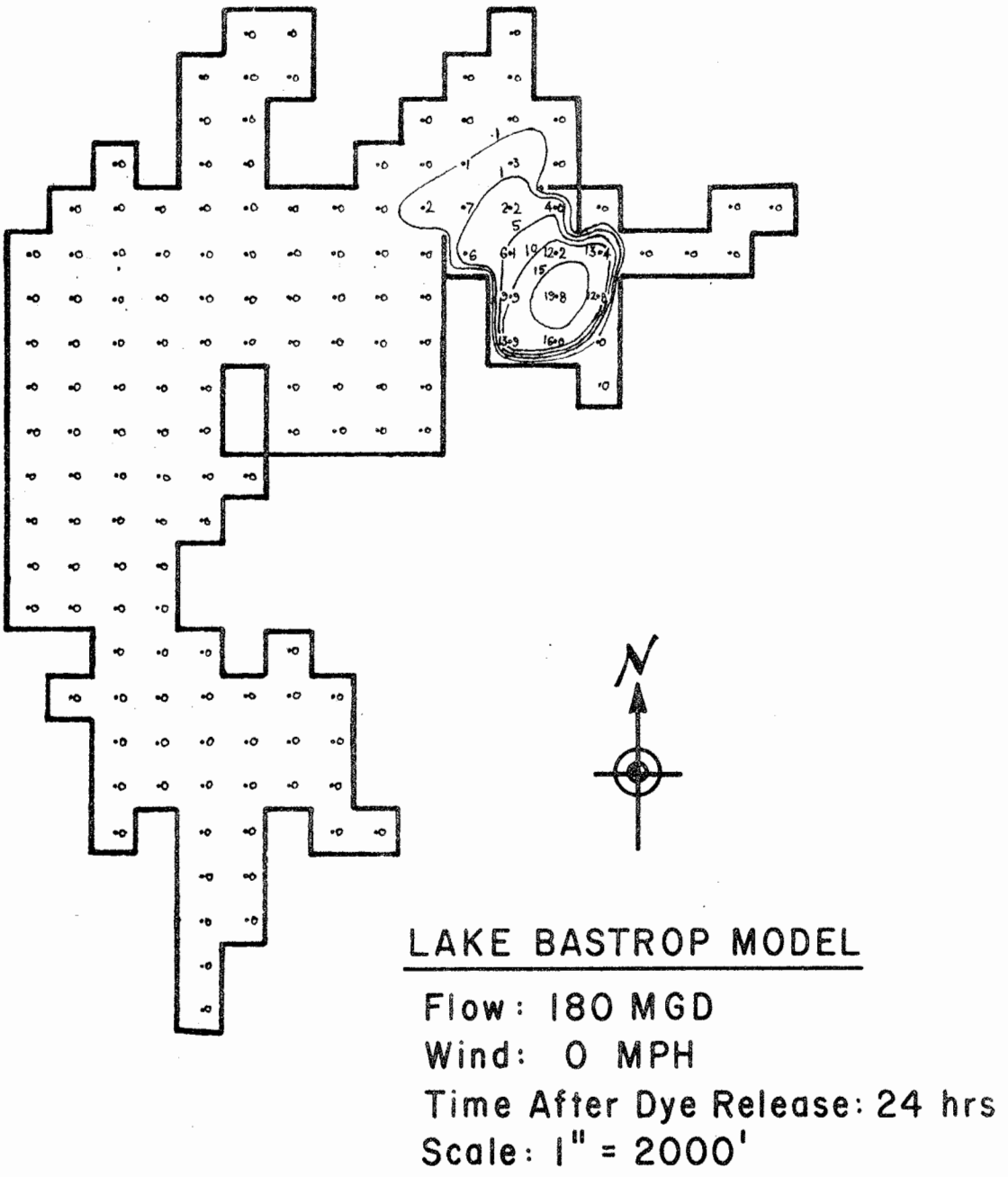

Figure 6-11. Computed Concentration Distribution

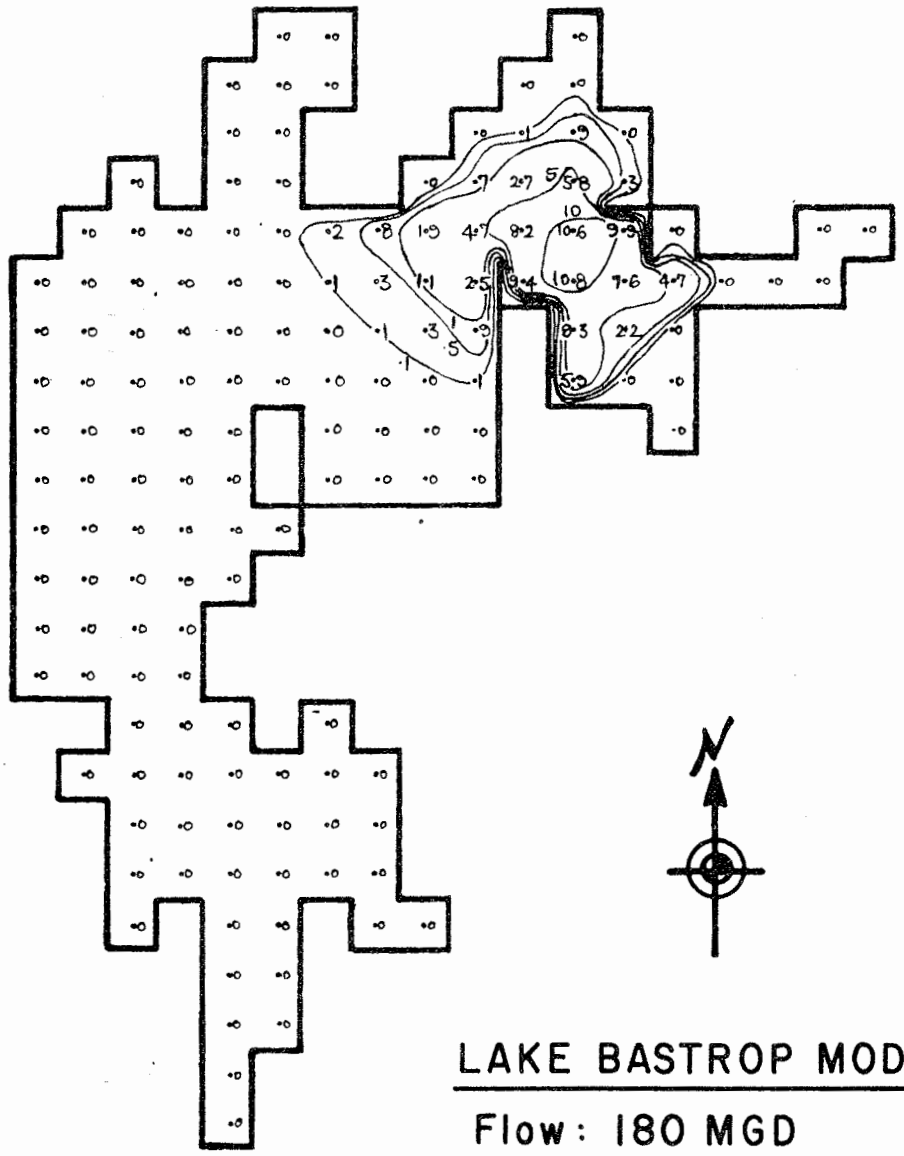

Figure 6-12. Computed Concentration Distribution

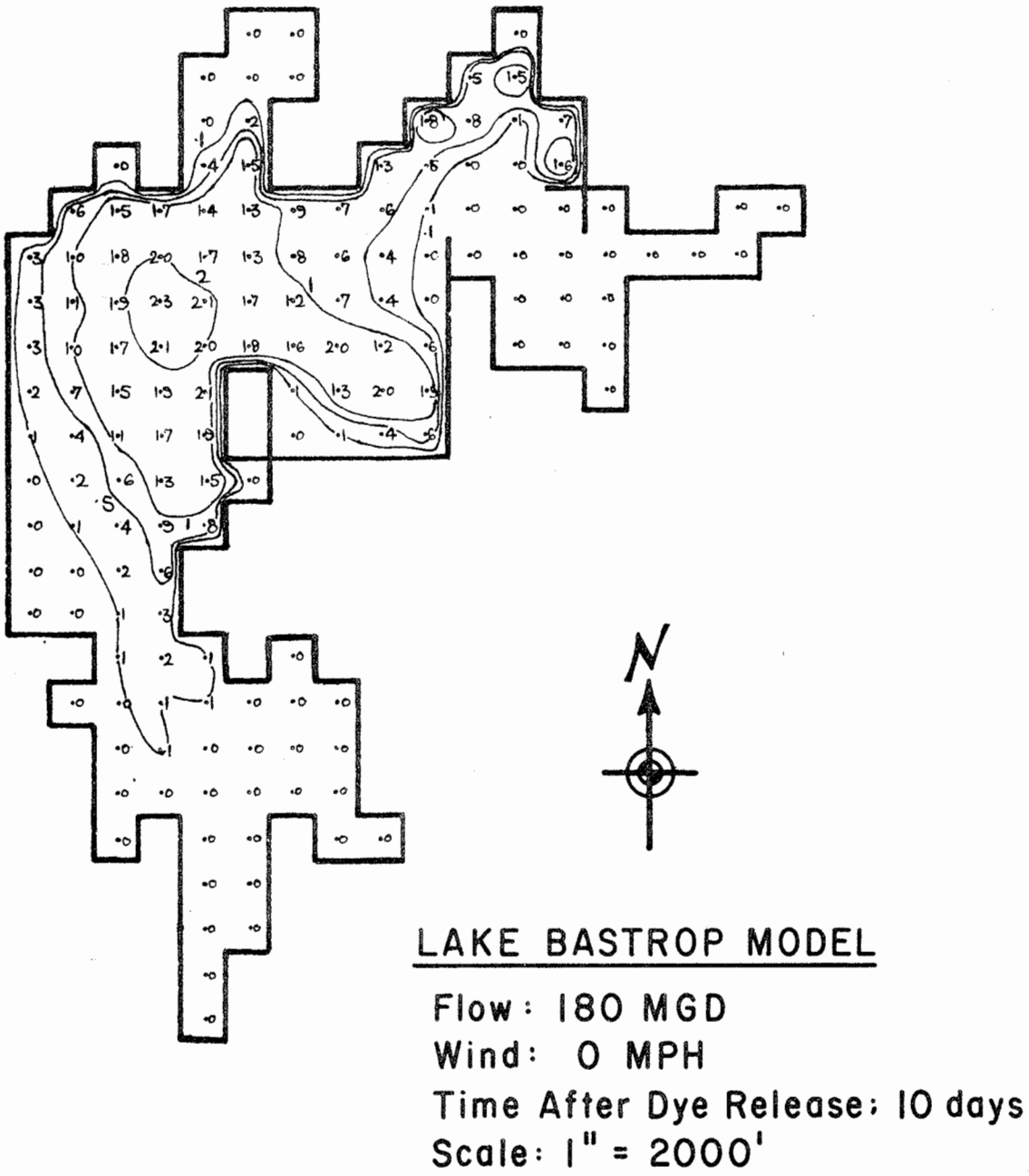

Figure 6-13. Computed Concentration Distribution

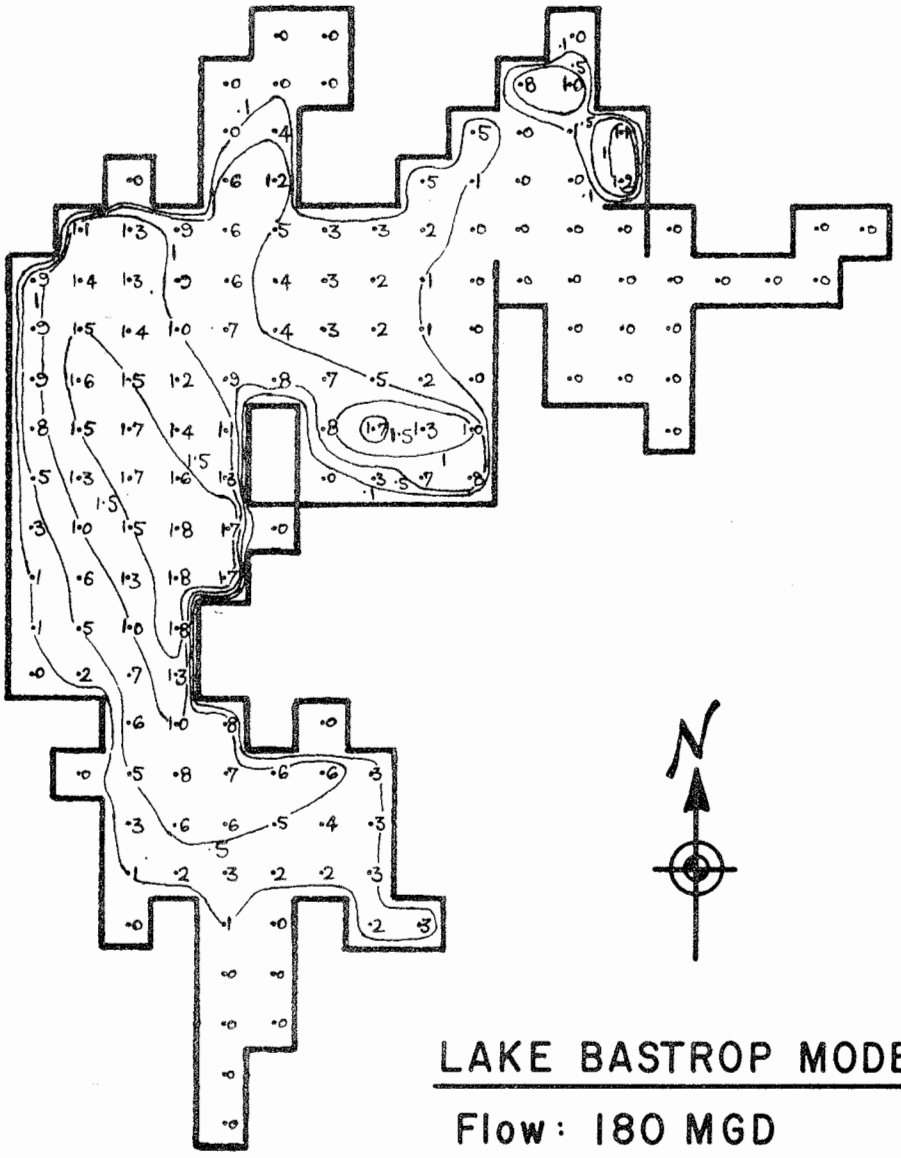

Figure 6-14. Computed Concentration Distribution

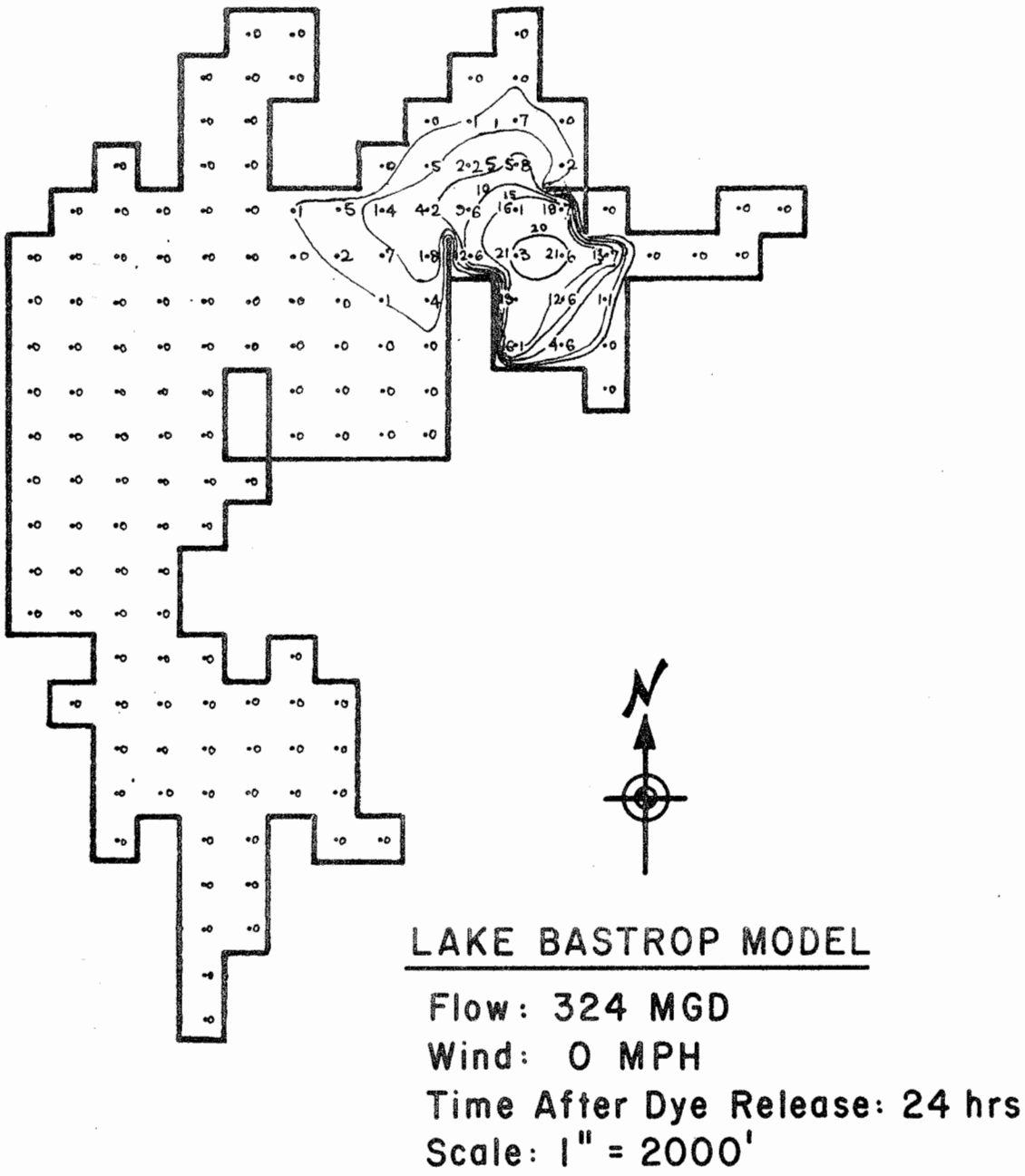

Figure 6-15. Computed Concentration Distribution

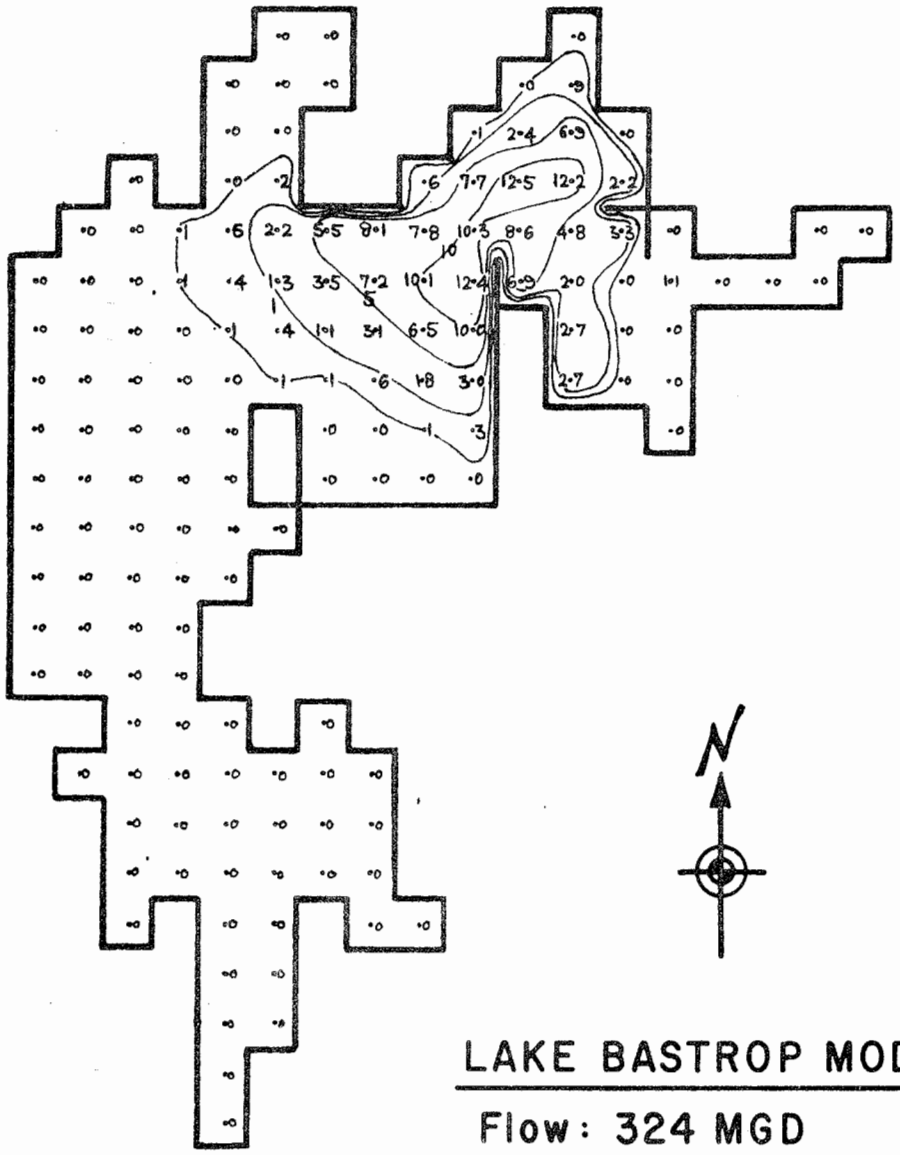

Figure 6-16. Computed Concentration Distribution

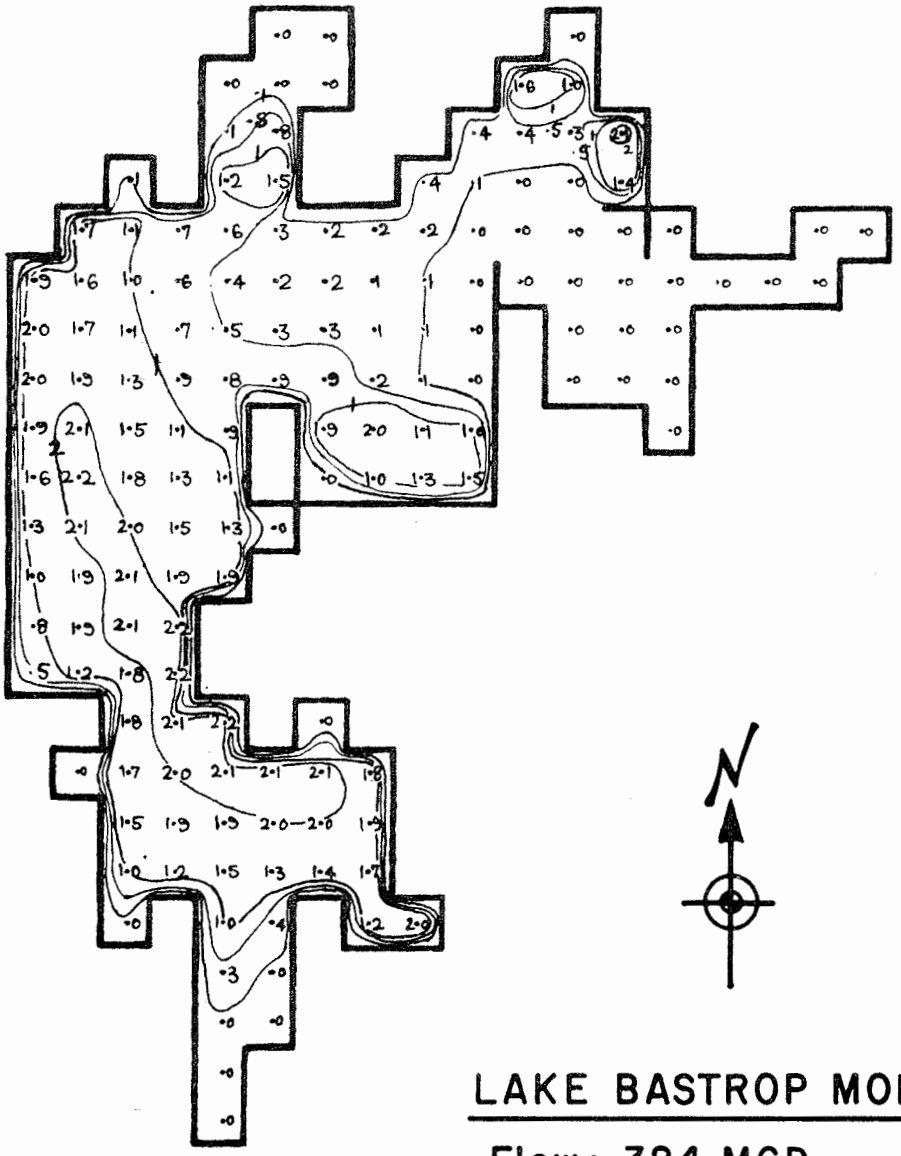

Figure 6-17. Computed Concentration Distribution

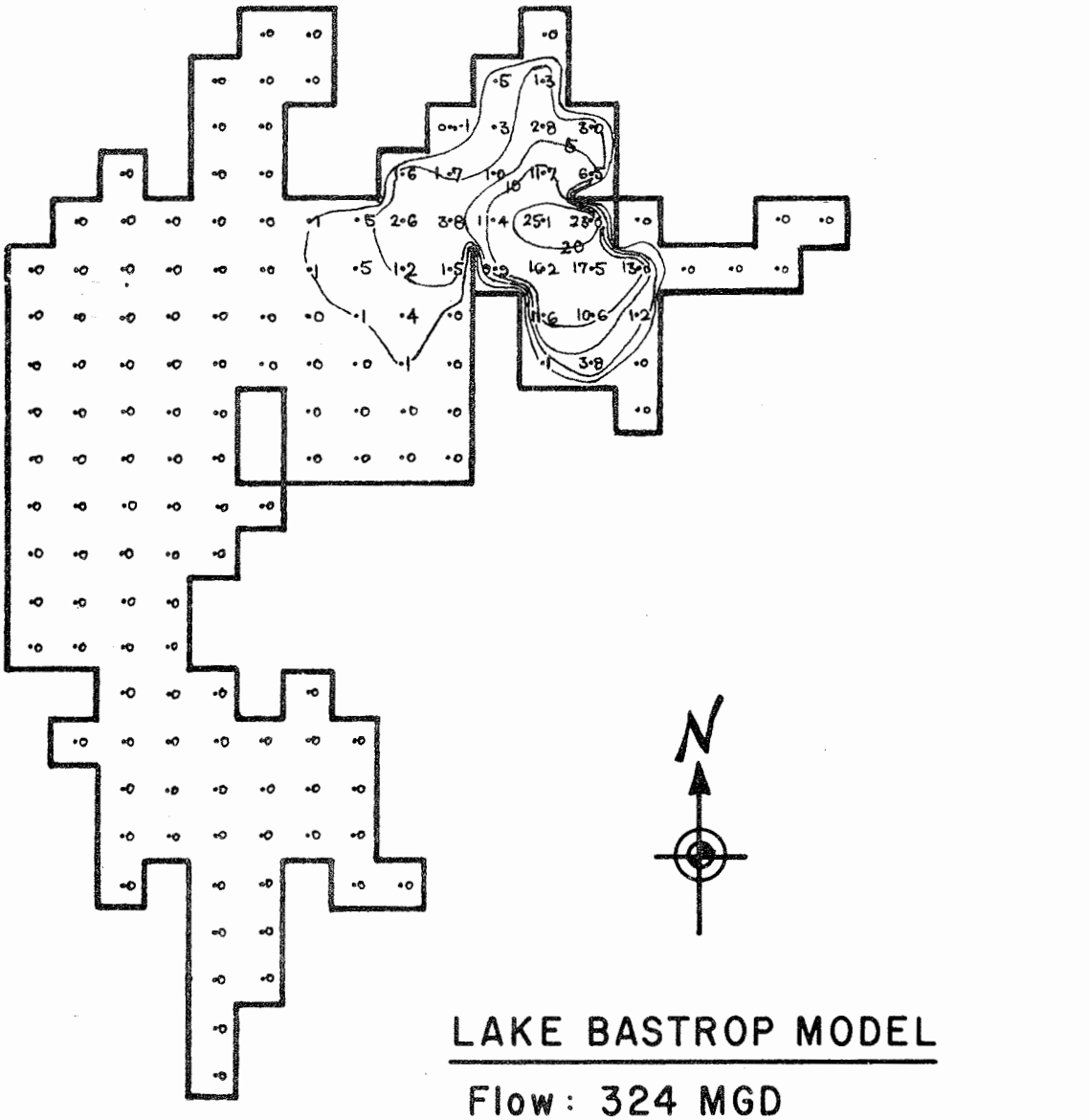

Figure 6-18. Computed Concentration Distribution

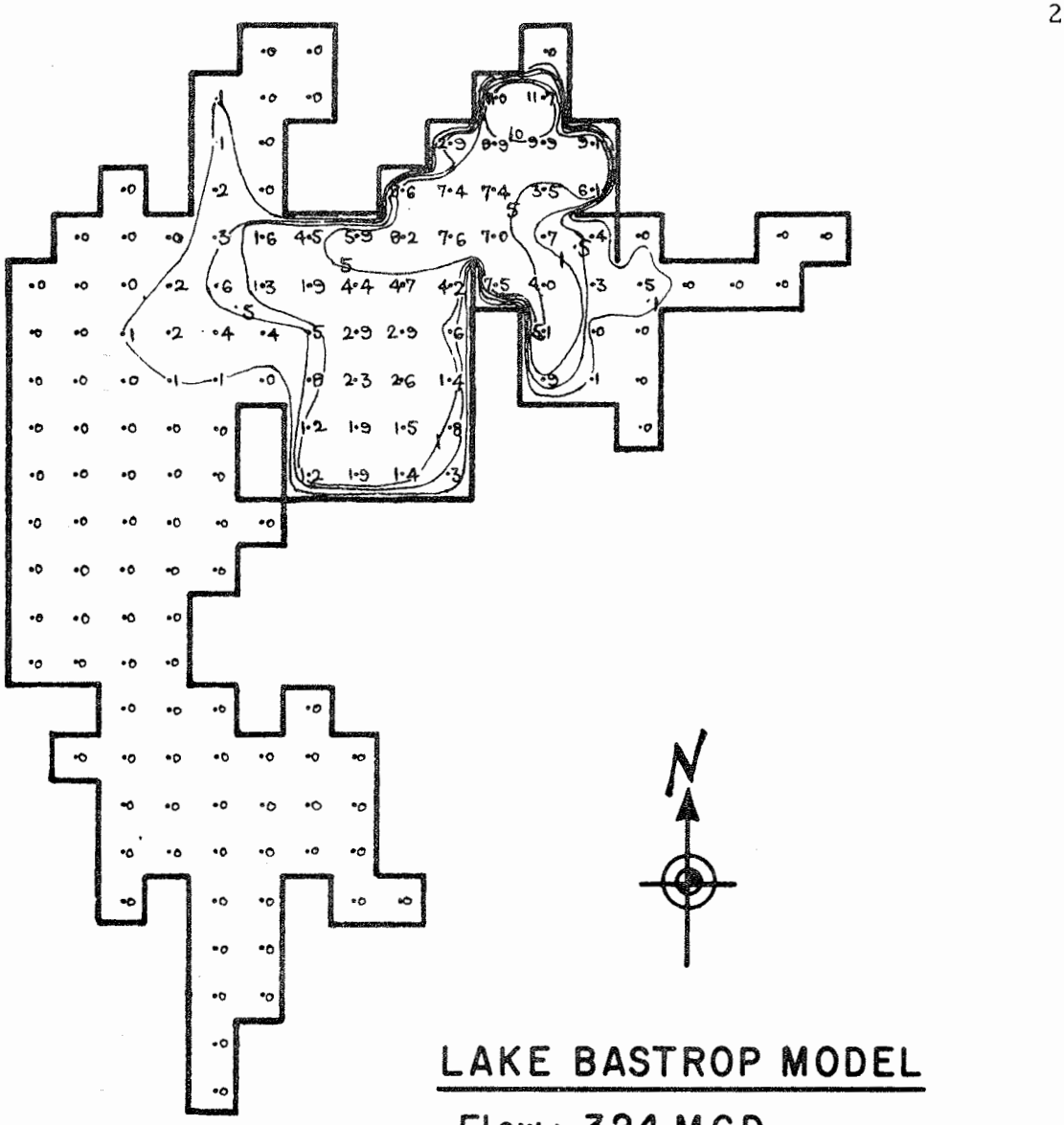

Figure 6-19. Computed Concentration Distribution

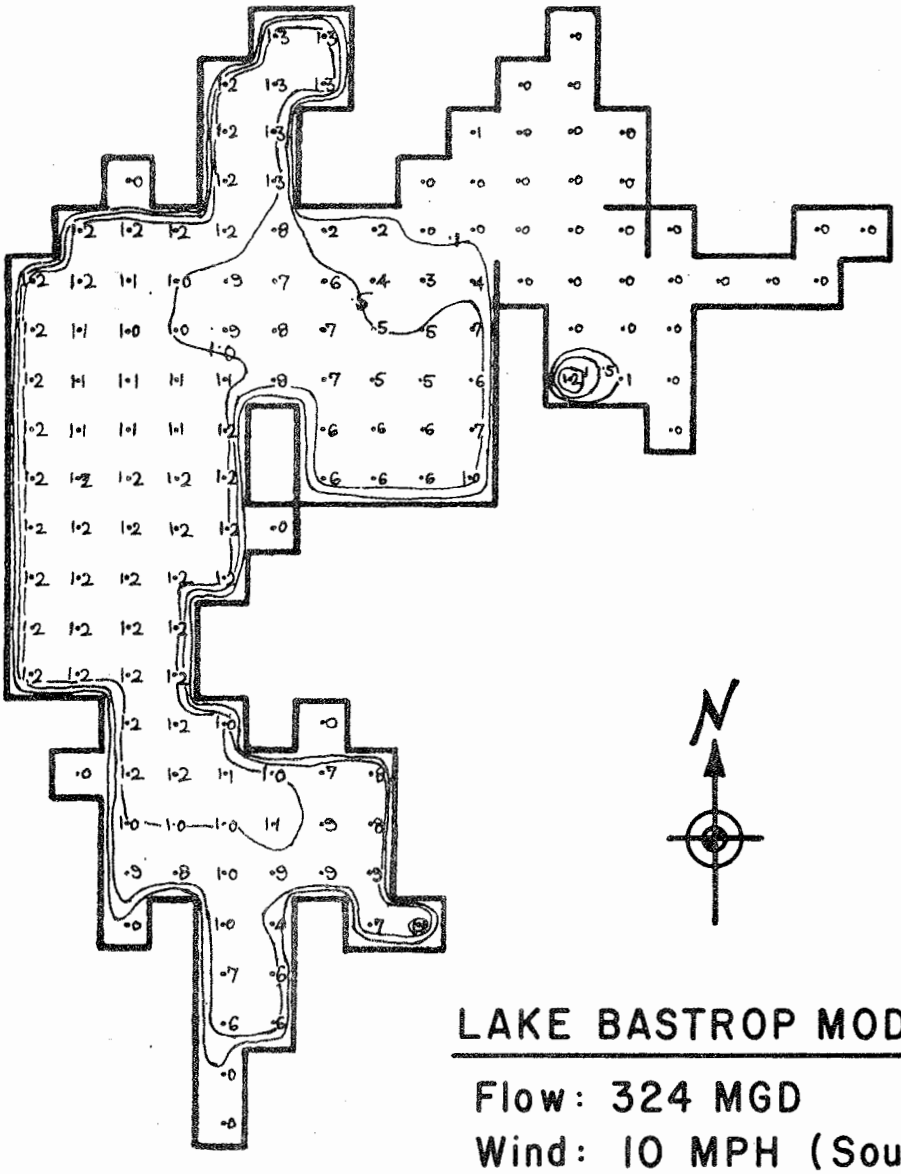

Figure 6-20. Computed Concentration Distribution

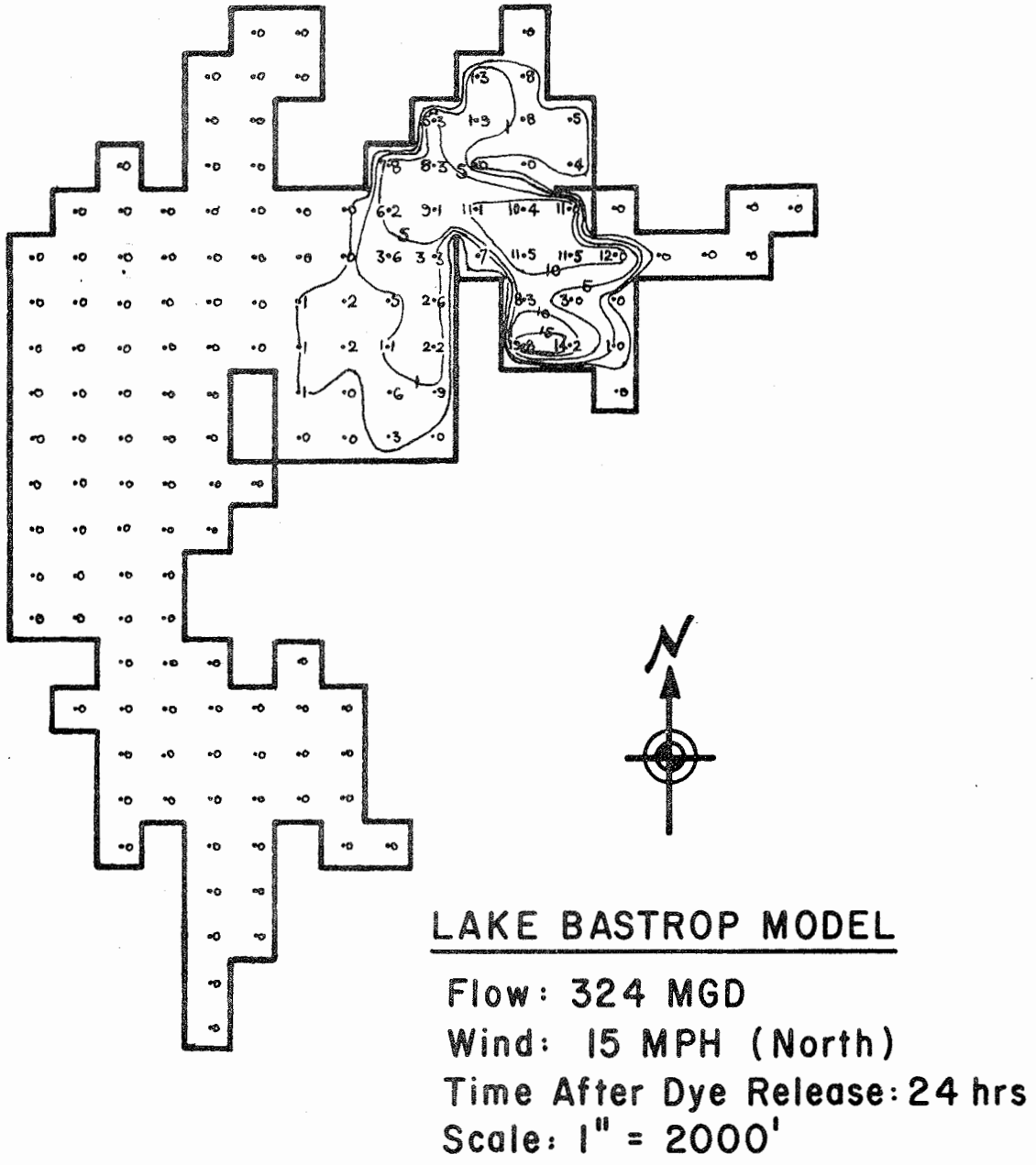

Figure 6-21. Computed Concentration Distribution

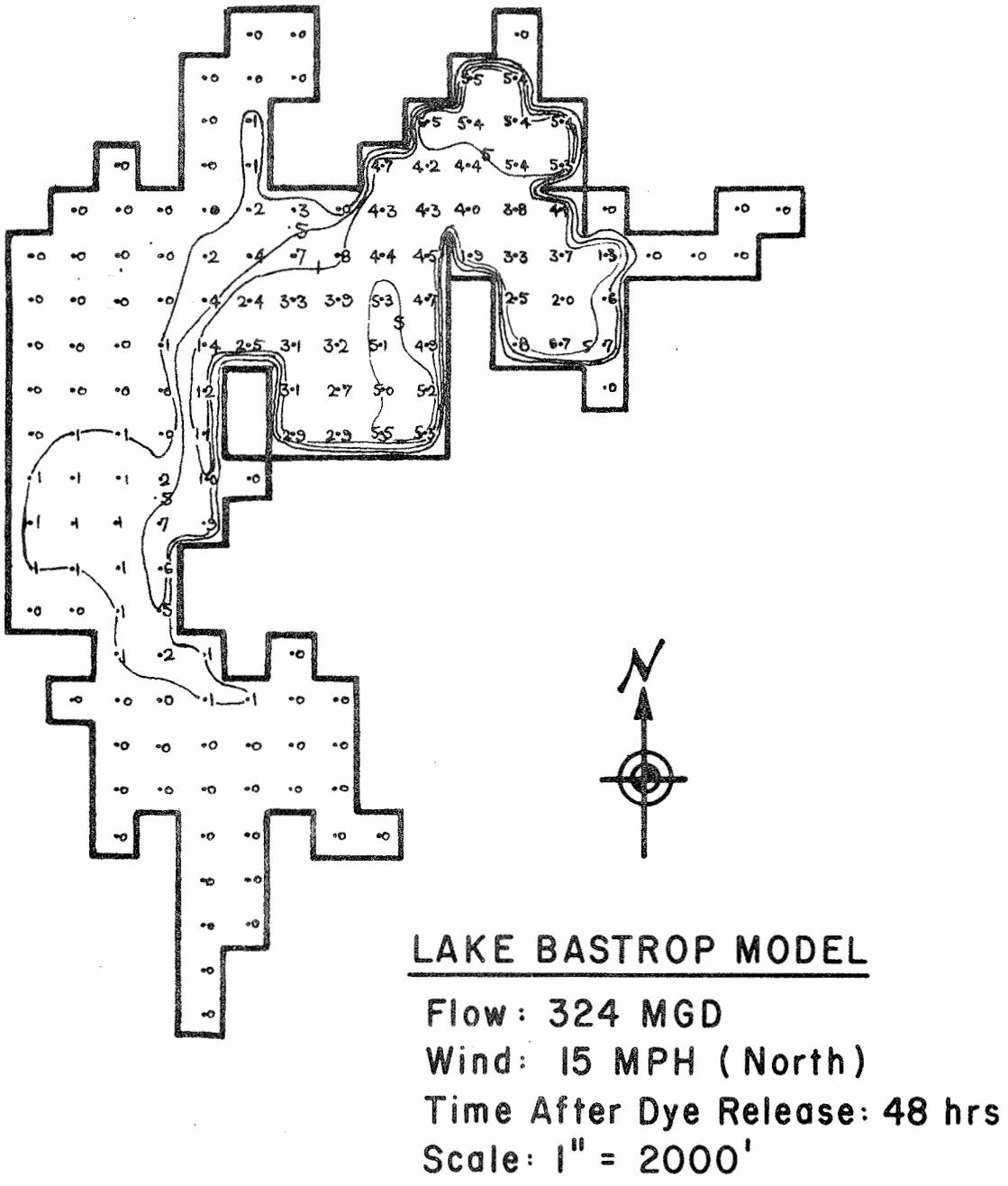

Figure 6-22. Computed Concentration Distribution

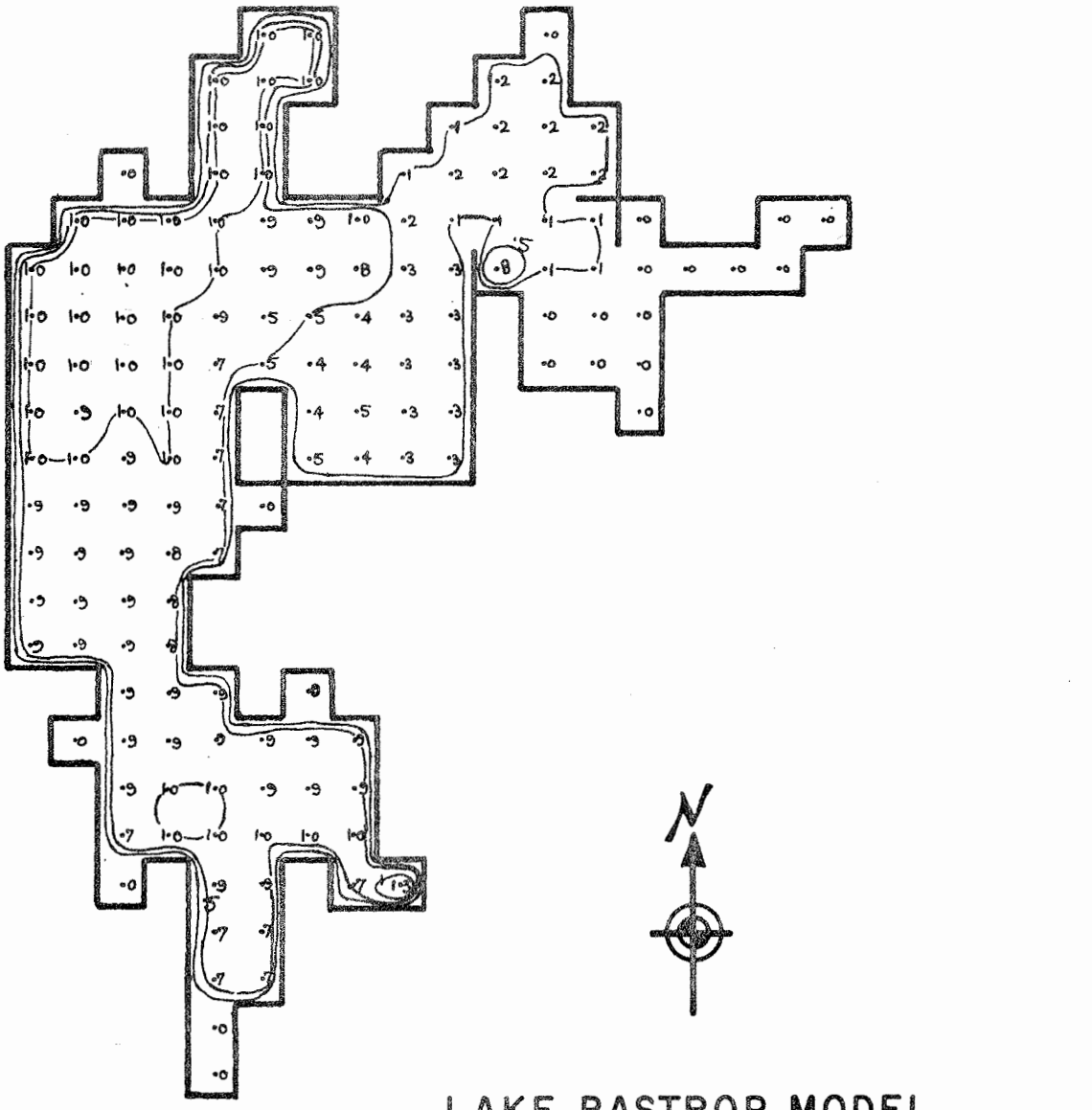

Figure 6-23. Computed Concentration Distribution

accommodates the small numerical magnitudes involved in parts per billion measurements. The transport concentration patterns do not appear to show any chaotic zones which would be signs of calculational instabilities or of serious truncation errors. However, the foregoing remarks do not intend to infer that an optimum, all-purpose computational cell system has been attained. Perhaps, a reduction in the 500' x 500' cell grid-size would achieve better density and definition of computed values, and this refined definition might be desirable for constricted areas of the lake. The smaller grid would permit a refinement of boundary and bottom topography description. However, the increase in computational effort must be considered. If the objective of a model study is to make an economical, rapid, macroscopic analysis of the entire lake, a coarse grid size is apropos. If the objective is to focus only a limited area of special interest, then a smaller, more refined boundary cell system should be used.

2. Determination of the Effects of Changes in Flow and Wind on Concentration Distribution and Peak Travel Time. Using the lake transport model, the effects of assumed combinations of flow and wind were examined.

Figures 6-24 to 6-27, inclusive, show the effects of changes in flow and wind on the concentration distributions in four consecutive cells: (10, 15), (9, 15), (8, 15) and (8, 14) after excitation of the model. Mixing causes the peak concentration to decrease and the slug to be diffused over longer distances in the direction of flow. The theoretical time-of-travel between consecutive cell centers can easily be computed from these plots. Figure 6-28 shows the expected, theoretical effects of various wind conditions on a typical lake cell (6, 12) located more remotely from the channel outlet. These model simulations typify the preliminary type of analyses which can be made of convective dispersion. They show the effects of mixing on peak concentrations of conservative materials transported through contiguous cells.

A general mathematical explanation for these results can be given using the most general form of Taylor's equation, applicable to

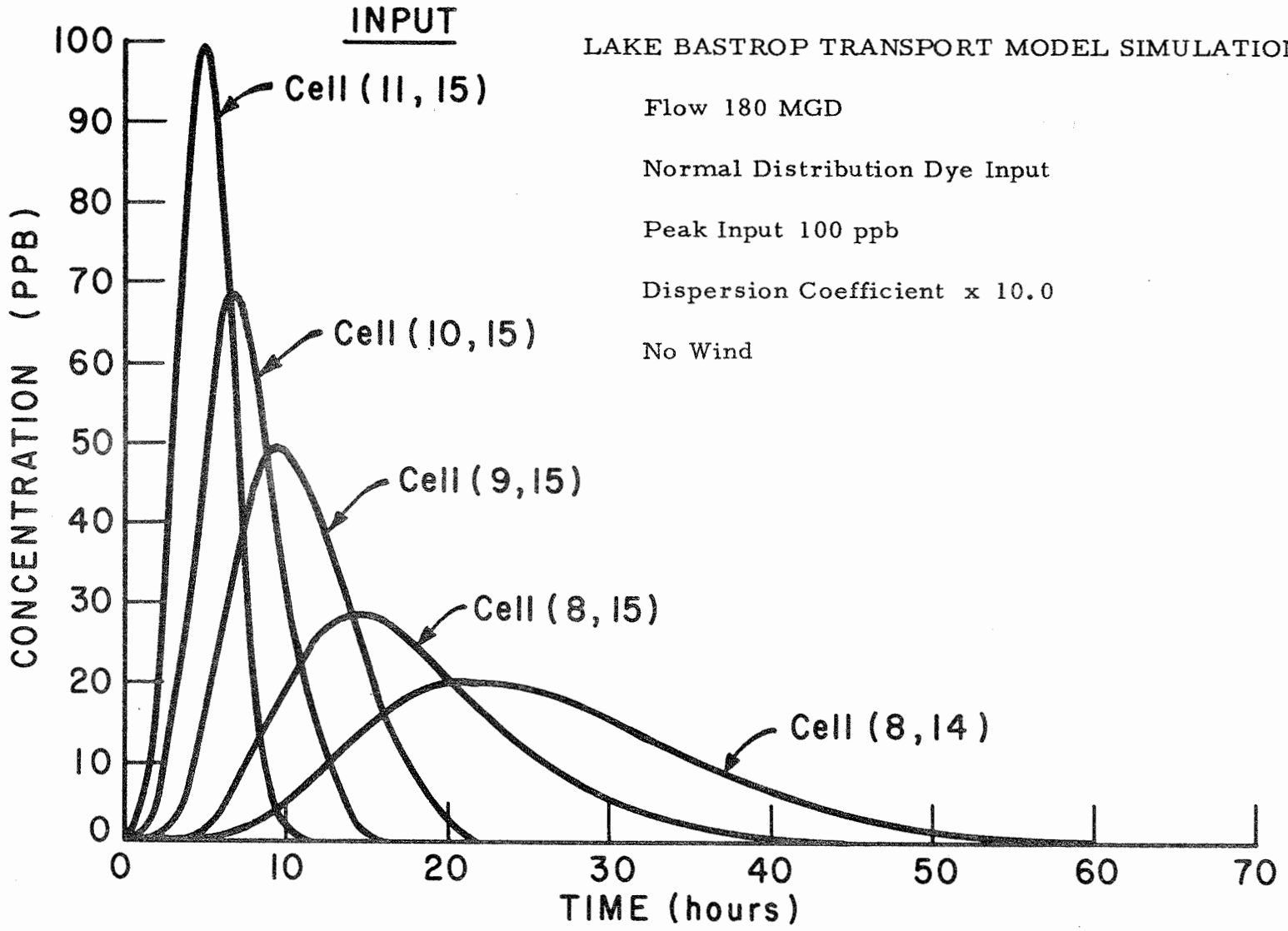

Figure 6-24. Wind and Flow Effects on Time-Concentration Function

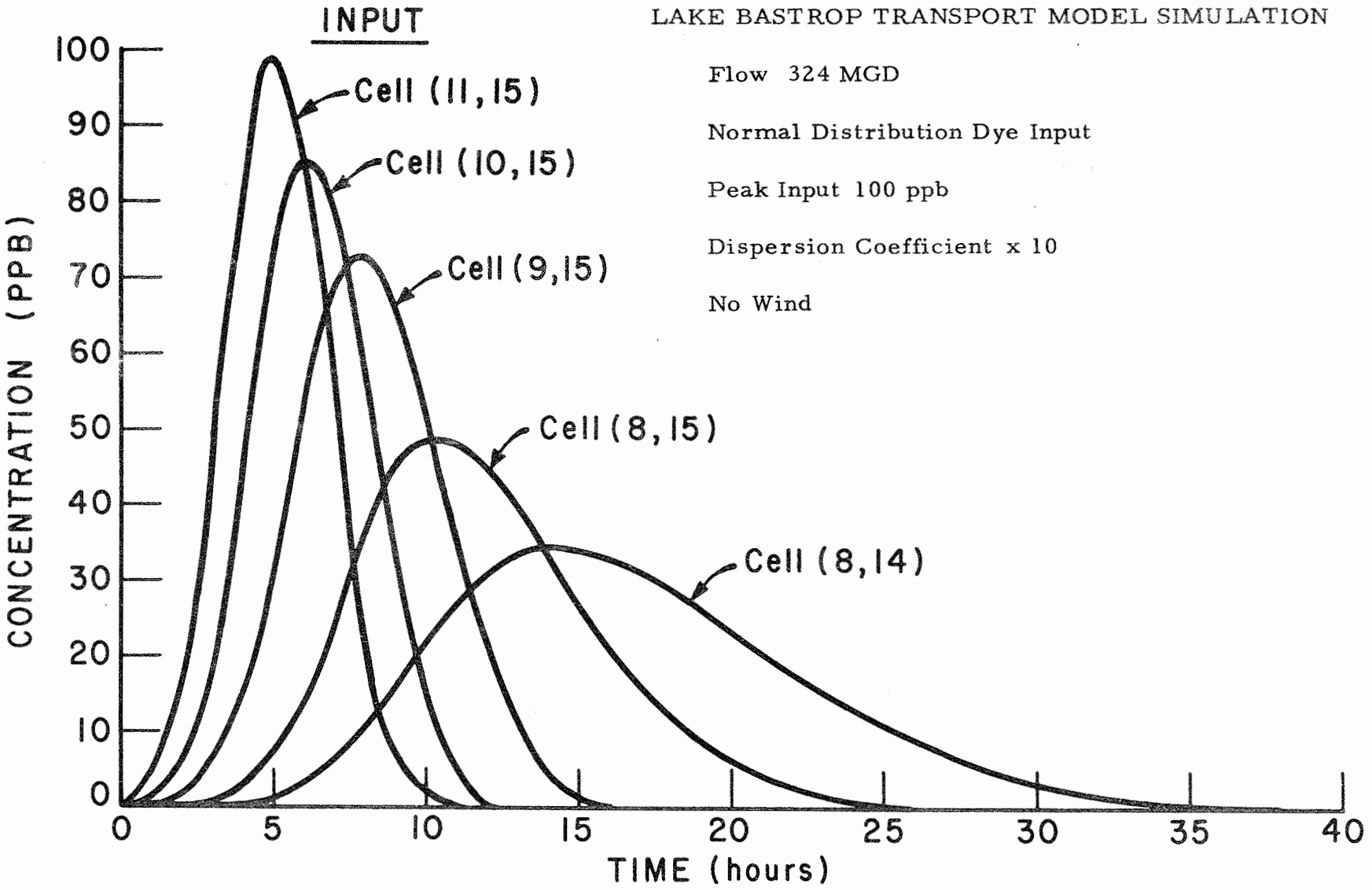

Figure 6-25. Wind and Flow Effects on Time-Concentration Function

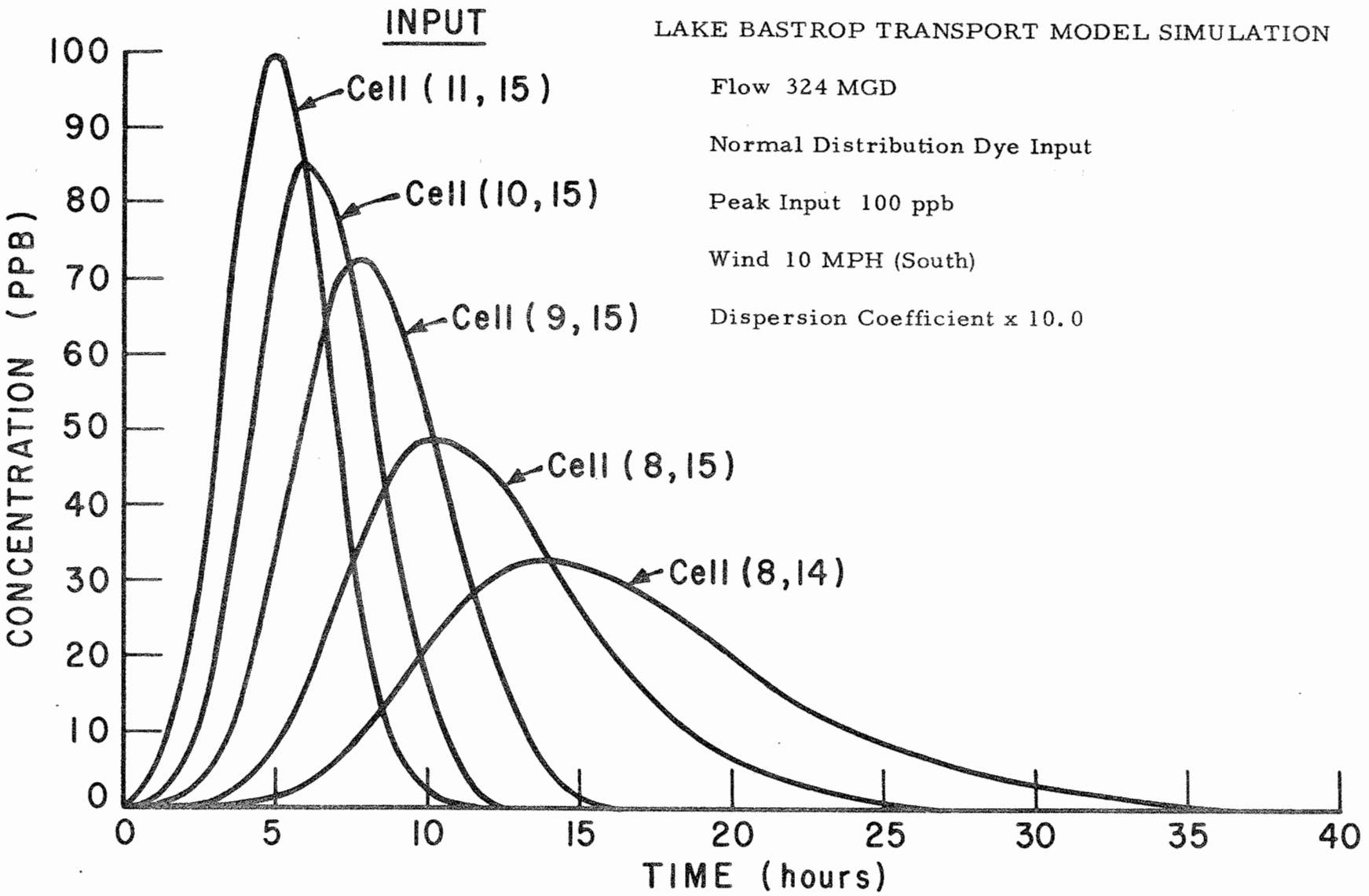

Figure 6-26. Wind and Flow Effects on Time-Concentration Function

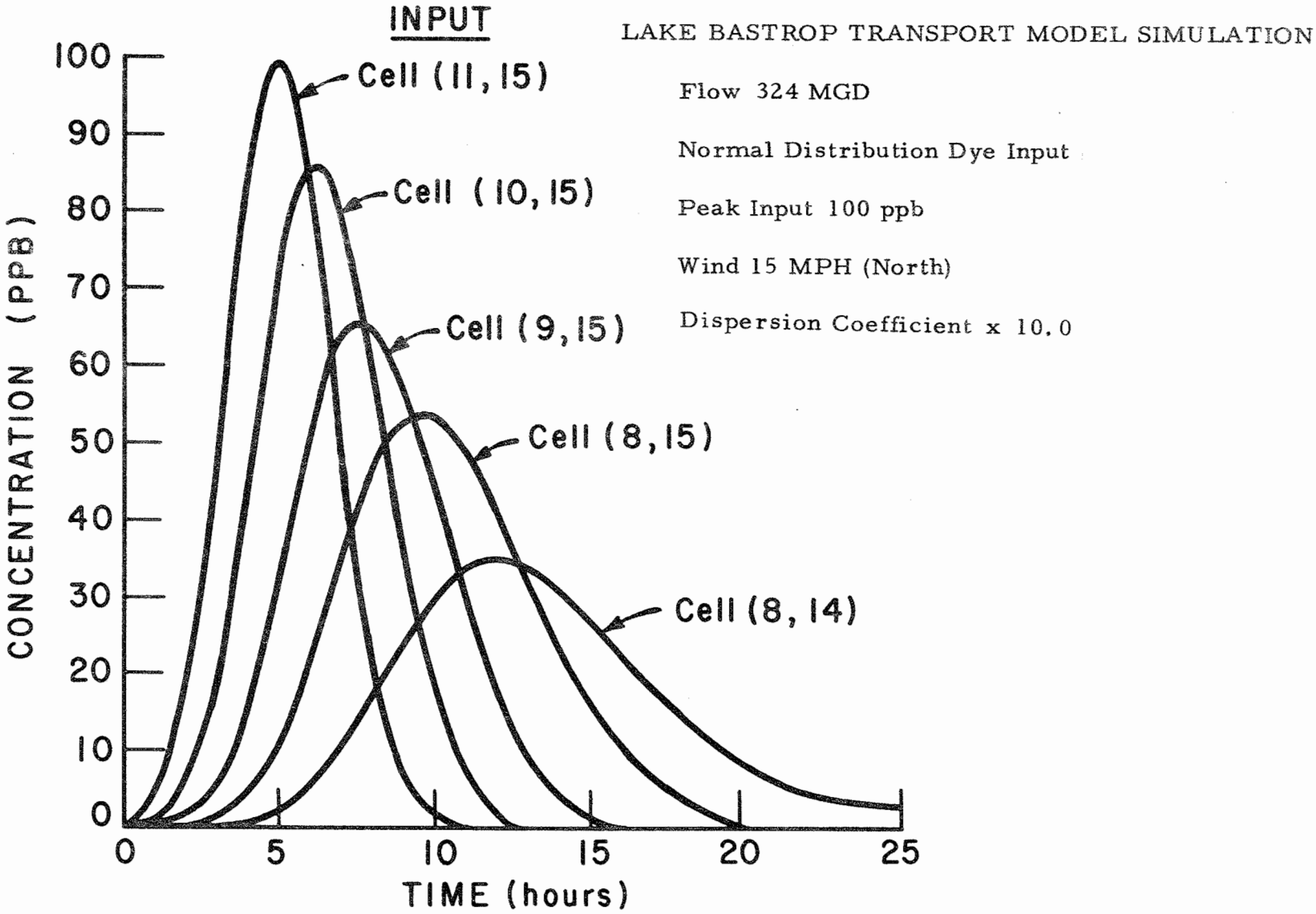

Figure 6-27. Wind and Flow Effects on Time-Concentration Function

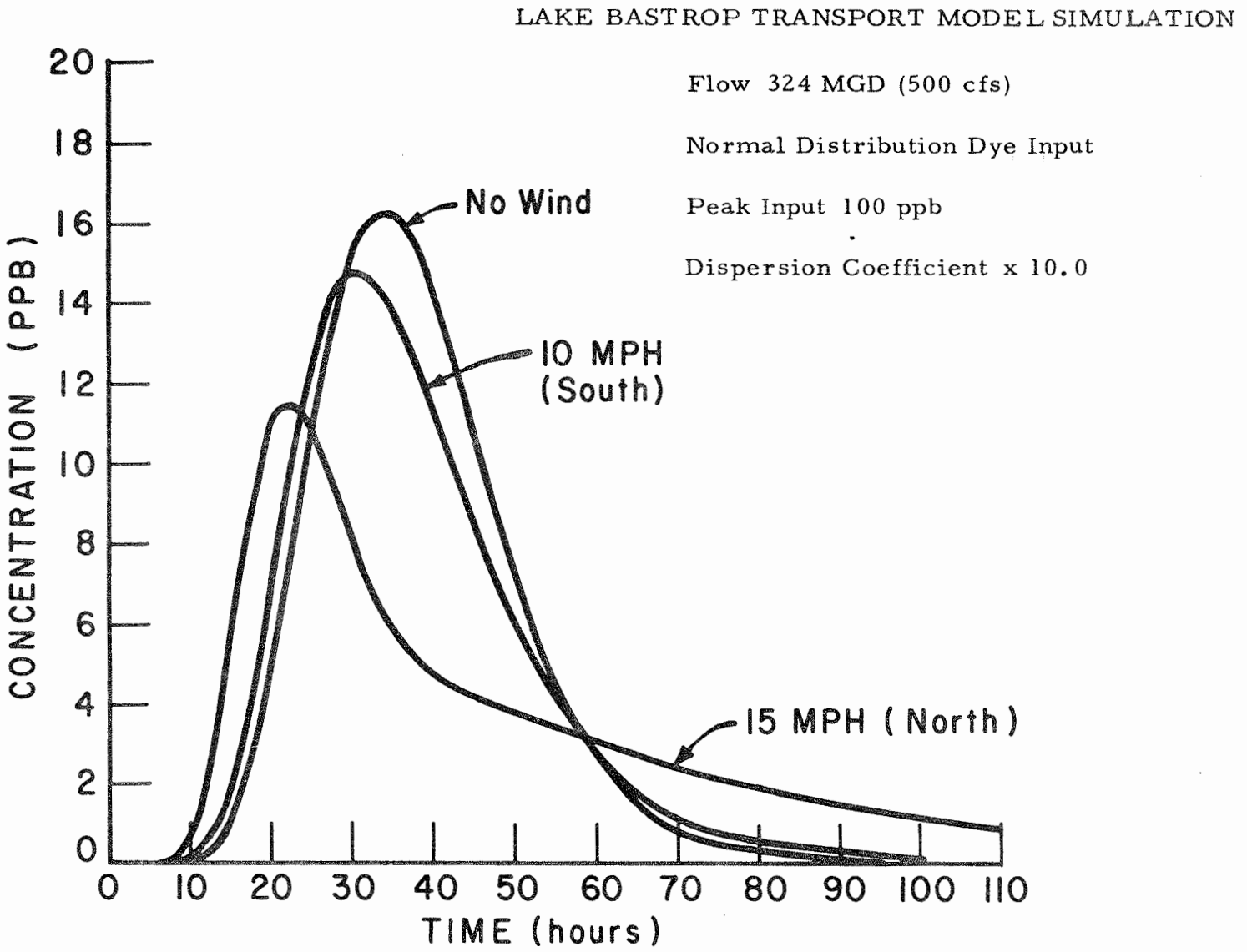

Figure 6-28. Wind Effects on Time-Concentration Function, Cell (6, 12).

either conservative or non-conservative substances, as suggested by the American Petroleum Institute (1969). The one-dimensional equation for the time-concentration curve at an observation point, located at a distance, x,downstream from a point of instantaneous injection, is:

$$m = \frac{W}{2A\sqrt{E_L t}} \exp\left[-K_d t - \frac{(x-vt)^2}{4E_L t}\right] \qquad (6-4)$$

where:

m = material concentration, in pounds per cubic foot.

W = material dose, in pounds.

A = stream cross-sectional area, in square feet.

E_L = longitudinal dispersion coefficient, square feet/second.

t = time, in seconds.

K_d = deoxygenation rate constant, in reciprocal seconds.

V = the mean stream velocity of receiving water in the x-direction, in feet per second.

Differentiation of the above Equation (6-4) yields the following equation for time of peak concentration at distance x:

$$t_{PEAK} = \frac{x}{\sqrt{4E_L K_d - V^2}} . \qquad (6-5)$$

For a conservative material, $K_d = 0$ and the above equation becomes

$$t_{PEAK} = \frac{x}{V} . \qquad (6-6)$$

And, the peak concentration becomes:

$$m = \frac{W}{2A\sqrt{E_L t_{PEAK}}} \quad . \tag{6-7}$$

From Equation (6-6) and (6-7), applicable to instantaneous injections, it can be seen that concentration peaks are inversely proportional to the square root of the dispersion coefficient, and that the time of peak at a given location is inversely proportional to an average stream velocity.

CHAPTER VII

FIELD VERIFICATION TESTS AND MEASUREMENTS

Introduction

This chapter will be subdivided into the following major topics:

1. A brief syllabus of the scope and objectives of preliminary field and laboratory reconnaissances, tests and, measurements involved in the verification process of the numerical model described.

2. A listing and general description of the essential equipment and materials used in the verification operations.

3. A general description of the various techniques used in the verification operations.

4. A detailed description of the sequential investigations and tests leading to verification, and a critical evaluation of the results and impacts of these tests.

Scope

The verification operations involved the methodical accomplishment of the following tasks with the specific objectives, as stated:

Preliminary Hydrodynamic and Hydromechanical Explorations. The following initial explorations, tests and measurements were made at Lake Bastrop and in the tributary discharge channel of the Sim Gideon power plant:

1. Discharge Channel: The work included confirmation of channel geometry and channel flow characteristics.

Objectives: (1) To evaluate the proposed use of the channel as an efficient, mixing and dispersive "feeder mechanism" of desired variable-concentration inputs into the lake. (2) To evaluate the feasibility of using the power plant discharge channel as the prototype for a uniform cross-section, open-channel transport model.

2. Lake. The work included observation of the effects of normal power plant operations on the lake level and plant cooling water discharge rates, essential features of lake configuration, and the extent of algal growth in prospective test zones of the lake. The work also included the measurement of velocity profiles and depths at critical points, the observation of general current and circulation patterns; and a depth reconnaissance from the confluence of the discharge channel and the lake to the power plant inlet, along "thalweg" of lake main channel. Objectives: (1) To confirm the major findings of the basic research on Lake Bastrop described in Chapter V, which led to the selection and use of the Lake Bastrop complex as the prototype lake hydrodynamic system. (2) To select feasible locations for test stations and model verification zones. (3) To determine essential and suitable test equipment, materials and prepare test.

Analysis of Initial Conditions; Procedure Familiarization Trials; Calibration of Equipment. The following tests and related actions were taken:

1. Laboratory. Using standard solutions of Rhodamine B tracer dye with lake water as a diluent, fluorometric calibration and temperature correction curves were prepared. Objectives: (1) To prepare for the conversion and temperature corrections over a wide range of fluorometric measurements.

2. Discharge Channel and Lake. Rhodamine B solutions of desired concentrations were prepared and measured quantities of the solutions were released instantaneously at the turbulent discharge outlets of the power plant for two separate trial tests. The solutions used in these two tests contained 60 grams and 90 grams, respectively, of Rhodamine B powder. The actual solution concentrations

were 1.997×10^6 ppb and 3.15×10^6 ppb, respectively. Objectives: (1) To check the validity and accuracy of the discharge channel transport model concentration versus time relationships at stations in the channel, especially at the end of the 4440-foot paved channel. (2) To compute the longitudinal dispersion coefficients using the method of variances based on observed dye concentration versus distance data in the channel. And, to compute this value with that obtained using conventional formulas. (3) To assess the accuracy of methods used to estimate dye quantities for controlled dye tests. (The quantity estimating method used is part of a conventional technique for computing flow measurement with fluorescent tracers. Reference: Replogle, et al, 1966). (4) To use and then evaluate the practicality of continuous, flow-through fluorometric procedures for dye tracing developed by other investigators. (Reference: Foxworthy and Kneeling, 1969; Wilson and Masch, 1967). (5) Analyze fluorometric measurements to ascertain the relative severity of adsorption or background fluorescence. (6) To ascertain the practical limit of dye concentration dosages to preclude "concentration quenching" - a factor to be considered for measurements in high-concentration tracer clouds likely to be experienced in the constricted channel. (The term "concentration quenching" is a reduction in the rate of increase of fluorometer read-out with increasing dye concentration due to the increasing optical density of the dye itself. This is a problem associated with very high concentrations.) (7) To ascertain the relative detectibility, or the extent to which the dye may be identified quantitatively in the lake. (It will be noted that special emphasis was given to the analysis of fluorometric measurement factors. This concern is prompted by the fact that the strength of verification depends inherently on achieving a reliable correlation between valid field fluorometric readings and dye concentrations.

3. Lake. Measured quantities of solution of known concentrations made up of 60 grams and 90 grams, respectively, of Rhodamine B powder were released instantaneously at the power plant outlets (which will be referred to henceforth as Station 0 + 00 of the discharge channel, or the dye release point), thus obtaining a fully-mixed influx into

the lake. Fluorometric readings versus time measurements were made from selected, anchored stations in the lake; and, fluorometric readings versus distance measurements were made by traversing marked known distances. Objectives: (1) To evaluate the dye dilution and loss effects sustained by the dye dosages over the approximate 2-mile run from point of dye release to the limit of the verification zone. (2) To estimate the range of dosage and concentrations which would insure reliable detection (i.e., not below 0.1 ppb and not so high as to cause concentration quenching) of fluorescent dye concentrations within the verification zone of the lake during the two or three days of the field verification period. (2) To compute localized lateral and longitudinal dispersion coefficients by the method of variances using measured concentration versus distance data taken over measured distances.

First Comprehensive Field Verification of the Lake Transport Model. The following data were used as input into the transport model computer programs: (1) The cell velocities computed by the hydrodynamic model corresponding to the actual lake flow, (324 MGD), and the actual wind conditions, (0 MPH), occurring at the Lake Bastrop verification zone during the period, June 23-24, 1970. (2) The concentration ordinates at uniform time intervals, obtained from a measured concentration versus time curve based on continuous fluorometer sampling taken from an anchored, marked position at the confluence of discharge channel and lake. This marked position at the center of lake cell (10, 15) was taken as the center of "excitation cell" for the numerical model. The concentration versus time curve was taken at cell (10, 15) after release of a solution of 1.17 lbs. of dye tracer dissolved in 28.5 liters of lake water at Station 0 + 00 of the discharge channel. Objectives: (1) To prepare predicted

concentration contour maps for verification zone at selected time intervals (3, 6, 12, 24 and 48 hours); (2) To plot computed versus field-measured concentration versus time data in several cells located a short distance inside the verification zone, during the first 24 hours after release of dye. (3) To plot on a contour map the averaged computed field-measured concentrations in several selected cells located in the middle of the verification zone measured during the second 24 hours after the release of dye. (4) To plot vertical concentration profiles for two cells in the verification zone. (Note: One cell is located a short distance inside the verification zone; another is located mid-zone.) Concentration measurements were made both in the laboratory on "grab" samples, and in the field by continuous flow-through fluorometer measurements. (5) To compute time-of-travel of peak concentration for selected areas in the verification zone.

Second Comprehensive Field Verification of Lake Transport Model. The following were used as input data into the transport model computer program: (1) The cell velocities computed by the hydrodynamic model corresponding to the actual lake flow, (324 MGD), and average wind conditions, (10 MPH - South), occurring at the verification zone on June 30, 1970. (2) The concentration ordinate values at uniform time intervals obtained from the measured concentration versus time curve based on continuous fluorometer sampling, taken from an anchored, marked position at the confluence of the discharge channel and the lake. This marked

position at the end of the concrete-lined channel is the center of model cell (11, 15). This cell was used as the "excitation cell" for the computations of the second verification test. The concentration versus time curve was taken at cell (11, 15) after release of 1.225 lbs. of dye dissolved in 28.5 liters of lake water at Station 0 + 00 of the discharge channel. Using as input in the channel transport model, the value of the actual dosage, (1.225 lbs), and the value of the average longitudinal velocity resulting from wind conditions (10 MPH - South) occurring on June 30, 1970, the concentration versus time curve for the end of the discharge channel was computed. This computed curve was compared with the temperature corrected measured curve. Objectives: (1) To prepare predicted concentration contour maps for the verification zone for 12 and 24 hours after dye release. (2) To plot computed predicted versus field-measured concentration versus time data for several selected cells in the verification zone during the first 24 hours after release of the dye. (3) To compute time-of-travel of peak concentration for selected areas in the verification zone.

General Description of Equipment and Materials

Main Testing Equipment. See Photos, Figure 7-1. The boat, a KENNER SKI BARGE, powered with 33 HP EVINRUDE outboard motor was equipped with the following instruments:

1. Fluorometer and Ancillary Equipment. TURNER Model III fluorometer equipped with the continuous-sampling door

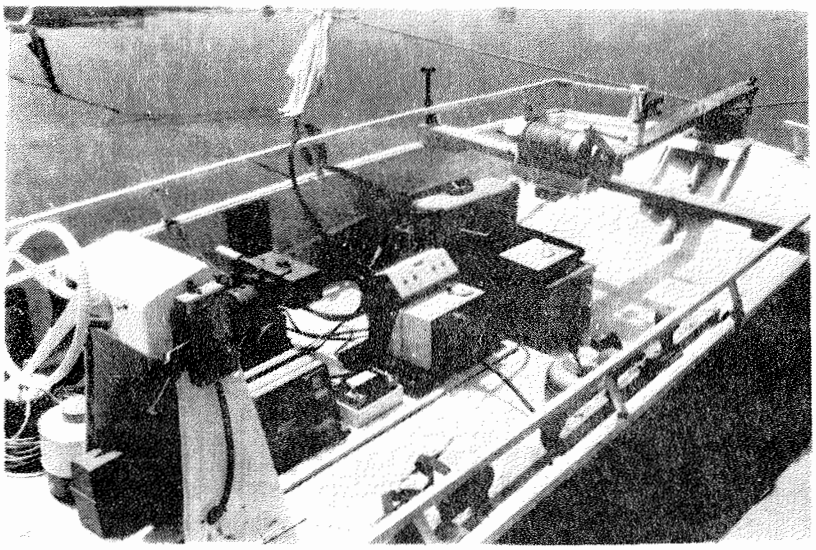

(a) General View of Equipment.
Note: Price Meter Cable Winch and Outrigger for Suspension of Meter at Upper (Bow) part of Boat.

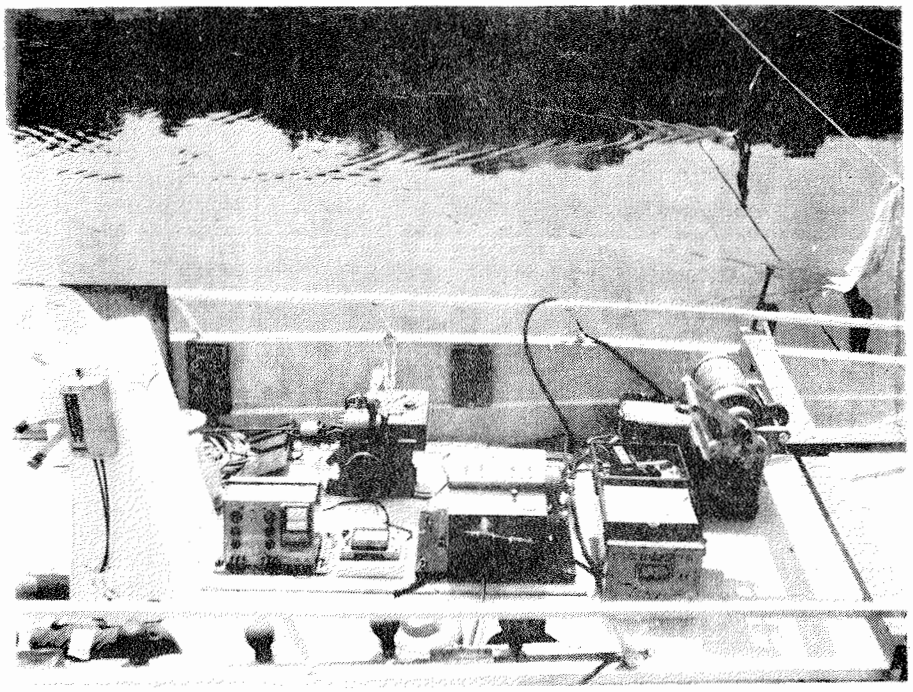

(b) Closer View of Equipment.
Note: Continuous Flow Fluorometer, Anemometer, Discrete Shallow Sampler, Photo Equipment

Figure 7-1. Boat and Test Equipment.

door fitted with intake and discharge hoses. A special hood was devised to reduce light, leakage into the instrument, and a base equipped with small shock absorbers was devised to dampen vibrations. Electrical power was supplied by a 1250 W., 115 V a.c., 60 cps alternator driven by 3.5 HP gasoline engine. A JABSCO model B3M6 pump supplied a 2 gpm flow through the fluorometer. A YELLOW SPRINGS INSTRUMENT COMPANY Model 410 thermistor probe was installed in the fluorometer discharge line and connected to a battery-powered YELLOW SPRINGS INSTRUMENT COMPANY field Model 43 TD Tele-thermometer. Input from the fluorometer and thermometer was transmitted and recorded on the strip chart of a YELLOW SPRINGS INSTRUMENT COMPANY Model 81 dual channel recorder. The chart speed was set at 30 inches per hour.

2. Water Velocity Meter. A PRICE current meter consisting of a 6-vane rotor equipped with audio-headphone attachment, and a standard 75-lb. lead weight was used. The boat was fitted with a cross-arm and outrigger for mounting and operating the cable winch. The winch was equipped with a depth dial which enabled the placement of the meter at desired depths.

3. Anemometer. A 3-cup CASELLA contact anemometer was used. The instrument was equipped with an audio-visual counter and a wind speed conversion chart.

4. Vertical Sampling Device. An improvised arrangement was used consisting of a series of nine storage battery-type rubber syringes spaced at one-foot intervals on a wood pole. The bulbs were evacuated of air and clamps placed on the collapsed bulbs. Simultaneous vertical sampling was done by pulling a clamp release cord.

Other Equipment.

1. The SAVONIUS current meter and fathometer used in this study, is equipment installed on the test boat of the Applied Research Laboratory, Balcones Research Center, The University of Texas at Austin.

2. Normal hydraulic laboratory equipment and ancillary fluorometer equipment for testing of discrete samples of lake water and, preparation of tracer standard solutions.

Materials.

1. Rhodamine B solution and powder. (More details are furnished in the next section of this chapter.)

2. Float markers.

General Description of Techniques Used in the Verification Operations.

General. The field verification operations conducted in this study required application or adaptation of the following techniques:

1. Estimation of Rhodamine B dye dosage requirements.

2. Fluorometric procedures for continuous sampling dye tracing.

3. Discrete vertical "grab" sample acquisition.

4. Velocity profile and depth measurements.

5. Wind velocity measurements.

6. Flow and lake level data determinations.

In Chapter II, a description was given of a several prominent extensive field investigations which illustrate the relatively advanced development and the variable uses in dye tracing techniques. In addition, the studies of Patterson and Gloyna (1963), Wilson and Masch (1967), furnished essential data based on practical field conditions. Hence, only the most essential aspects of these techniques will be discussed in the following sections.

Dosage Requirements Estimates. The determinations of optimum dosages of tracer required considerable research and trial efforts. This arose from the decision to consider the channel and lake as part of a comprehensive hydrodynamic system. The channel controlled the initial conditions and thus warranted special analysis. The results of computed dye injections into a virtually-closed recirculation system subject to thermal stratification could not be fully anticipated without field trials and observations. Several formulas and methods were analyzed. Three were found to be satisfactory for making rational estimates:

1. The Cobb-Bailey Formula

$$V_d = 3 \times 10^7 \frac{C_p}{C_d} Q t_p \qquad (7\text{-}1)$$

where:

V_d = Volume of dye solution to be injected (ml).

C_p = Peak dye concentration desired at terminal site (ppb).

C_d = concentration of dye solution injected (ppb).

Q = average discharge (cfs).

t_p = Estimated time in hours for dye peak to travel from injection point to terminal site.

3×10^7 = combination of conversion factors. (See Dunn 1968).

2. The Wilson Formula

$$V_d = f \frac{Q\ L}{V} \qquad (7\text{-}2)$$

where:

V_d = (as defined above).

f = Coefficient equal to 0.06/dye solution strength in ratio form (For example, 0.4 for 40%).

Q = (as defined above).

L = Length of reach (miles).

V = Estimated average velocity of stream (cfs).

C_p = (as defined above). (See Dunn 1968)

3. Replogle Formula (1966)

$$S = Q(62.4)\frac{C}{10^9} \cdot \frac{L}{V} \qquad (7\text{-}3)$$

where:

S = Amount of tracer, (lbs).

Q = Flow, (cfs).

C = Expected average concentration in an integrated sample (ppb).

L = Distance from release point to sampling section (ft).

V = Average longitudinal velocity (fps).

t = Time of travel between injection and sampling station.

Using the normal flow, Q = 500 cfs and the measured channel average velocity of 1.3 fps, a field check was made of computed, expected concentrations at L = 1700 ft. and 4900 ft. for four dosages gradually increased from 0.11 lbs. to 1.225 lbs. of active Rhodamine B. These dosages were made up and released in concentrations ranging from 1.9×10^6 ppb to 19.5×10^6 ppb, using 28.5 liters of channel water as a diluent at an average temperature of 95° F. In tests for sensitivity, detectability and stability, it was found that observed readings in the 10-70 ppb range, corrected for temperature, were within 4.0% of predicted values. Wider variations were noted in tests involving low initial concentrations below 10 ppb.

Two forms of Rhodamine B were used:

1. Powder, with measured dry weight density of 3.50 lbs/cu. ft.

2. Solution, with following analysis:

   Active ingredient: 42.0 $\pm$ 2% by weight.

   Specific gravity: 1.120 $\pm$ 0.005, at 20/4° C.

   Total acidity: 48.0 $\pm$ 1.5%, as acetic acid.

   Special trait: Shows complete dispersion when dropped in seawater.

Slightly better predictive results were obtained using concentrations prepared with the powder form and with lake water as a diluent.

The limit of detectability of Rhodamine B concentrations warranted close attention. According to Patterson and Gloyna (1963), the minimum limit of concentration detectability is 2.0×10^{-4} mg/liter; and, the amount of dye needed per 10^6 cubic feet for minimum detectability is 0.01248 lbs. Using these data, a theoretical, minimum amount of 10 lbs of Rhodamine B would be needed to achieve a minimum detectable concentration level throughout the entire 16,590 acre-feet content of the lake, assuming a fully-mixed condition. However, this figure should be considered only as a guide because of the following realistic factors which influence mixing and dispersion in Lake Bastrop:

1. The practical limit of continuous flow-through fluorometer dial accuracy and the limit of sensitivity of detection obtained in laboratory calibrations was 0.1 ppb, using standard solutions with lake water as a diluent. The fluorometer was stable to $\pm$ 1/2 unit.
2. Stratification effects.
3. Temperature effects.
4. Electronic gain and light leakage.

Thus, the foregoing estimated dye values served purely for preliminary planning. Laboratory and on-site tests, and observations using varying amounts of dosages were found to be indispensable. As a result, an optimum dosage of about 2.00 lbs of Rhodamine B was determined to insure reliable, detectable readings for tests contemplated in the discharge channel and in the restricted confines of the selected verification zone of the lake.

Of paramount importance in this analysis of determining optimum dosages was the avoidance of large, frequent, or poorly-placed injections which would result in an excessive, persistent "background" build-up of fluorescent activity in stagnant zones. Such accumulations and subsequent sporadic releases which result from high concentration dosages in low-velocity impoundments containing considerable aquatic growth and silt, would require constant fluorometer re-calibration due to "background" variation. This would complicate and prolong the conditions for consecutive tests which must be conducted with a minimum of delay in order to operate under reasonably similar hydrometeorological conditions.

Based on the foregoing considerations, separate dosages of 56.9 grams, 90 grams, 1.17 lbs and 1.225 lbs were selected for use in separate formal field tests. The actual hydrometeorological conditions occurring on June 8, 10, 18, 23, 24 and 30, 1970 were used as input into the hydrodynamic and transport model to generate predicted values for necessary verification.

Fluorometric Procedures. The basic dye tracing techniques used in the verification tests are those described in U. S. Geological Survey, Water Supply Paper No. 1892 (1968), for continuous sampling at a depth of 2 feet below the surface with a continuous record of temperature and dimensionless fluorometric dial readings.

One aspect warranting special emphasis is the need for careful calibration of fluorometric equipment and adjustment of field readings. Since temperature is the predominant environmental factor influencing the fluorescence of Rhodamine B, all fluorometer readings must be taken at or adjusted to a common temperature. In this study fluorometer calibration and temperature correction curves were prepared and used to make the adjustments. See Figures 7-2 and 7-3.

Another important point is the variance which exists in the fluorometer sensitivity range controls. It must be remembered that the four range selector positions: 30X, 10X, 3X and 1X, indicate only the approximate relative sensitivity of the four positions. There are indications that these sensitivity ratios vary with intensity of ultraviolamp output.

Discrete Vertical Sampling. The sampling method used was that which developed by Wilson and Masch (1967). A series of syringes are installed at one-foot intervals on a rigid wood pole. Prior to lowering, all the syringe bulbs are evacuated of air and the nozzles clamped. For sampling, the pole was lowered and all clamps were released simultaneously by pull-cord.

Velocity Profiles and Depth Soundings. Two methods of velocity measurements were used:

1. In the discharge channel: velocity profile measurements were taken from anchored positions at the channel center-line and at the two adjacent quarter points of a channel transection at Station 17 + 00. Measurements were made at 1-foot depth intervals from surface to channel bed, using a Price current meter.

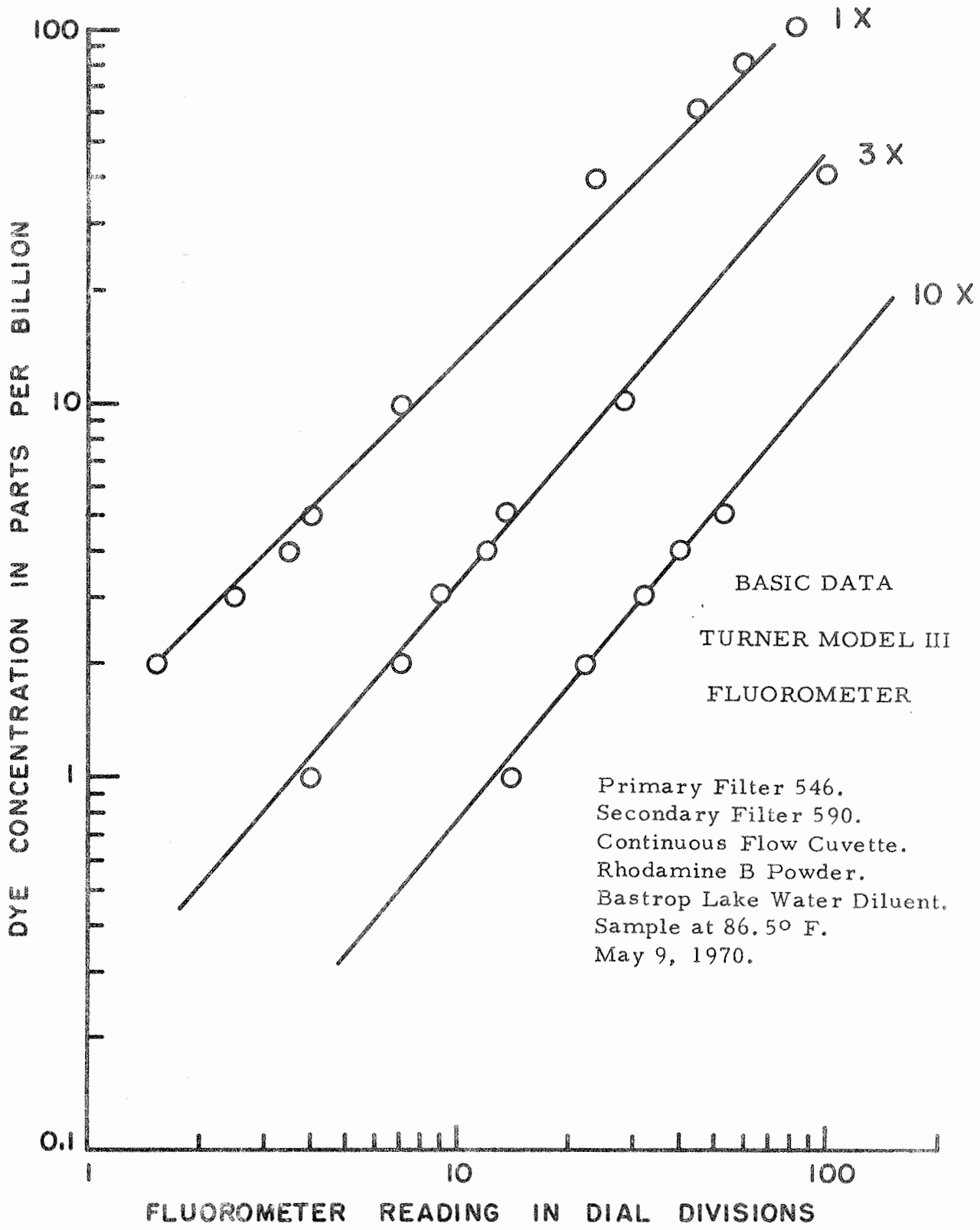

Figure 7-2. Fluorometer Calibration Curves.

Temperature Range	Concentration	Fluorometer Scale
14° C to 32° C	1.3 ppb	30 x
42° C to 25° C	17.0 ppb	1 x

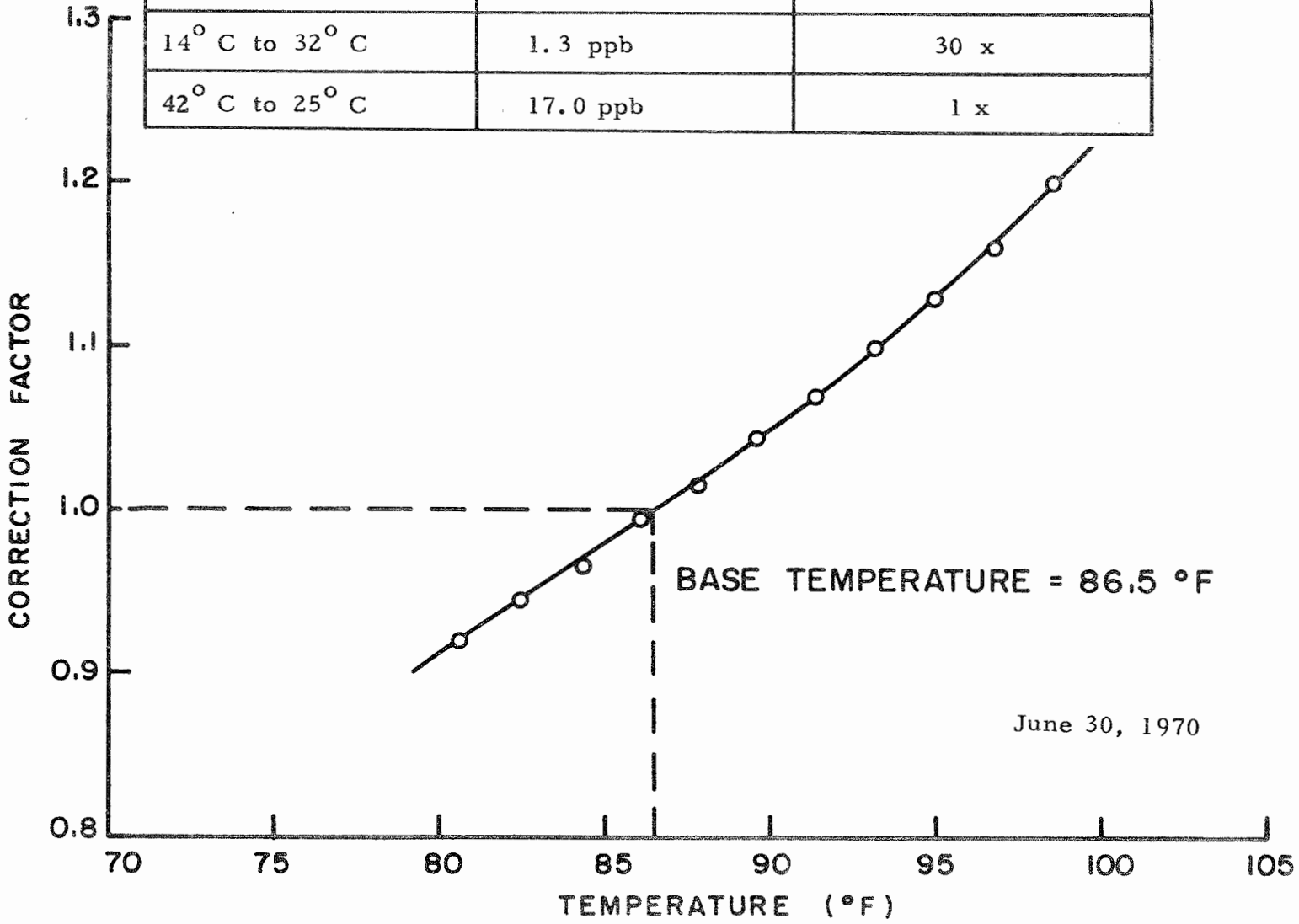

Figure 7-3. Temperature - Correction Curve for Rhodamine B Dye.

2. In the lake: velocity profile measurements were taken from selected anchored stations at one-foot depth intervals, using a continuously-recording, directional Savonius current meter.

Depth soundings were made using a continuously-recording fathometer for a traverse along the thalweg of the lake extending from the end of the inlet to the end of the discharge channel.

Wind Velocity Measurements. Wind measurements were obtained using an anemometer with audio-visual counter. The instrument was placed about six feet above water surface.

Lake Flow and Lake Level Determinations. Flow quantities and rates were obtained directly from power plant operational records. Lake levels were determined from the Lower Colorado River Authority gaging station at the dam.

Description of Field Verification Tests and Measurements

The sequence of items in this final section of the chapter is keyed to the sequence established in the section on Scope.

Preliminary Hydrodynamic and Hydromechanic Explorations. Following are results of actions taken to systematize lake geometry, grid systems, boundary conditions and reference stations as preparations for model computations and field verification. The average depth of cells used as input to both the hydrodynamic and transport models, shown earlier in Figure 6-1, were re-checked using the following map sources:

1. Lower Colorado River Authority Topographic Map: Sheet 600-A-17 (R-100-C-7) BASTROP POWER PLANT RESERVOIR.

2. Lake Bastrop - Fisherman's Reference Map, 1969. On June 18, 1970, a continuously-recorded fathometer survey was made of the 3-mile lake channel extending from the end of power plant inlet channel to the terminus of the discharge channel, and also the 12-cell test area at the confluence of the channel and lake. (See Figure 5-5). The map data and fathometer data reconciled satisfactorily. The average cell depths (Figure 6-1) are reasonable for the 500-foot grid used in this macro-model study.

Figure 7-4 shows the cell system coded by numbers ("flags") representing specific combinations of cell boundary flow conditions. The "flags" are integral elements of the transport model computer program (PROGRAM TRACER), described in the Appendix A. A similar flag system was used in the hydrodynamic model computer program (PROGRAM HYDROD [11]), which generated cell velocity input for PROGRAM TRACER.

Also, on June 18, 1970 velocity profiles were measured using a Savonius meter at selected locations to "spot-check" velocities generated by the hydrodynamic model. Figure 7-5 shows velocity profiles in a vertical plane, measured at two selected cells, which typify four profiles taken equidistantly along the lake main channel between cell centers (9, 15) and (6, 12). Figure 7-5 also shows the computed average velocities for the two given cells. The values were generated using the hydrodynamic model assuming that the upper 30 percent of the lake is a fully-mixed stratum. Measurable steady velocities were restricted to an 8-foot surface stratum. Velocity measurements at greater depths were hampered by a profusion of aquatic plants, and the insensitivity of the Savonius current meter to low velocities of 10^{-1} to 10^{-2} fps order of magnitude.

---

[11] See Chapter IV regarding the algorithm developed by Masch, et al, 1969.

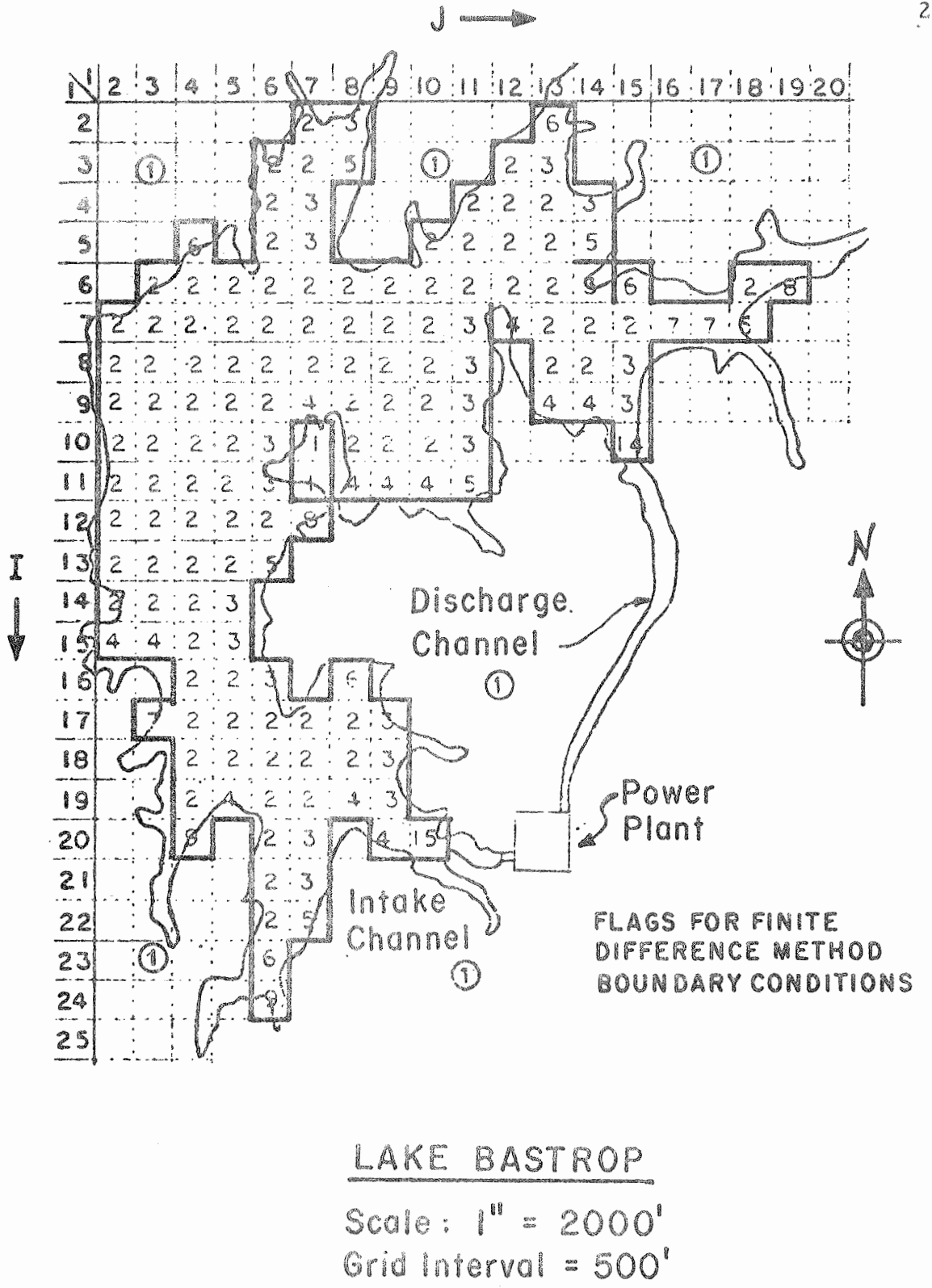

Figure 7-4. Cell Boundary Designations Used in Lake Bastrop Transport Model - Computer Program TRACER.

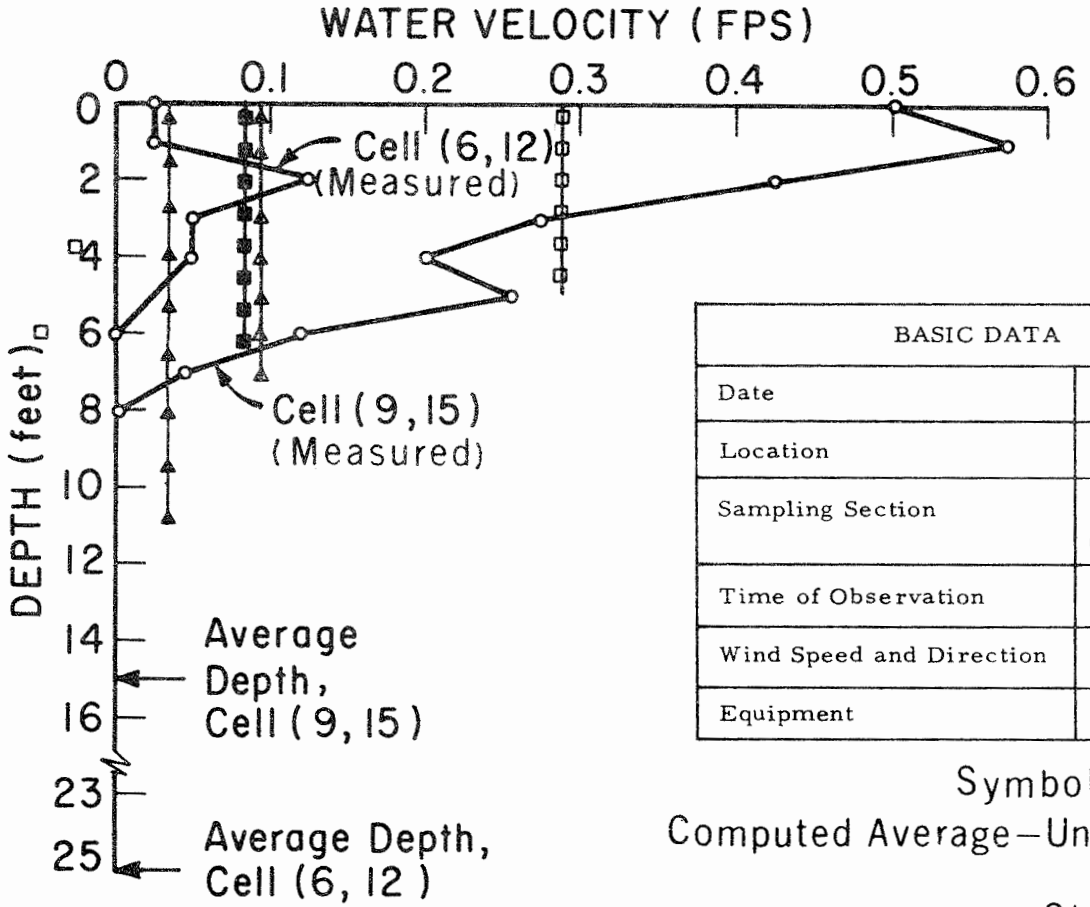

BASIC DATA	
Date	June 18, 1970
Location	Lake Bastrop
Sampling Section	Cell (9, 15); Cell (6, 12) (Marker 1)
Time of Observation	10:30 A.M. ; 1:40 P.M.
Wind Speed and Direction	10 MPH (SE) ; 10 MPH (SE)
Equipment	Savonius Velocity Meter

Symbols

Computed Average—Unstratified: (9,15) —△— (6,12) —▲—

—Stratified: (9,15) —□— (6,12) —■—

Figure 7-5. Velocity Profiles - Cells (9, 15) and (6, 12)

The velocity profile measurements confirm that a two-layer stratification prevails in most of the lake. The top stratum is essentially a fully-mixed, highly-advected layer, the lower is essentially a "dead zone" region which is stabilized vertically by temperature gradients and horizontally by resistance to flow due to dense aquatic growth and a highly-indented bottom topography. The following tabulation is an extract of computed velocity component values for consecutive cells in line with cell (6, 12) and cell (9, 15):

Table 7-1. Extract from Computed Velocity Output of Hydrodynamic Model Assuming Stratification.

I	J	(Velocity Component, feet per second) x-direction[1]	y-direction[2]
2	12	+0.000000	+0.000000
3	12	+0.053169	-0.069926
4	12	+0.044114	-0.019667
5	12	-0.022946	+0.014873
6	12	-0.081686	-0.049065
7	12	+0.000000	-0.081715
8	12	+0.000000	+0.000000
. . . . .			
6	15	-0.000072	+0.000000
7	15	-0.062486	+0.000108
8	15	-0.132563	+0.000000
9	15	-0.282459	+0.000000
10	15	-0.405988	+0.000000
11	15	+0.000000	+0.000000

[1] Negative sign indicates vector direction is north; positive sign indicates south direction.

[2] Negative sign indicates vector direction is west; positive sign indicates east direction.

The tabulated extract of velocities typifies the order of magnitude of computed velocities throughout the lake. It is also of interest that the average cell velocities based on a 30% depth stratification were only slightly larger than the computed velocities based on a fully-mixed lake.

Analysis of actual velocity and temperature profiles compelled further action regarding the initial assumption made in the hydrodynamic model of a homogeneous, shallow, fully-mixed lake. Therefore, effort was turned first to the task of examining the feasibility of developing a realistic adjustment for thermal stratification in the transport model while still using velocities computed from the hydrodynamic model, and then to the task of examining the velocities based on a fully-mixed surface stratum of variable thickness. A rational basis for these examinations was afforded by the following theoretical concepts and field studies:

1. The concept of the "baroclinic layer" that has become firmly established in oceanography, and which involves the dependence of the depth of the lower boundary of a current on water stratification and on the wind field over the sea, (Fomin 1964). According to Fomin (1964), "the baroclinic layer is the layer of water extending from the surface to some depth, which is under the influence of the wind-induced current. The current velocity and tangential stress must be zero at the lower boundary of this layer. A wind-driven current does not propagate beyond the baroclinic layer."

2. The findings of Okubo (1968) regarding oceanic diffusion and Wiegel (1961) regarding engineering aspects of wave spectra and mixing of surface waters - suggest valid

> approximations regarding temperature - density- depth relationships in stratified impoundments. These findings appear to be macroscopic applications of the "baroclinic layer" concept. These concepts will be discussed further in developing the "depth ratio correction" for stratification later on in this section.

In addition, following Fischer's (1966) approach for determining dispersion coefficients, a realistic adjustment was developed for the dispersion coefficient algorithm in the transport model to be discussed later. These "adjustments" represent crucial points, encountered sooner or later in all modeling. Hays, et al (1966), for example, found that:

> "The complexity and variety of the geometry and hydrodynamics of rivers indicates that some rigor will have to be sacrificed to obtain a soluble description."

Regarding transport phenomena Bird, et al (1960) wrote:

> "Quite often, a simpler mathematical model based upon sounder premises will yield far more advantages than a quite sophisticated model based upon a less firm foundation. Approximation, after all, may be in two places - in the construction of the model and in the solution of the associated equations. It is not at all clear which yields a more judicious approximation."

Analysis of Initial Conditions, Procedure Familiarization Trials and Calibration of Equipment. Following are results of tests to determine if the channel model could be used to produce predictable, simulated, initial concentration conditions for the lake model. Incident to these tests, all field dye tracing techniques and equipment were evaluated for suitability and reliability.

1. Check on Channel Model Parameters and Mixing Properties. Figures E-1, E-2, and E-3 (Appendix E) show channel test data based on release of 56.9 grams of Rhodamine B at Station 0 + 00. Figure E-1, shows the time-concentration distribution at Station 17 + 00. This near-Gaussian distribution is typical of other plots taken at this station and confirms the validity of the channel model algorithm which incorporates the following "physical constants":

   Velocity = 1.30 fps

   Hydraulic radius = 5.74

   Manning's n = 0.016

   Using these values in Taylor's equation for the open-channel longitudinal dispersion coefficient gives a value of $D_L = 6.85$ ft^2/sec which also was adopted as another "physical constant" for the Bastrop Channel.

2. Measurements for Lake Dispersion Coefficients. Figures E-2 and E-3 show concentration versus distance curves between selected cells. These data were obtained to compute the longitudinal, (D_{LX}), and lateral, (D_{LY}), coefficients of dispersion in the lake. Using the method of variances $D_L = 1/2\ (d\ \sigma^2/dt)$, (PROGRAM TRACE, Appendix C), values of $D_{LX} = 17.71$ ft^2/sec and $D_{LY} = 5.60$ ft^2/sec were computed for the localized 3-cell area shown in the cited Figures.

3. Additional Tests: Determine the Conditions Produced by the Channel Model. Figures F-1, F-2, F-3 and F-4 (Appendix F) show channel and lake dye test data based on a dye release of 90 grams. Figure F-1 confirms the Gaussian-type concentration vs. time distribution at channel Station 17 + 00. Figure F-2 shows a characteristically-skewed concentration distribution delivered as input to the first computational cell. Figure F-3 and F-4 show concentration vs. distance data for the channel and lake used to compute dispersion coefficients. Conforming to earlier values computed for the same localized area, coefficients of $D_{LM} = 6.65$ ft^2/sec and $D_{LX} = 17.25$ ft^2/sec were obtained for the channel and lake, respectively.

These tests showed that the discharge channel could be used as a reliable time-varying input mechanism for the lake model. However, two important adjustments are necessary to reconcile more closely the observed and computed concentration vs. time curves for channel stations:

1. The average velocity used in the channel model must be corrected for wind effect.

2. The fluorometer must be calibrated carefully and the observed concentrations must be corrected for high-temperature effects which prevail in the channel.

Fluorometer sensitivity checks throughout the 12-cell test area of the verification zone indicated minimum readings of 0.5 ppb were detectable as far out as cell marker 6, located about 2,000 feet from the end of discharge channel. After widespread checking, it was determined that a dosage of 1 to 2 lbs of active Rhodamine B material would be adequate to insure measurable and recordable detection throughout the verification area selected for field tests. See Figures 7-6A and 7-6B.

First Comprehensive Field Verification of the Lake Transport Model.

1. Determination of Stratification Correction for Computed Concentrations. It was indicated earlier in this chapter that due to stratification correction factors would be determined for the dispersion coefficient algorithm and for the computed concentrations.

   a. The dispersion coefficient algorithm correction. It was determined that the Taylor dispersion coefficient algorithm in the lake transport model computer program should be multiplied by a factor of fifty (a

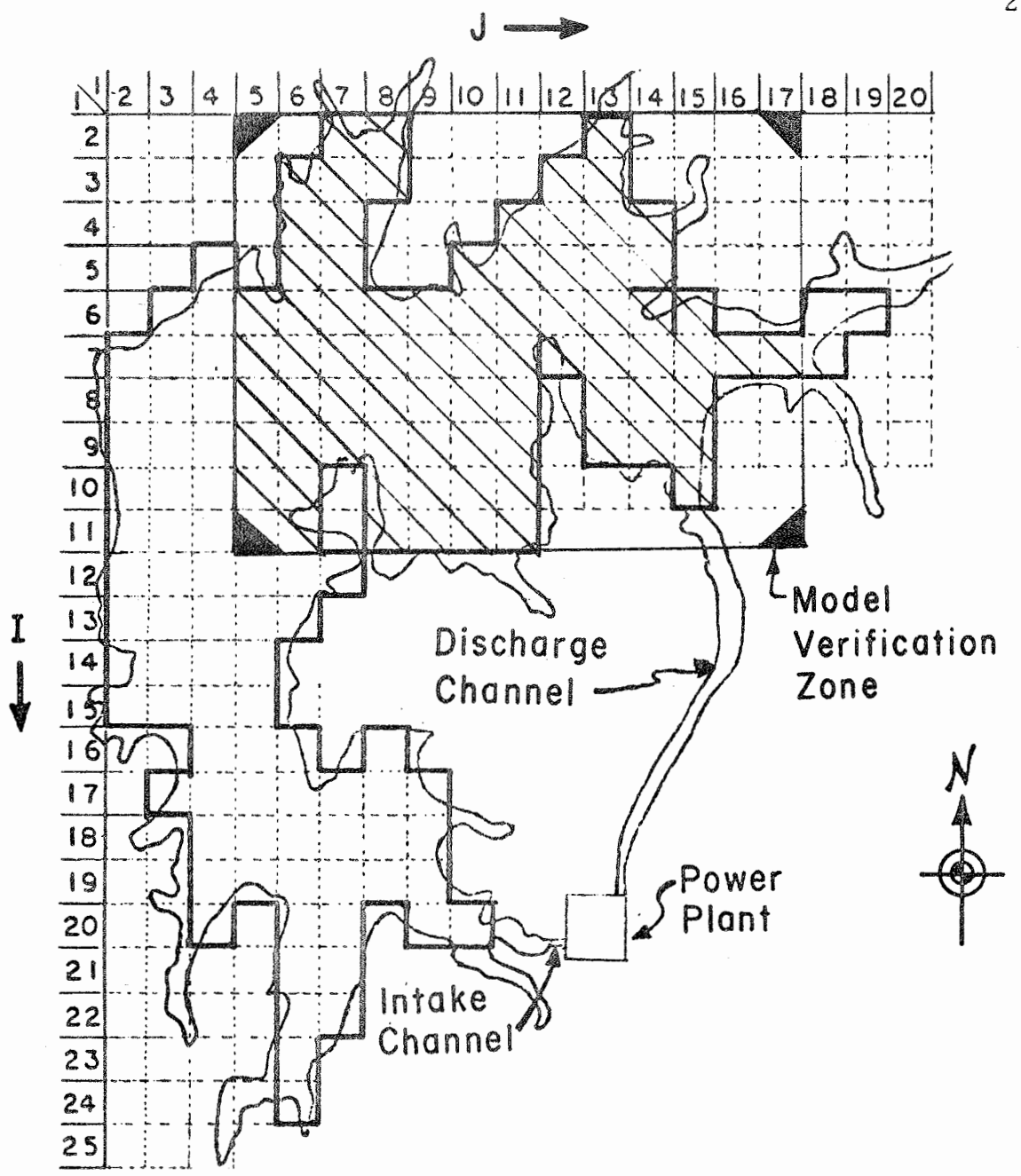

Figure 7-6A. Model Verification Zone

Figure 7-6B. Oblique Aerial Photograph of Lake Bastrop Test Area and Sim Gideon Power Plant Complex. (View to the Northwest.)

Source: Lower Colorado River Authority and The Austin Statesman.

value found after testing a series of factors ranging from 10 to 100). This correction factor produced coefficients in the transport model that were compatible with values of coefficients in the x-and y-directions, computed by the method of variances using observed dye tracer distribution data. The correction to the Taylor dispersion coefficient algorithm was necessary in order to accommodate pronounced wind shear effects and the stochastic nature of surface fluctuations of the lake surface. These two factors overshadow the effects of other cellular variations due to: stratification, profuse aquatic plant growth, irregular bottom topography, and sedimentation. It was evident from results of the first comprehensive tests, that unique prototype conditions, as discussed above, compel a "feedback" readjustment to the initial experimental numerical model. Test results indicate that this correction was an effective part of the adjustment needed to reconcile the observed and computed concentration values.

b. The Depth Ratio Correction for Computed Concentrations. The second component of adjustment, the depth ratio correction, stems basically from a macroscopic application of the concept of the "baroclinic layer", and Okubo's (1968) oceanic diffusion studies. These concepts and studies were alluded to earlier in this section. The following rationale is presented. A study of the velocity and temperature profiles in the lake show a relative constancy only in a surface layer of limited thickness. The reason seems to be that all turbulence in the lake flow remains confined within this surface layer, and make the profiles uniform. Therefore, it can be assumed the phenomena of turbulent dispersion takes place in this surface layer only, while molecular diffusion predominates elsewhere. However, the latter diffusion is of a very low order of magnitude. This is true because the velocities encountered in the lake are very small, with an order of magnitude of 10^{-1} fps. In experimenting with the lake transport model, it was decided to assume initially that turbulent flow existed throughout the entire depth of the lake. And, if this was found not to be true, then effort would be directed toward

finding the "effective stratum" in which turbulent flow could be assumed to be confined. As expected, observations of dye releases indicated that the dye was not uniformly distributed throughout the depth of the lake but rather was confined to the surface layer of the lake. The "effective stratum" can be determined by a series of successive approximations regarding the value of the fully-mixed depth used in the hydrodynamic model until velocities are obtained which produce realistic, verifiable concentration distribution patterns requiring only minor adjustment when used in the lake transport model. In order to facilitate the explanation of the successive approximation technique, first refer to Figure 7-7. Let D_{EXCIT} = depth of the excitation cell. And, suppose that the bulk of the tracer dye concentration in the excitation cell is in a top layer of thickness x. Further let

$$\frac{D_{EXCIT}}{x} = \text{a constant}, \xi \, . \tag{7-4}$$

At some other near-by cell of average depth, $D_{I, J}$, the thickness of the top layer is $x + x'$, where x' is very small, such that $x + x' \approx x$, because diffusion is considered negligible at the interface.

Therefore, if we assume "bringing all concentration to the top layer", the correction factor for cell (I, J) is:

$$F_{I, J} = \frac{D_{I, J}}{x} \, . \tag{7-5}$$

Substituting the value of x from Equation (7-4) we obtain:

$$F_{I, J} = \frac{D_{I, J}}{D_{EXCIT}/\xi} = \xi \frac{D_{I, J}}{D_{EXCIT}} \, . \tag{7-6}$$

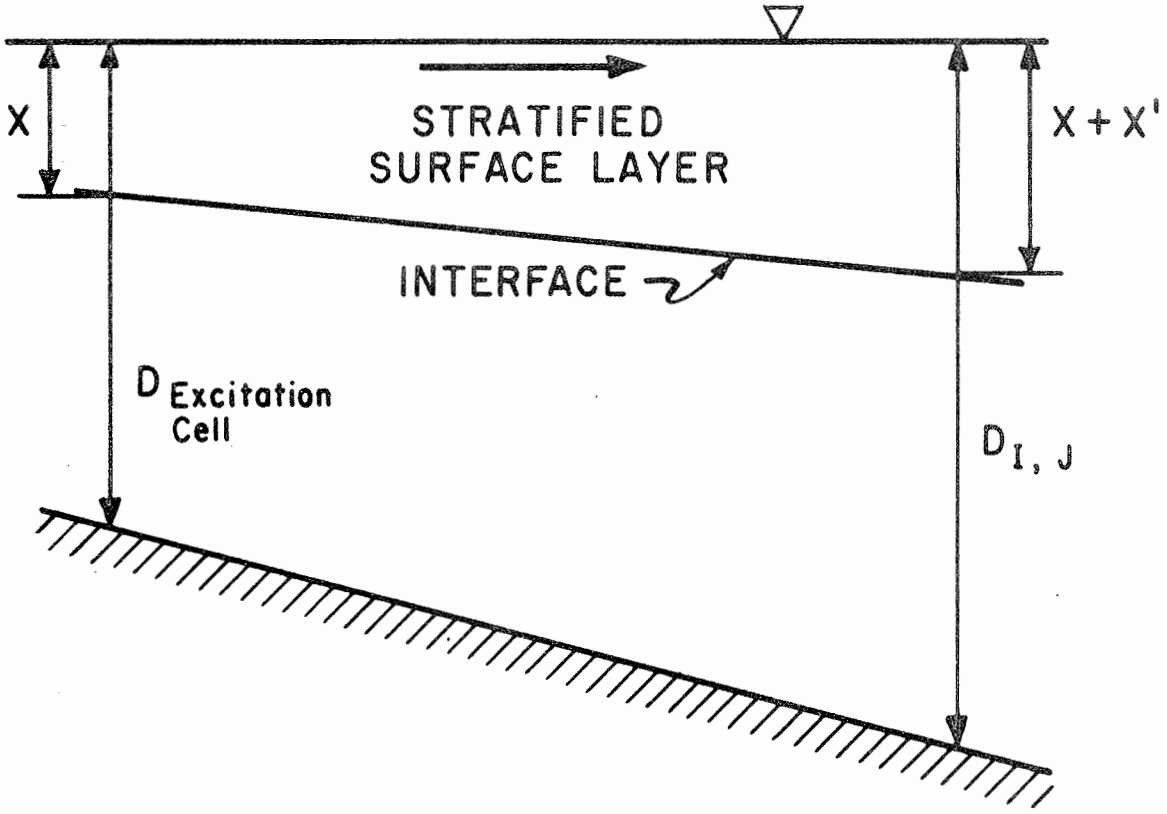

Figure 7-7. Depth Ratio Correction for Stratification

The value of the constant, $F_{I,J}$ is unique for each cell, and is also unique insofar as a given combination of wind speed, wind direction, temperature profile, velocity profile, and flow rate. The factor expressed in Equation (7-5) is determined for each cell and applied to the computed concentration of each cell. These corrected values form the basis of concentration distribution contour maps developed and discussed later.

The foregoing technique is used successively, starting with the assumption of a fully-mixed lake in the hydrodynamic model. Then using the resulting velocities in the transport model determine the tentative values of ξ and $F_{I,J}$ based on a comparison of computed versus observed concentration values. This process is repeated until a value of ξ is determined, which when used to adjust the depths of the hydrodynamic model for stratification effects, produces velocities for the transport model which yields concentration distributions that can be closely reconciled with those observed. For example, in the two verification tests made in this study, the initial velocities used in the transport model were generated from the hydrodynamic model assuming a fully-mixed lake. Initial tentative values of ξ = 4.0 and 3.25 respectively were used to compute the individual cell correction factors needed to reconcile observed and computed concentrations. New velocities were again computed from the hydrodynamic model assuming an upper layer of stratification amounting to 1/4 and 1/3.25 of the total depths. Using the new velocities, a new ξ factor of 2.3 was determined, and adequate reconciliation between computed and observed values was achieved.

The feasibility and practicality of the above-described method for the correction of computed concentration values in order to reconcile them with the observed concentration values pertaining to the Lake Bastrop transport model and tests are strongly enhanced by relevant quantitative and qualitative results of laboratory flume tests conducted by Stefan (1970).

These flume tests simulated the various basic flow patterns of heated water from an open channel into a relatively-colder and essentially stagnant reservoir. The flume tests revealed quantitative and qualitative composite effects of buoyancy, viscosity and temperature stratification conditions of channel discharge on the reservoir flow, assuming a two-layer, inviscid flow system downstream from the channel outlet. The Stefan (1970) flume experiment simulations included flow and stratification conditions analogous to those encountered in this study incident to the field verification operations of the Lake Bastrop transport model. The Stefan (1970) report indicated the possible types of time-averaged, isotherm configurations and interface patterns at the confluence of the channel outlet and the reservoir. Patterns were revealed in the flume tests where mass transfer and mixing occurred at the wedge, wave or, stratification interfaces and, patterns also occurred, however, where these phenomena did not evolve, depending on the distance from the channel outlet. Analogous situations were encountered in Lake Bastrop model verification zone in areas away from the immediate confluence zone. Both in the Stefan (1970) flume tests and in the actual field explorations and verification tests of the Lake Bastrop transport model, it was noted that near the open channel outlet the thermal stratification or concentration gradient interface was subject to random vertical displacements. Of course, in the field operations these displacements were not as easily or as rapidly detected as they appear to be in the flume tests. Stefan (1970) indicated that the maximum thickness, d_1, of the heated water layer downstream from the outlet was found from the flume experiments in three ways: (1) The distance from the water surface to the visual interface. (2) The distance from the water surface to the temperature inflection point. (3) The distance from water surface to the temperature mid-point, which is the arithmetic mean between the greatest heated water and cold water temperatures. The following specific conclusions of the Stefan (1970) flume tests form strong practical justification for the adoption of the successive approximation technique

and the adjustment factors represented by Equations (7-4), (7-5) and (7-6):

> "For rough estimates, the flow from a channel into an impoundment in the presence of buoyant forces may be characterized in terms of outlet geometry, Reynolds number, densimetric Froude number at the outlet, and average depth of the warm water layer downstream of the outlet. The latter is controlled by the cooling process and the flow in the reservoir."

It is also significant that in analyzing the Stefan (1970) plots of the dimensionless depth ratio d_1/d_0 versus the internal or reduced Froude numbers at the outlet, the three ways in which d_1 could be defined seemed to have no major effect on results. (Note: d_1 is the depth of the warm water layer downstream from the channel outlet, and d_0 is the depth of the heated water.)

Based on the foregoing, it is believed that successive technique, using Equations (7-4) through (7-6), inclusive represents a rational synthesis of the "baroclinic layer" concept, Okubo's (1968) oceanic diffusion studies, and Stefan's (1970) flume studies to simulate stratification of flow from channel into a deep lake. This synthesis is more realistic than adopting constant-thickness epilimnion simplifications. It is well to reiterate the point made in connection with the Equation (7-6), that the concentration correction factor for a given cell of the transport model must be based on the composite effects of wind speed and direction, temperature profile, velocity profile and flow-through rate.

2. Model Verification, June 23-24, 1970. On June 23, 1970 a release dye of 1.17 lbs was made at Station 0 + 00 in the discharge channel. Figure (7-8) is a plot of the concentration vs. time curve measured at cell (10, 15),

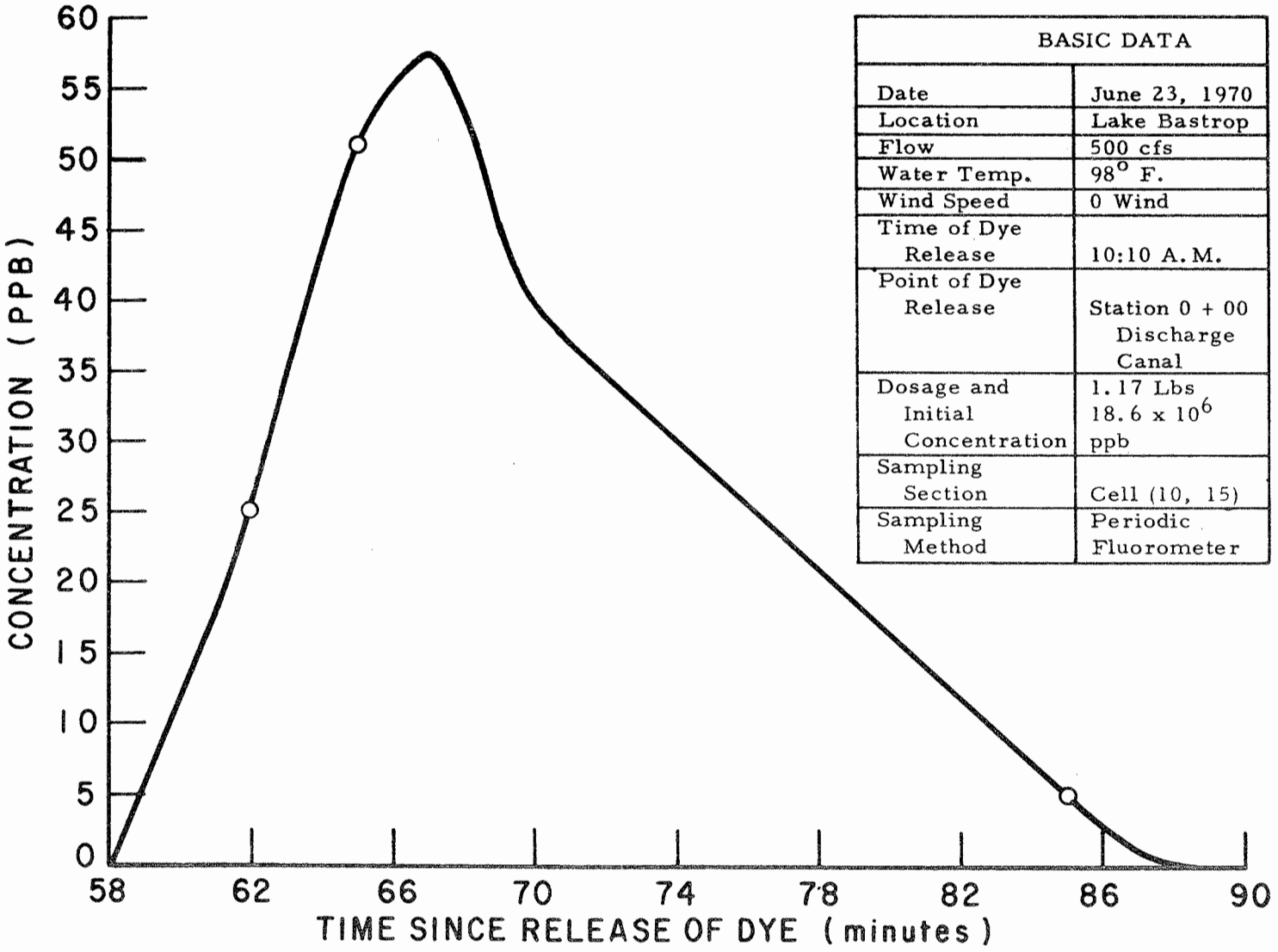

BASIC DATA	
Date	June 23, 1970
Location	Lake Bastrop
Flow	500 cfs
Water Temp.	98° F.
Wind Speed	0 Wind
Time of Dye Release	10:10 A.M.
Point of Dye Release	Station 0 + 00 Discharge Canal
Dosage and Initial Concentration	1.17 Lbs 18.6×10^6 ppb
Sampling Section	Cell (10, 15)
Sampling Method	Periodic Fluorometer

Figure 7-8. Concentration vs. Time at Cell (10, 15)

the first computational cell. The curve shows the characteristic shape obtained in earlier tests.

Concentration ordinates of this curve at 3-minute intervals were used as input to computer PROGRAM TRACER, (Appendix A), using cell (10, 15) as the excitation cell. And, pursuant to the decisions explained in the previous section (1) the dispersion coefficient algorithm was multiplied by a factor of 50, and (2) a value of $\xi = 4$ was determined for the ratio $\frac{D_{EXCIT}}{X}$ (See Equation 7-4).
In other words, in the excitation cell, the thickness of the homogeneously-mixed stratum which transports the bulk of the dye concentration was determined to be equal to 1/4 the total depth. This ratio was determined by considering temperature profiles, the effects of zero wind conditions, and sub-normal lake levels (5 inches below normal) specific conditions which prevailed on June 23 and 24, 1970. These conditions enhanced vertical and lateral diffusion at the expense of longitudinal dispersion and tended to increase the thicknesss of the well-mixed surface stratum.

Figures 7-9 to 7-13, inclusive, show the predicted dye concentration plots in the verification zone to 3, 6, 12, 24 and 48 hours after dye input to the lake. Computed data for each cell was corrected by its individual cell factor, using Equation (7-6).

Figure 7-14 shows a comparison of computed vs. observed concentrations for two typical cells in the verification zone within the first 24 hours after release of the dye. For each cell, the mean of observed values is compared with the appropriate segment of the computed concentration vs. time curve. Figures 7-15 and 7-16 contain the supporting field data.

Verification observations were then carried on during the second 24 hours after dye release. Figure 7-17 (11 spot check points) shows a concentration contour plot of 48 hours after release of dye and location of the points where positive verification was made. Table 7-2 lists the verification points and measurements taken 24 to 30 hours after dye release. Due to the onset of a steady 12 mph

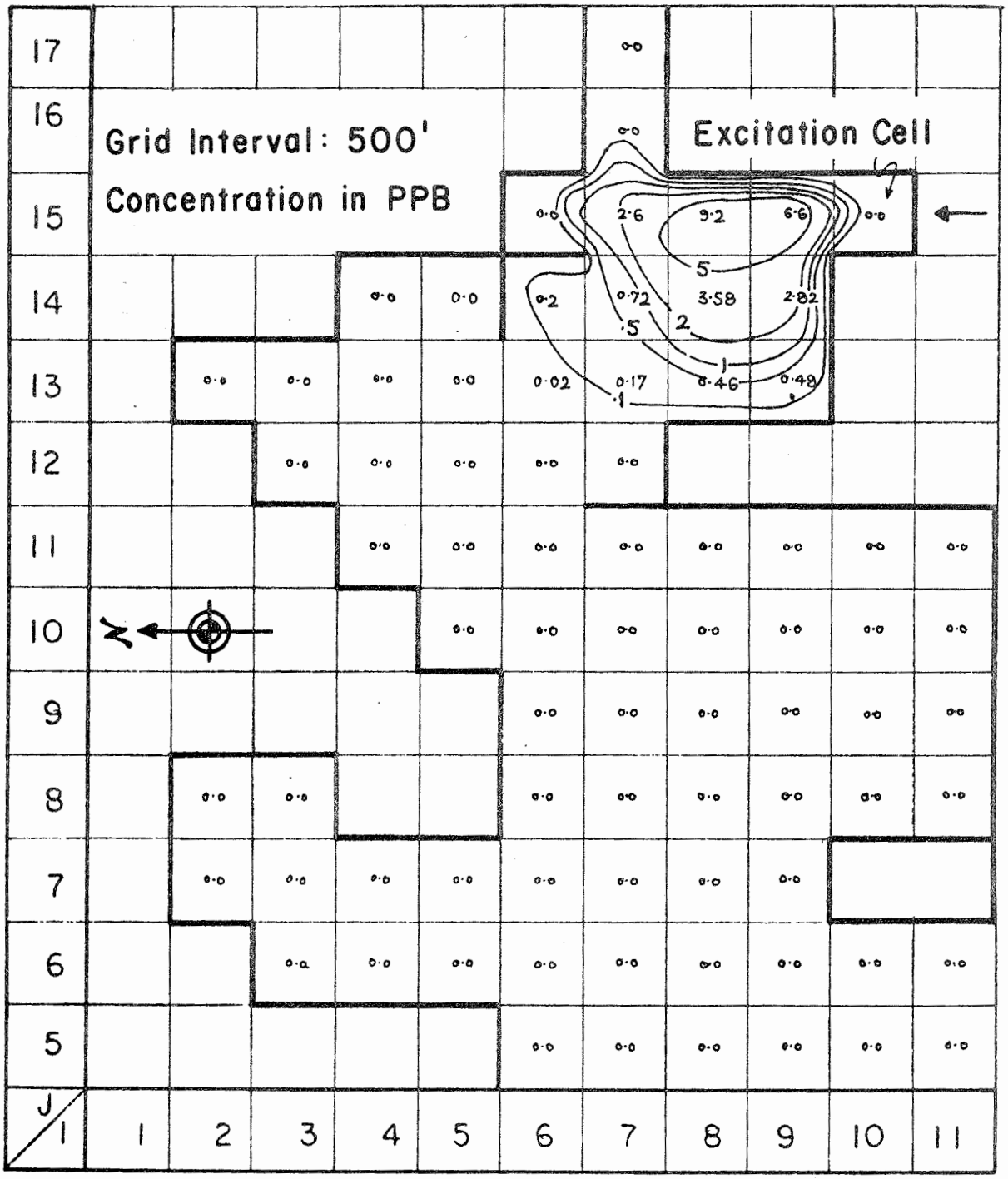

LAKE BASTROP MODEL VERIFICATION ZONE

Flow: 324 M. G. D.
Wind: 0 M. P. H.
Dosage: 1.17 Lbs.
Time After Dye Release: 3 Hrs.

Figure 7-9. Predicted Transport of Concentrations.

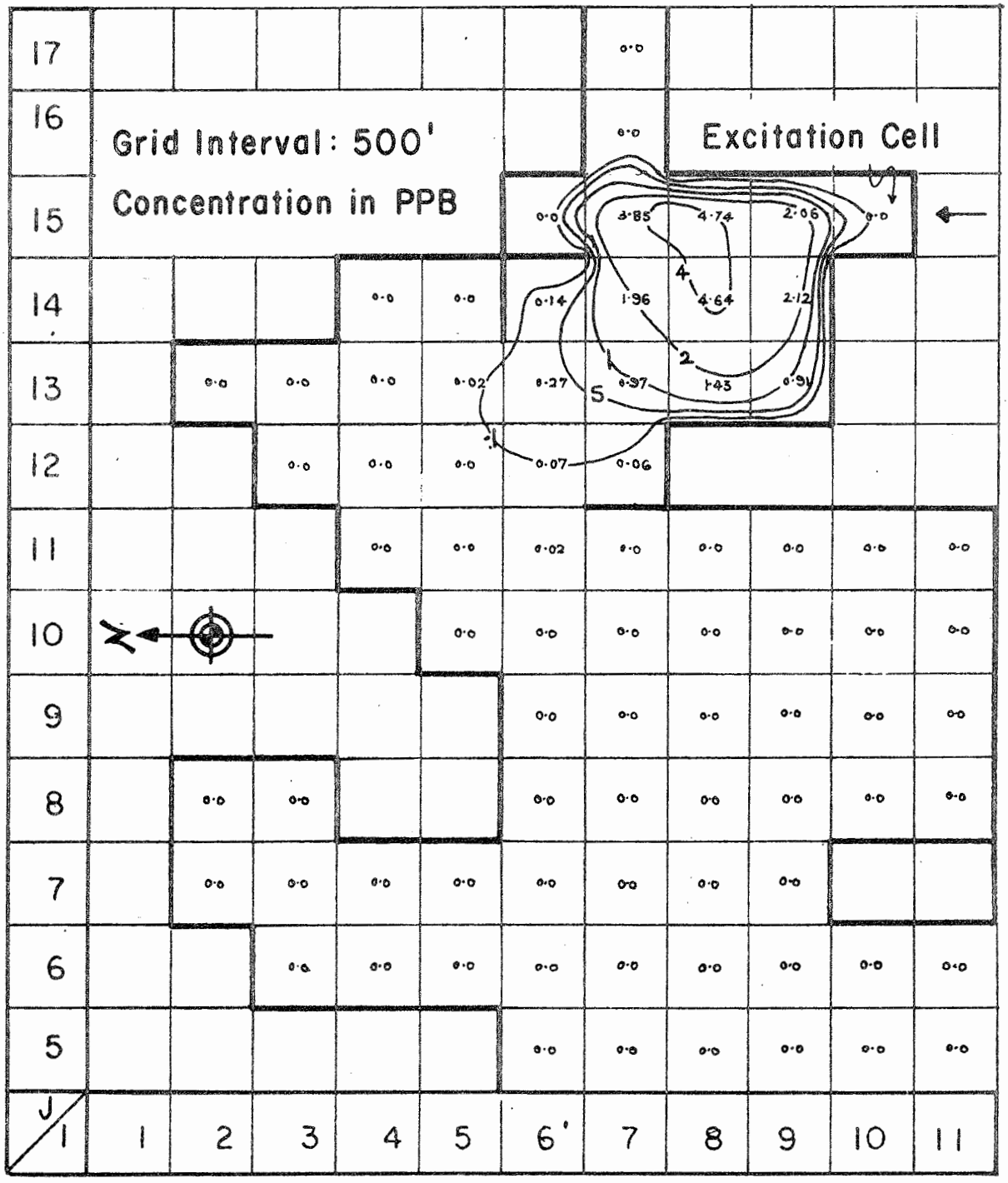

LAKE BASTROP MODEL VERIFICATION ZONE

Flow: 324 M. G. D.
Wind: 0 M. P. H.
Dosage: 1.17 Lbs.
Time After Dye Release: 6 Hrs.

Figure 7-10. Predicted Transport of Concentrations.

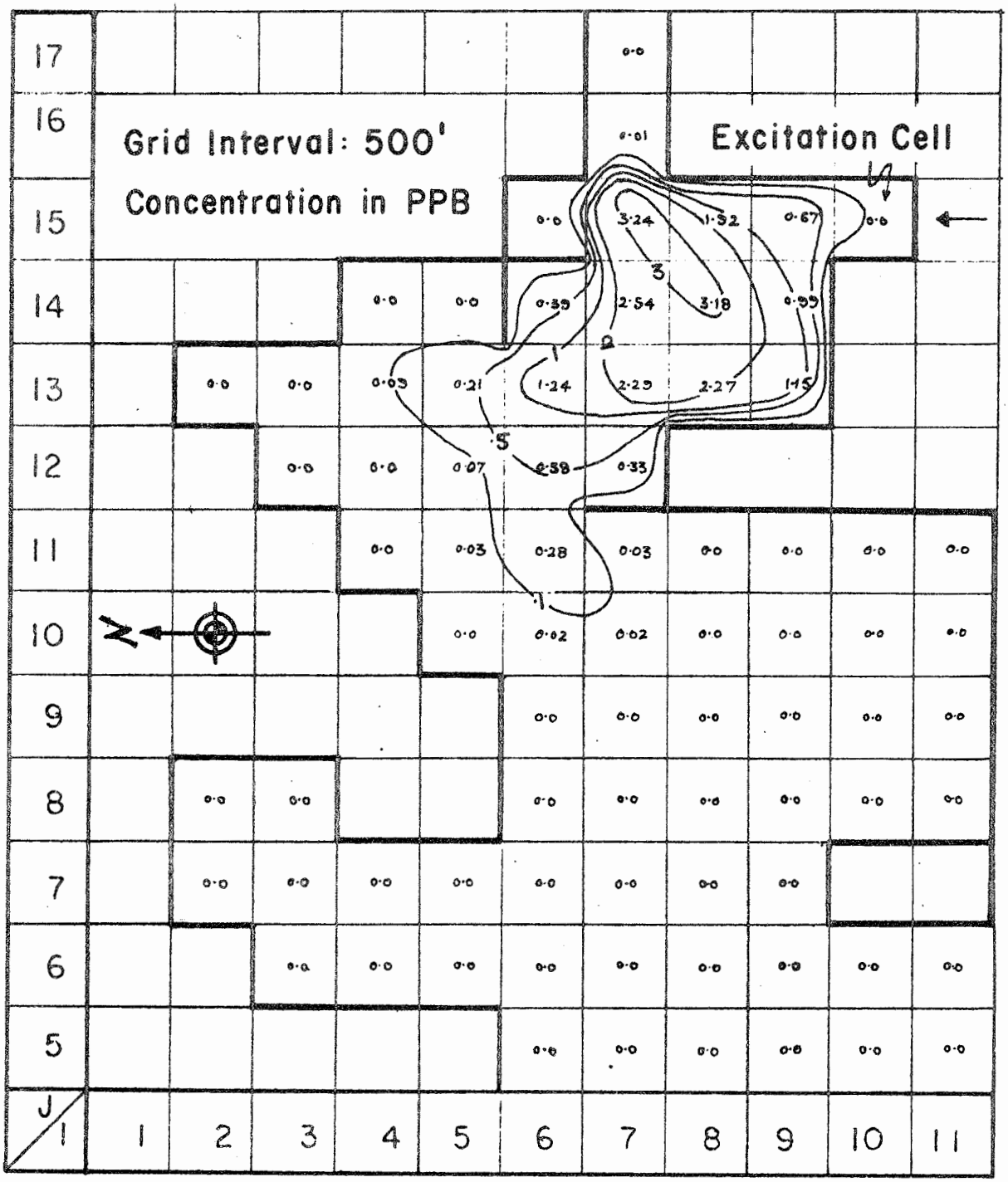

LAKE BASTROP MODEL VERIFICATION ZONE

Flow: 324 M. G. D.
Wind: 0 M. P. H.
Dosage: 1.17 Lbs.
Time After Dye Release: 12 Hrs.

Figure 7-11. Predicted Transport of Concentrations.

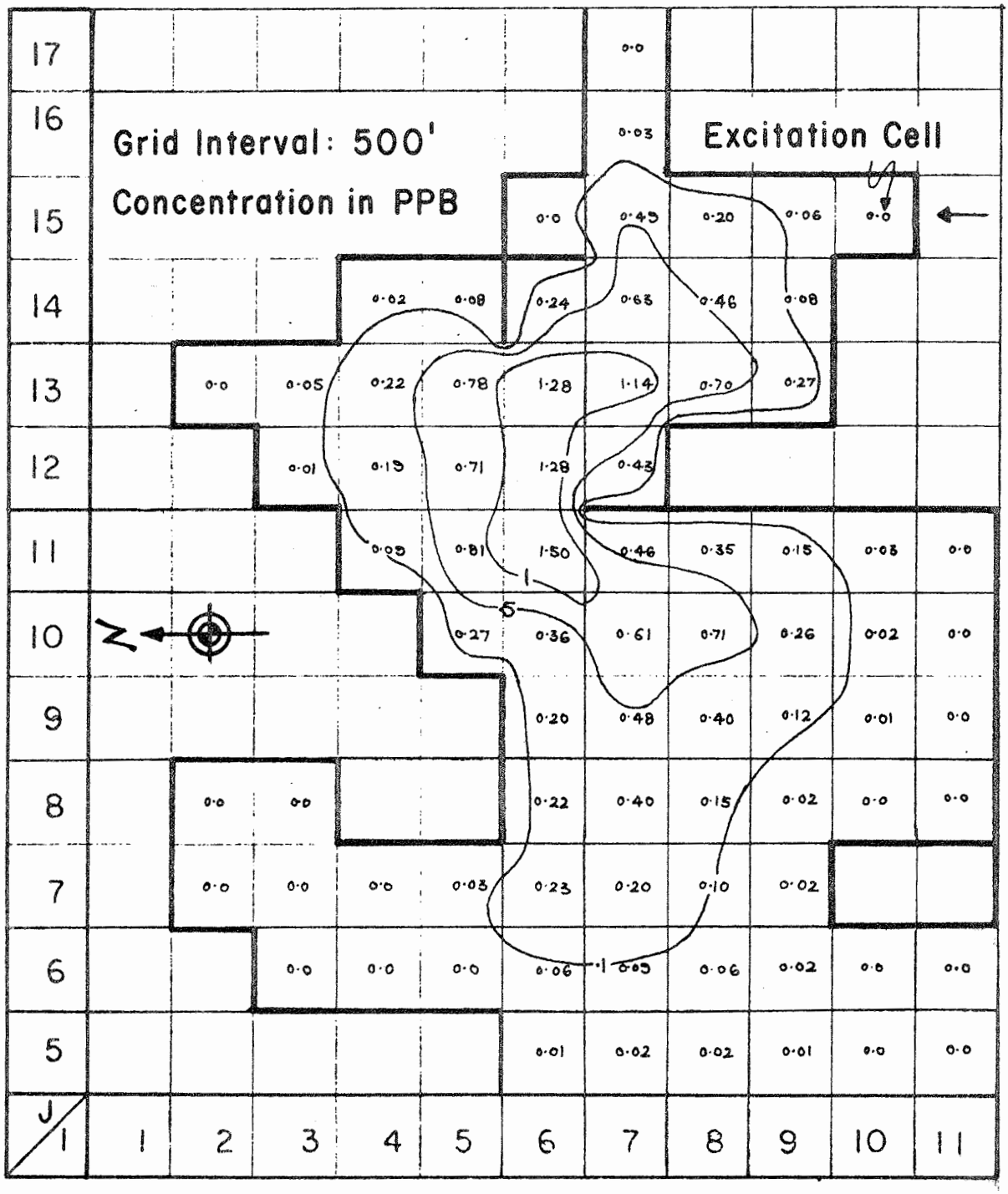

LAKE BASTROP MODEL VERIFICATION ZONE

Flow: 324 M.G.D.
Wind: 0 M.P.H.
Dosage: 1.17 Lbs.
Time After Dye Release: 48 Hrs.

Figure 7-13. Predicted Transport of Concentrations.

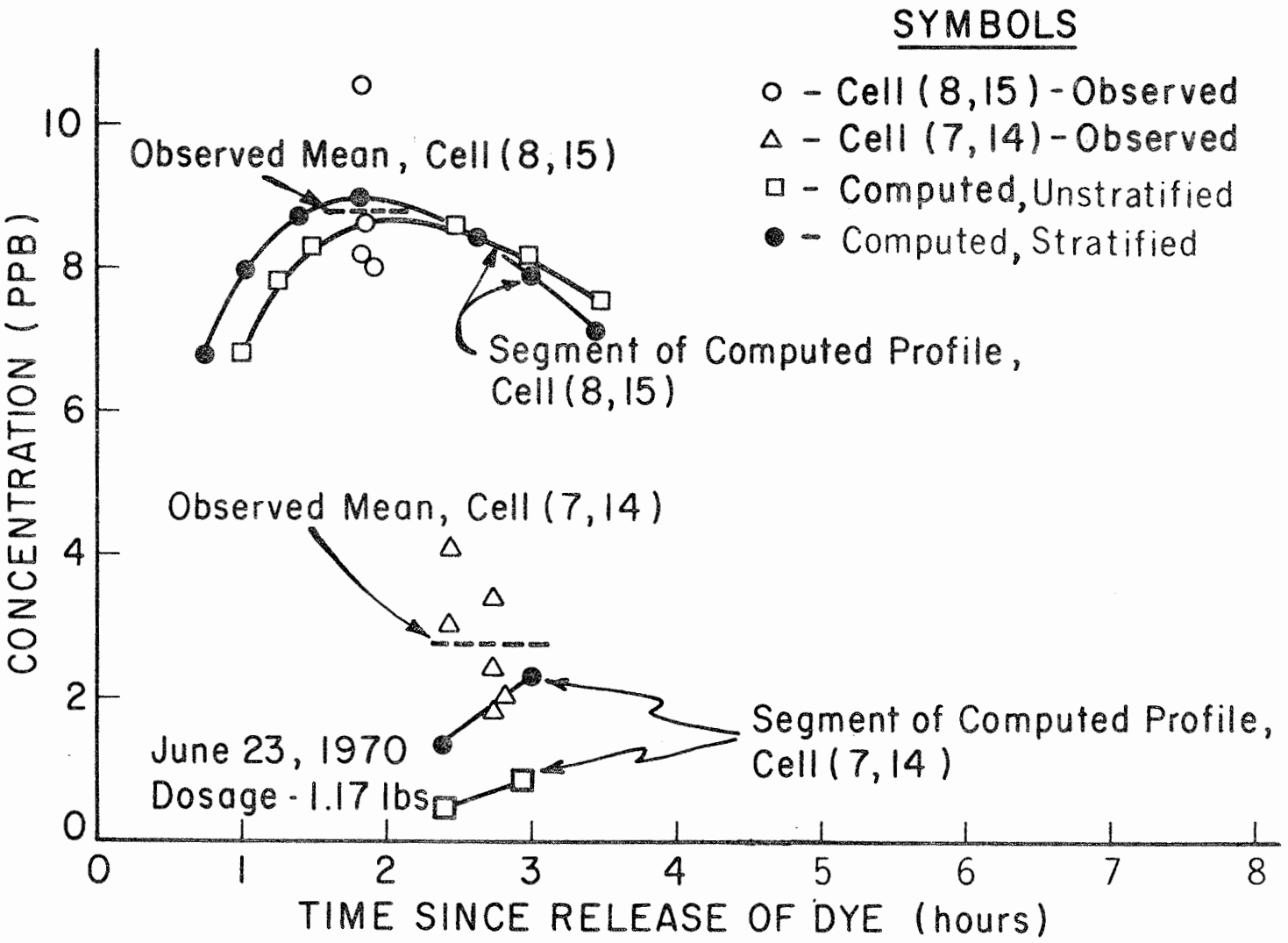

Figure 7-14. Comparison of Computed and Observed Concentrations Lake Bastrop Transport Model

BASIC DATA	
Date	June 23, 1970
Location	Lake Bastrop
Power Plant Discharge	500 cfs
Water Temperature	98° F
Wind Speed and Direction	No Wind
Time of Dye Release	10:10 A.M.
Point of Dye Release	Station 0 + 00 Discharge Channel
Initial Concentration	1.17 Lbs 18.6×10^6 ppb
Sampling Section	Cell (7, 14) Marker 6
Sampling Method	Periodic, Fluorometer

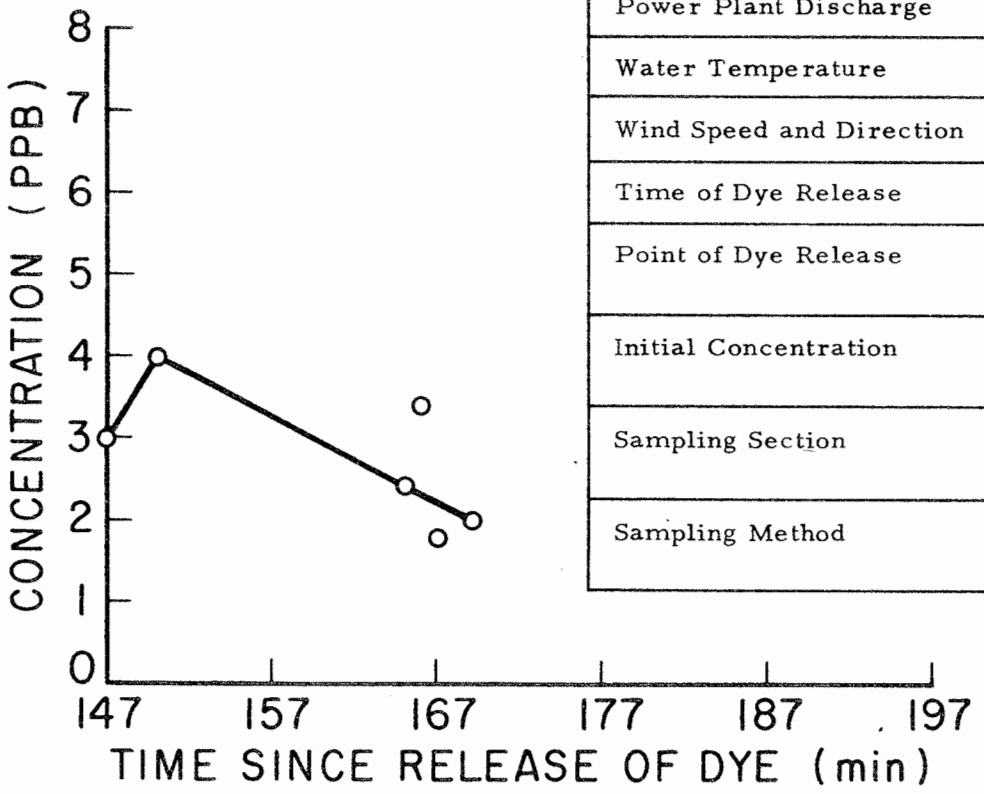

Figure 7-15. Concentration vs. Time, Cell (7, 14)

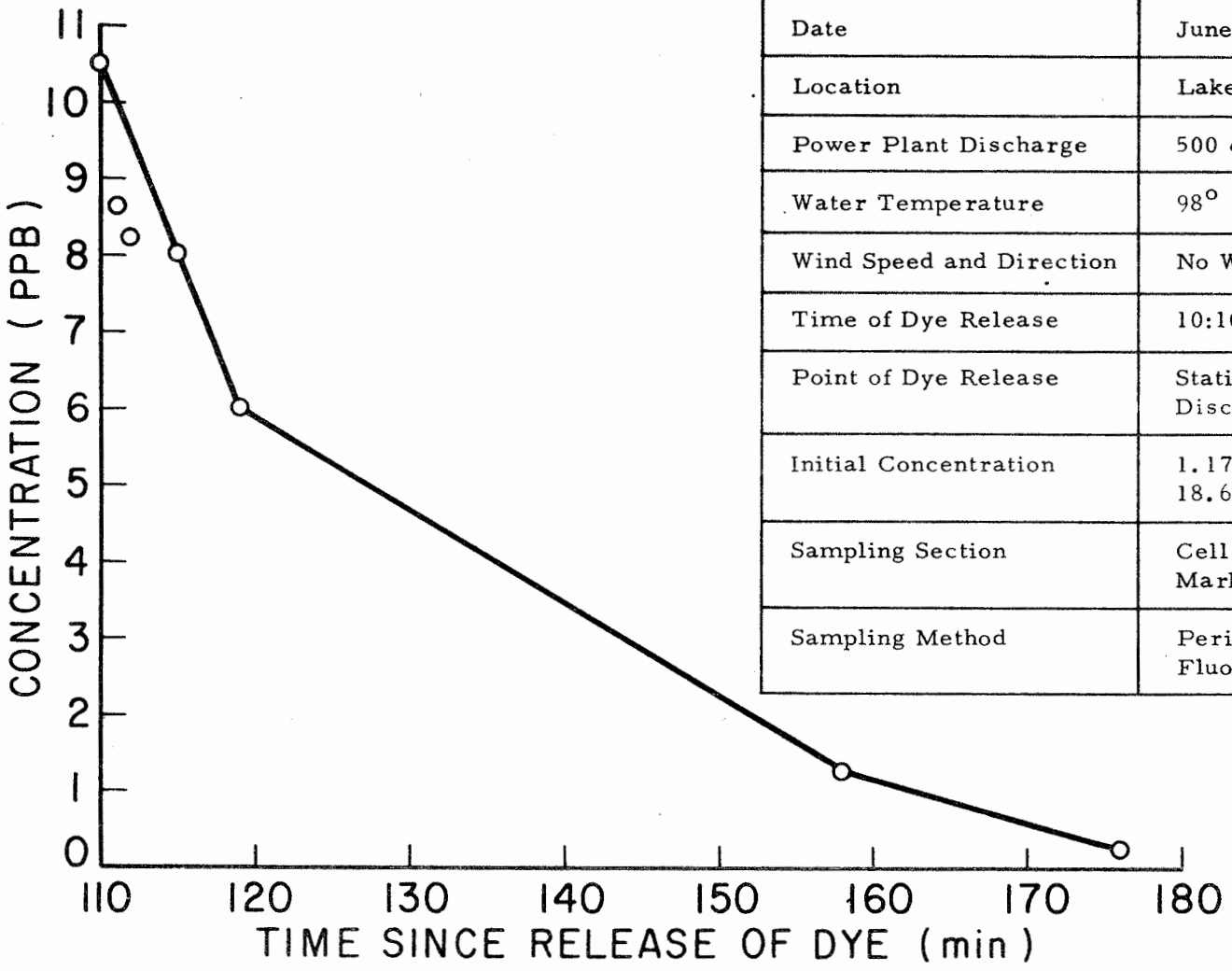

BASIC DATA	
Date	June 23, 1970
Location	Lake Bastrop
Power Plant Discharge	500 cfs
Water Temperature	98° F
Wind Speed and Direction	No Wind
Time of Dye Release	10:10 A.M.
Point of Dye Release	Station 0 + 00 Discharge Channel
Initial Concentration	1.17 Lbs 18.6×10^6 ppb
Sampling Section	Cell (8, 15) Marker 2
Sampling Method	Periodic Fluorometer

Figure 7-16. Concentration vs. Time, Cell (8, 15)

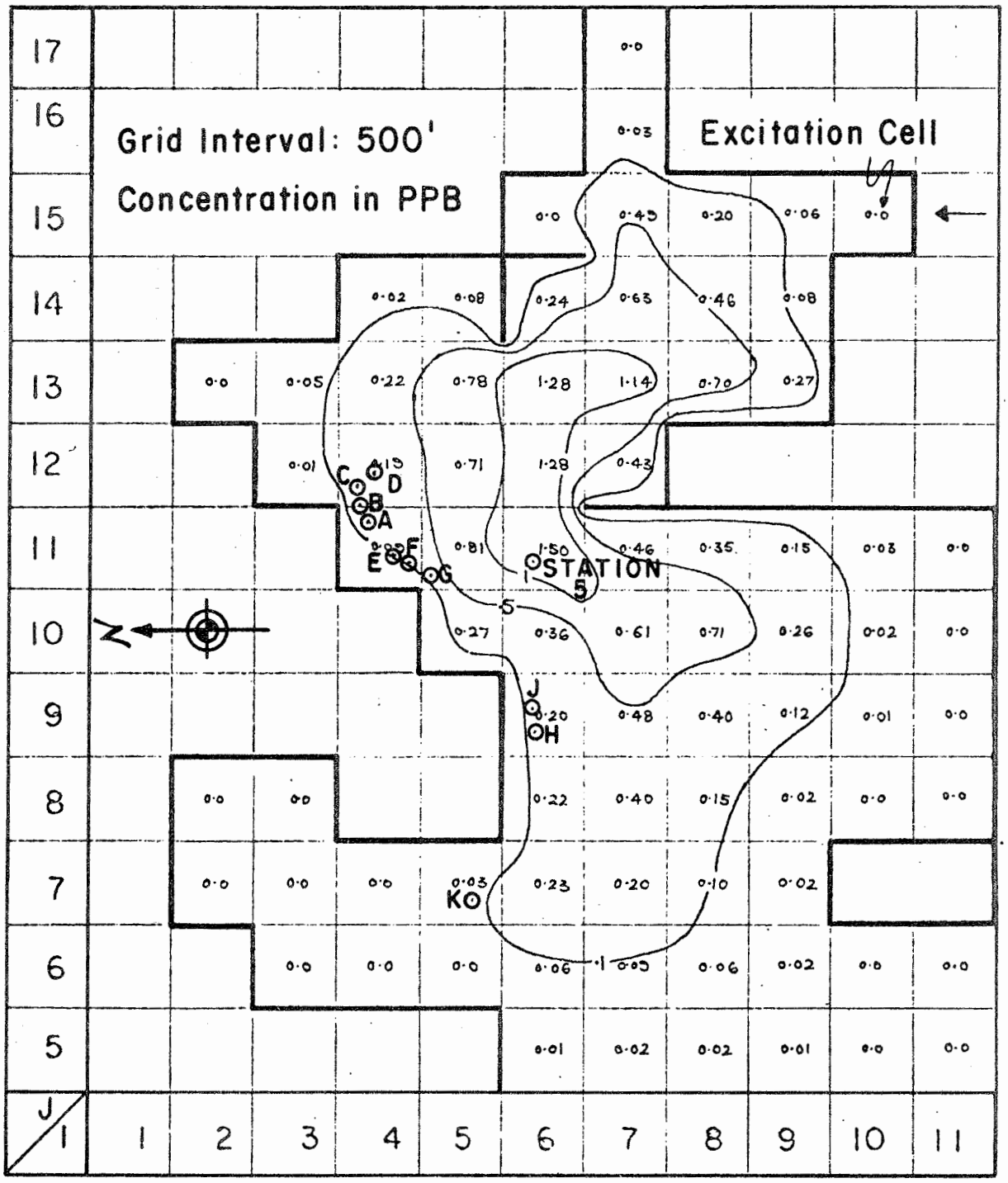

LAKE BASTROP MODEL VERIFICATION ZONE

Flow: 324 M. G. D.
Wind: 0 M. P. H.
Dosage: 1.17 Lbs.
Time After Dye Release: 48 Hrs.

Figure 7-17. Field Verification of Concentration Distributions.

TABLE 7-2

Field Measurement of Tracer Concentrations in Lake Bastrop

24 - 30 Hours after a Dye Injection of 1.17 Lbs.

Sampling Point		Rhodamine B
Cell Number	Station[1]	Concentration (ppb)
(7, 11)	5	1.30
(4, 11)	A	0.20
(4, 11)	B	0.20
(4, 12)	C	0.22
(4, 12)	D	0.20
(4, 11)	E	0.15
(4, 11)	F	0.13
(5, 11)	G	0.13
(6, 9)	H	0.10
(6, 9)	J	0.10
(5, 7)	K	0.00

[1] See Figure 7-17. Field Verification of Concentration Distributions.

south wind 28 hours after dye release, it was necessary that the computer model, (originally based on zero wind), be "pushed ahead" to the 48-hour condition in order to make allowance for the accelerated transport in the wind direction. This provided a realistic basis of comparison between observed and computed concentration for the second 24 hours. Satisfactory reconciliation was found between computed and observed values in the selected cells for the 2-day verification tests.

As part of the verification, the following subsidiary analyses were made:

a. Time-of-travel;

b. Vertical concentration profiles.

Figure 7-18 is the concentration contour or isopleth plot in the verification zone after 48 hours, indicating the plotted positions of the dye peak and cloud leading edge (assume the leading edge is the 0.1 ppb contour) at known times. Table 7-3 lists salient data showing the peak and leading edge velocities, and the relation between the two. The results correspond favorably with results encountered in time-of-travel studies made for streams in Illinois and Indiana by Stall and Hiestand (1969), who recommended that the following generalized relationship be adopted for the dye peak and edge velocities in streams of the two states:

$$V_E = 1.25\ V_p \tag{7-7}$$

In contrast, the Lake Bastrop model, indicates an average relationship over a 45 hr. period of:

$$V_E = 1.74\ V_p \tag{7-8}$$

In order to check the extent of the dye concentration with depth, both discrete and continuous samplings made during the two-days test period. Figure 7-19 shows the concentration profiles at the center marker for cell (10, 15),

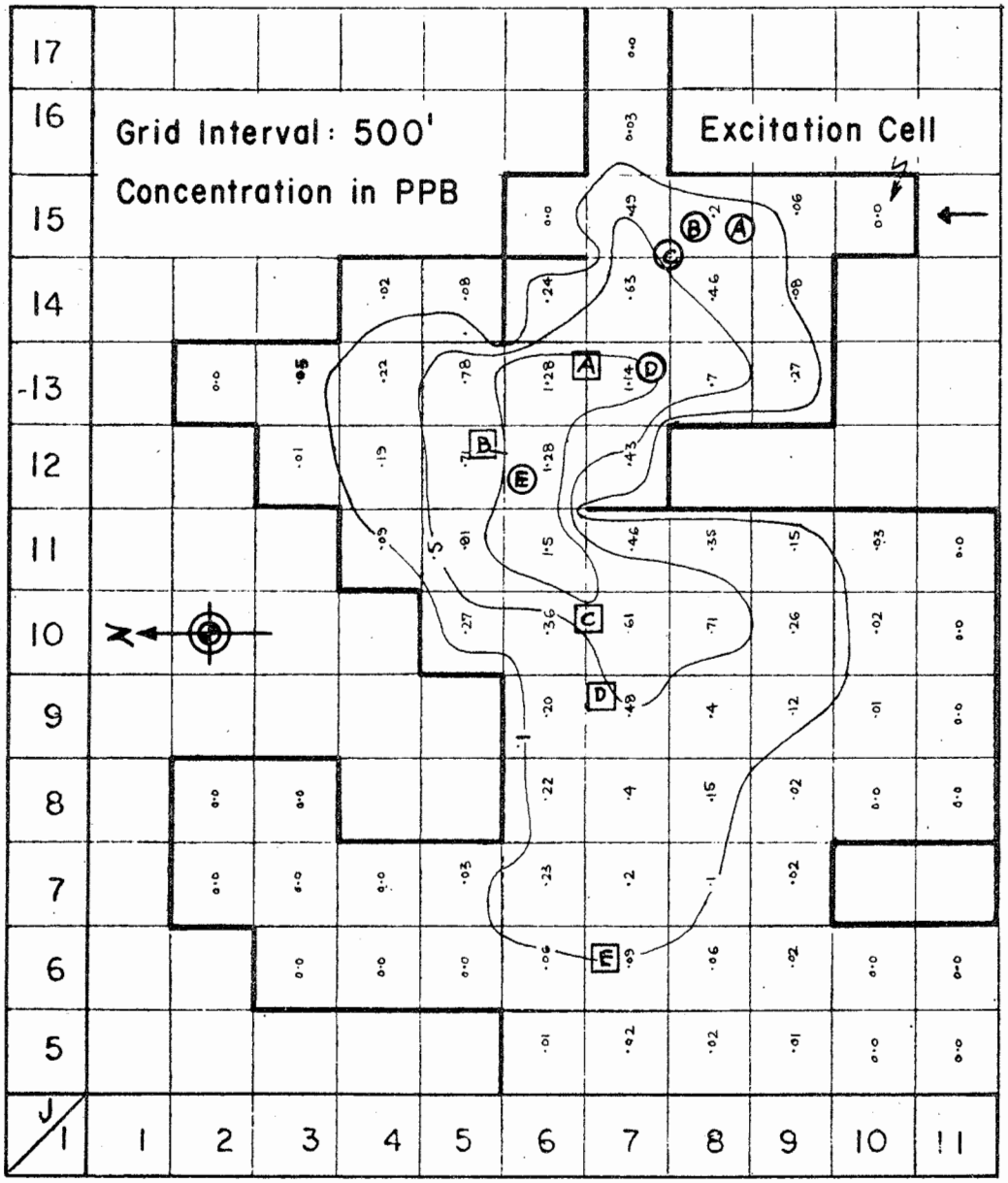

LAKE BASTROP MODEL VERIFICATION ZONE

Flow: 324 M. G. D.
Wind: 0 M. P. H.
Dosage: 1.17 Lbs.
Time After Dye Release: 48 Hrs.

Peak (A) (B) (C) (D) (E) — Edge [A] — 3 hours; [B] — 6 hours; [C] — 9 hours; [D] — 24 hours; [E] — 48 hours

Figure 7-18. Peak and Leading Edge Velocities and Time-of-Travel

Table 7-3. Peak and Leading Edge Velocities and Time-of-Travel Data, June 23-24, 1970.

Course[1] and Hrs. after Dye Release	Elapsed Time (Hrs)	Distance		Velocity		Ratio $\frac{V_E}{V_P} = K$	Remarks
		Peak (Ft)	Edge (Ft)	Peak, V_p (Ft/Hr)	Edge, V_E (Ft/Hr)		
A - B (6)	3	300	825	100	275	2.75	
B - C (12)	6	225	1300	38	217	5.70	Denotes increase in dye-spreading rate.
C - D (24)	12	825	500	69	42	0.60	Denotes rapid advance of peak in cloud.
D - E (48)	24	1100	1650	46	69	1.50	Denotes approach to an equilibrium rate.
A - D (24)	21	1350	2625	64	125	1.95	21-hour basis.
A - E (48)	45	2450	4275	55	95	1.74	45-hour basis.

[1] See Figure 7-18 for plotted locations of A to E, inclusive.

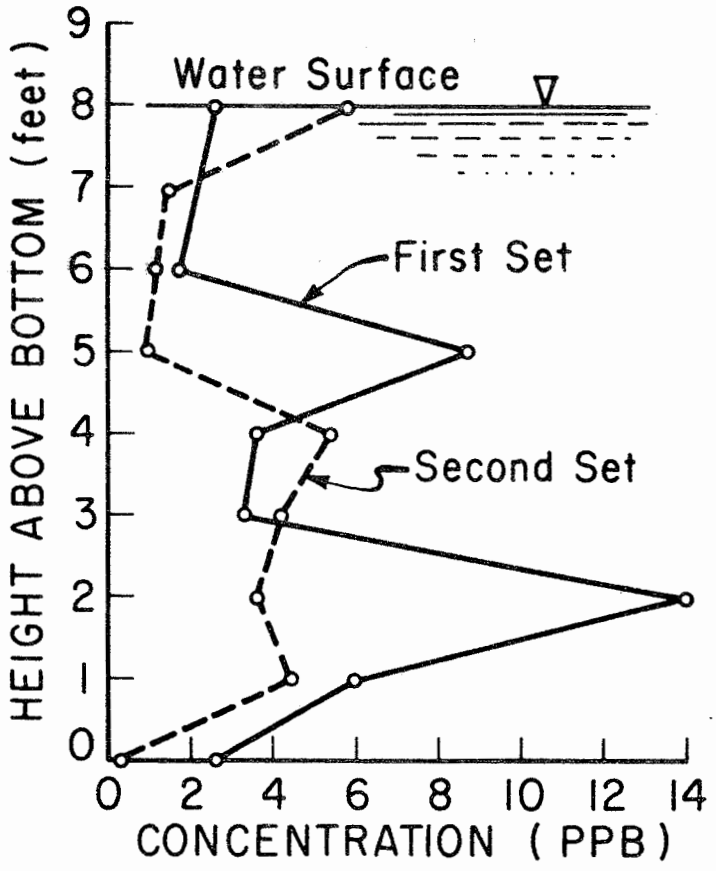

BASIC DATA	
Date	June 23, 1970
Location	Lake Bastrop
Power Plant Discharge	500 cfs
Water Temperature	98° F.
Wind Speed and Direction	0 Wind
Time of Dye Release	10:10 A.M.
Point of Dye Release	Station 0 + 00, Discharge Channel
Dosage: Initial Concentration	1.17 Lbs. 18.6×10^6 ppb
Sampling Location	Cell Marker 1 (I = 10, J = 15)
Sampling Method	Grab Samples at Depth Intervals of 1 Ft.
Date and Time of Sampling: Grab Set 1 Grab Set 2	June 23, 1970 (11:50 A.M.) June 23, 1970 (12:18 A.M.)
Date and Time of Testing: Grab Set 1 Grab Set 2	June 24, 1970 (7:20 P.M.) June 24, 1970 (8:30 P.M.)

Figure 7-19. Concentration vs. Depth - Cell (10, 15).

the excitation cell of the model, based on two sets of discrete samples at one-foot intervals, taken about 3 hours after release of dye at Station 0 + 00, of the discharge channel.

It would appear that an uniform distribution profile exists at the excitation cell center marker location. Quantitatively, the results may not be representative of the entire 500' x 500' cell. However, it is noted that the 5.5 ppb average of these data taken at the marker over an elapsed period of about 30 minutes compared favorably with the contemporaneous fluorometric sampling average of 6.6 ppb taken at a depth of 2 feet below the surface.

Figure 7-20 shows a concentration profile for cell (4, 12), on the 2nd day, based on continuous fluorometric sampling. This sample illustrates the relatively-homogeneous, mixed condition in shallow stagnant areas where vertical diffusion gradually thickens the initial, dye-carrying stratum.

However, observations and findings of the first comprehensive verification tests were regarded as tentative, subject to re-evaluation after completion of the second comprehensive field tests. The section on "Realistic Considerations" at the end of this chapter provides this re-evaluation.

Second Comprehensive Field Verification of the Lake Transport Model. The second comprehensive test was conducted on June 30, 1970, using a dosage of 1.225 lbs of Rhodamine B, diluted in 28.5 liters of lake water. The first phase consisted of verifying the concentration-time curve produced by the channel model for cell (11, 15) which was selected to serve as the excitation cell for the model. This cell encompasses the lower 500 ft of the discharge channel. Figure 7-21 shows the observed vs. computed values at Station 44 + 40 of the channel, the assumed center of

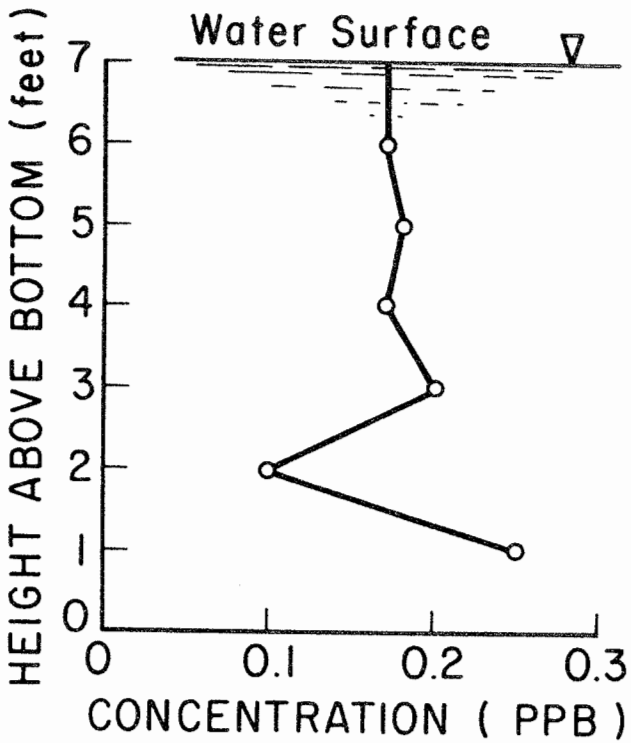

BASIC DATA	
Date	June 24, 1970
Location	Lake Bastrop
Power Plant Discharge	500 cfs
Water Temperature	96.5° F
Wind Speed and Direction	5 MPH (South)
Date and Time of Dye Release	June 23, 1970 (10:10 A.M.)
Point of Dye Release	Station 0 + 00, Discharge Channel
Dosage: Initial Concentration	1.17 Lbs. 18.6×10^6 ppb
Sampling Location	Point D in Cell (4, 12)
Date and Time of Sampling	June 24, 1970 (12:03 P.M.)
Sampling Method	Continuous Fluorometer Sampling from Surface to 7 Ft. Depth
Time of Sampling	June 24, 1970 (12:03 P.M.)

Figure 7-20. Concentration vs. Depth - Cell (4, 12).

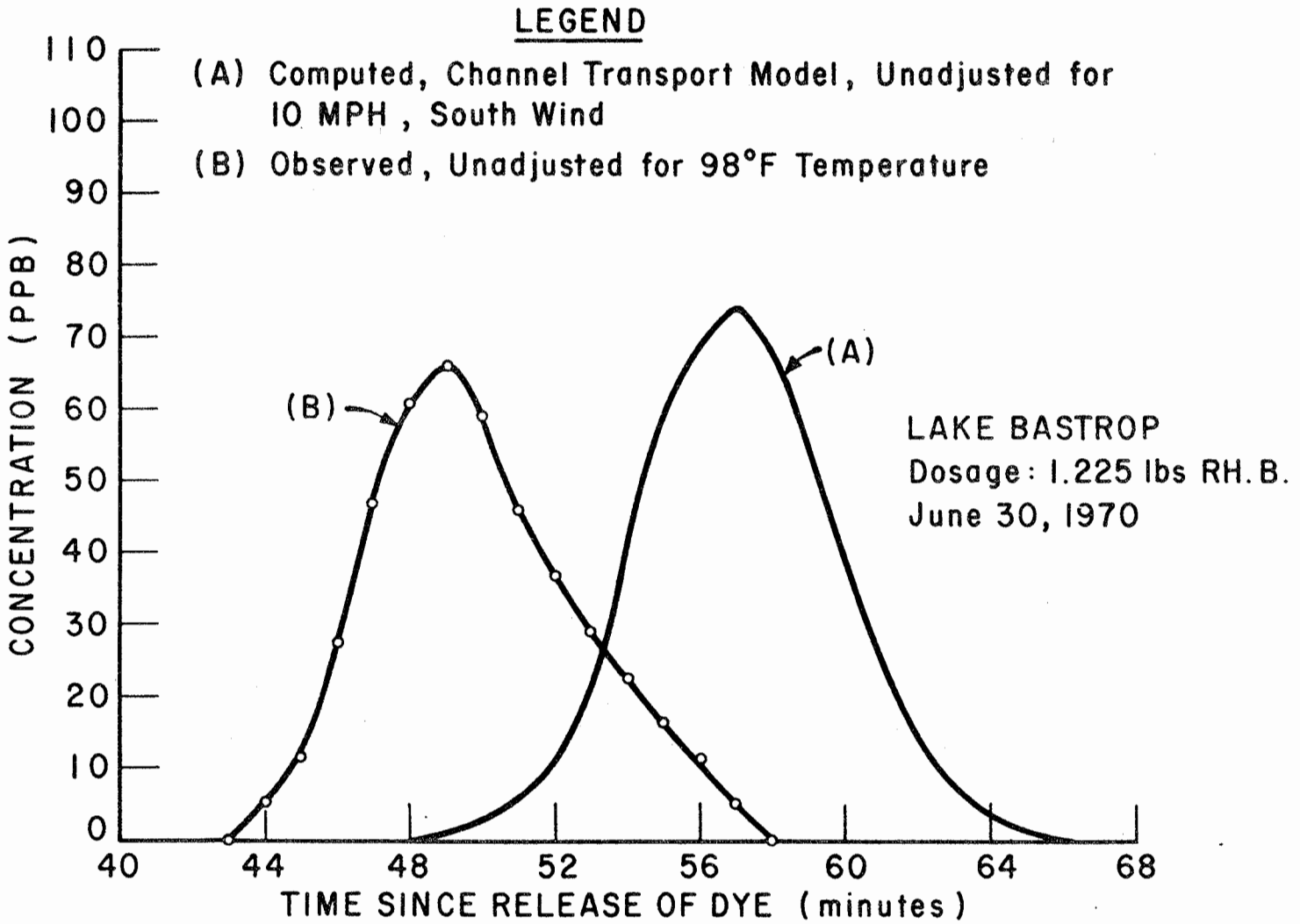

Figure 7-21. Concentration vs. Time, End of Discharge Channel, Station 44 + 40 - Showing Unadjusted Computed and Observed Values.

the excitation cell. Figure 7-22 shows the computed curve corrected for channel wind, and the observed values corrected for temperature. This confirms earlier results of the predictable nature of the channel concentration distribution discharges. The time-concentration curve at channel Station 44 + 40 (cell 11, 15) has a more normal Gaussian configuration than the curve for cell (10, 15). Figure 7-23 is the concentration-time curve, whose ordinates at 3-minute intervals, were used as temporal concentration input to PROGRAM TRACER, with cell (11, 15) serving as the excitation cell. Pursuant to decisions explained previously, the Taylor dispersion coefficient algorithm was corrected by a factor of 50, and a value 3.25 was determined for the depth ratio D_{EXCIT} / x [See Equation (7-4)], due to increased wind shear and decreased surface stratum thickness effects. Figures 7-24 and 7-25 depict the predicted concentration contours after 12 and 24 hours. Figure 7-26 shows a comparison of computed vs. observed mean concentration for each of 3 consecutive cells, at the southern end of the verification zone. Figures G-1, G-2, G-3 (Appendix G) are the supporting field data for the aforementioned comparisons. Figure 7-27 shows a comparison of computed vs. observed mean concentrations in two cells located in the middle of the zone. Figure G-4 and G-5 (Appendix G) are the supporting field data for the comparisons. Figure 7-28 shows a similar comparison for a cell located at the far end of the zone. Figure G-6 (Appendix G) is the supporting field data.

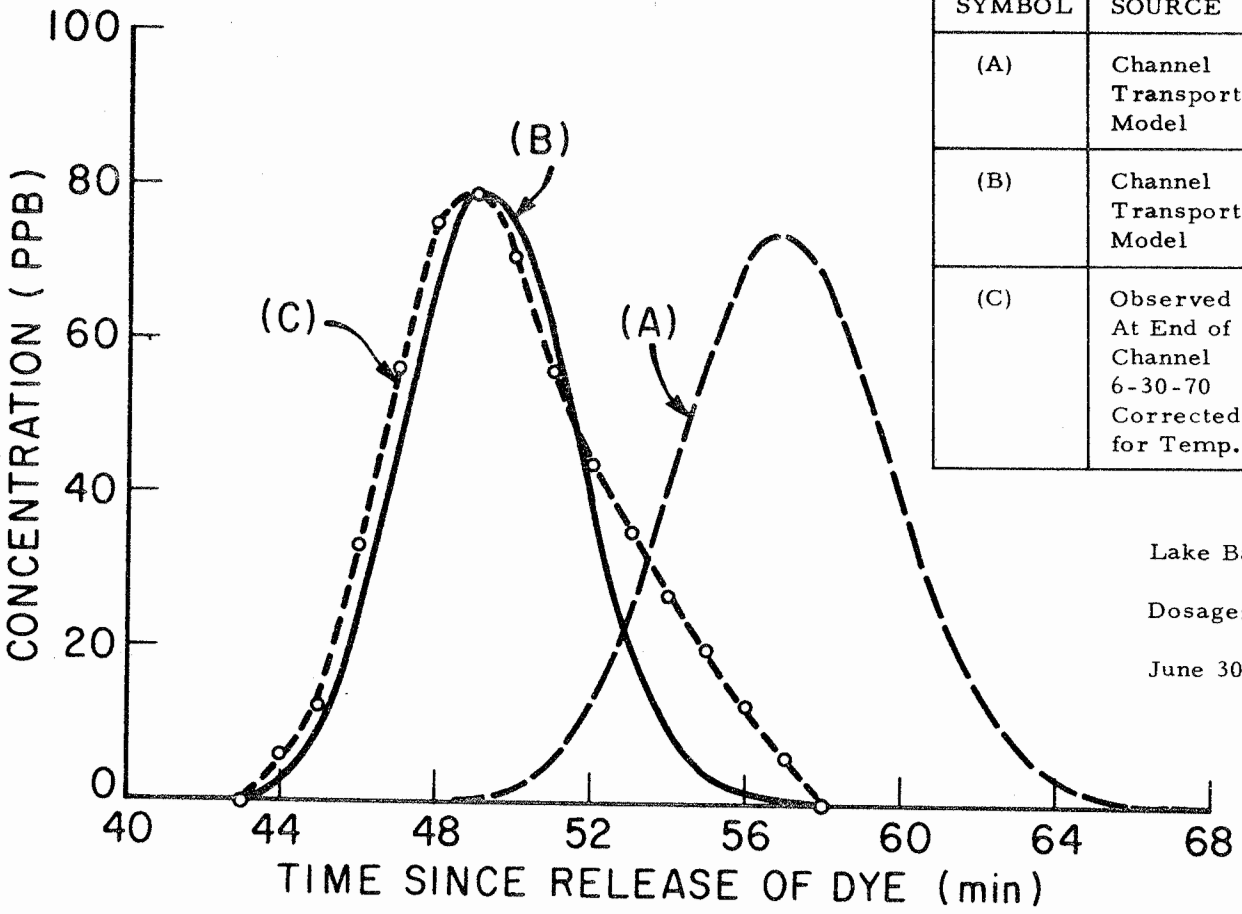

LEGEND			
SYMBOL	SOURCE	VELOCITY	WIND
(A)	Channel Transport Model	1.30 fps	0 MPH
(B)	Channel Transport Model	1.50 fps	10 MPH (South)
(C)	Observed At End of Channel 6-30-70 Corrected for Temp.		10 MPH (South)

Lake Bastrop

Dosage: 1.225 Lbs. Rhodamine B

June 30, 1970

Figure 7-22. Concentration vs. Time, End of Discharge Channel, Station 44 + 40. - Showing Basis for Reconciling Channel Model and Observed Values. (Model Values Corrected for Wind; Observed Values for Temperature)

BASIC DATA	
Date	June 30, 1970
Location	Lake Bastrop
Power Plant Discharge	500 cfs
Water Temperature	98° F
Wind Speed and Direction	10 MPH (South)
Time of Dye Release	12:58 P.M.
Point of Dye Release	Station 0 + 00 Discharge Channel
Initial Concentration	1.225 Lbs 19.5×10^6 ppb
Sampling Section	Station 0 + 4440 Discharge Channel
Sampling Method	Continuous Fluorometer Sampling

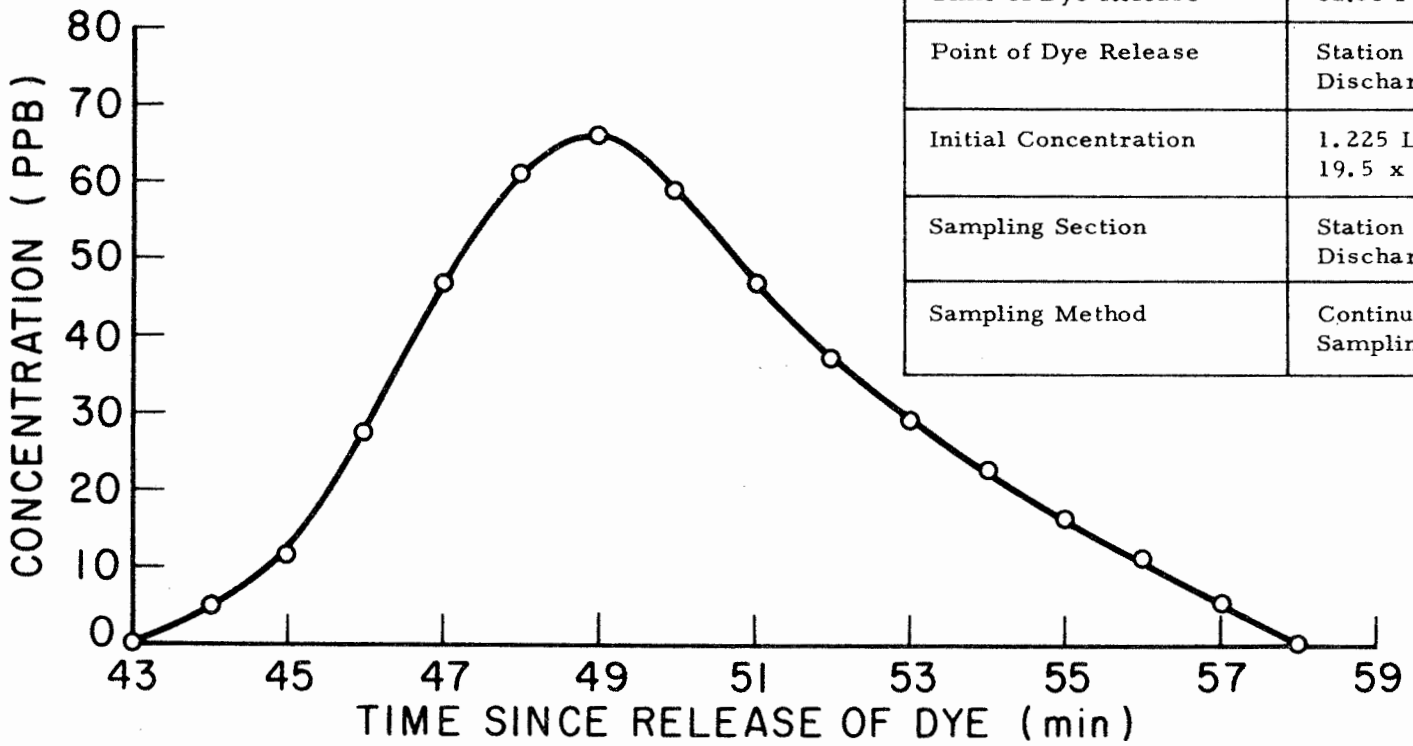

Figure 7-23. Observed Concentration vs. Time at End of Discharge Channel, Lake Bastrop

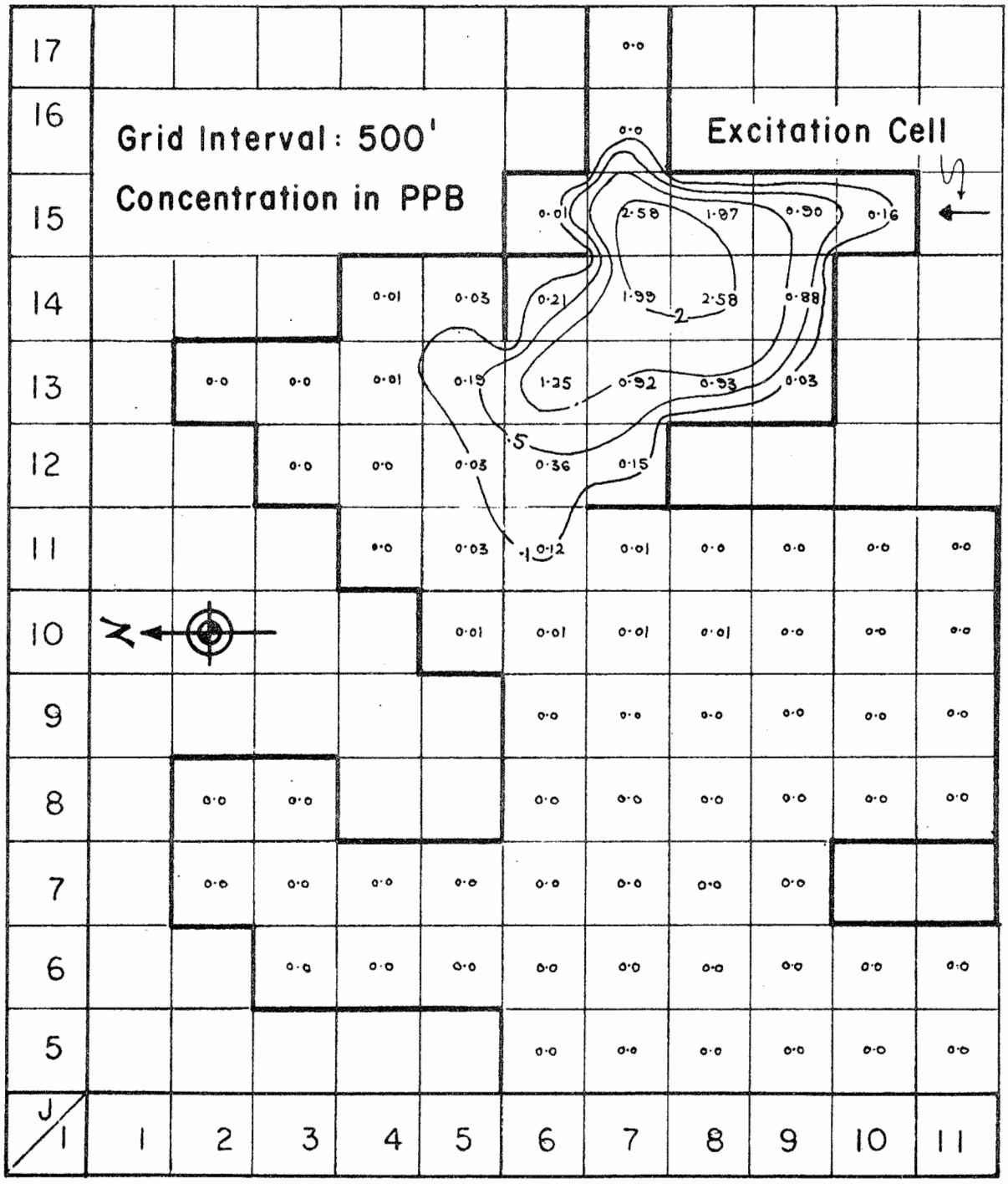

LAKE BASTROP MODEL VERIFICATION ZONE

Flow: 324 M. G. D.
Wind: 10 M. P. H. South
Dosage: 1.225 Lbs.
Time After Dye Release: 12 Hrs.

Figure 7-24. Predicted Transport of Concentrations.

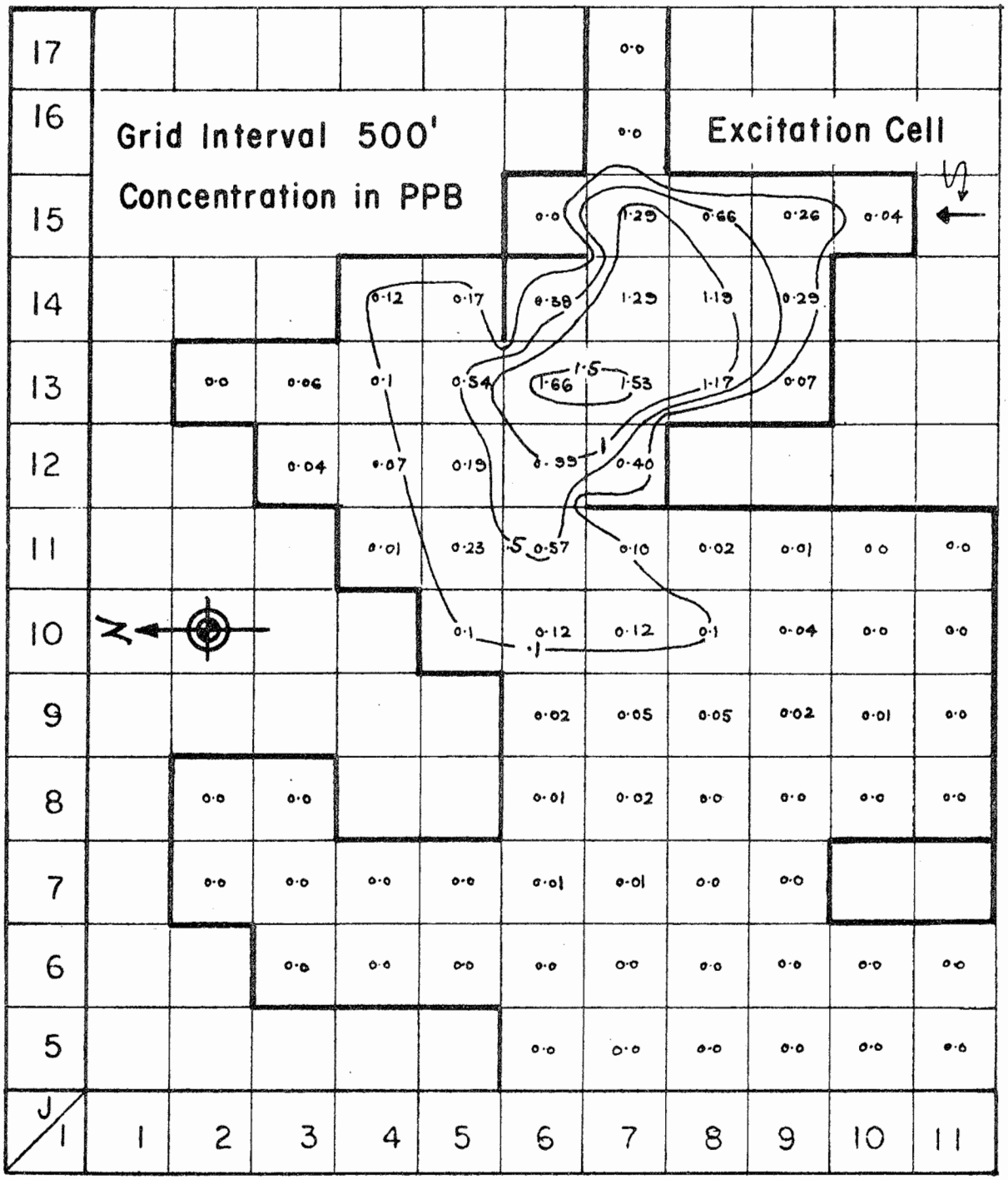

LAKE BASTROP MODEL VERIFICATION ZONE

Flow: 324 M. G. D.
Wind: 10 M. P. H. South
Dosage: 1.225 Lbs.
Time After Dye Release: 24 Hrs.

Figure 7-25. Predicted Transport of Concentrations.

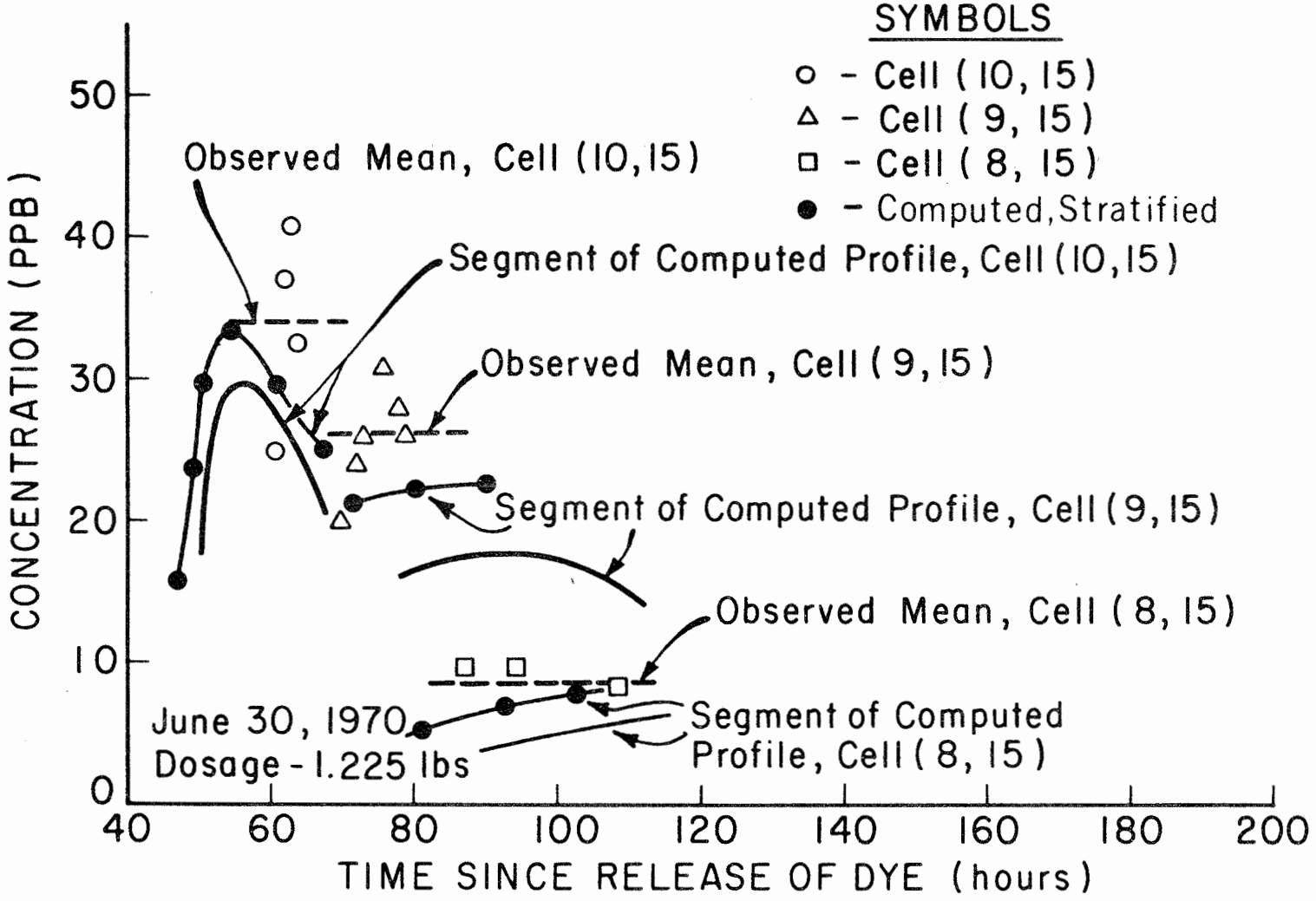

Figure 7-26. Comparison of Computed and Observed Concentrations Lake Bastrop Transport Model

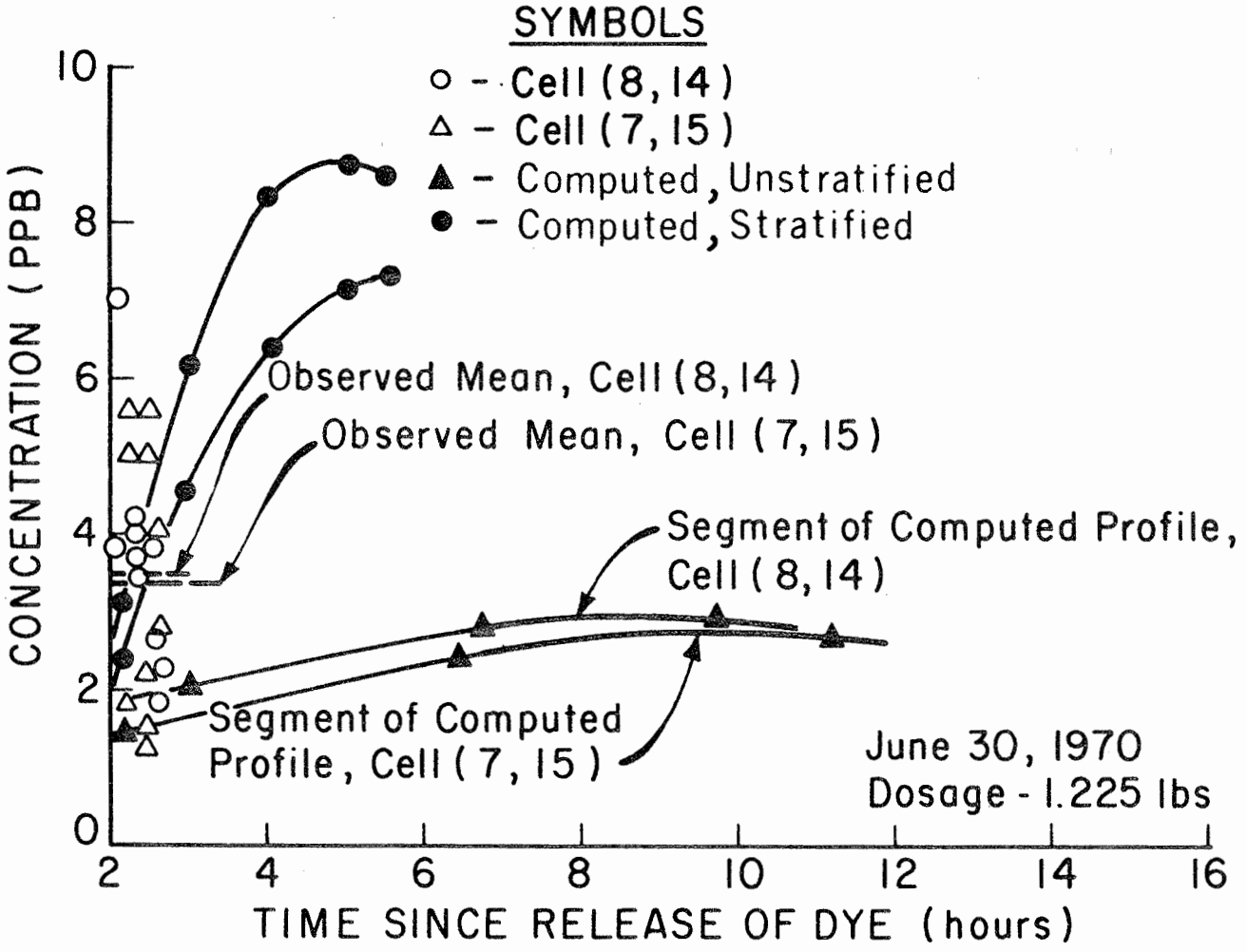

Figure 7-27. Comparison of Computed and Observed Concentrations Lake Bastrop Transport Model

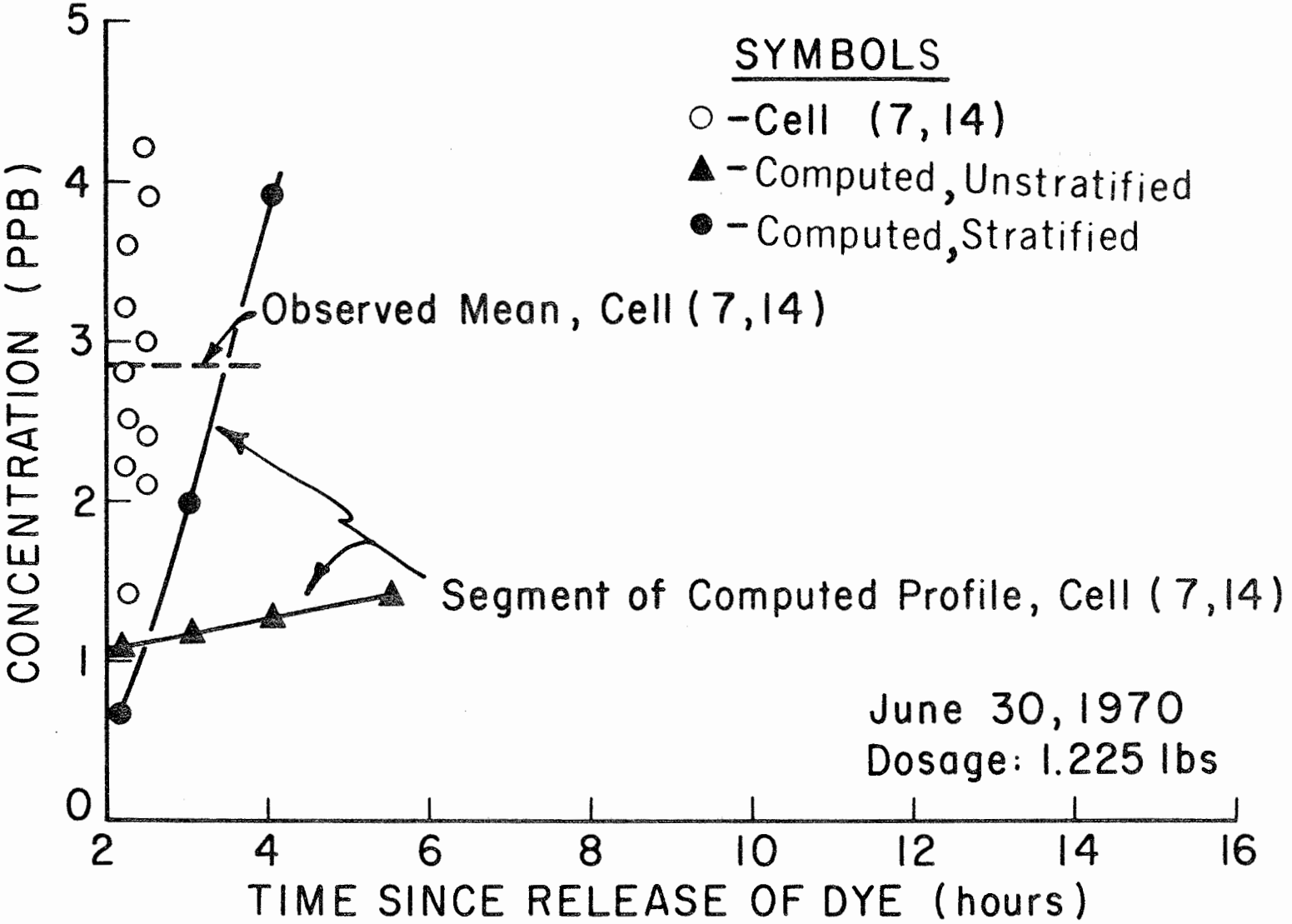

Figure 7-28. Comparison of Computed and Observed Concentrations - Lake Bastrop Transport Model

Figure 7-29 shows a time-of-travel analysis of the concentration contour plot indicating that in the period between 12 and 24 hours after excitation of the model, the velocity of peak, V_P averaged 83.5 ft/hr and the velocity, V_E of the 0.1 ppb isopleth which represents the leading edge averaged 96 ft/hr. The ratio is $V_E / V_P = 1.17$.

Tabulated below for comparison are the time-of-travel results of the first and second comprehensive tests:

Table 7-4. Time-of-Travel Comparisons

Date	Dosage (lbs)	Time after Dye Release (hrs)	Wind Velocity (MPH)	V_P (ft/hr)	V_E (ft/hr)	V_E / V_P
6/23/70	1.170	12 to 24	0	58.5	100	1.70
6/30/70	1.225	12 to 24	10 (south)	83.5	96	1.17

The comparison reflects the substantial effect of wind velocity on the peak velocity and a decidedly minor effect on the leading edge velocity. The ratio of the peak and leading edge velocities is materially reduced by wind effect.

Realistic Considerations. The full scale verification tests indicated the need for recognizing certain basic realistic hydrodynamic effects of mixing in a lake. This recognition was necessary in order to interpret and evaluate properly the observed dye concentration data. These basic aspects are:

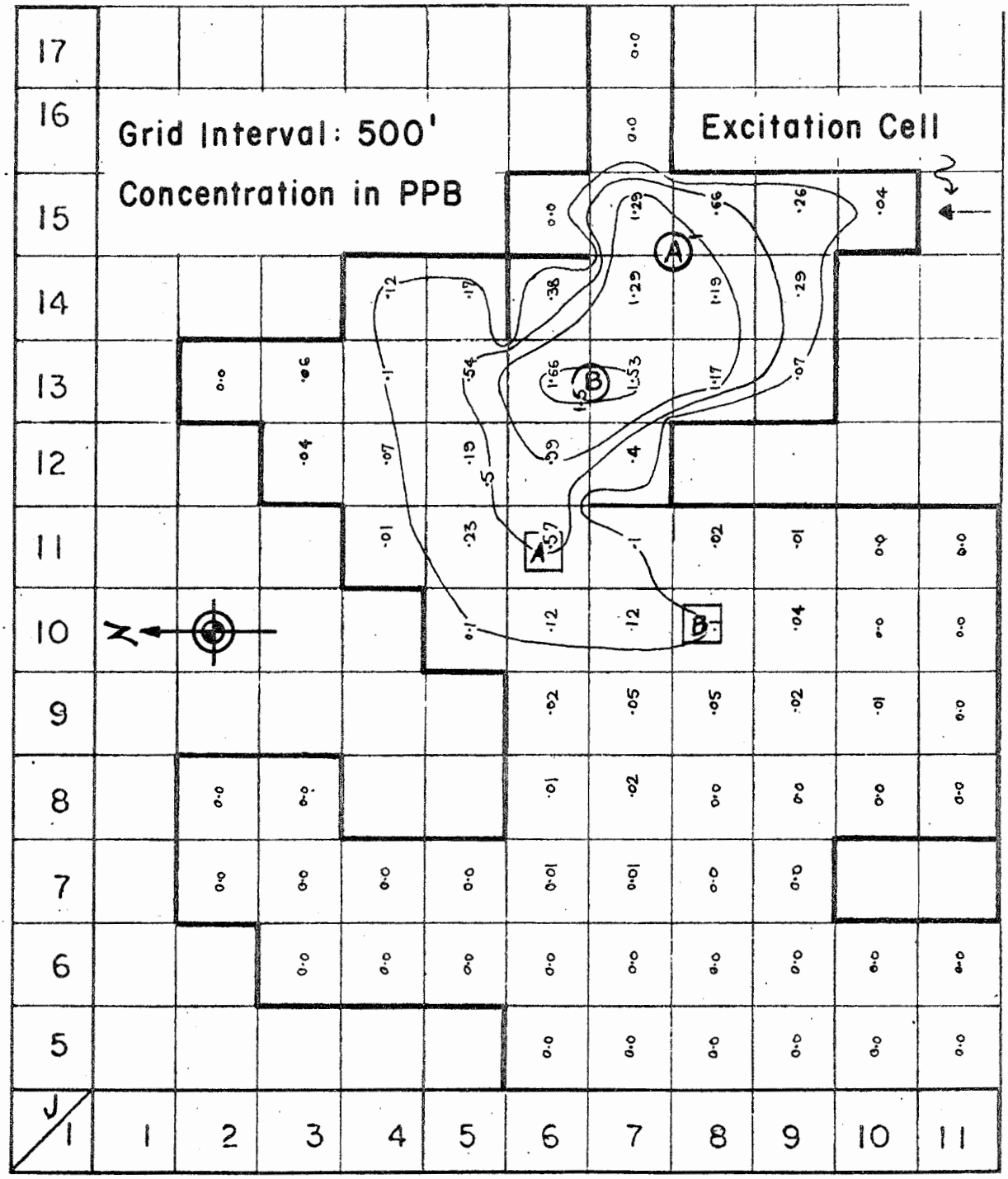

LAKE BASTROP MODEL VERIFICATION ZONE

Flow: 324 M. G. D.
Wind: 0 M. P. H. South
Dosage: 1.225 Lbs.
Time After Dye Release: 24 Hrs.

Peak (A) (B) Edge [A] - 12 Hours [B] - 24 Hours

Figure 7-29. Peak and Leading Edge Velocities and Time-of-Travel.

1. Mixing in water of a lake arises mainly from wind-induced currents and the physical and metabolic activity of layer organisms. (Lee 1970).

2. The existence of lake currents does not insure that appreciable mixing will occur. Mixing occurs only if velocity gradients exist.

3. Appreciable sub-surface currents may exist in lakes even under conditions of thermal stratification, including wind-induced hypolimnetic currents along the bottom, (Bryson and Kuhn 1955). However, concentration-depth profiles of stratified lakes indicate poor mixing between strata including the sediment-water interface, (Hutchinson 1957).

4. In open-lake conditions, and with normal wind velocities, about 18 hours lapse before a shifted wind establishes its new current; in very shallow waters and along shore a new current can occur within two hours after a wind shift. The induced current has a velocity of about 2% of the causative-wind.

Since the wind on any given day must modify the existing currents before it can set up its own, the wind of a given observation day cannot be assigned full value in making comparisons of wind to current noted on the observation day. During the major part of the observation day (open lake), the observed currents are largely those produced by the previous days winds but contain diminishing effects of the currents of days even earlier. Simple vector plots of wind or wind stress seldom are in agreement with observed current directions. But, Ayers (1962) found that if the wind stress vectors of the days in question are corrected by a series of effectiveness factors, according to their time-position relative to the observation day and if the resultant vector is considered to be modified by the Coriolis force, the result is generally in agreement with the observed local current directions. Thus, according to Ayers (1962), a suitable expression of wind-stress energy content of a lake at a given time is:

$$T_t = T_o\left(\frac{1}{4}\right) + \sum_{n=1}^{k} T_n \left(\frac{1}{2}\right)^{n-1} \qquad (7\text{-}9)$$

where:

T_t = total stress.

T_o = observation day stress.

T_n = stress on the nth day prior to the observation day.

n = number of the day prior to the observation day such that n = 1, 2. . .K.

K = number of days prior to the observation day for which the summation is carried out.

5. The "jet effects" which take place at the confluence of a warm water channel discharge and a relatively quiescent lake, described by Stefan (1970), are characterized by pronounced stratification. (Thus, the correction factors for stratification developed and applied in this study appear realistically warranted.)

The foregoing realistic factors serve to explain the major discrepancies between model predictions and field observations such as the time lags between observed and computed dye peak concentration values, with increasing lapse of time. (See Figures 7-14, 7-26, 7-27 and 7-28).

The verification tests brought out some of the major realistic factors encountered in the field measurement of environmental data. For example, the adsorption and release of dye from sediments and aquatic

growth; and, the sporadic introduction of non-steady wind conditions during prolonged test periods on the lake, constituted the major obstacles to "testing'control".

The tests demonstrated the need for more detailed sampling preparations which would consider both the spatial and temporal distribution of adsorbing materials in the area under study. Delfino (1968) in his lake studies suggests also the continuous and close observation of hydro-meteorological conditions at the test site for several days before the verification test days.

CHAPTER VIII

CONCLUSIONS AND RECOMMENDATIONS

Conclusions

This study confirmed the vital need for practical judgement and decision in the hydrodynamic modeling process which has been recognized also by others incident to modeling research for reservoirs (Elder, et al 1968), (Fruh 1970); for streams (Shull and Gloyna 1968); for bays and estuaries (Masch, et al 1969), (Bailey, et al 1966); and for flood control reservoir systems (Sauer and Masch 1969). Every impoundment or water body possesses its own unique hydrodynamical complex of forces and energy. A knowledge of these hydrodynamics is a pre-requisite to any practical engineering control or usage of the impoundment. The consensus of the experience is that the engineering task of gaining the essential hydrodynamic knowledge unique to a certain water body can be made more tractable by the adoption of a macro-synthetical investigation and problem-solving approach which synthesizes three major processes, namely: analysis, mathematical or hydraulic modeling, and prototype verification. Referring specifically to reservoirs and lakes, for example, the analysis process involves the specification of impoundment system concept or configuration such as shoreline and bottom geometry, inflows and other basic input variables. Then, the mathematical or hydraulic

modeling process involves the development of tractable equations solved by numerical models capable of being energized by a wide range of input combinations. The model furnishes by computer solution an output of concentration, temperature or other property distributions as a function of time. Finally, the field verification process involves field observations, measurements and tests, guided by prior model simulations and hypothetical predictions, on a selective basis to facilitate sampling operations and to ascertain important correlations between key hydrodynamic and hydrometeorological parameters.

The efficacy, versatility and value of the macro-synthetic approach just described was demonstrated in this study of Lake Bastrop, a power plant cooling-water impoundment of considerable hydrodynamical and thermodynamical complexity. First, an analysis was made of available hydrological and hydromechanical data, supplemented by field reconnaissances. This preliminary action revealed the predominant mechanisms of motion, unique boundary conditions, and other parameters which are "characteristic" of the system. This knowledge enabled the formulation of the lake system. Then, the physical system was discretized into two, complementary, numerical, steady-state, macro-models - a hydrodynamic model and a conservative-substance transport model. These computer models were capable of being energized with hypothetical inputs to simulate a wide assortment of combinations of variables. In the third

phase, field verification, highly useful and reliable correlations between observed and computed values were obtained in the following specific aspects of dispersive and transport phenomena of Lake Bastrop:

1. Mixed layer concentration (of conservative substances) distribution vs. time.
2. Circulation patterns.
3. Time-of-travel values, involving peak concentrations, and leading edge versus peak.
4. Coefficients of dispersion.

Also, a by product of the "model simulation - field verification" process was the opportunity to analyze the spectra of effects resulting from assumed univariate or multivariate changes in the following:

1. Coefficients of dispersion.
2. Wind velocities and directions.
3. Flow rates.
4. Depth of homogeneous, fully-mixed surface stratum.

After careful analysis, and from a macroscopic view point, it is concluded that the most powerful dispersion, mixing and transport mechanisms in impoundments are the wind-induced surface currents. These currents are caused by wind shear at the surface. The turbulent motion possessed by these currents enables them to transport large bulk masses and to disperse materials concentrated in the water.

In contrast, wind-induced surface waves transport a large amount of energy. But, waves are not the bulk mass transport mechanism. Generally, wind-induced currents assume even greater importance when it is considered that the surface stratum on which wind stress acts is also in most cases a stratum which is virtually captured and held within an epilimnetic rigidity of temperature stratification. Analysis of the results of the hypothetical simulations made in this study confirms the general, quantitative relationships between lake current velocities and wind velocities, which are analagous to the quantitative, empirical relationships found by other investigators in their work on ocean coastal waters and large lakes. Based on dye-travel studies, it was found that in shallow waters, the upper "skin" layer of 6 to 12 inches moves at about 2.5% of the wind velocity, decreasing to about 1.5% at depths of 4 feet, and is negligible at 8 to 10-foot depths. In deeper waters (i.e., over 40 feet) the current-wind factor is about 2% at 10 feet and negligible at depths of 15 to 20 feet. However, the practical measurement of reverse flows below the stagnation plane for winds transverse to shores and velocity changes in flows below the stagnation plane, due to sustained duration of winds are beyond the scope of study. But, these considerations more than any others, gives overwhelming impetus to the adoption of a horizontal, two-dimensional model for the analysis of the dispersive and transport mechanisms of lakes and reservoirs.

Natural phenomena are probabilistic. Therefore, in the field verification observations, the means of values measured over a 5-minute or a 30-minute interval were taken for comparison with the computed values of the deterministic model. The study confirms the essential fact that exact prediction of the phenomena is impractical, but that the prediction of its distribution is reasonable. Averaging over measurable time intervals is more appropriate than instantaneous values for macroscopic analysis purposes.

A recent report by Stefan (1970) on stratification of flow from channel to lake, based on laboratory flume studies, sheds light on some of the phenomena observed in the field verification tests at Bastrop, especially in the two or three cells which constitute the physical confluence of the channel and lake. The flow of the heated water discharged from the Bastrop channel entered the slow-moving, colder confluence zone of the lake under conditions virtually as described by Stefan (1970). He reported that various types of stratification can occur at such a confluence of channel and lake: (1) A cold water wedge can penetrate into the outlet channel, or at least underlie the greater part of the confluence zone. (2) Internal gravity waves can be generated, and (3) Internal hydraulic jump phenomena can be formed. Evidence of a combination of all these actions were recognized in the two or three cells forming the "mixing bowl" of the confluence zone. However, beyond the juncture, the warm channel discharge formed a "gliding stratum"

of warm, highly-concentrated water-dye mixture. Then, approximately mid-way in the verification zone the water-dye stratum, having attained the ambient surface temperature, seemed to come under the influence of density stratification phenomena, "diving" to a level from two to six feet below the surface. However, these phenomena are not easily separable by field observations and the net effects noted in the field appear to be more highly-attenuated compared to the laboratory test effects described in the Stefan (1970) report. In view of the foregoing considerations, the verification zone was selected to cover a sufficiently large area to insure analysis of dispersive and transport phenomena under a wide range of hydrodynamic and hydrometeorological regimens.

Recommendations

While the model developed in this study is essentially deterministic, and the tests conducted on it have involved deterministic inputs, it should not be inferred that the stochastic aspects are either disregarded or excluded. It was beyond the scope of this study to introduce aspects of randomness in the model. However, it is believed that it would have been entirely feasible to use stochastic, time-concentration inputs into the excitation cell of the lake transport model in lieu of the relatively uniform Gaussian type distributions actually used. It is recommended that further tests be conducted using stochastic inputs into a deterministic

transport model. In theory, this should give better statistical ranges of transport behavior in a given impoundment.

Since wind effects have such a preponderant effect on dispersive and transport process in the water environment, it appears desirable that provision be made for obtaining continuous records of wind data and water current data as part of the permanent instrumentation for large, multiple-use water impoundments. These data should be used to develop, test and improve the correlations between observed and computed transport and current patterns. The use of high-capacity, self-contained recording current meters; buoy-mounted wind recorders; temperature profile recorders; and, associated automatic data processing similar to that used in oceanographic instrumentation, would greatly enhance verification and adaptation of impoundment modeling. Velz and Gannon (1960) from studies on forecasting heat losses from ponds and streams, came to similar conclusions regarding the utility, establishment and use of localized weather record stations.

These recommendations are in consonance with the macro-synthetical approach of harmonizing model data at every practical step with easily-obtained, readily-measured field "state" conditions, in order to inject realism into the process of applying numerical models to specific cases. Mathematical model technology is similar to scale model technology in one vital respect: in all cases, models have to be adjusted experimentally in order to reproduce correctly the natural phenomena to be studied. (Le Mehaute 1962).

Renewed emphasis should be placed on the rational analysis and management of individual bodies of water. It appears productive to focus on a flexible, adaptive methodology whose objective is to understand the hydrodynamics of a particular body rather than focusing exclusively on the task of applying a universal model in sterile fashion to all cases. The compelling trend today is to regulate, manage and protect the "renewability" of individual water bodies for specific multi-purposes. Thus, while continued emphasis should be given to pursuing further advances in modeling such as development of three-dimensional model, and the reduction in the number of empirical coefficients and in the number of simplifying assumptions, - it should be remembered that professional engineering usually inherits the task of having to design and construct facilities based on highly-selective, economically-available and measurable hydrodynamic knowledge of a specific reservoir or lake. The macro-synthetical approach demonstrated in this study, involving system analysis, numerical modeling and field test methodology provides a rational strategy for this engineering task.

The two-dimensional horizontal transport model developed in this study, using Lake Bastrop as the "typical hydrodynamic system", and Rhodamine B as the "typical conservative substance" transported, has a potentiality for general application to macro-synthetical analyses of numerous practical cases involving transport of conservative substances in a hydrodynamic regime characterized by shallow, stratified, well-mixed

or stabilized surface strata. Of course, implied in each application is the pre-requisite of obtaining the hydrodynamic data unique to the water body as input for the transport model. The macro-synthetical two-dimensional transport model approach affords a methodology to make useful estimates of the general magnitude and extent of "shocks" on water bodies brought about by "peaks" or instantaneous onsets of various phenomena (e.g., pollutant, thermal, flood, or run-off from rainfall).

Table A-1. A Lake Transport Model Using the Finite Differences Notations and Conversions

Fortran Notation	General Notation	Description
IMAX		Number of cells in x-direction.
JMAX		Number of cells in y-direction.
NSORCS		Number of source points. (Inflow/Outflow)
DELX	ΔX	Spatial increment in x-direction, (feet).
DELY	ΔY	Spatial increment in y-direction, (feet).
DELT	ΔT	Computational increment.
CSORC		Concentration at source point. (Inflow/Outflow)
U		Velocity in x-direction at cell boundary, (feet/second).
V		Velocity in y-direction at cell boundary, (feet/second).
I FLAG		Control for boundary conditions. (Lateral, longitudinal, inflow and outflow boundaries.)
CAVE		Depth at the center of cell, (feet).
CO		Concentration at the Excitation cell, (parts per billion, ppb).

Table A-1 (Continued)

Fortran Notation	General Notation	Description
NDATA		Number of values of temporally-varying concentration data read into excitation cell.
CONCN (I, J)	$C_{i,j}^{k}$	Concentration (parts per billion, ppb) at the center of cell at time t = k.
DX	Ex	Turbulent dispersion coefficient in x-direction, (feet^2 / second).
DY	Ey	Turbulent dispersion coefficient in y-direction, (feet^2 / second).
(IS, JS)		Grid point location of source points.
(I, J)		Grid point location of cell.

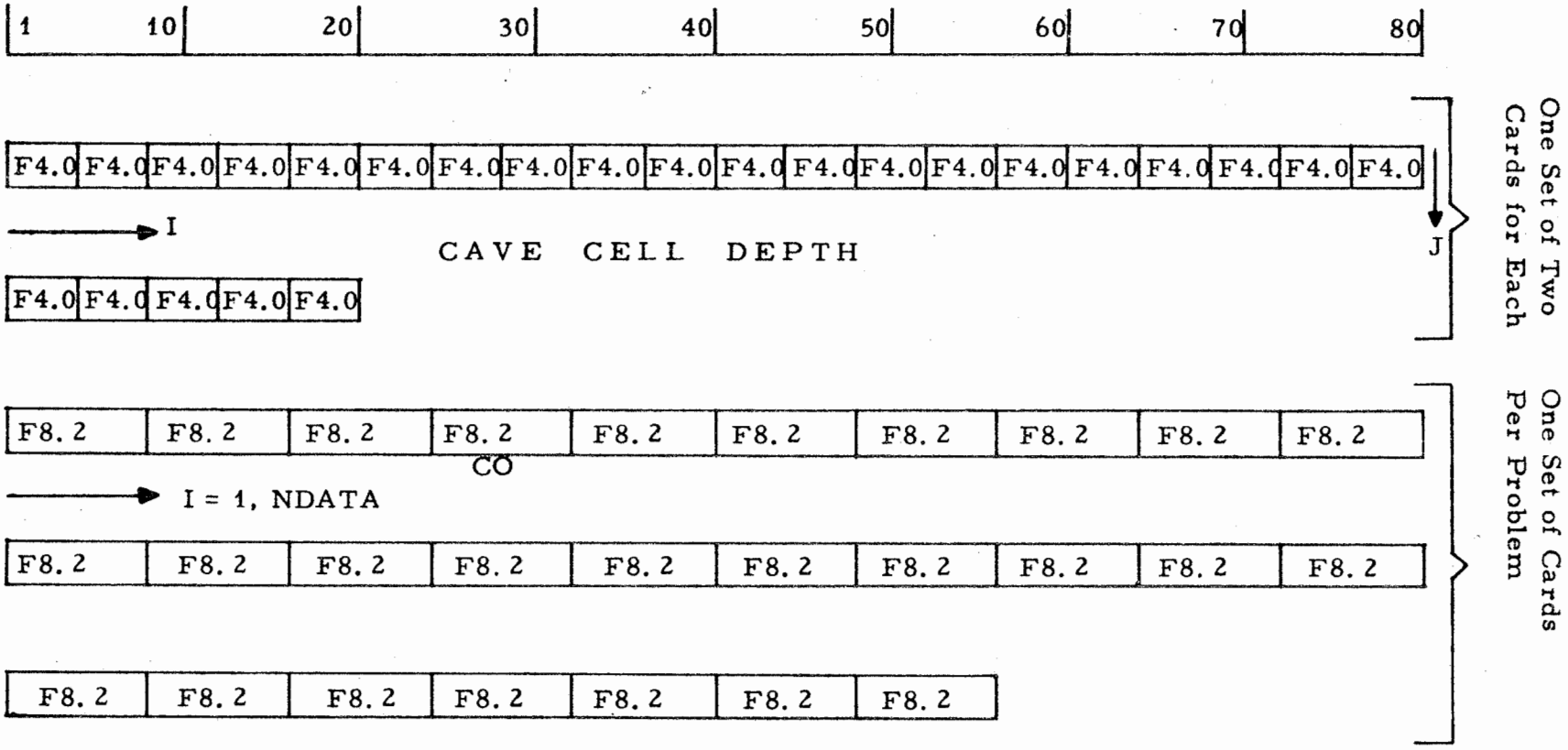

FIGURE A-1 FORMAT FOR DATA INPUT FOR PROGRAM TRACER -- A LAKE TRANSPORT MODEL USING THE ALTERNATE DIRECTION IMPLICIT METHOD OF FINITE DIFFERENCES.

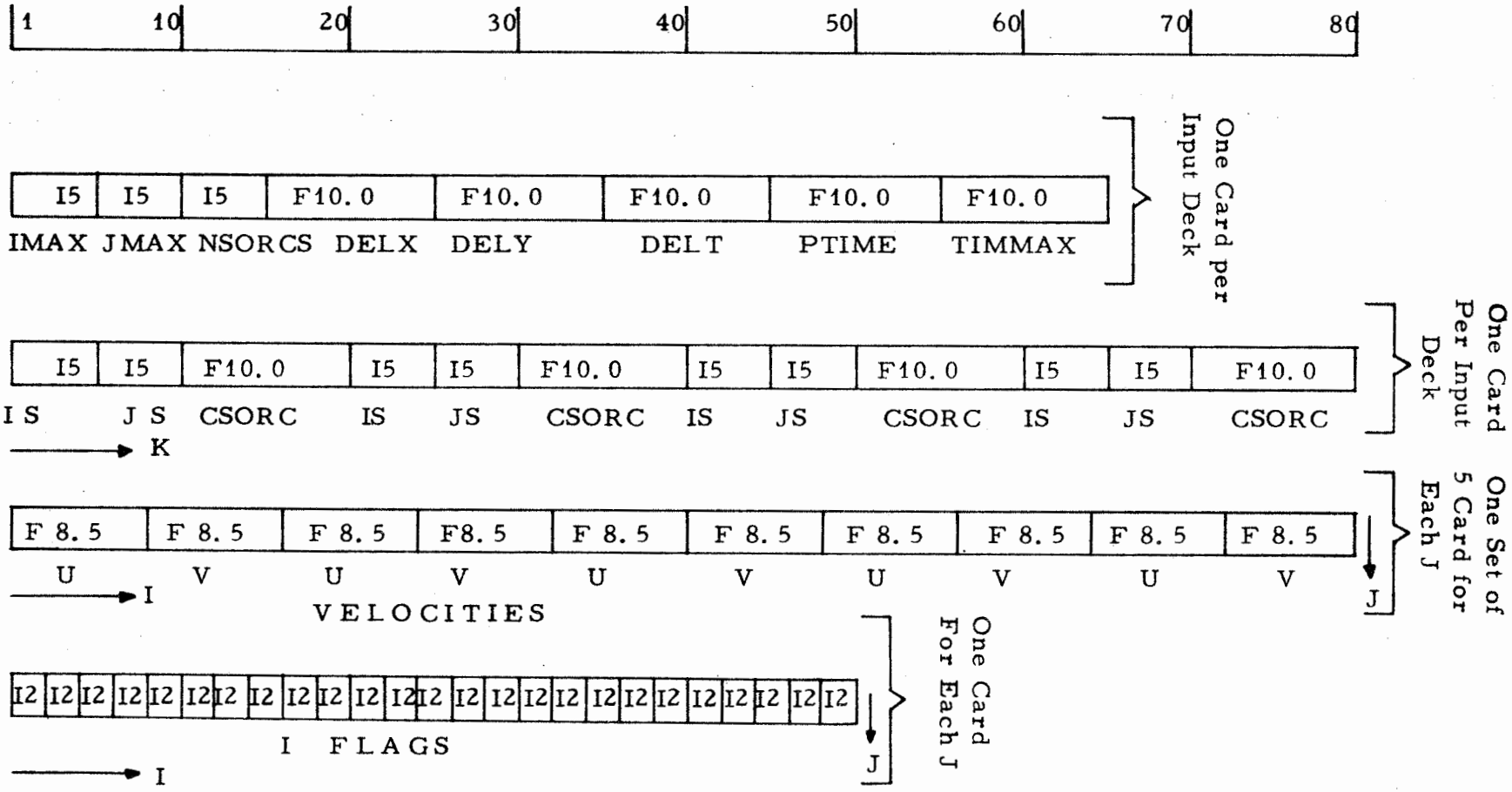

FIGURE A-1 (continued) FORMAT FOR DATA INPUT FOR PROGRAM TRACER--A LAKE TRANSPORT MODEL USING THE ALTERNATE DIRECTION IMPLICIT METHOD OF FINITE DIFFERENCES.

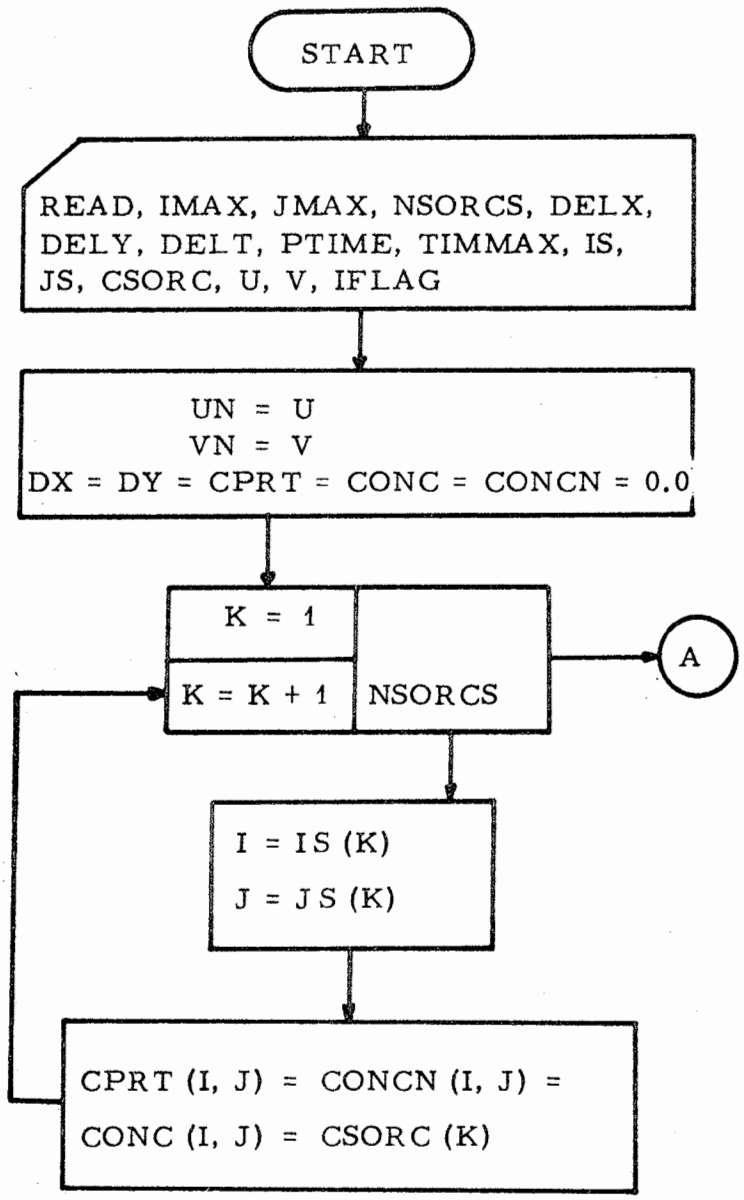

FIGURE A-2-1. FLOW DIAGRAM FOR PROGRAM TRACER

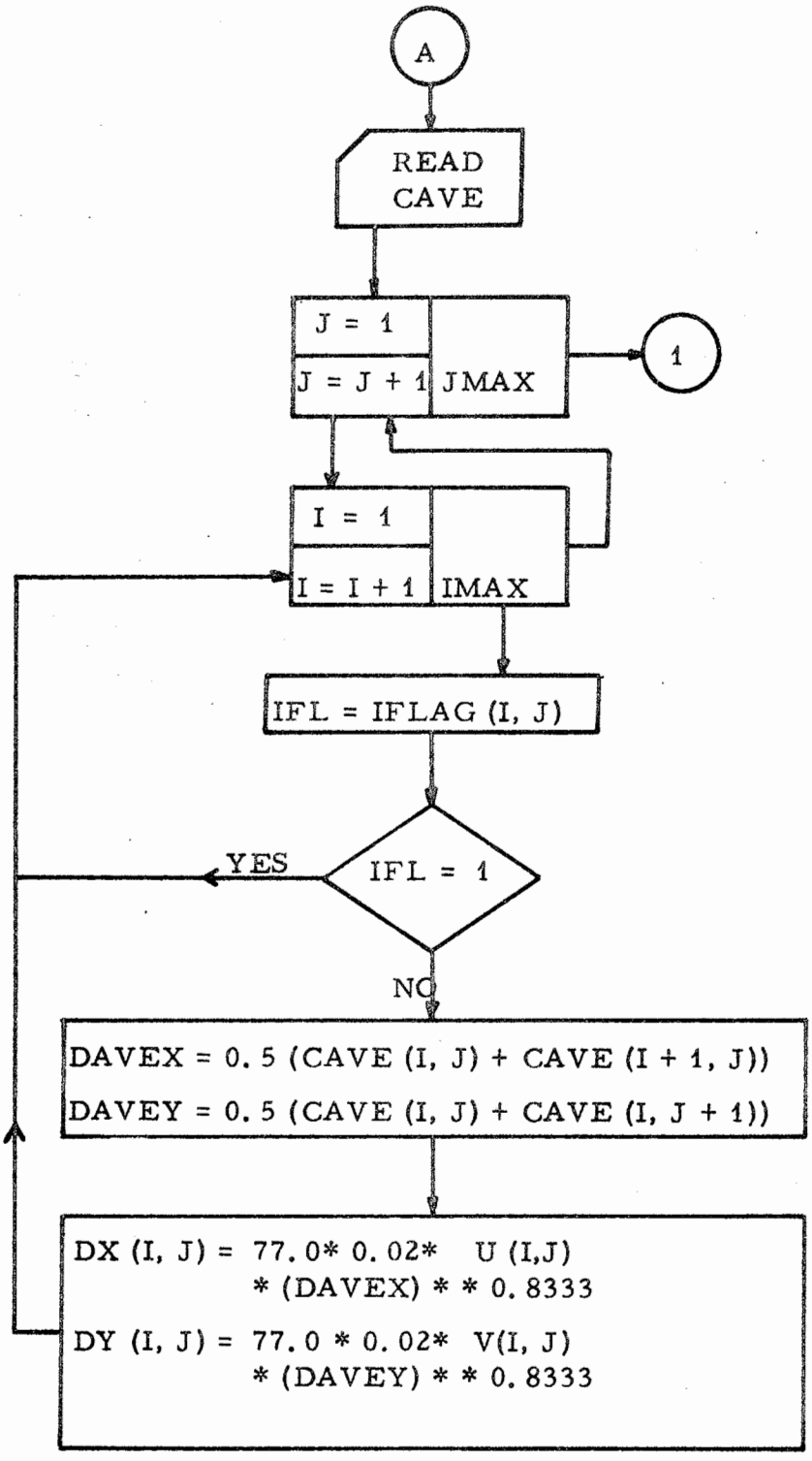

FIGURE A-2-2. FLOW DIAGRAM FOR PROGRAM TRACER
(continued)

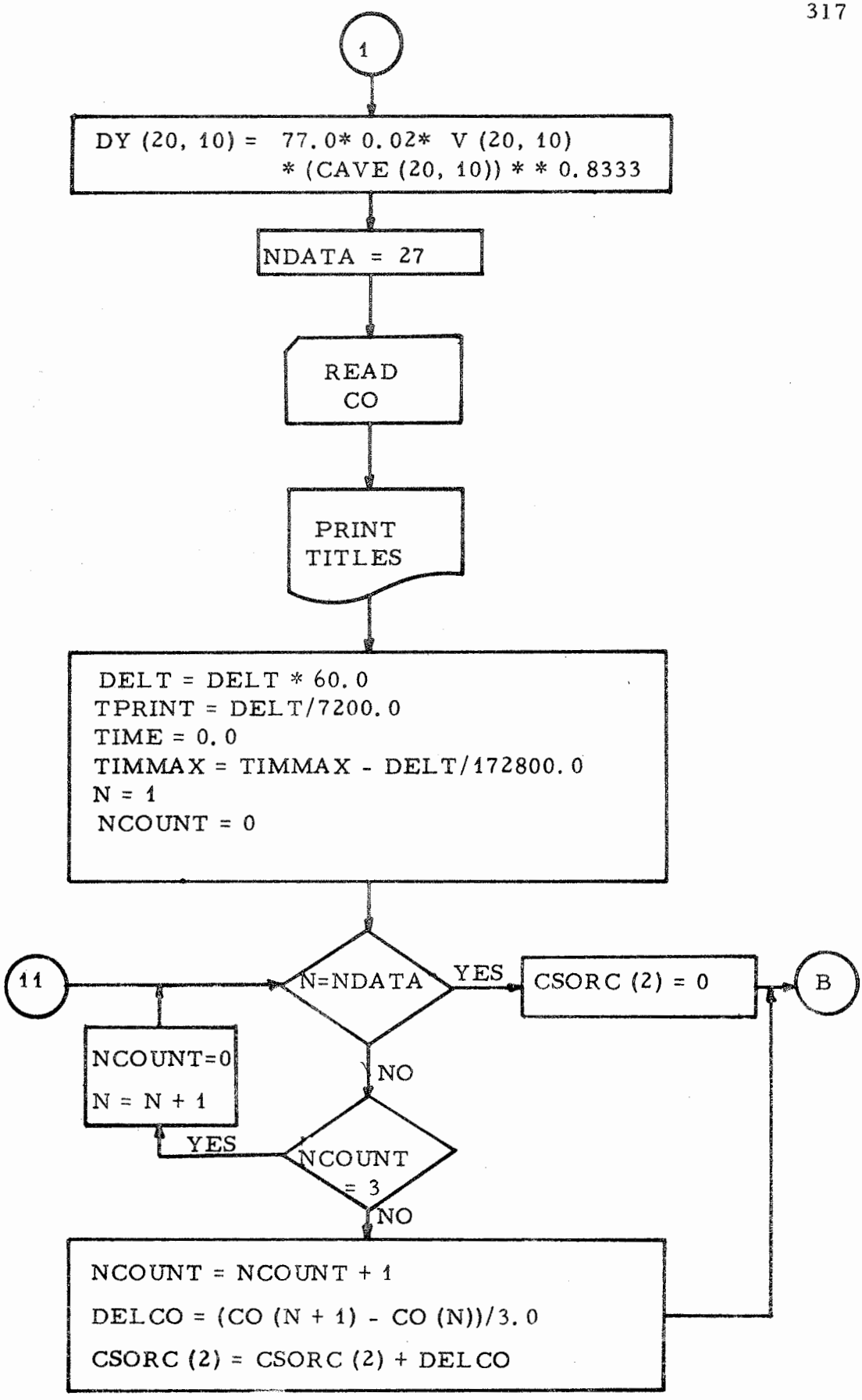

FIGURE A-2-3. FLOW DIAGRAM FOR PROGRAM TRACER (continued)

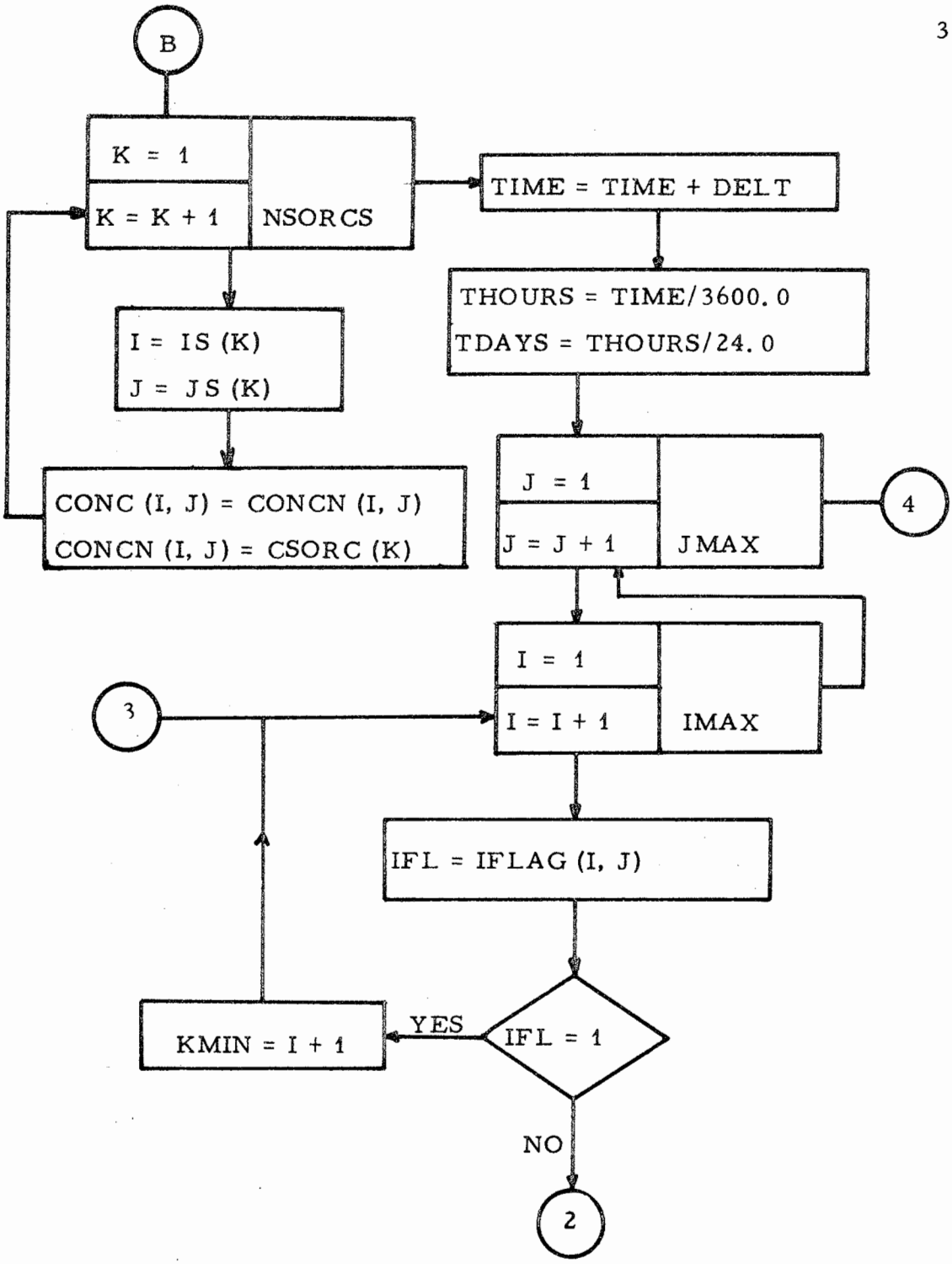

FIGURE A-2-4. FLOW DIAGRAM FOR PROGRAM TRACER (continued)

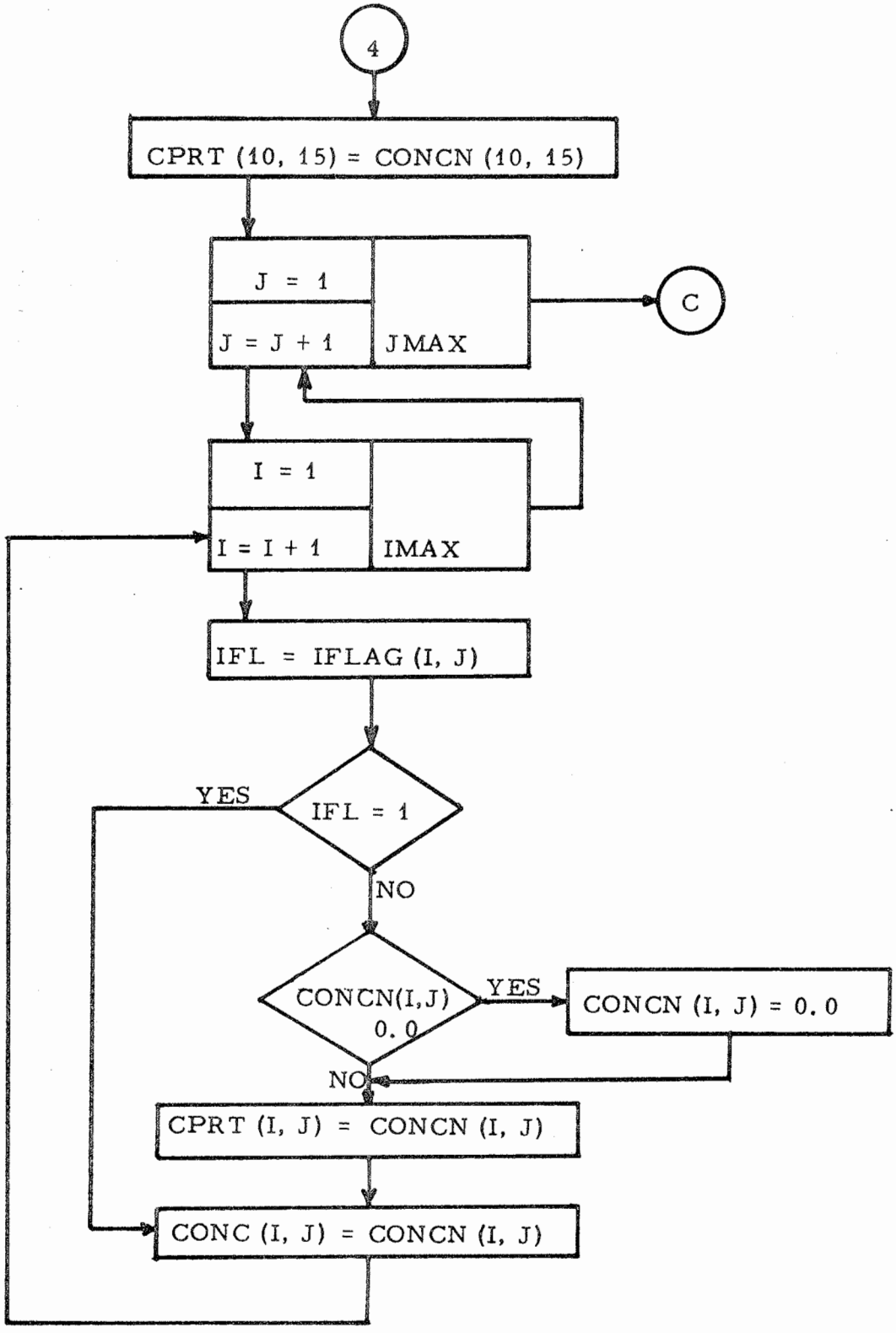

FIGURE A-2-5. FLOW DIAGRAM FOR PROGRAM TRACER (continued)

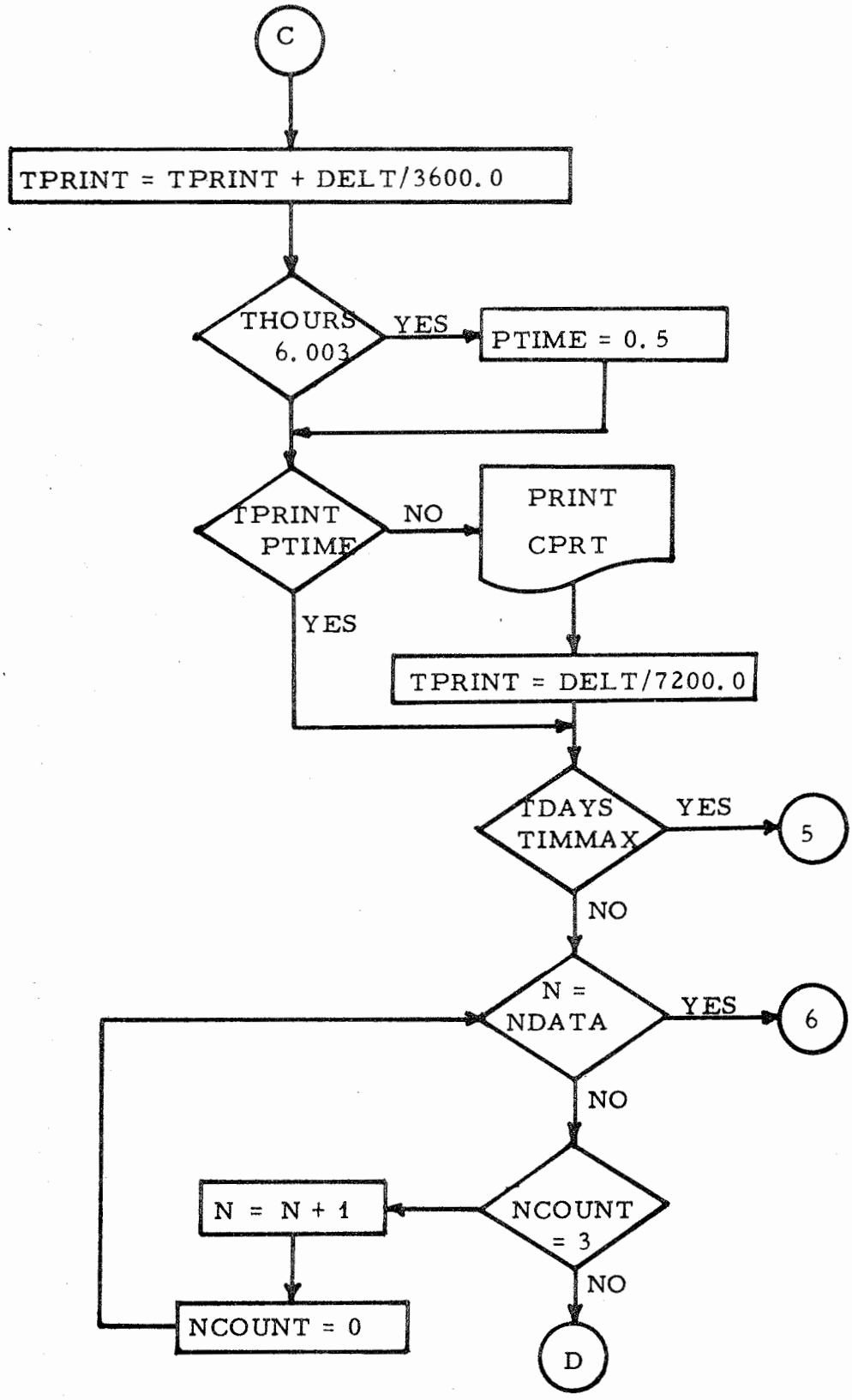

FIGURE A-2-6. FLOW DIAGRAM FOR PROGRAM TRACER
(continued)

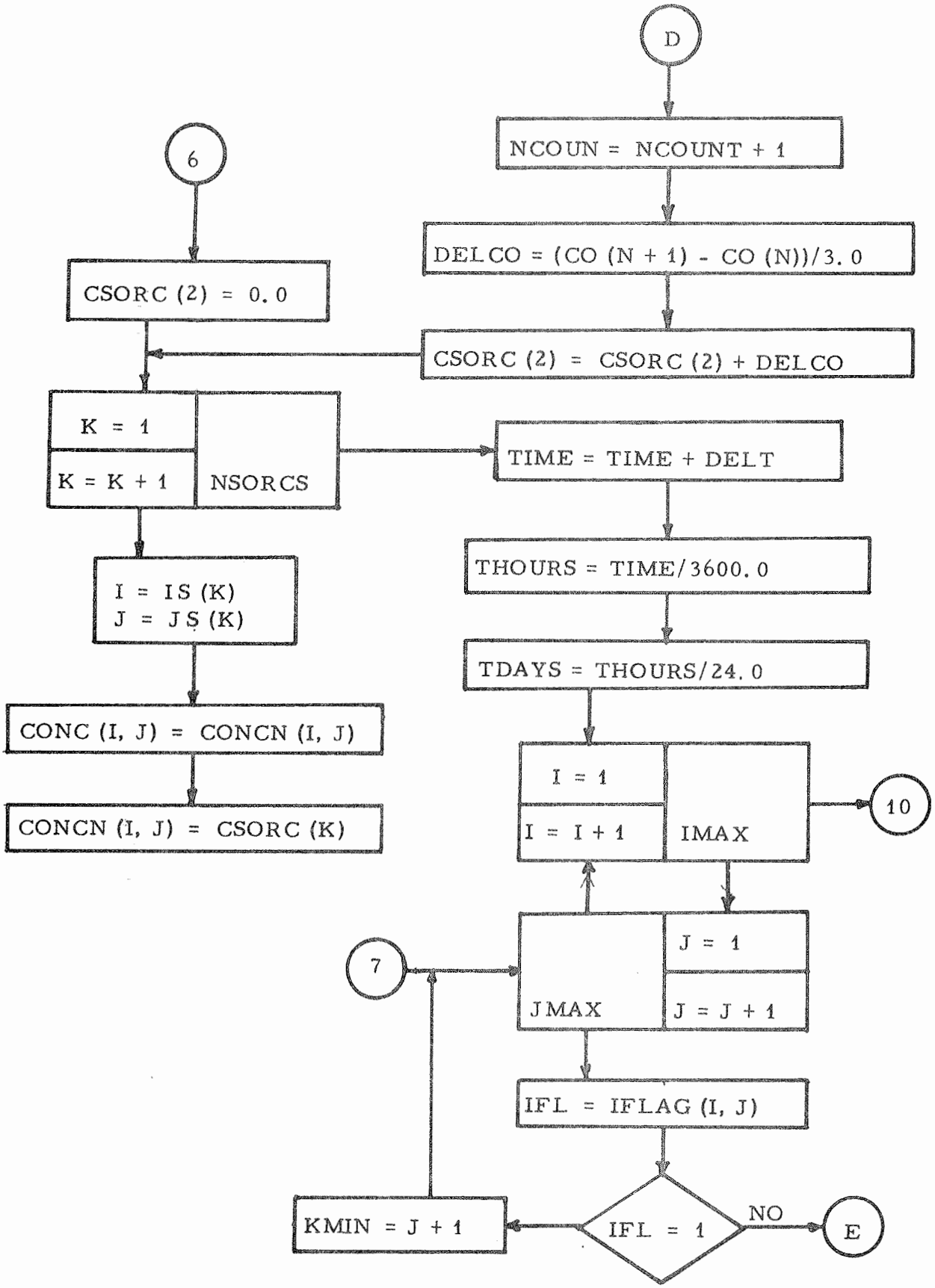

FIGURE A-2-7. FLOW DIAGRAM FOR PROGRAM TRACER (continued)

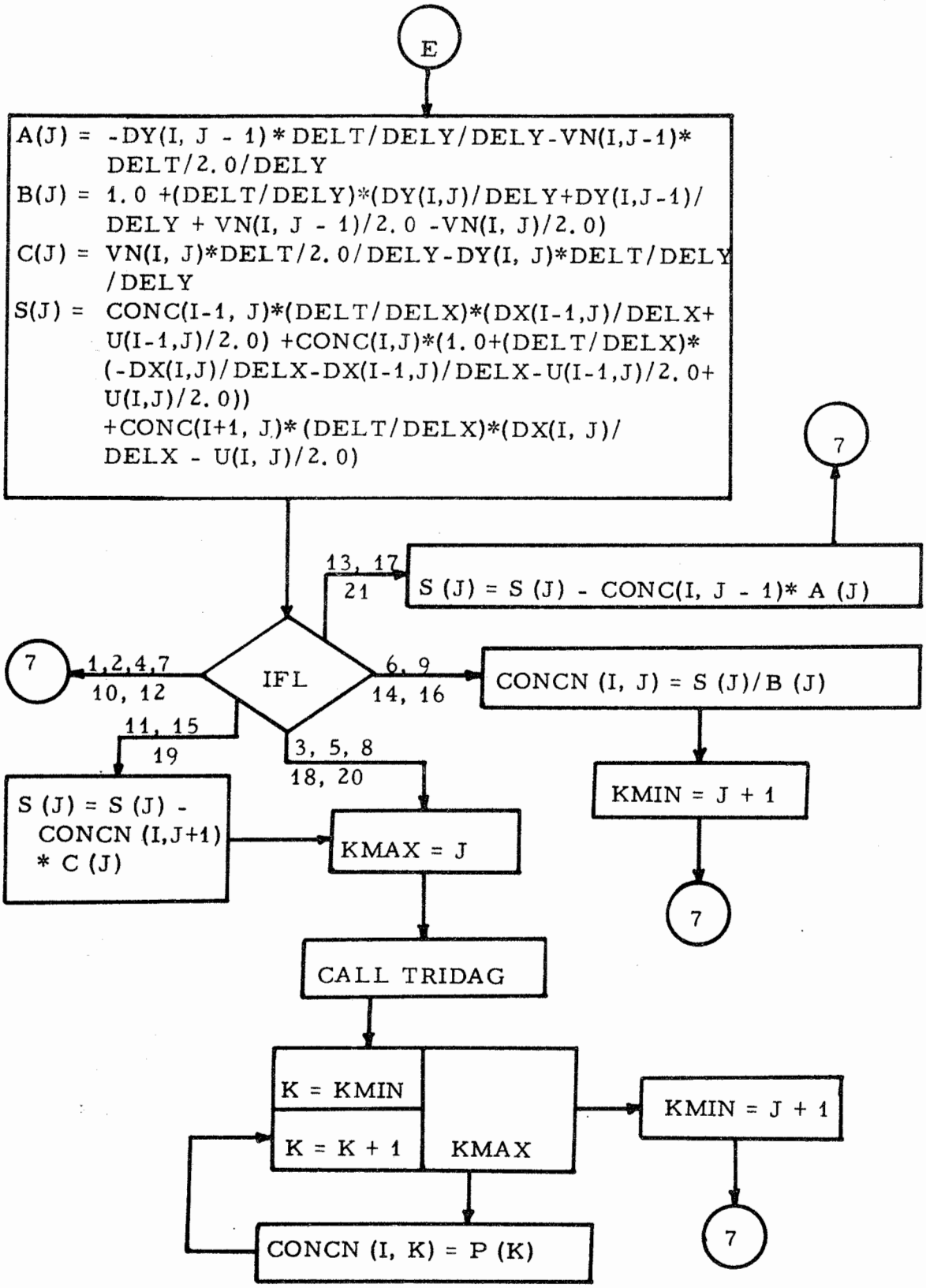

FIGURE A-2-8. FLOW DIAGRAM FOR PROGRAM TRACER (continued)

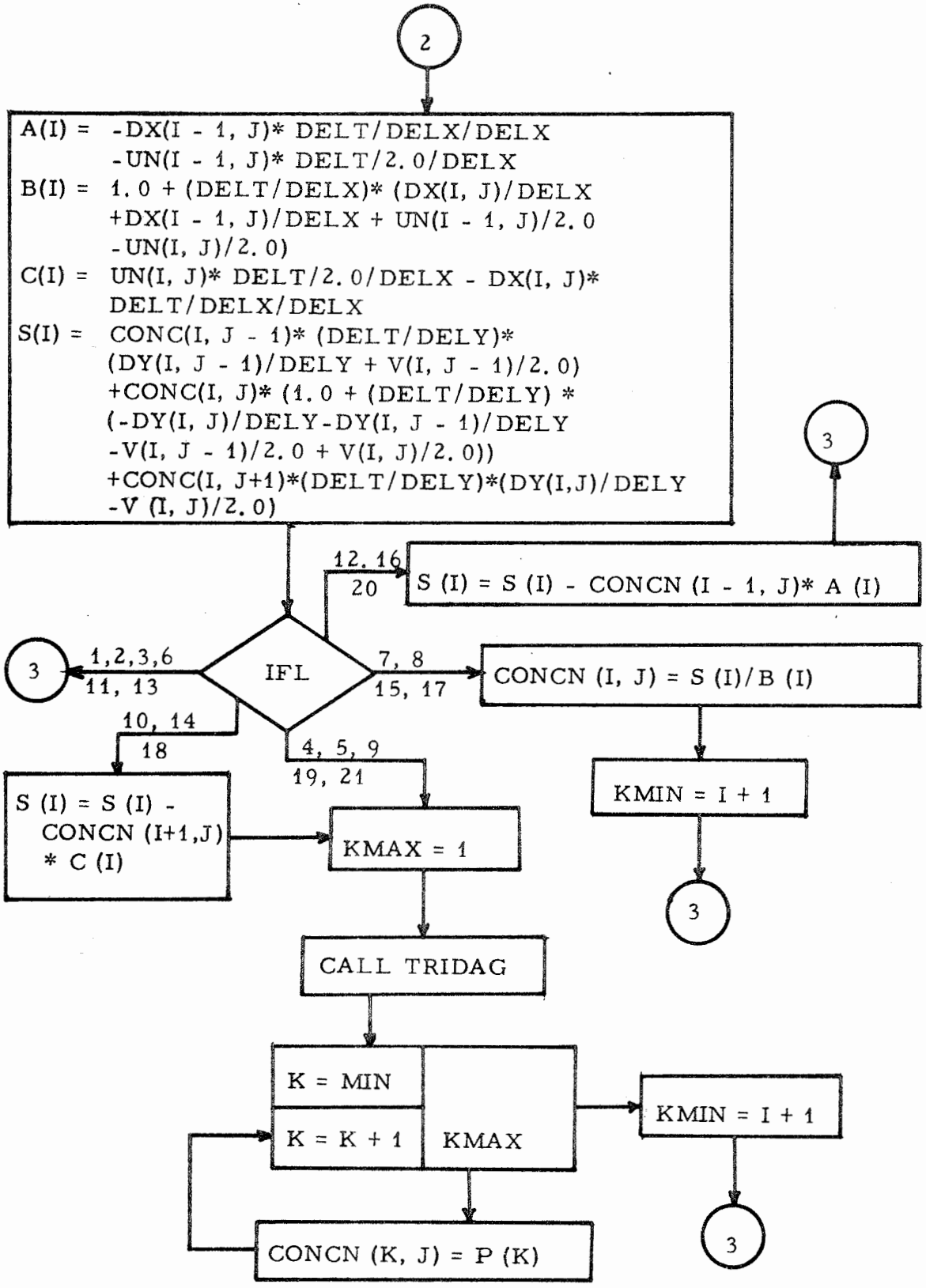

FIGURE A-2-9. FLOW DIAGRAM FOR PROGRAM TRACER
(continued)

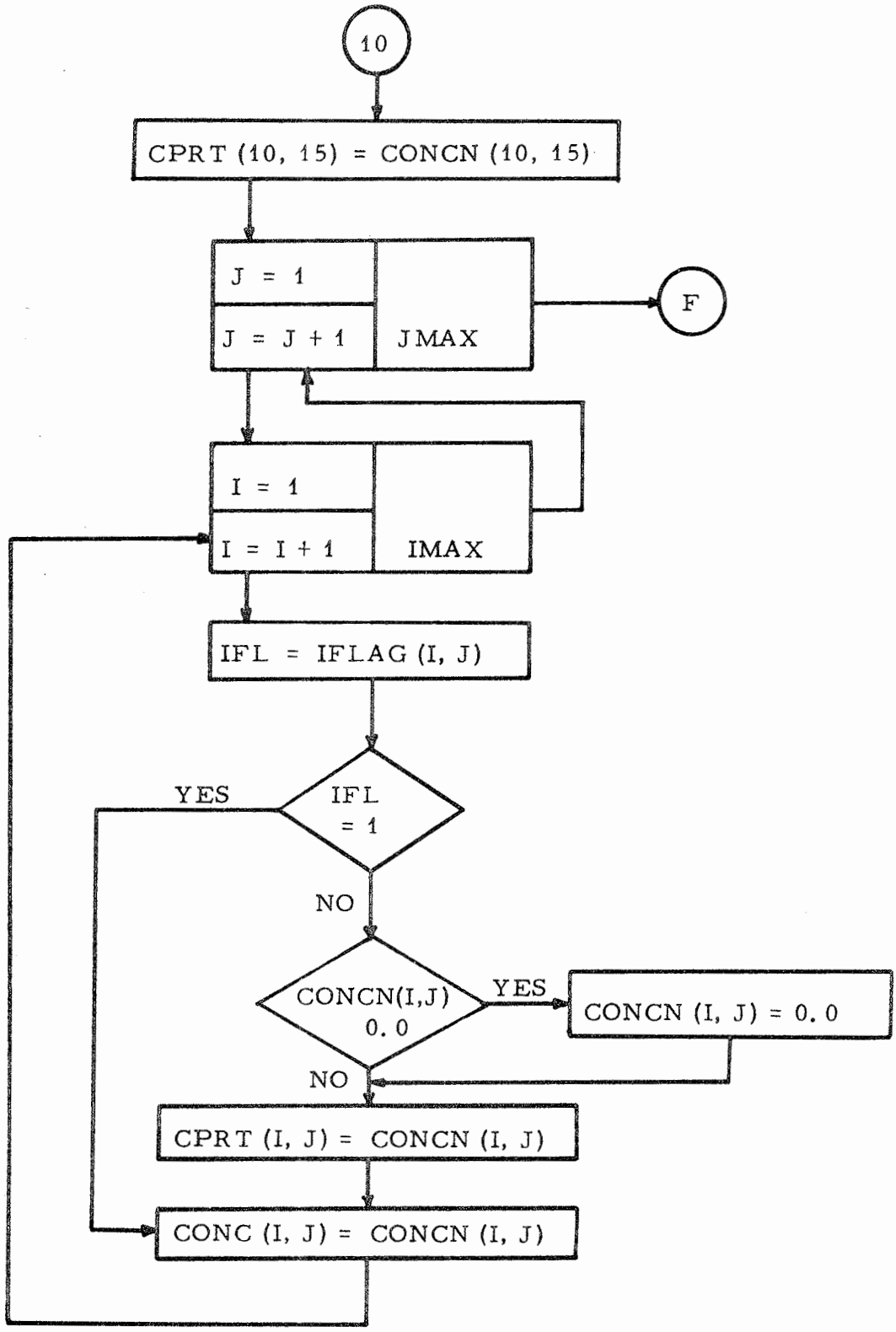

FIGURE A-2-10. FLOW DIAGRAM FOR PROGRAM TRACER (continued)

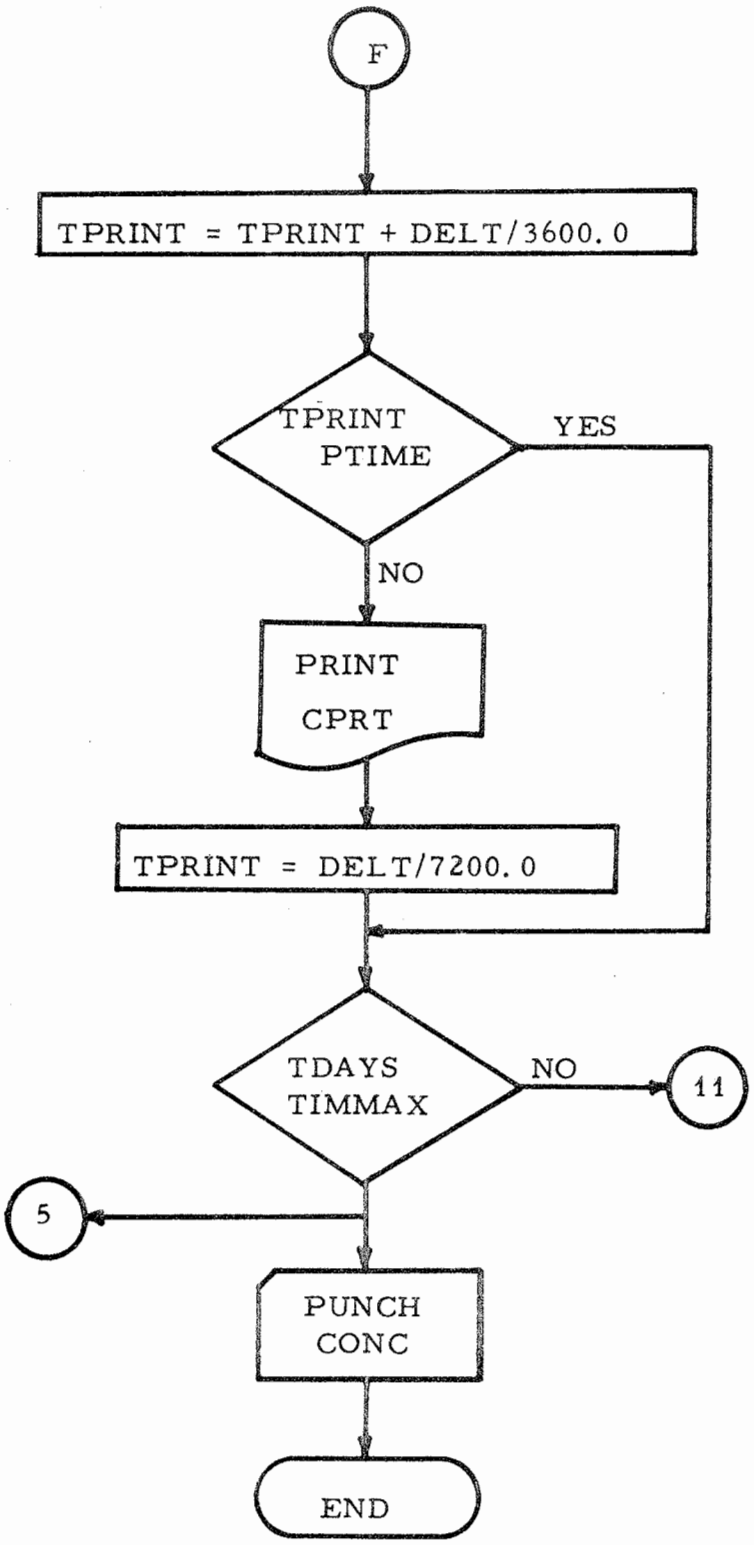

FIGURE A-2-11. FLOW DIAGRAM FOR PROGRAM TRACER (continued)

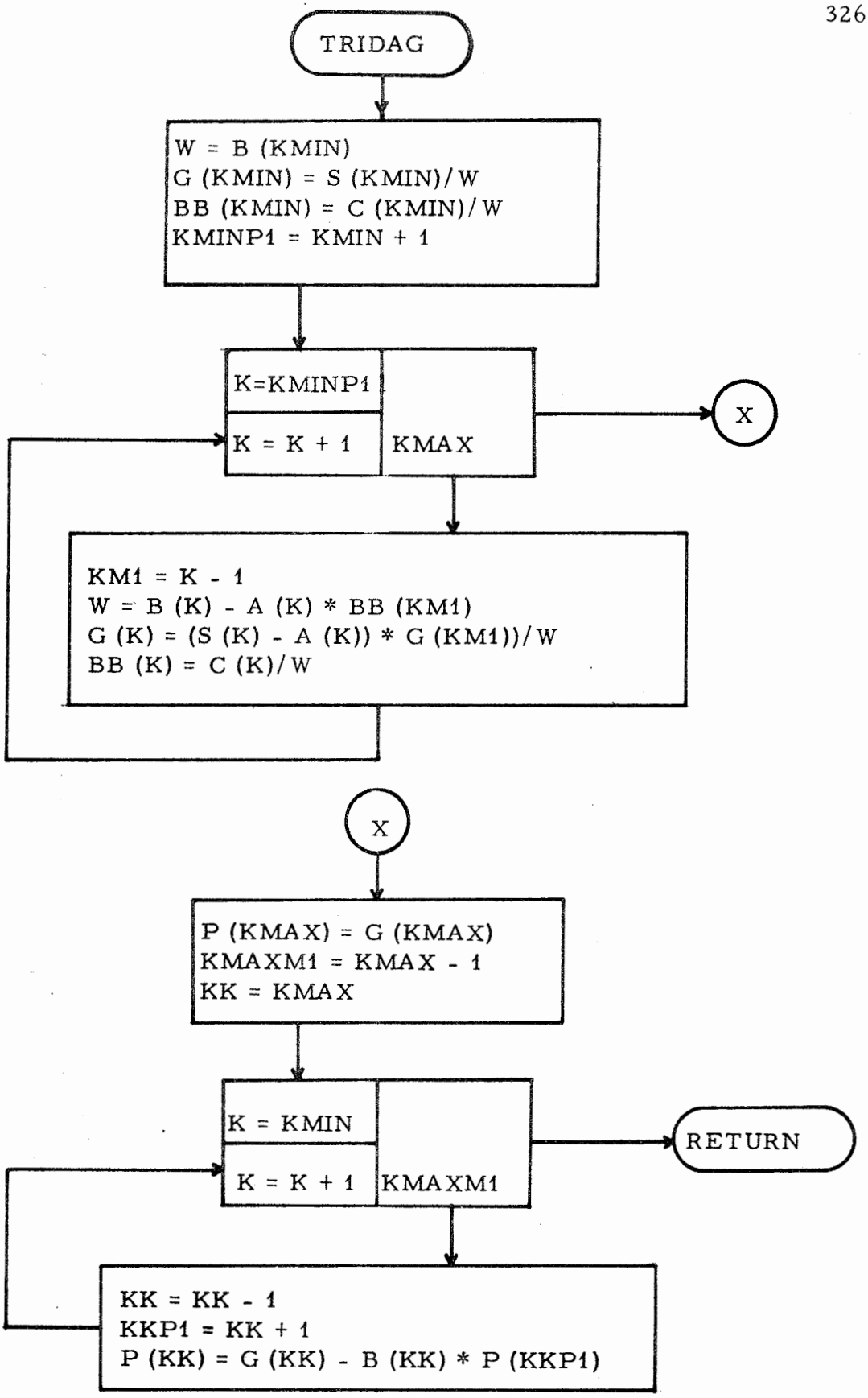

FIGURE A-2-12. FLOW DIAGRAM FOR PROGRAM TRACER

Table B-1. PROGRAM CONC - An Open-Channel Transport Model Using the Taylor Approximation for the One-Dimensional Dispersion Equation - Notations and Conversions

Fortran Notation	General Notation	Description
X		Distance down-channel.
DX	D	Turbulent dispersion coefficient, (ft^2 / sec.)
U		Velocity in channel, (feet / second).
AM	m	Mass, (pounds).
A		Cross sectional area, (square feet).
RHO	ρ	Density of powder Rhodamine B, (lbs/ft^3).
W		Volume of Rhodamine B per unit area of cross-section, (feet).
T	t	Time since release of Rhodamine B, (hours).
C		Concentration, (ppb).

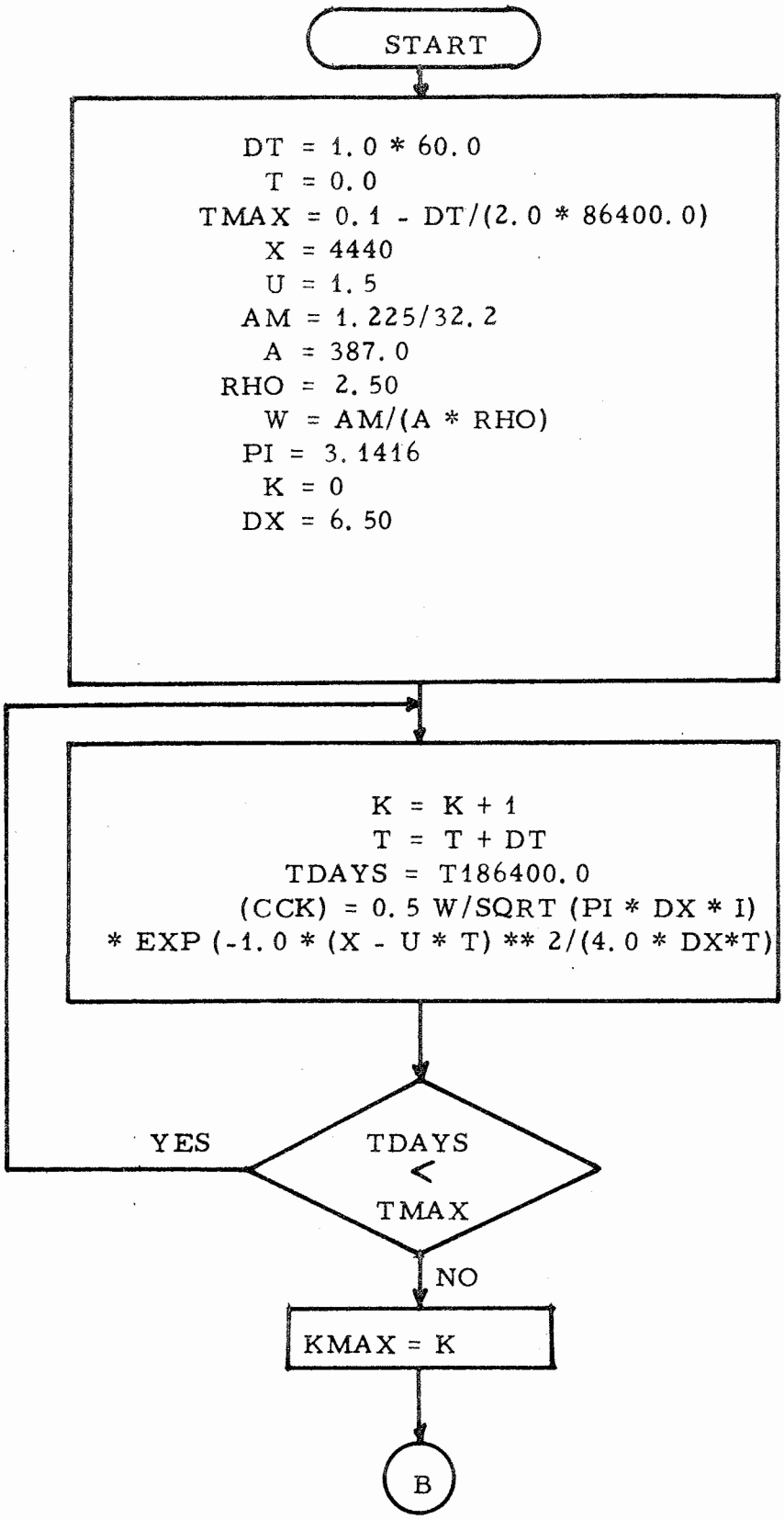

FIGURE B-1-1. FLOW DIAGRAM FOR PROGRAM CONC

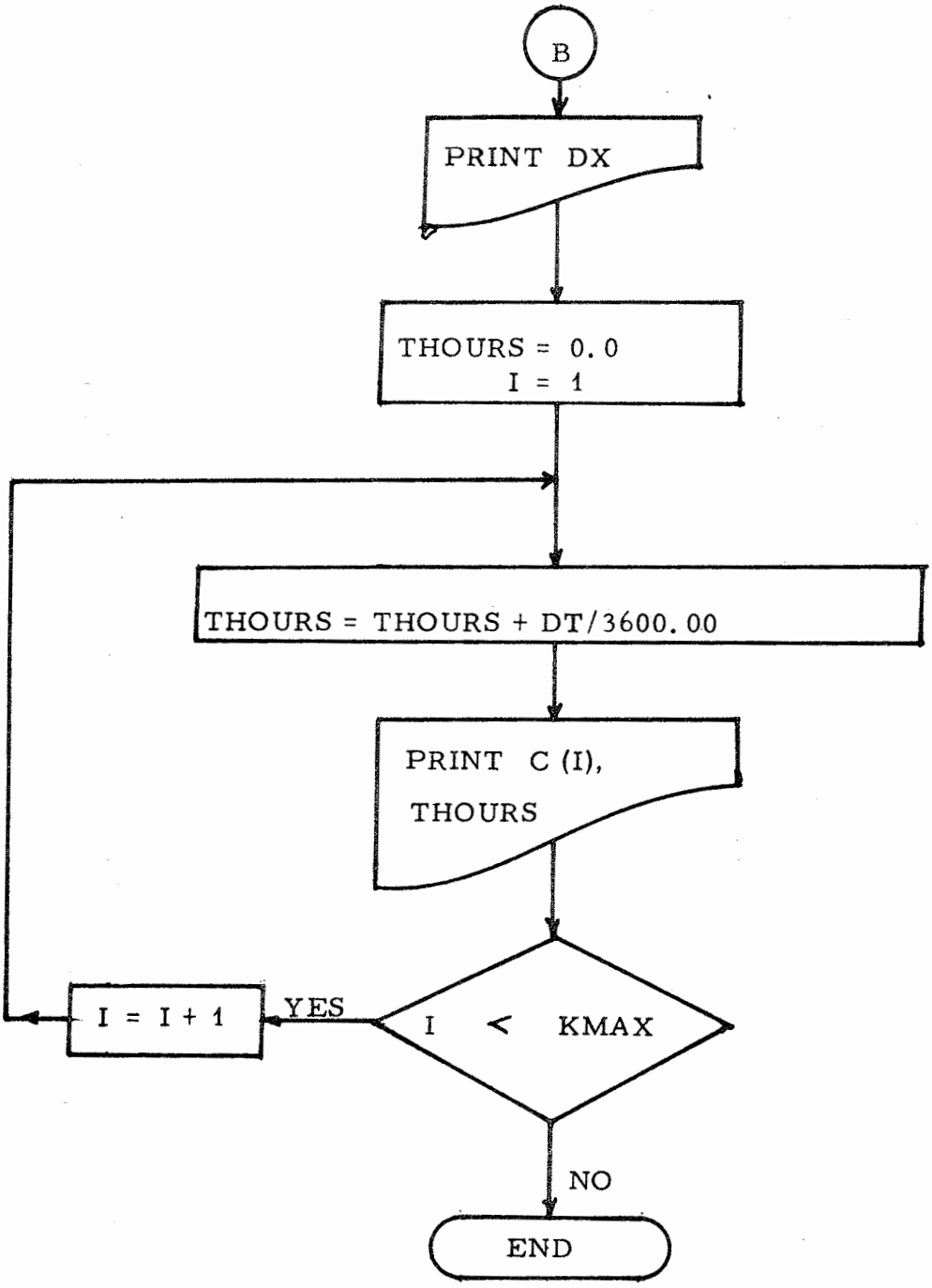

FIGURE B-1-2. FLOW DIAGRAM FOR PROGRAM CONC (continued)

Table C-1. PROGRAM TRACE - An Algorithm for Computing Dispersion Coefficients by Method of Variances

Notations and Conversions

Fortran Notation	General Notation	Description
C		Concentration.
X		Distance, (feet).
XBAR	μ	Arithmetic Mean.
V	σ^2	Variance, (Square feet).
DISCOF	D	Turbulent Dispersion Coefficient, (ft^2 / sec.).
DELT		Change in time, (seconds).

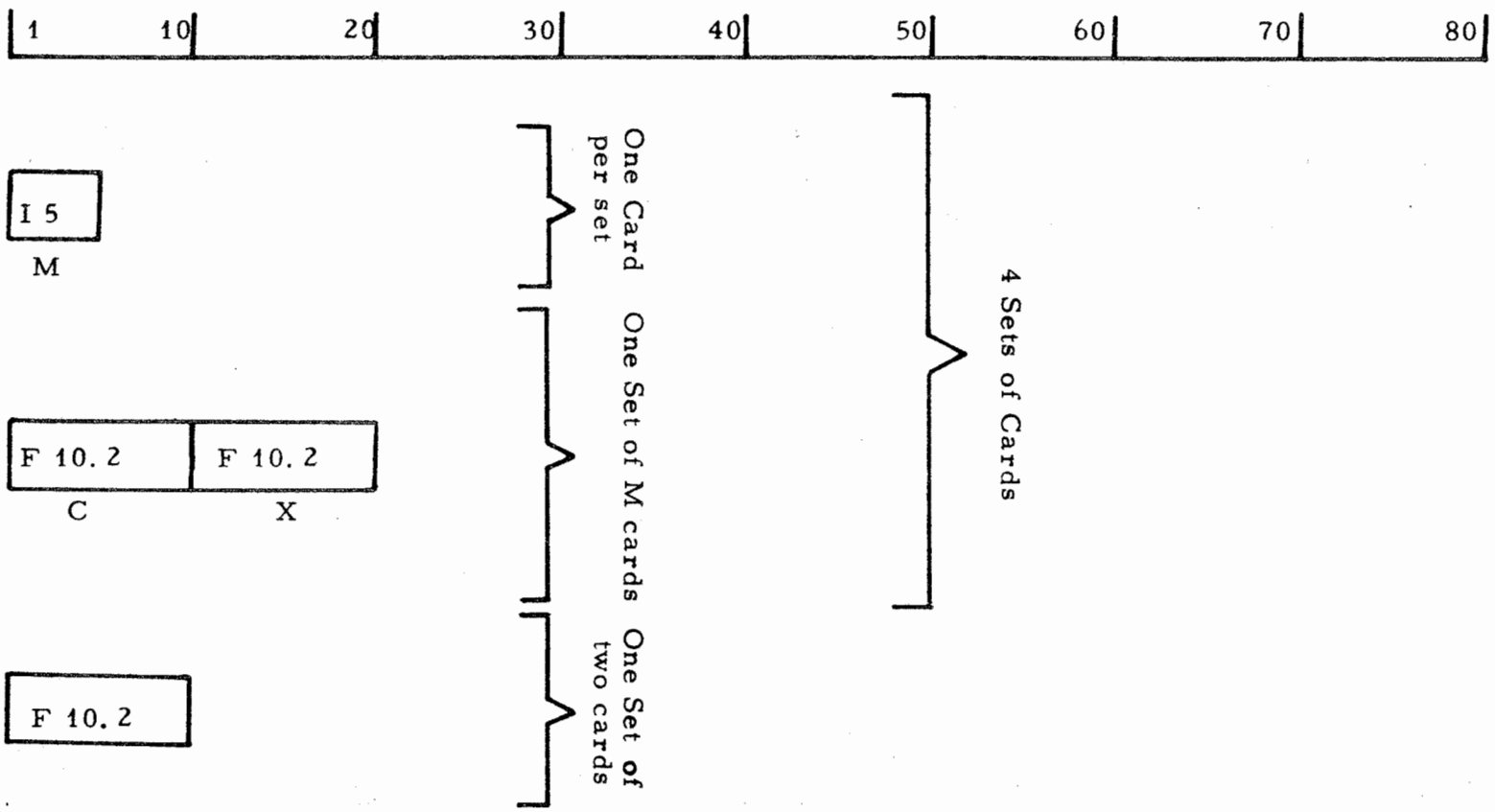

FIGURE C-1. FORMAT FOR DATA INPUT FOR PROGRAM TRACE

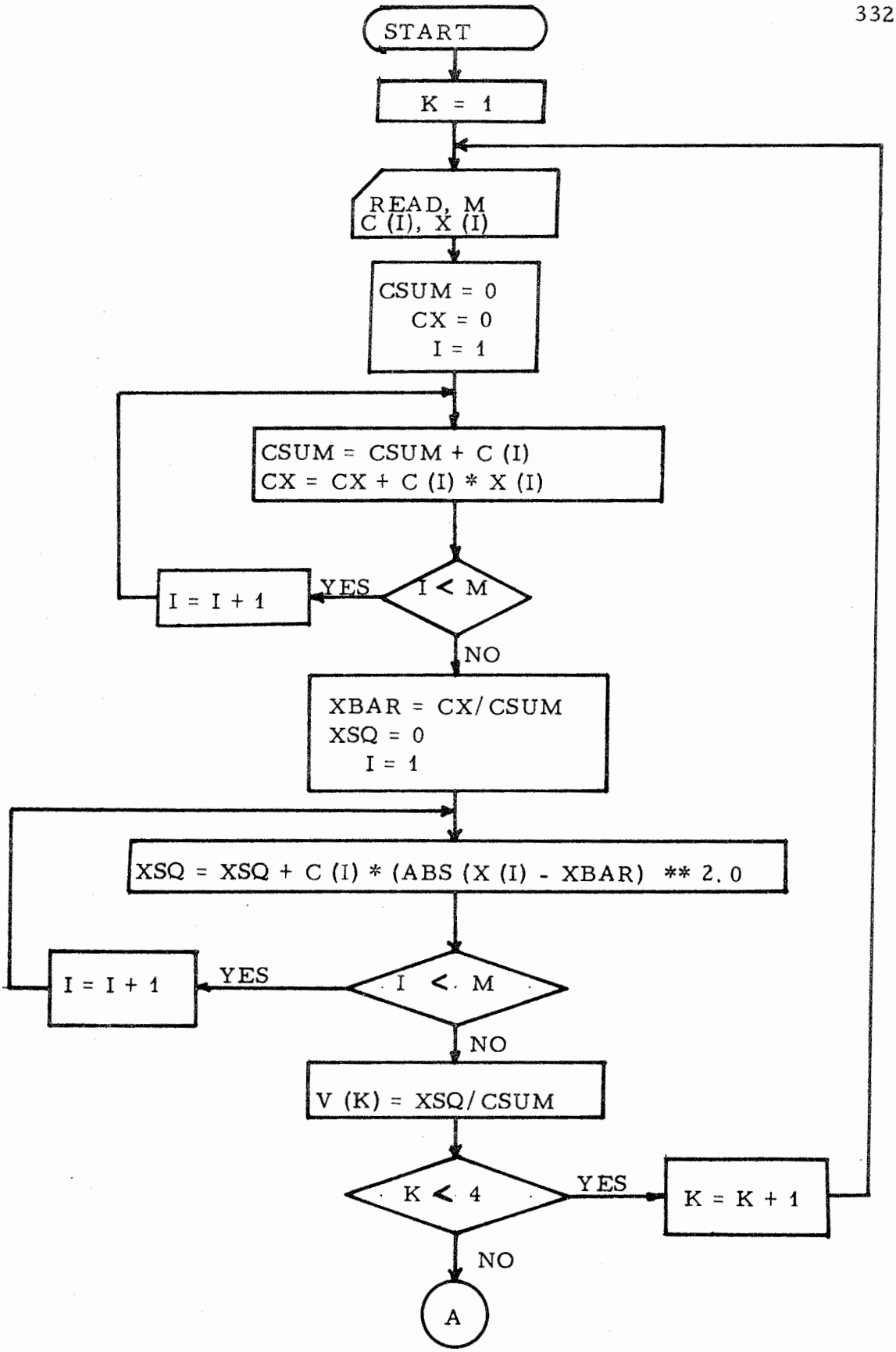

FIGURE C-2-1. FLOW DIAGRAM FOR PROGRAM TRACE

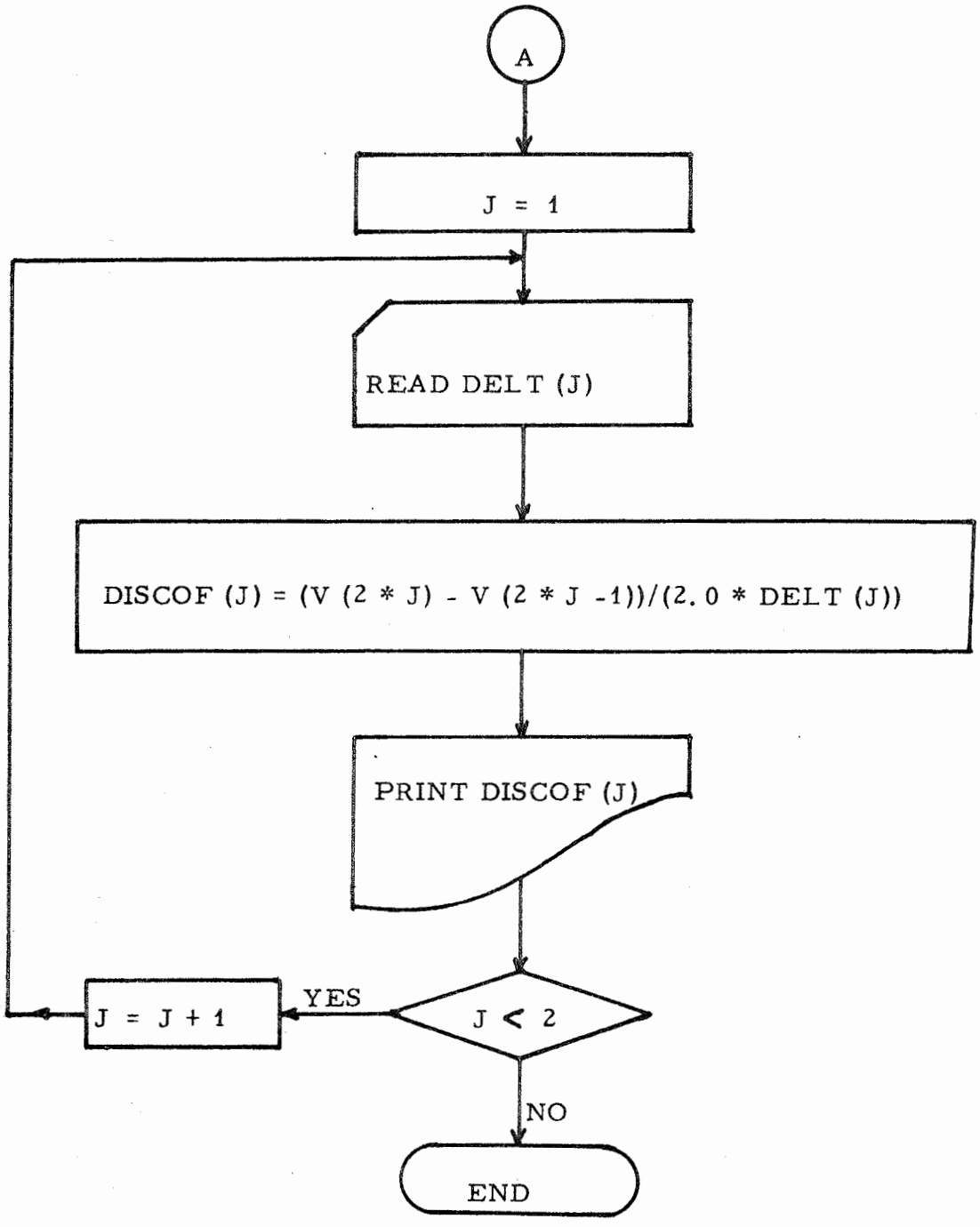

FIGURE C-2-2. FLOW DIAGRAM FOR PROGRAM TRACE (continued)

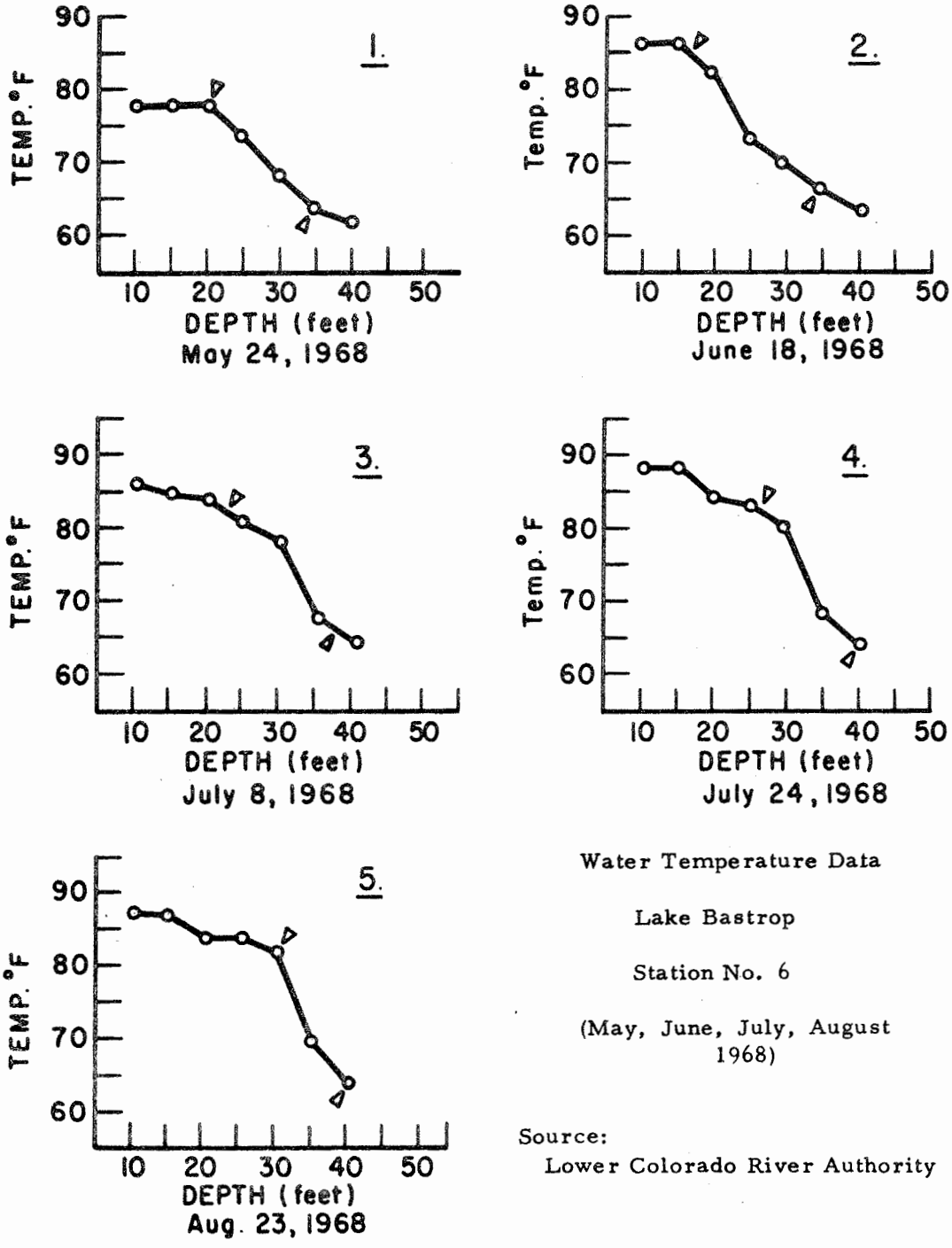

Water Temperature Data

Lake Bastrop

Station No. 6

(May, June, July, August 1968)

Source:
Lower Colorado River Authority

Figure D-1. Lake Bastrop Temperatures - Station 6, May - August Profiles, 1968 - 1969.

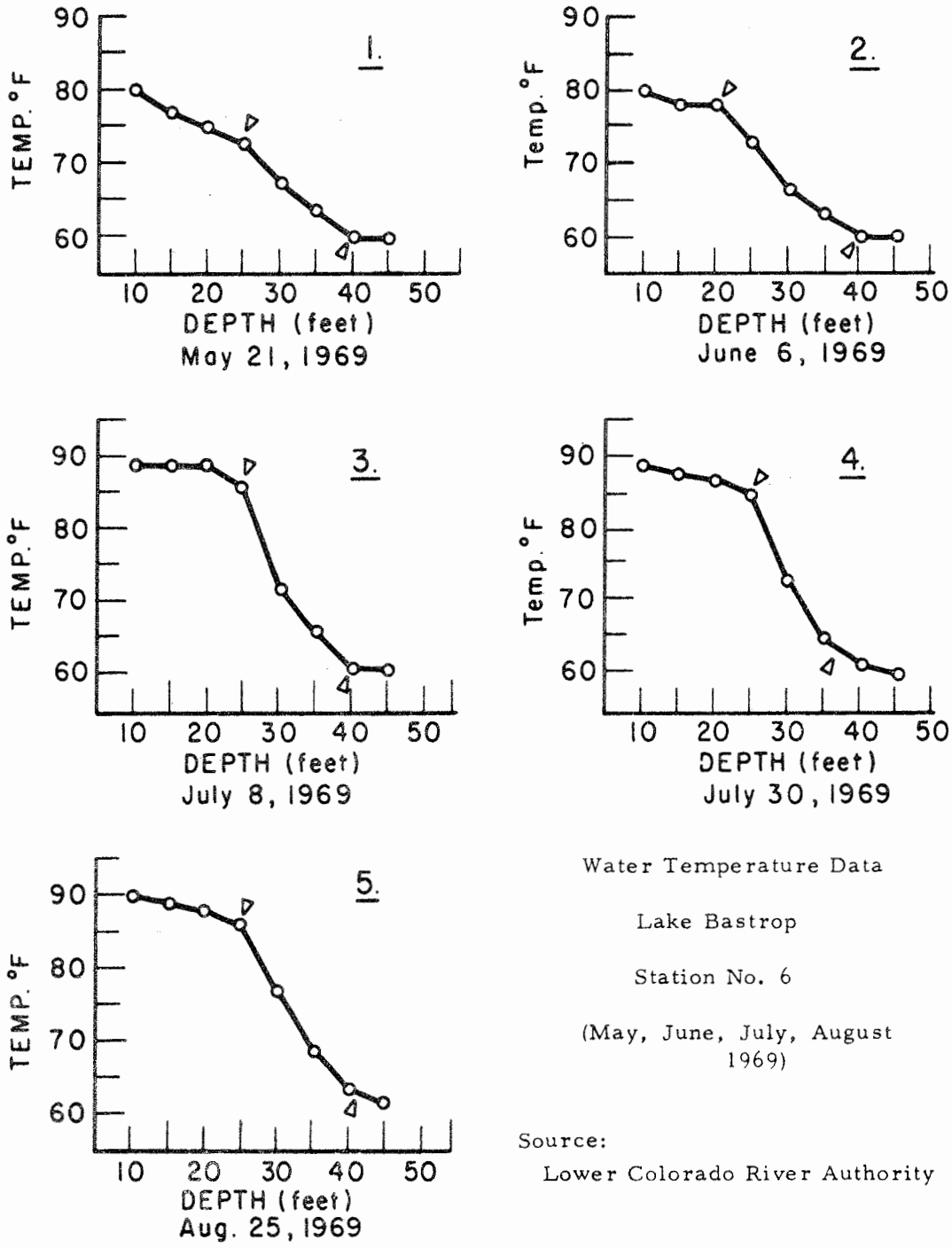

Water Temperature Data

Lake Bastrop

Station No. 6

(May, June, July, August 1969)

Source:
Lower Colorado River Authority

Figure D-2. Lake Bastrop Temperatures - Station 6, May - August Profiles, 1968 - 1969.

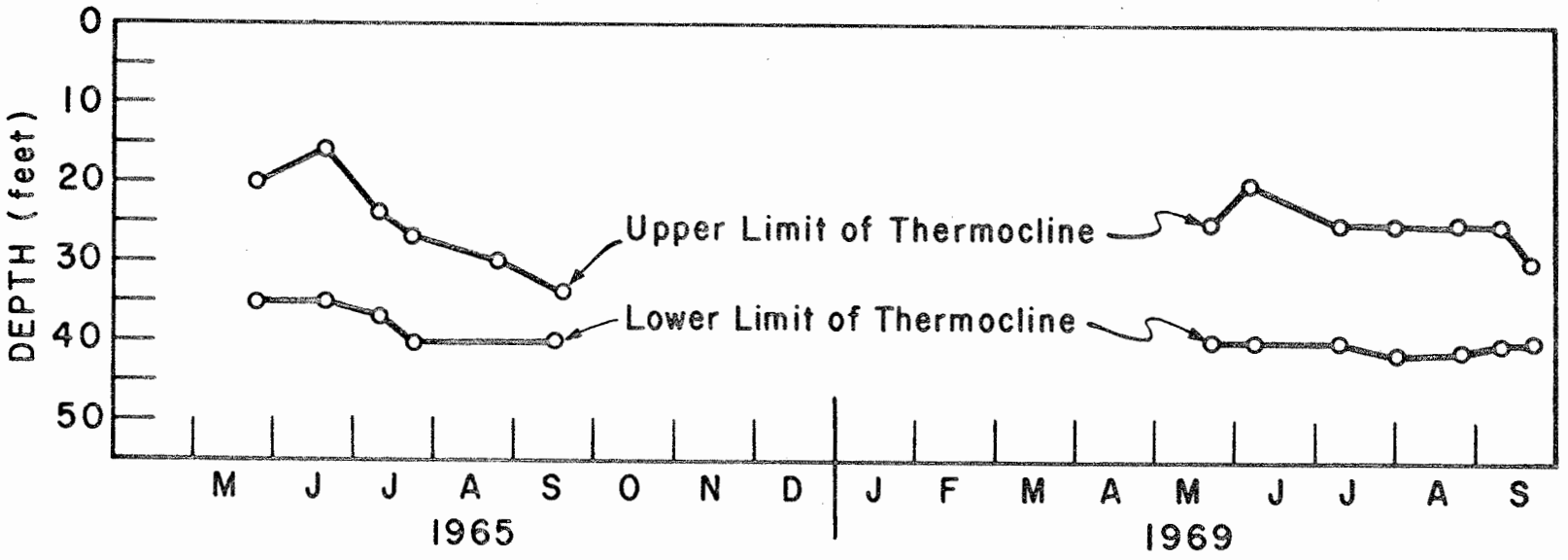

Water Temperature Data

Lake Bastrop

Thermocline Data at
Station No. 6

Source: Lower Colorado River Authority

Figure D-3. Lake Bastrop, Thermocline Data.

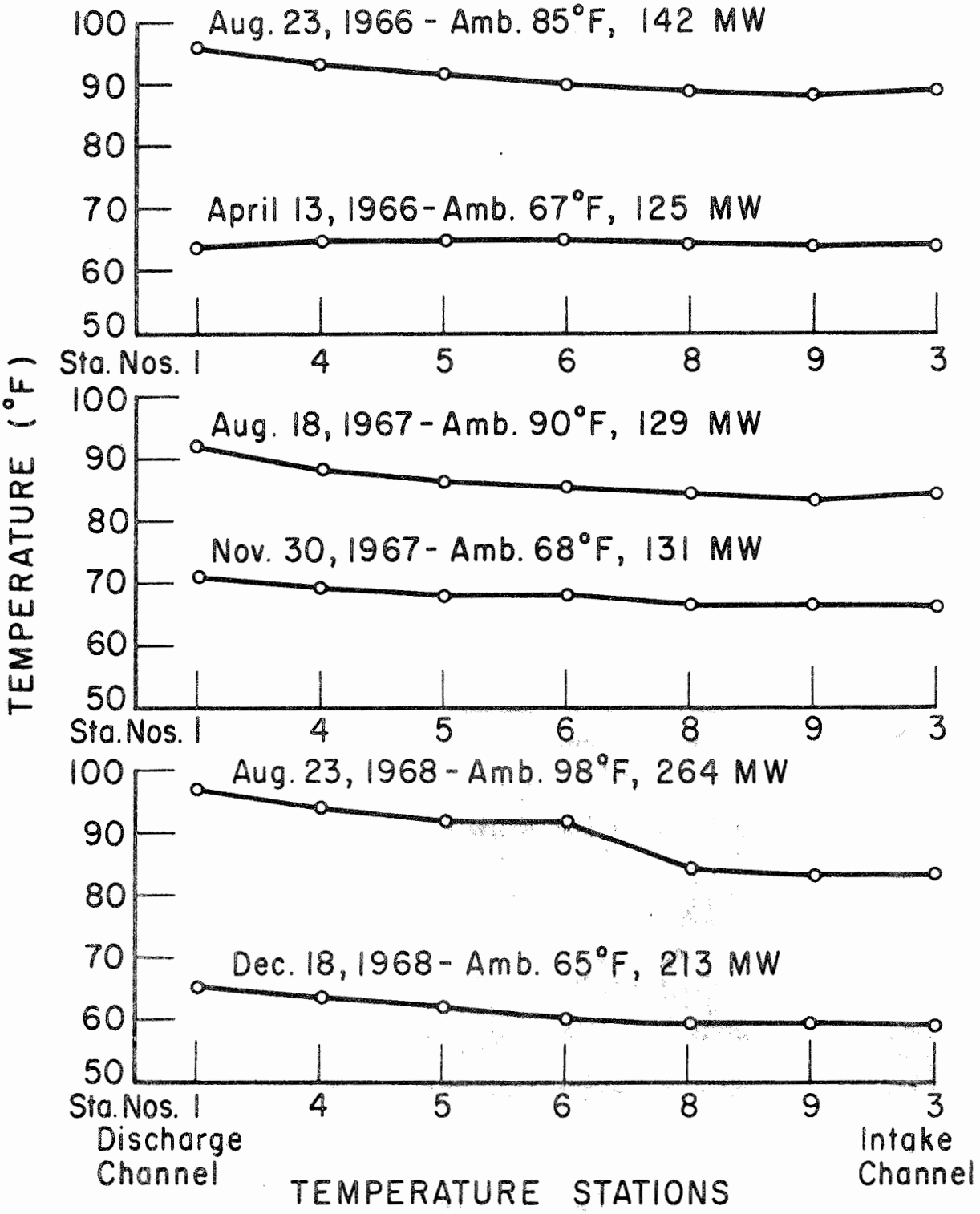

Figure D-4. Lake Bastrop Surface Temperatures, Annual Maximum and Minimum, 1966 - 1970.

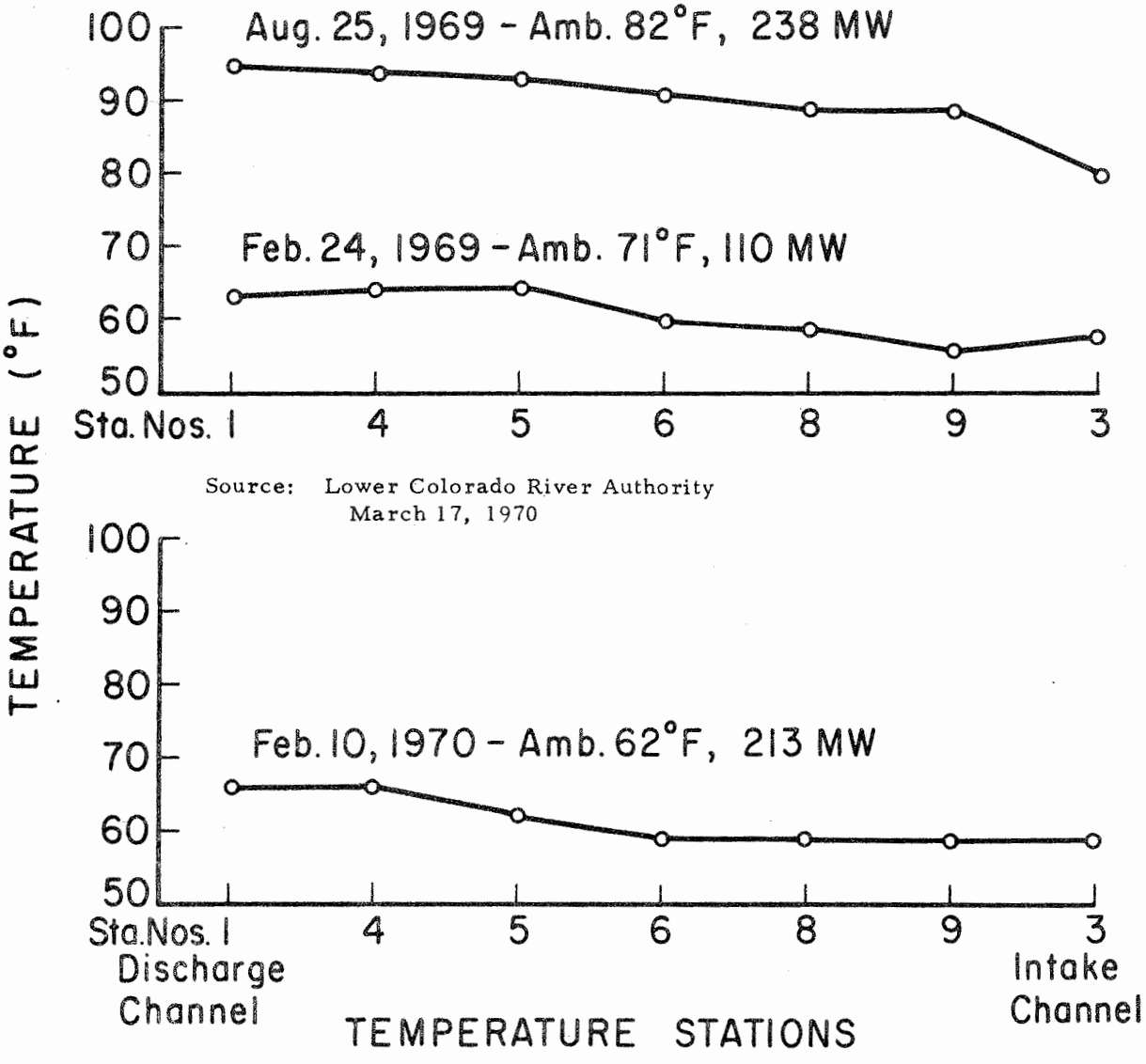

Source: Lower Colorado River Authority
March 17, 1970

Figure D-5. Lake Bastrop Surface Temperatures, Annual Maximum and Minimum, 1966 - 1970.

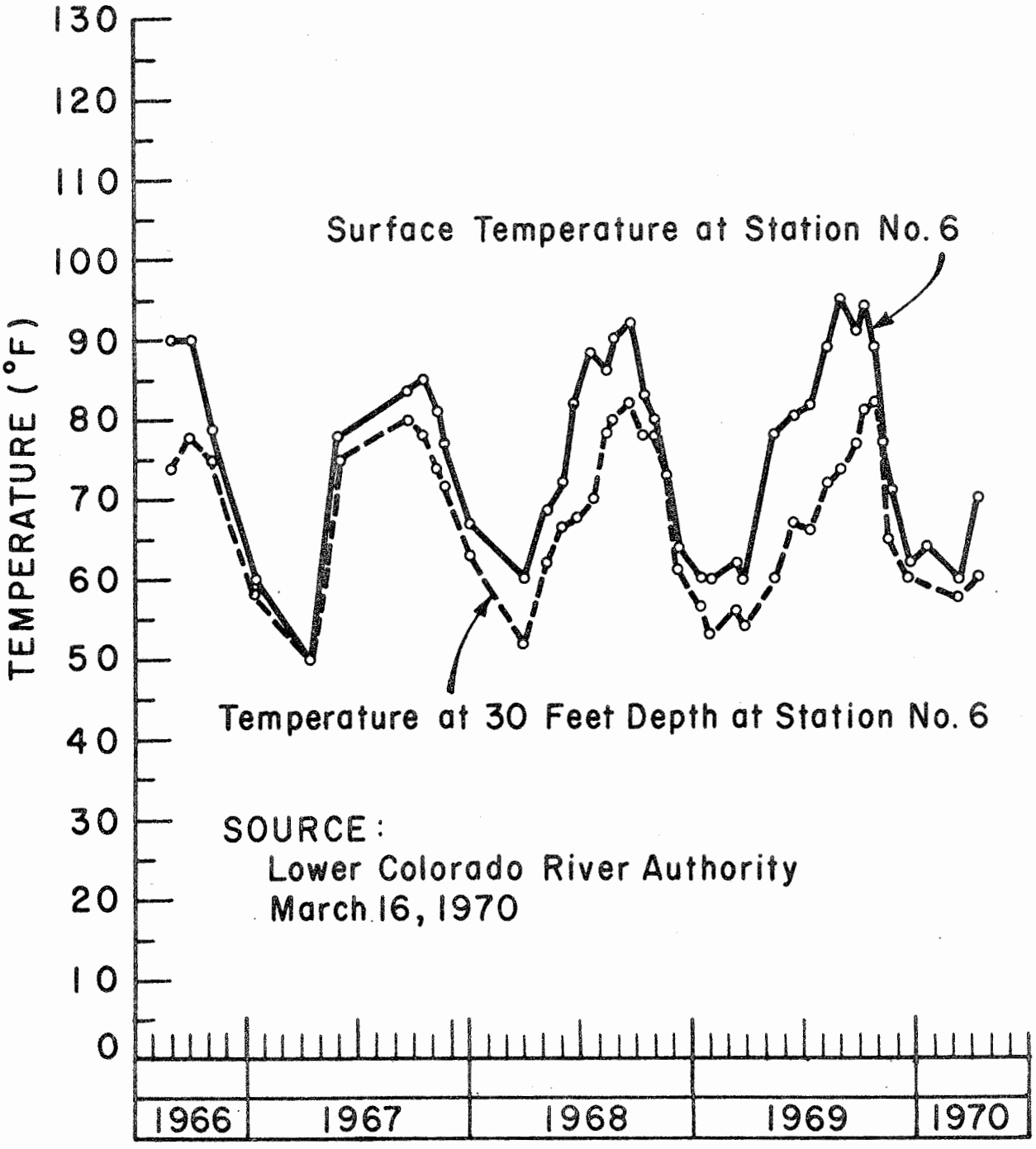

Figure D-6. Lake Bastrop Temperature Station No. 6 Temperatures at Surface and 30-Ft. Depth 1966 - 1970, Monthly Averages

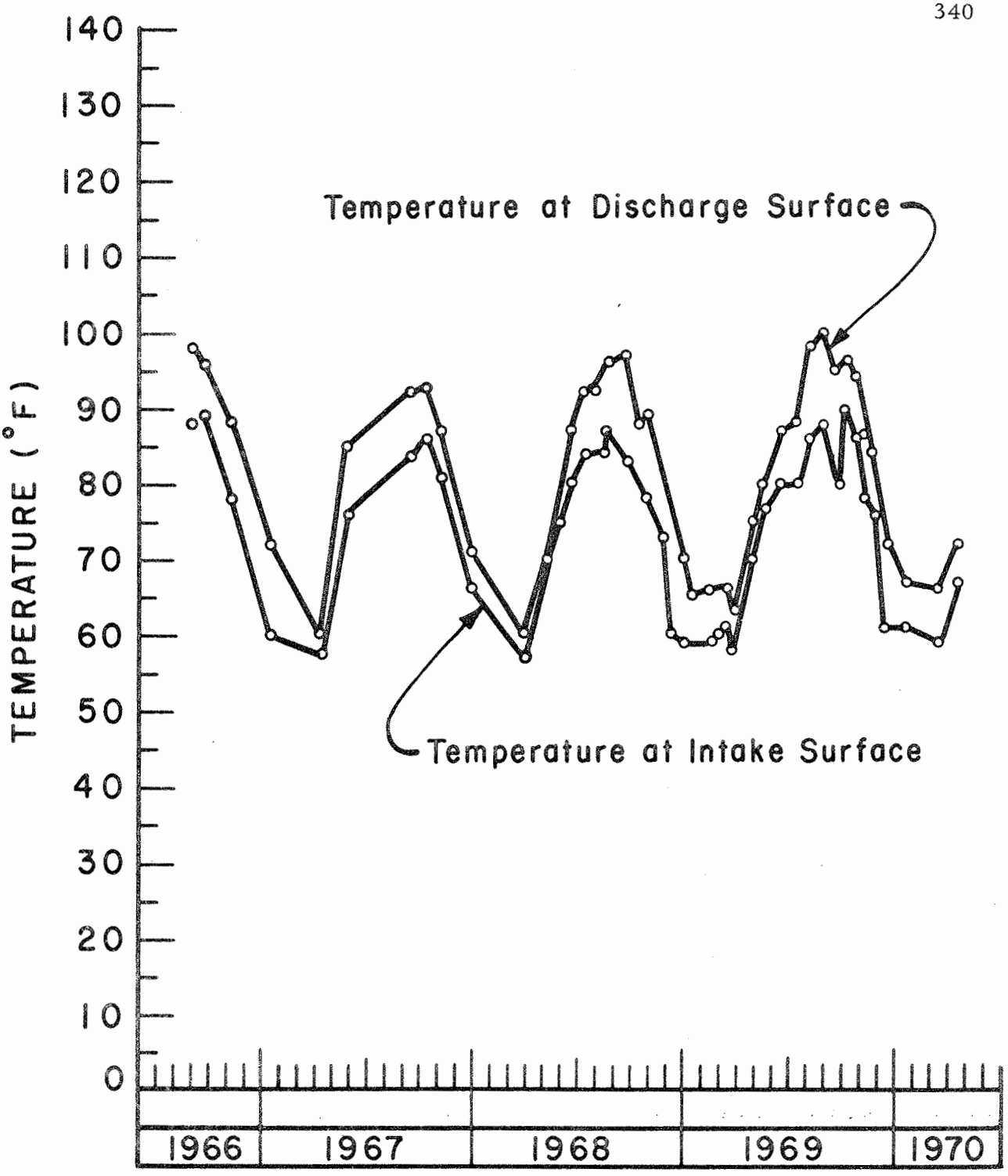

Figure D-7. Lake Bastrop, Surface Temperatures at Discharge and Intake, 1966 - 1970, Monthly Averages.

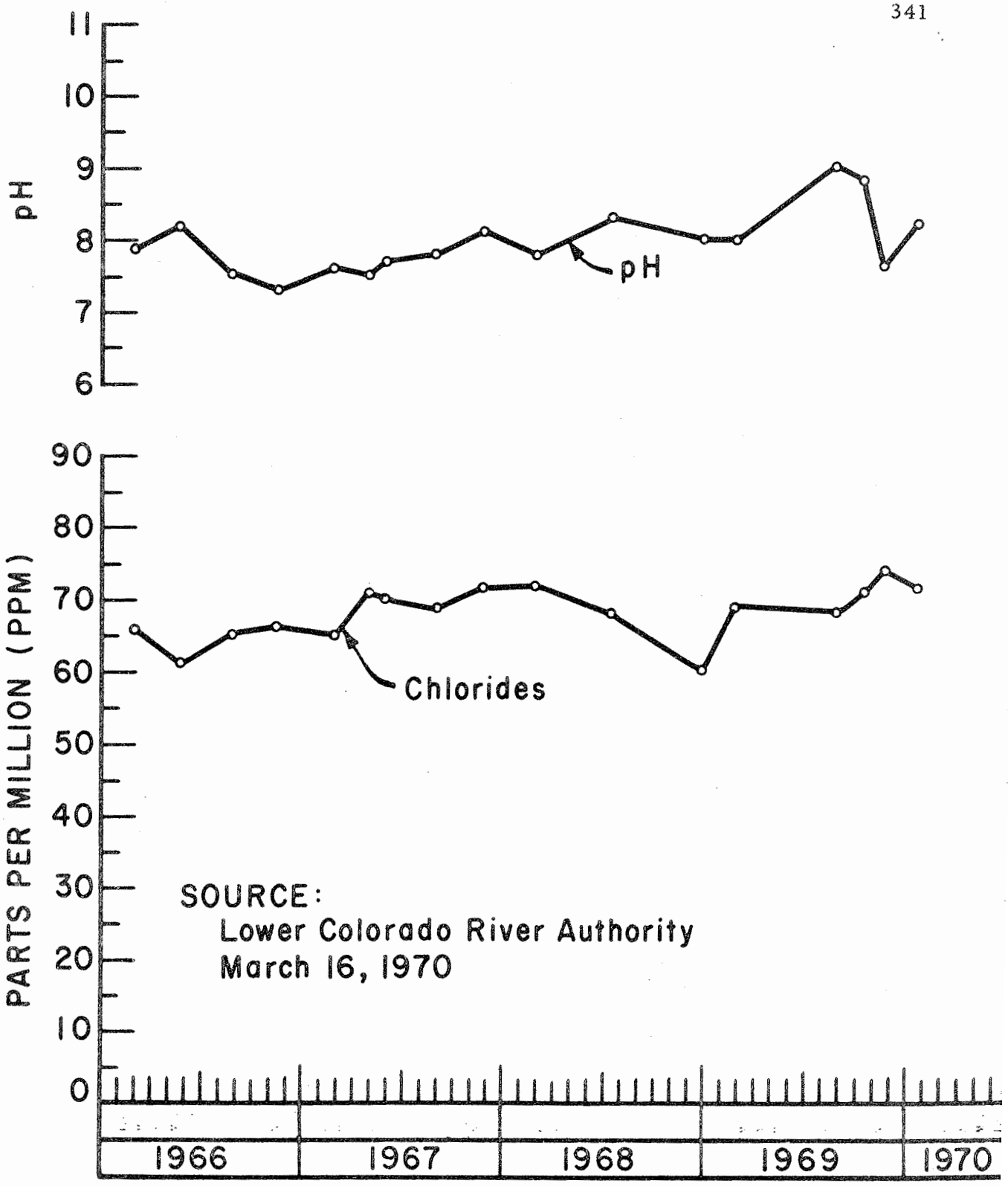

Figure D-8. Lake Bastrop Water Analysis Data
PH and Chlorides, 1966 - 1970.

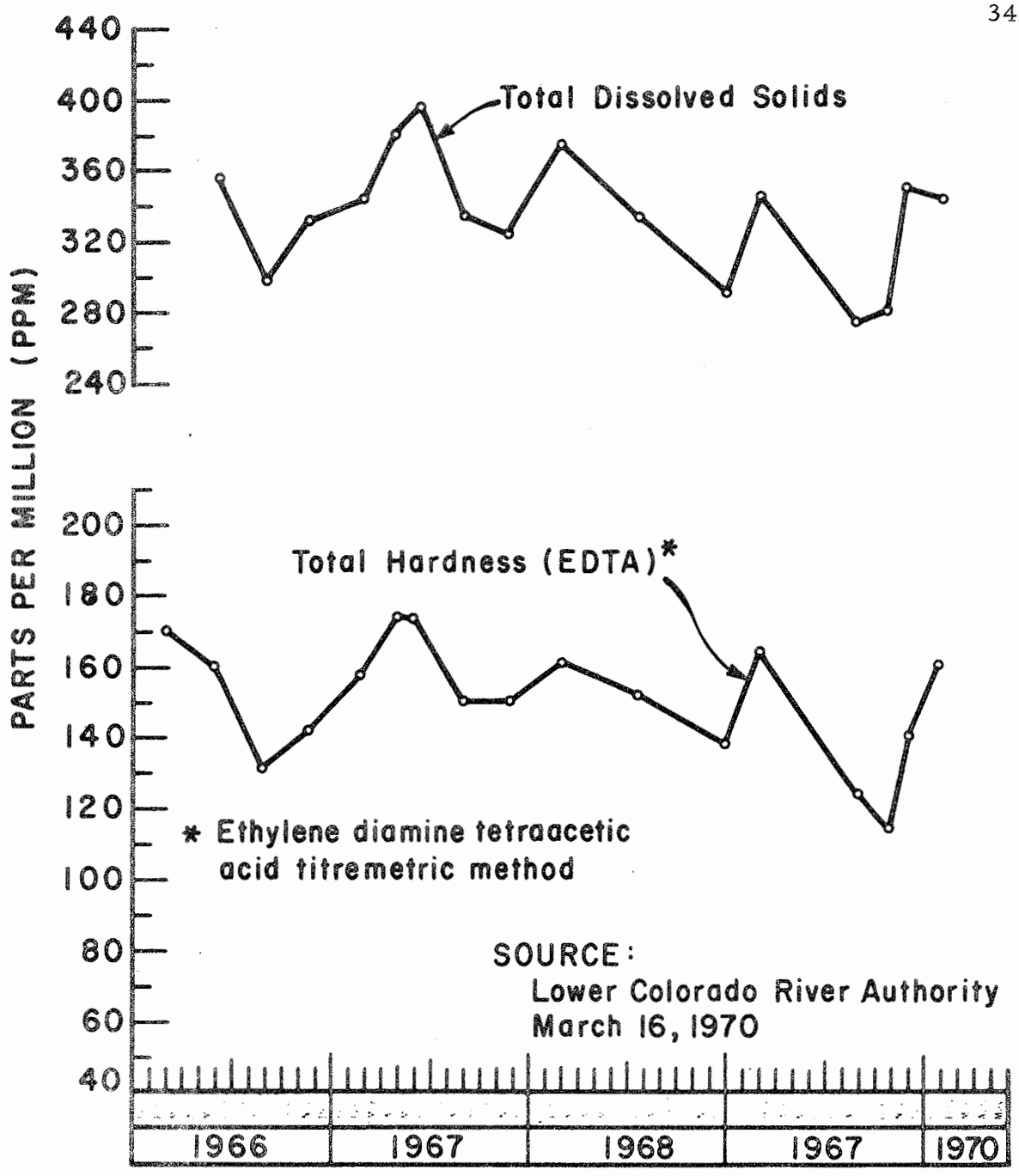

Figure D-9. Lake Bastrop Water Analysis Data, Dissolved Solids and Hardness, 1966 - 1970.

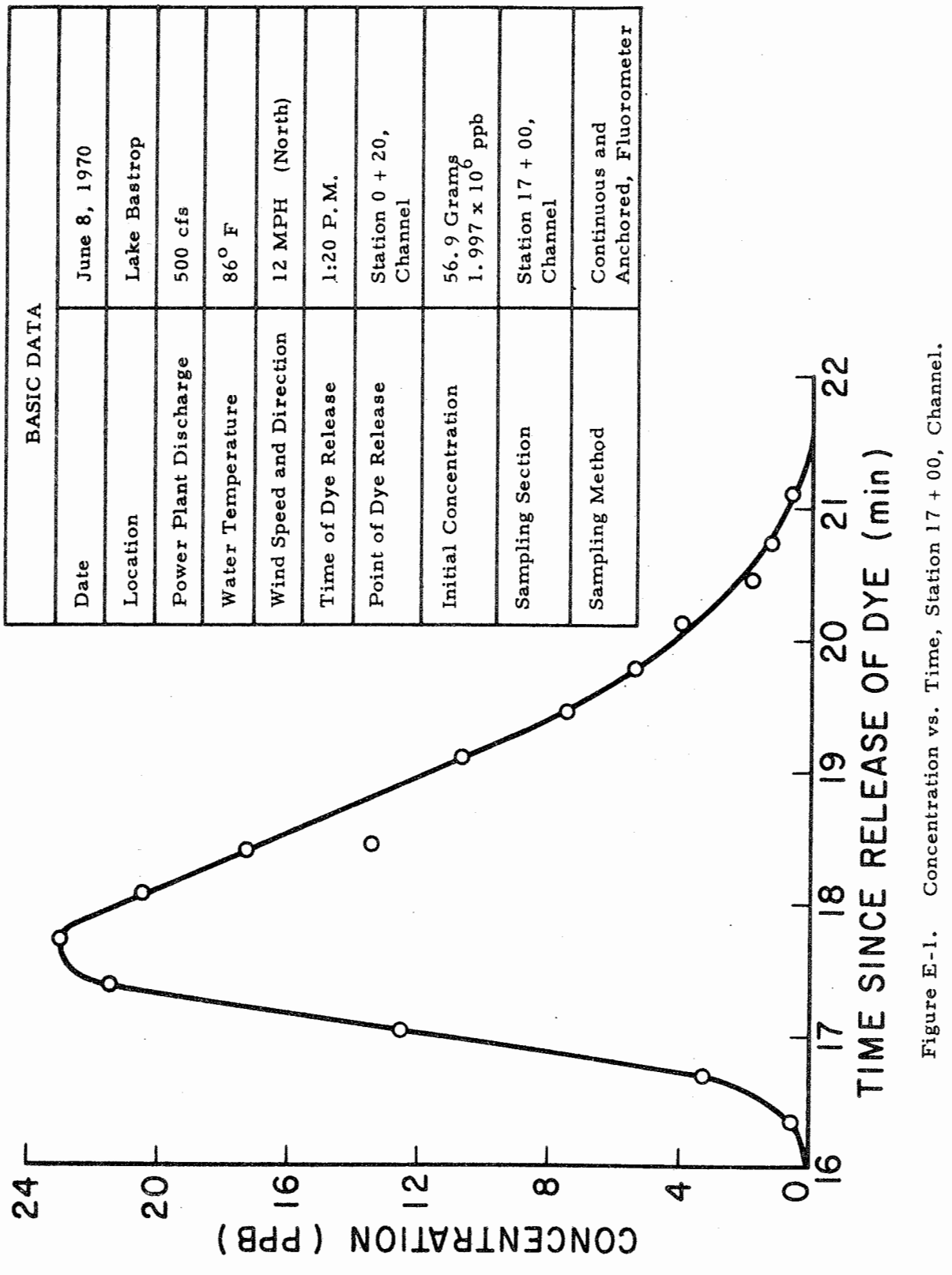

Figure E-1. Concentration vs. Time, Station 17 + 00, Channel.

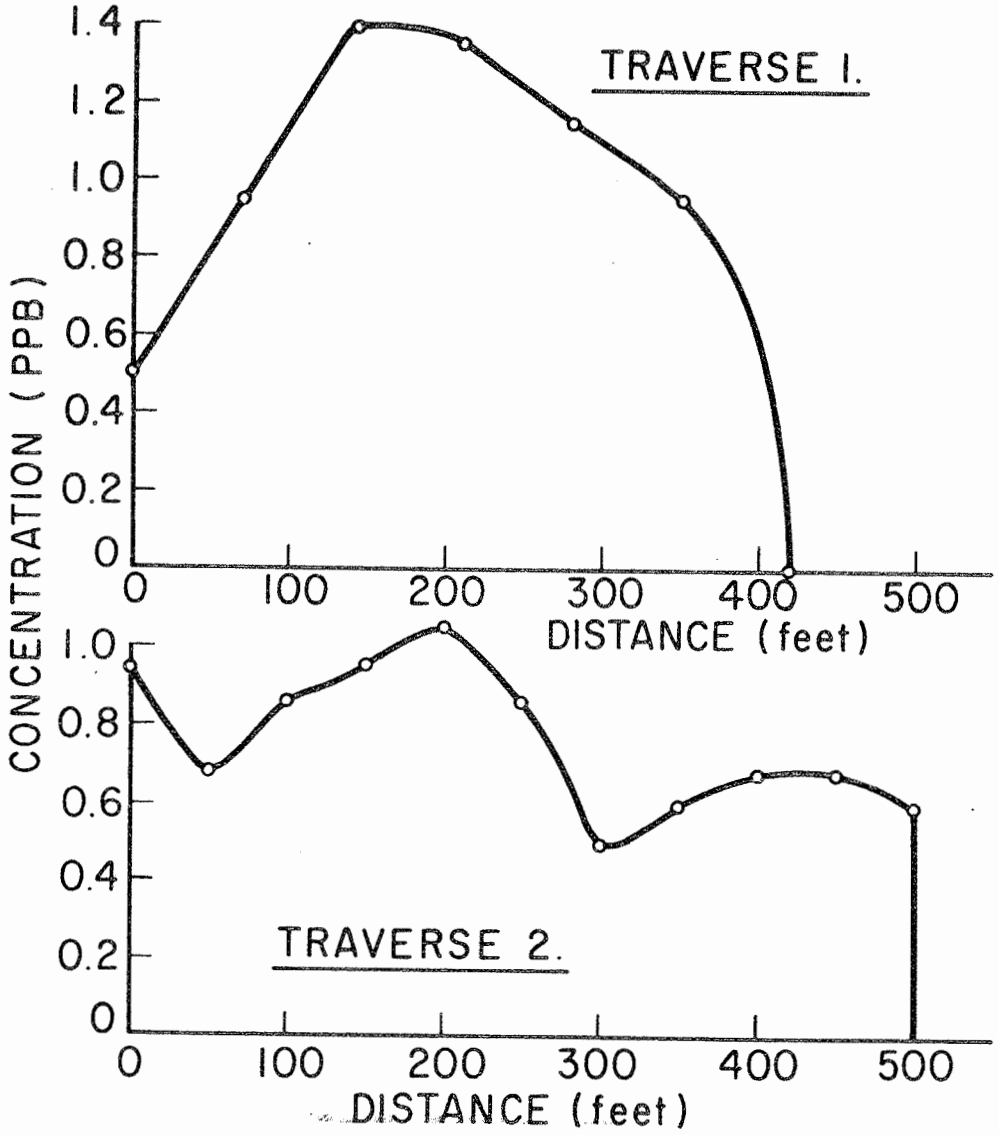

BASIC DATA	
Date	June 8, 1970
Location	Lake Bastrop
Power Plant Discharge	500 cfs
Water Temperature	86° F
Wind Speed and Direction	12 MPH (North)
Time of Dye Release	1:20 P.M.
Point of Dye Release	Station 0 + 20, Channel
Initial Concentration	56.9 Grams 1.997×10^6 ppb
Traverse 1	Start 2:55 P.M.
Traverse 2	Start 3:00 P.M.
Sampling Section	Cell (9, 15) to Cell (8, 15)
Sampling Method	Continuous and Moving Fluorometer

Figure E-2. Concentration vs. Distance, Between Cells (9, 15) and (8, 15).

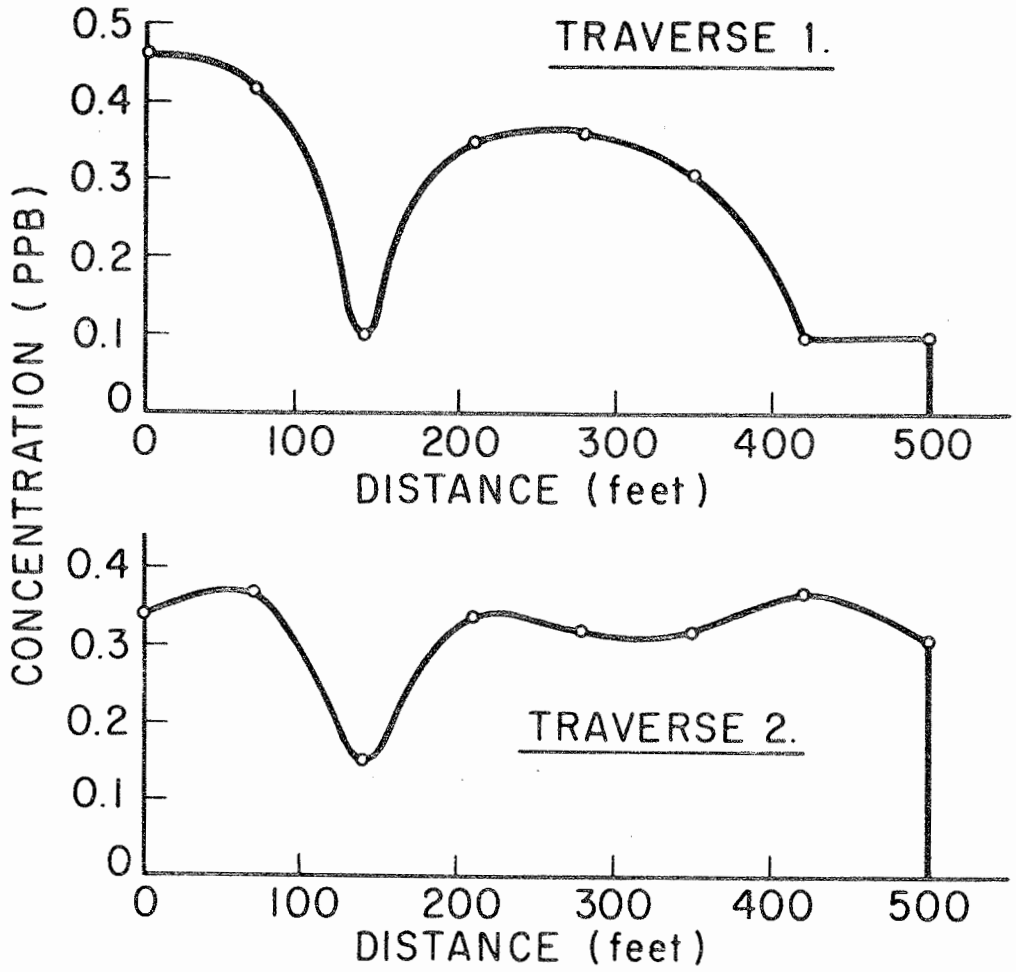

BASIC DATA	
Date	June 8, 1970
Location	Lake Bastrop
Power Plant Discharge	500 cfs
Water Temperature	86° F
Wind Speed and Direction	12 MPH (North)
Time of Dye Release	1:20 A.M.
Point of Dye Release	Station 20 Ft Discharge Channel
Initial Concentration	56.9 Grams 1.997×10^6 ppb
Traverse 1	Start 3:10 P.M.
Traverse 2	Start 3:17 P.M.
Sampling Section	Cell (8, 15) to Cell (8, 14)
Sampling Method	Continuous and Moving Fluorometer

Figure E-3. Concentration vs. Distance, Between Cells (8, 15) and (8, 14).

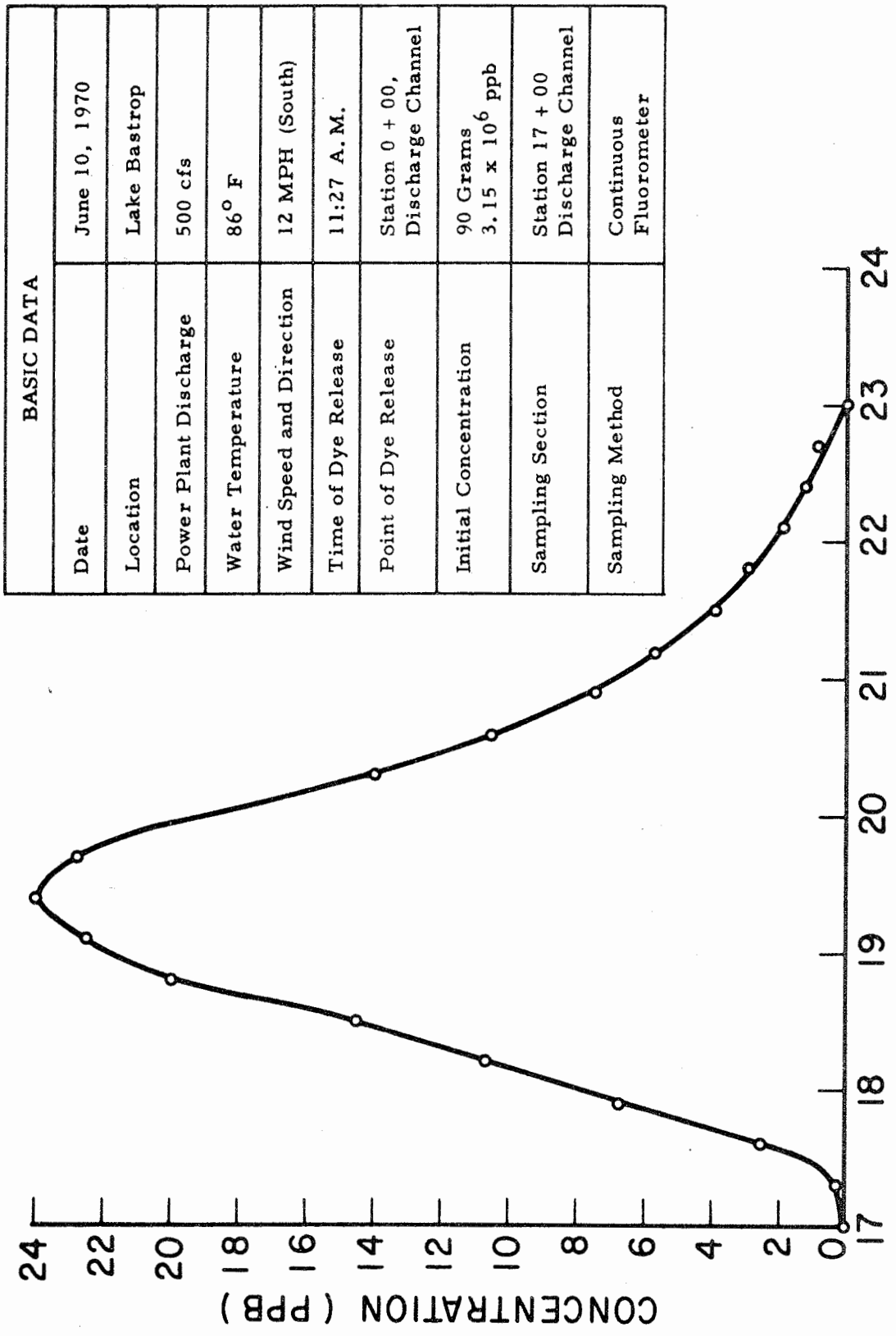

Figure F-1. Concentration vs. Time, Station 17 + 00, Channel.

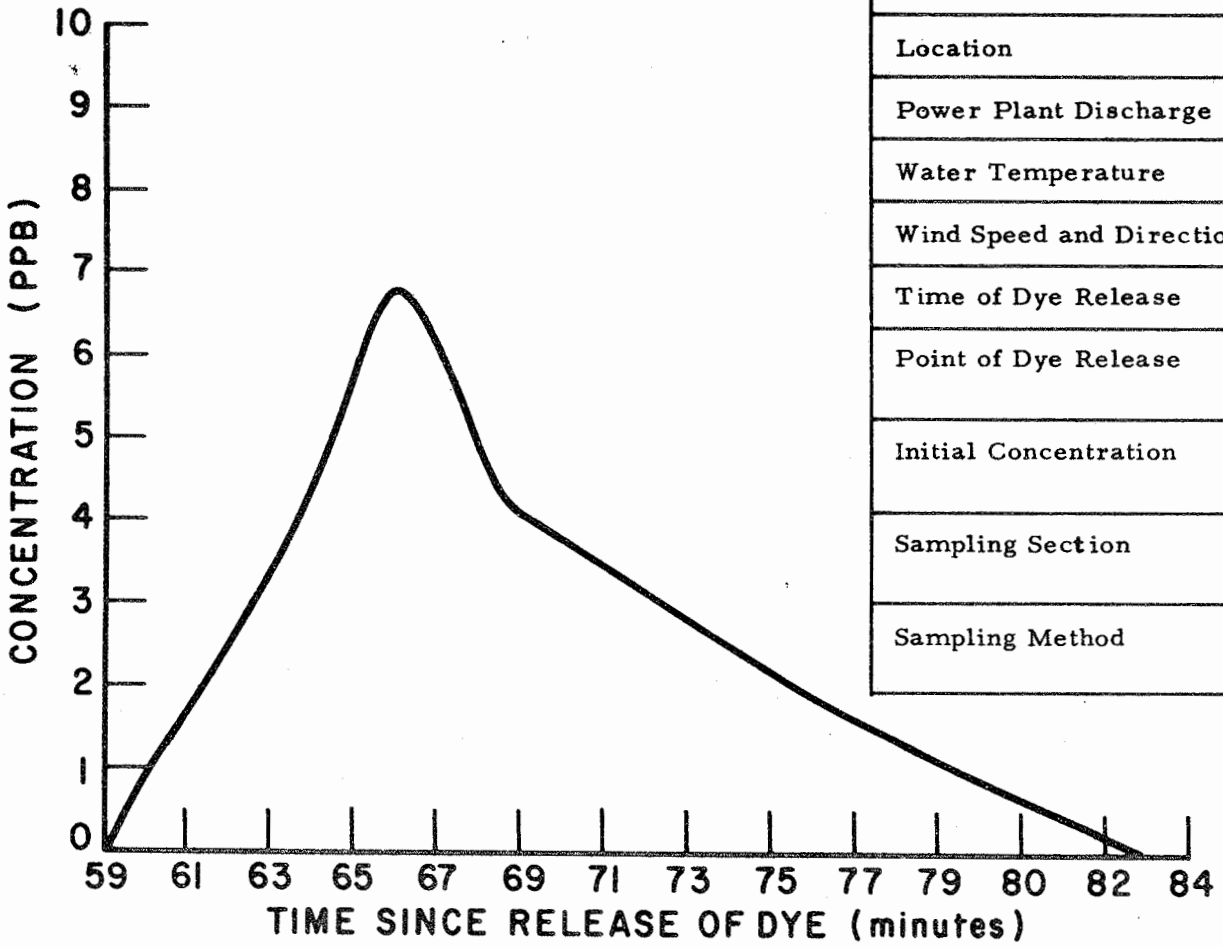

BASIC DATA	
Date	June 10, 1970
Location	Lake Bastrop
Power Plant Discharge	500 cfs
Water Temperature	86° F
Wind Speed and Direction	12 MPH (South)
Time of Dye Release	11:27 A.M.
Point of Dye Release	Station 0 + 00 Discharge Channel
Initial Concentration	90 Grams 3.15×10^6 ppb
Sampling Section	Cell (10, 15) Marker 0
Sampling Method	Continuous Fluorometer

Figure F-2. Concentration vs. Time, Cell (10, 15)

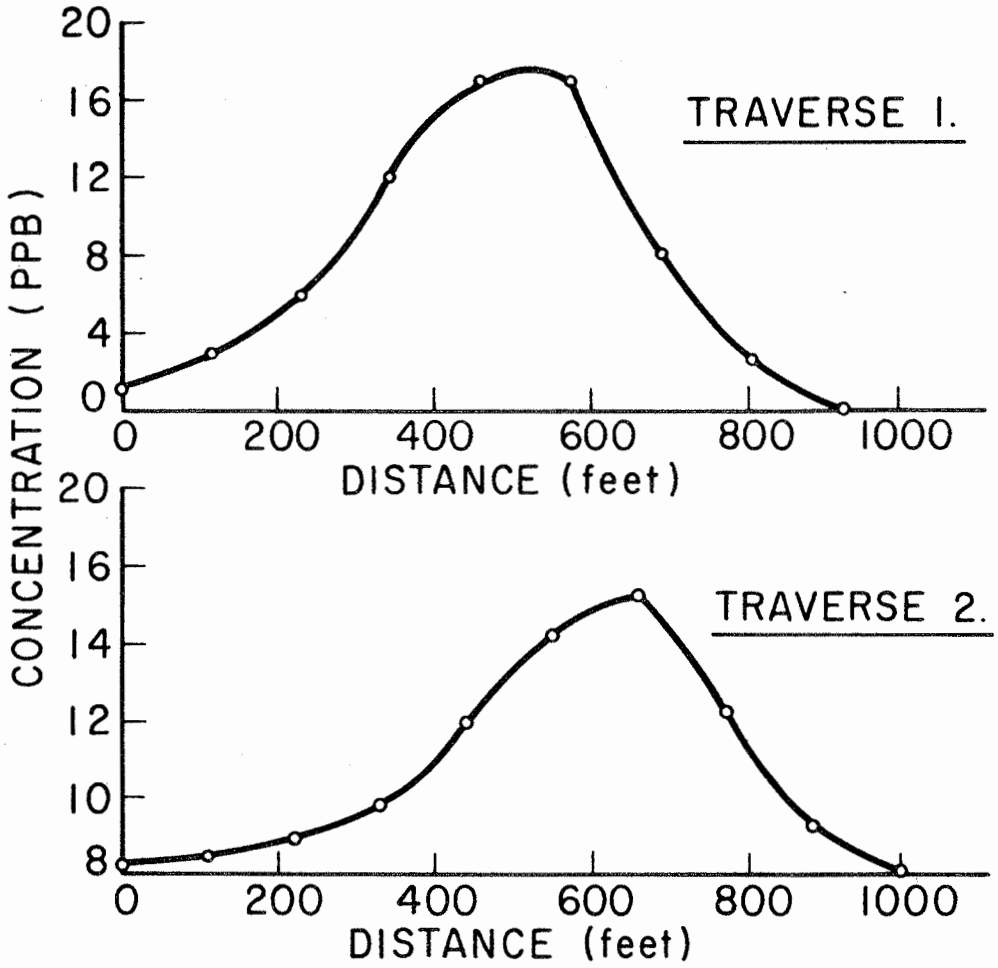

BASIC DATA	
Date	June 10, 1970
Location	Lake Bastrop
Power Plant Discharge	500 cfs
Water Temperature	86° F
Wind Speed and Direction	12 MPH (South)
Time of Dye Release	11:27 A.M.
Point of Dye Release	Station 0 + 00 Discharge Channel
Initial Concentration	90 Grams 3.15×10^6 ppb
Traverse 1	Start 11:53 A.M. End 11:55 A.M.
Traverse 2	Start 12:00 Noon End 12:02 P.M.
Sampling Section	17 + 00 - 27 + 00 Channel
Sampling Method	Continuous and Moving Fluorometer

Figure F-3. Concentration vs. Distance, Channel.

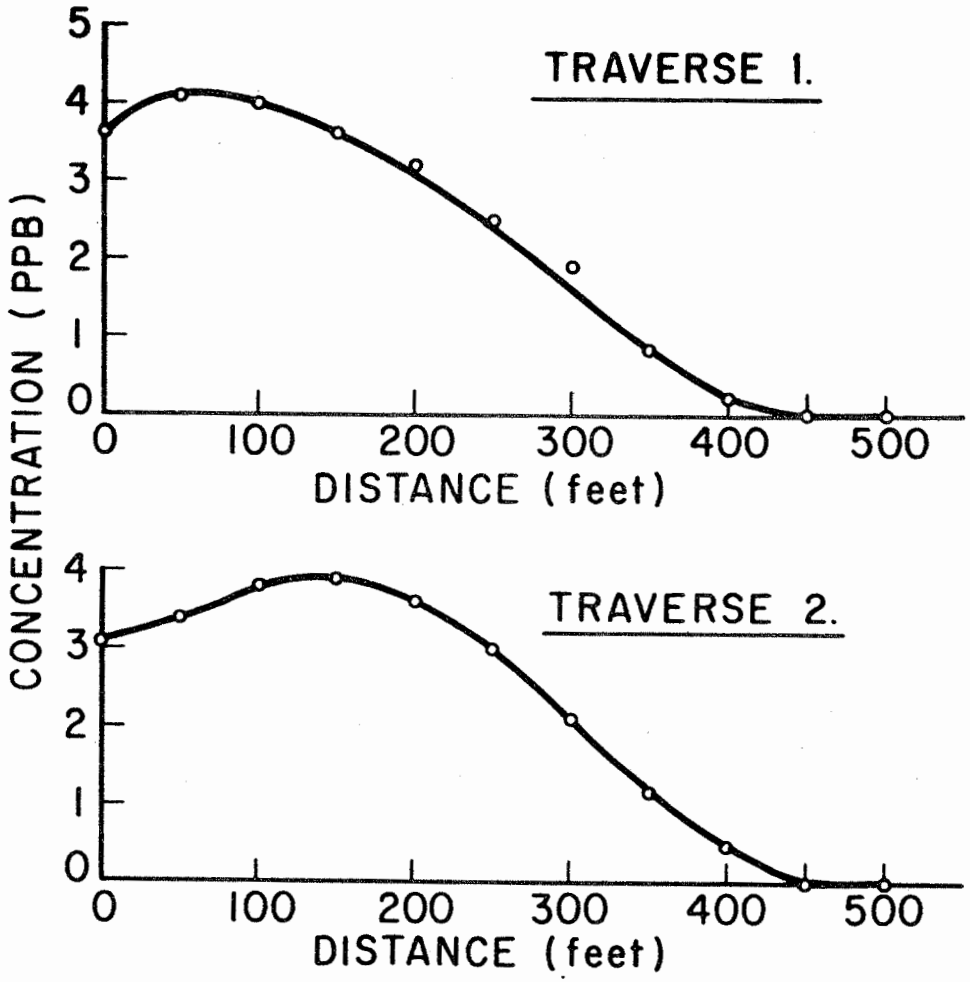

BASIC DATA	
Date	June 10, 1970
Location	Lake Bastrop
Power Plant Discharge	500 cfs
Water Temperature	86° F
Wind Speed and Direction	12 MPH (South)
Time of Dye Release	11:27 A.M.
Point of Dye Release	Station 0 + 00 Discharge Channel
Initial Concentration	90 Grams 3.15×10^6 ppb
Traverse 1	Start 12:53 P.M.
Traverse 2	Start 12:57 A.M.
Sampling Section	Cell (9, 15) to Cell (8, 15)
Sampling Method	Continuous and Moving Fluorometer

Figure F-4. Concentration vs. Distance between Cells (9, 15) and (8, 15).

APPENDIX G - SUPPORTING DATA FOR VERIFICATION

TESTS ON JUNE 30, 1970

BASIC DATA	
Date	June 30, 1970
Location	Lake Bastrop
Power Plant Discharge	500 cfs
Water Temperature	98° F
Wind Speed and Direction	10 MPH (South)
Time of Dye Release	12:58 P.M.
Point of Dye Release	Station 0 + 00, Discharge Channel
Initial Concentration	1.225 Lbs 19.5 x 10^6 ppb
Sampling Section	Cell (10, 15) Marker 0
Sampling Method	Periodic, Fluorometer

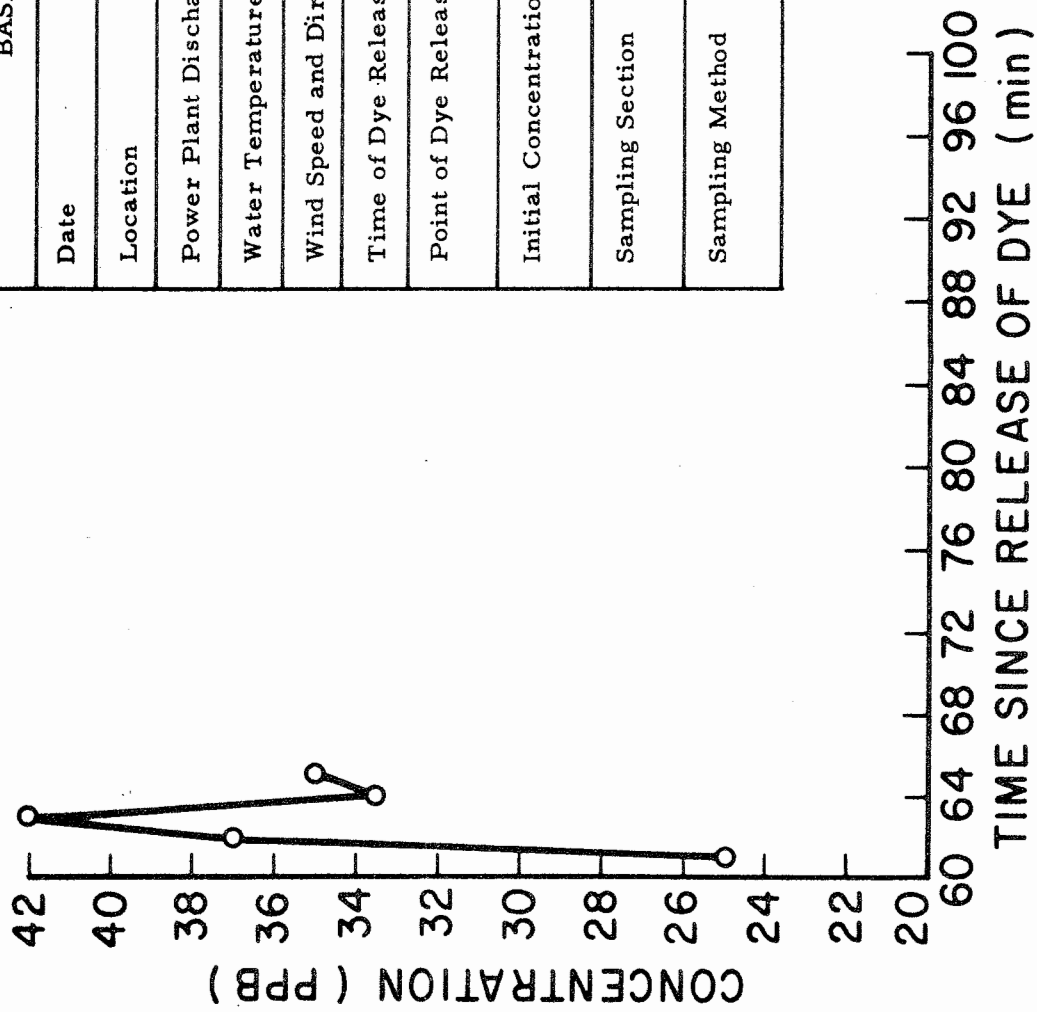

Figure G-1. Concentration vs. Time, Cell (10, 15).

BASIC DATA	
Date	June 30, 1970
Location	Lake Bastrop
Power Plant Discharge	500 cfs
Water Temperature	98° F
Wind Speed and Direction	10 MPH (South)
Time of Dye Release	12:58 P.M.
Point of Dye Release	Station 0 + 00, Discharge Channel
Initial Concentration	1.225 Lbs 19.5×10^6 ppb
Sampling Section	Cell (9, 15) Marker 1
Sampling Method	Periodic, Fluorometer

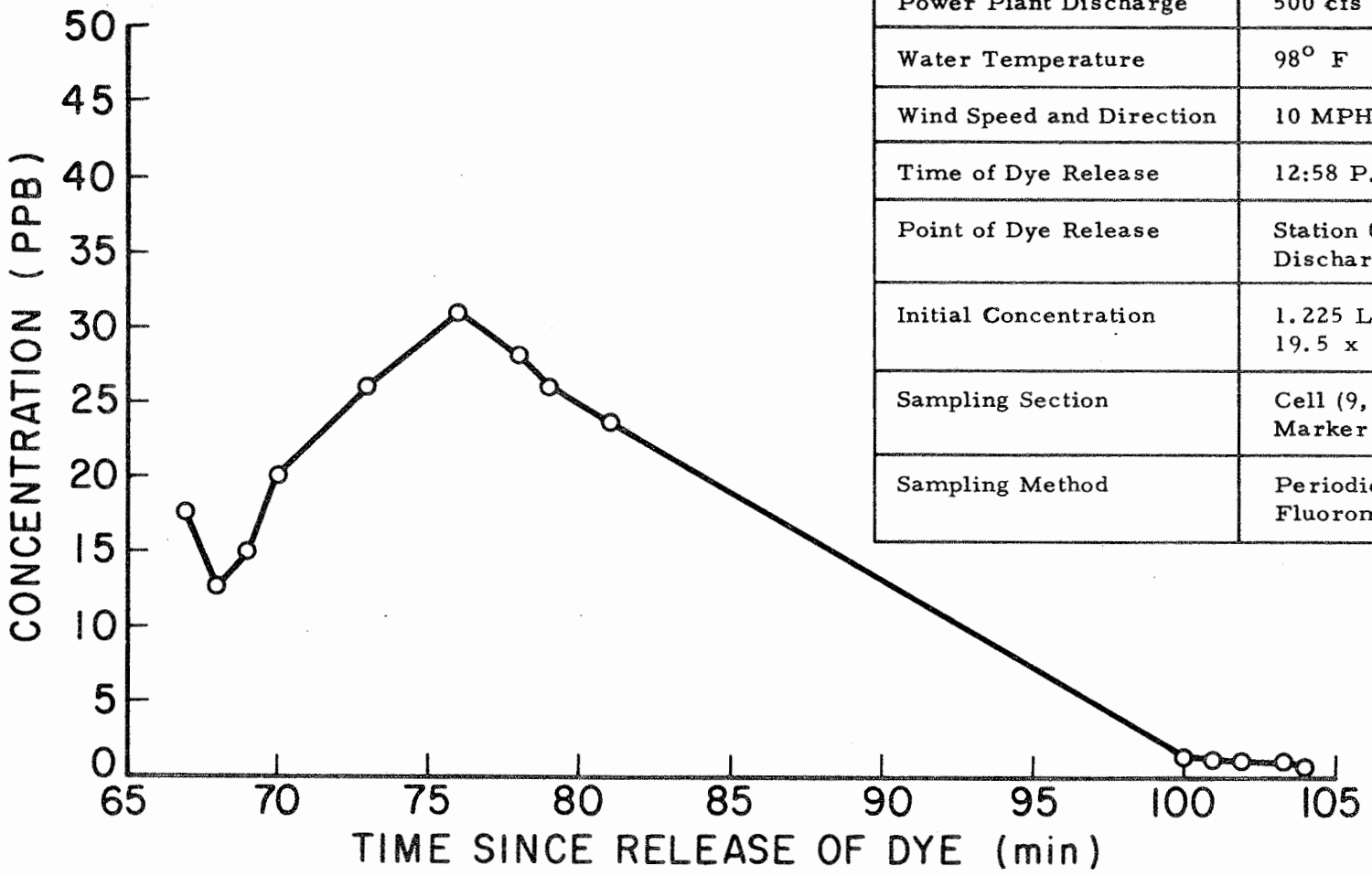

Figure G-2. Concentration vs. Time, Cell (9, 15).

BASIC DATA	
Date	June 30, 1970
Location	Lake Bastrop
Power Plant Discharge	500 cfs
Water Temperature	98° F
Wind Speed and Direction	10 MPH (South)
Time of Dye Release	12:58 P.M.
Point of Dye Release	Station 0 + 00, Discharge Channel
Initial Concentration	1.225 Lbs 19.5×10^6 ppb
Sampling Section	Cell (8, 15) Marker 2
Sampling Method	Periodic, Fluorometer

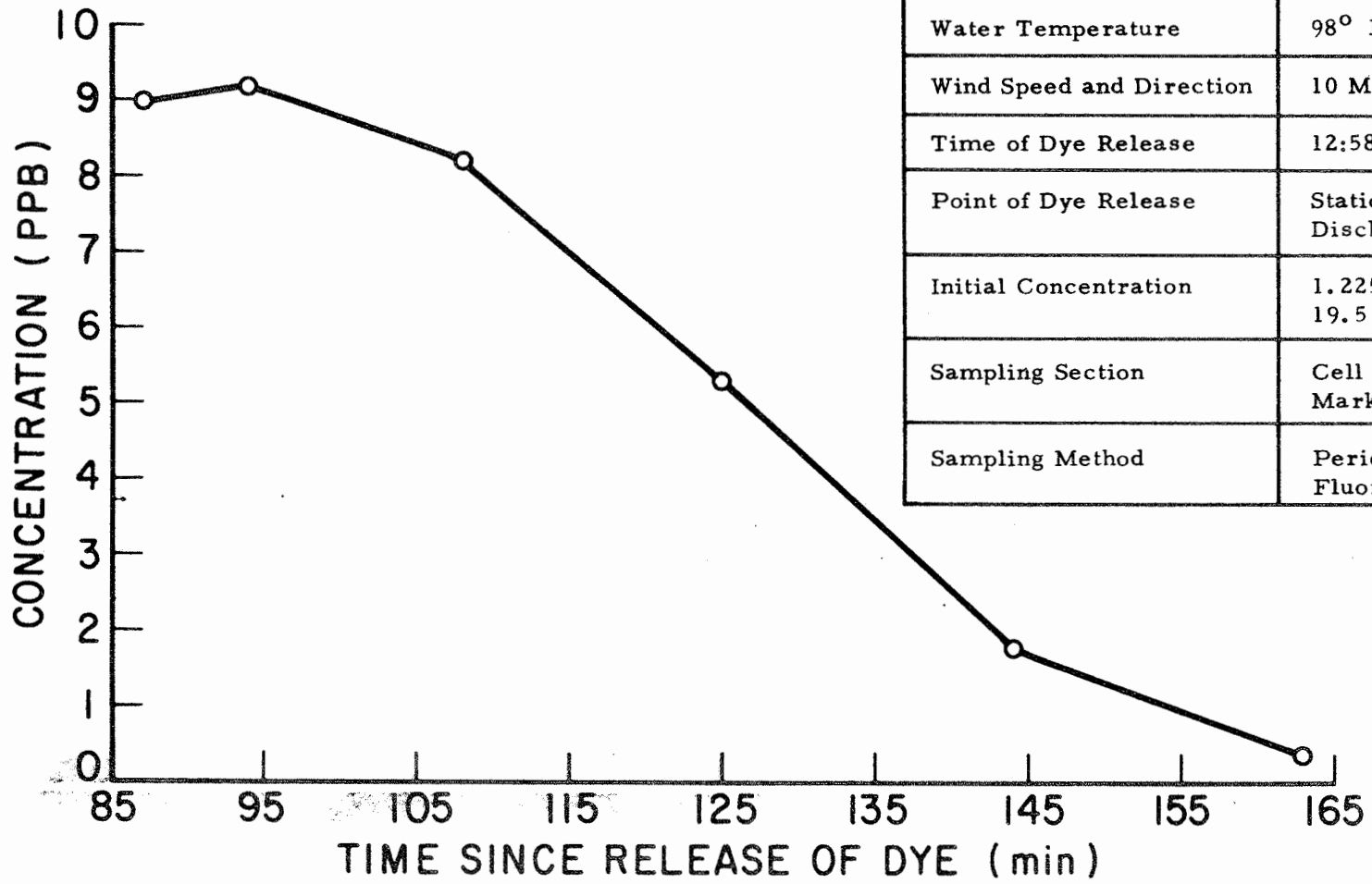

Figure G-3. Concentration vs. Time, Cell (8, 15).

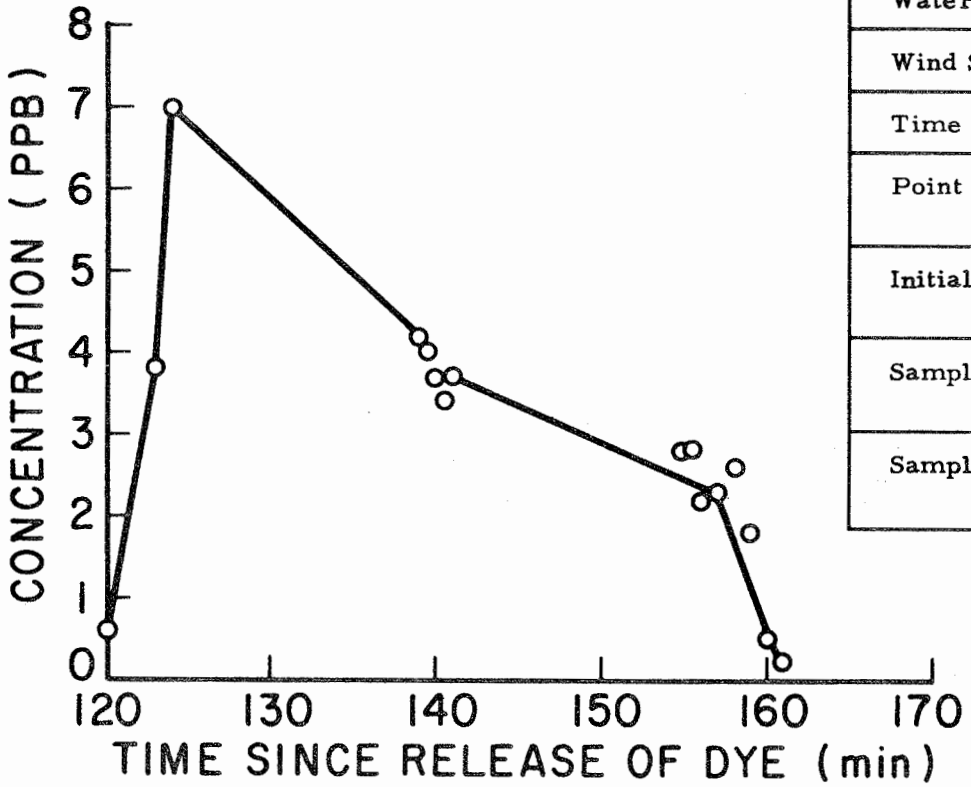

BASIC DATA	
Date	June 30, 1970
Location	Lake Bastrop
Power Plant Discharge	500 cfs
Water Temperature	98° F
Wind Speed and Direction	10 MPH (South)
Time of Dye Release	12:58 P.M.
Point of Dye Release	Station 0 + 00, Discharge Channel
Initial Concentration	1.225 Lbs 19.5×10^6 ppb
Sampling Section	Cell (8, 14) Marker 3
Sampling Method	Periodic Fluorometer

Figure G-4. Concentration vs. Time, Cell (8, 14)

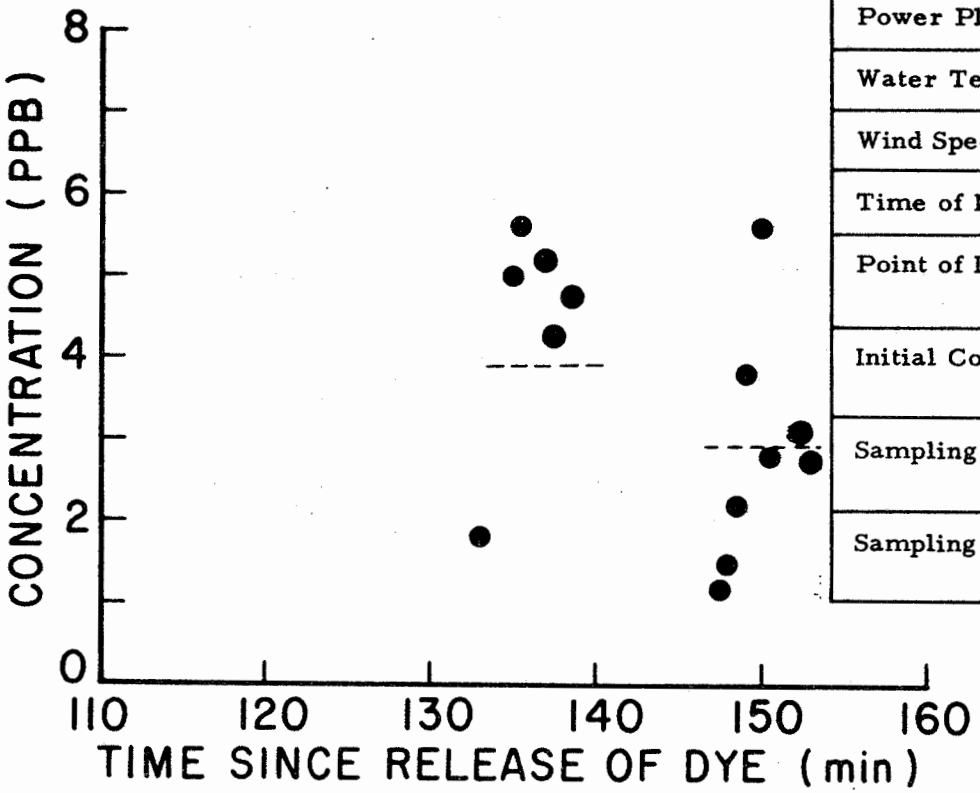

BASIC DATA	
Date	June 30, 1970
Location	Lake Bastrop
Power Plant Discharge	500 cfs
Water Temperature	98° F
Wind Speed and Direction	10 MPH (South)
Time of Dye Release	12:58 P.M.
Point of Dye Release	Station 0 + 00 Discharge Channel
Initial Concentration	1.225 Lbs 19.5×10^6 ppb
Sampling Section	Cell (7, 15) Marker 5
Sampling Method	Periodic Fluorometer

Figure G-5. Concentration vs. Time, Cell (7, 15).

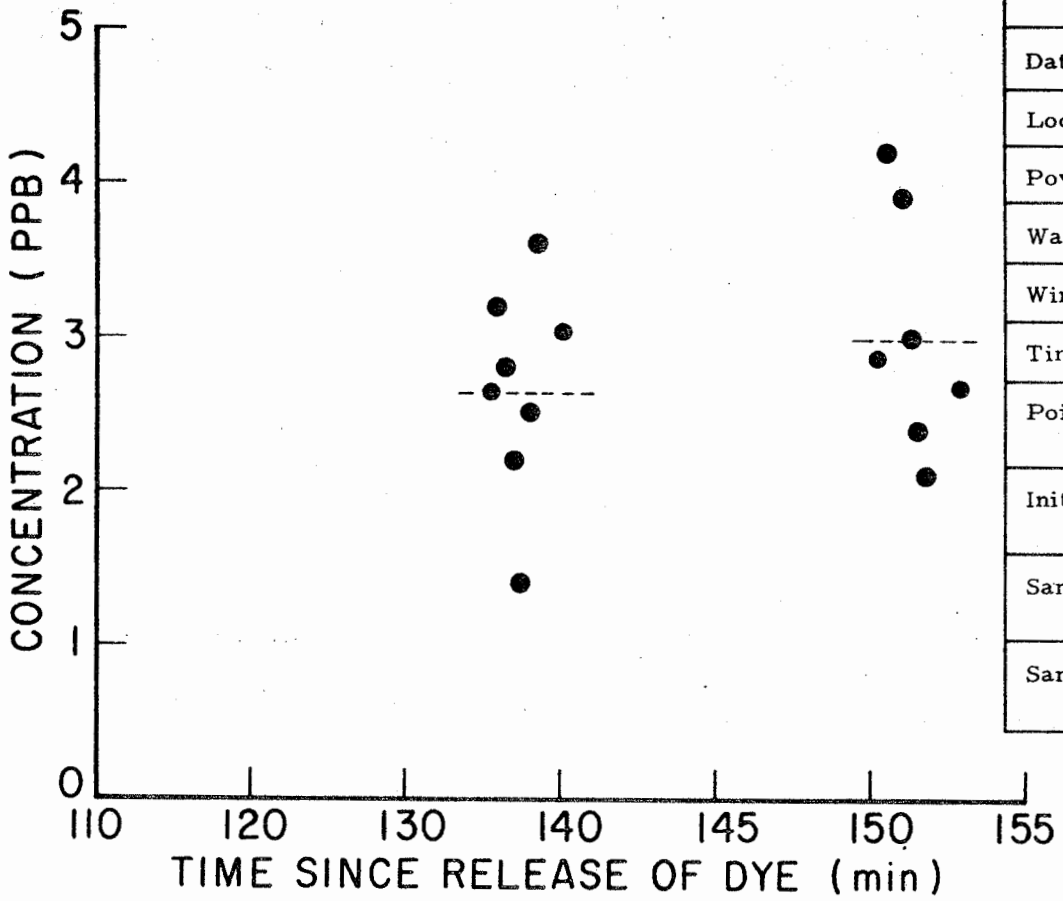

BASIC DATA	
Date	June 30, 1970
Location	Lake Bastrop
Power Plant Discharge	500 cfs
Water Temperature	98° F
Wind Speed and Direction	10 MPH (South)
Time of Dye Release	12:58 P.M.
Point of Dye Release	Station 0 + 00 Discharge Channel
Initial Concentration	1.225 Lbs 19.5×10^6 ppb
Sampling Section	Cell (7, 14) Marker 6
Sampling Method	Periodic Fluorometer

Figure G-6. Concentration vs. Time, Cell (7, 14)

BIBLIOGRAPHY

[1] American Petroleum Institute. (1969). "Diffusion on Effluents into Receiving Waters," (Chap. 18), Manual on Disposal of Refinery Wastes, Volume on Liquid Wastes, Amer. Pet. Inst., New York.

[2] Ames, William F. (1968). Nonlinear Ordinary Differential Equations in Transport Processes, Academic Press, New York.

[3] Ayers, John C. (1962). "Great Lakes Waters, Their Circulation and Physical and Chemical Characteristics," Great Lakes Basin. Publ. 71, Amer. Assoc. of Adv. of Science, (Edited by H. J. Pincus), The Horn-Shafer Company, Baltimore, Md., pp. 71-89.

[4] Bailey, Thomas E., McCullough, Charles A., and Gunnerson, Charles G. (1966). "Mixing and Dispersion Studies in San Francisco Bay," J. San. Engr. Div. Amer. Soc. Civil Engrs., 92, (SA5), pp. 23-45.

[5] Batchelor, G. K. (1967). An Introduction to Fluid Dynamics, The University Press, Cambridge, Mass.

[6] Batchelor, G. K. (1952). "Diffusion in a Field of Homogeneous Turbulence, (II): The Relative Motion of Particles," Proc. Camb. Phil. Soc., 48, pp. 345-362.

[7] Bella, David A. (1970). "Dissolved Oxygen Variations in Stratified Lakes," J. San. Engr. Div. Amer. Soc. Civil Engrs., 96, (SA5), pp. 1129-1146.

[8] Bird, R. Byron, Stewart, Warren E., and Lightfoot, Edwin N. (1960). Transport Phenomena, John Wiley and Sons, Inc., New York.

[9] Bortelson, G. C. (1968). Chemistry of Lake Sediment Cores, M.S. Thesis, Water Chemistry, University of Wisconsin, Madison.

[10] Bowden, K. F. (1965). "Horizontal Mixing in the Sea due to a Shearing Current," J. of Fluid Mech., 21, pp. 83-96.

[11] Bridgman, P. W. (1959). The Way Things Are, The Viking Press, New York.

[12] Bryson, R. A., and Kuhn, P. M. (1955). "On the Measurement of Bottom Stress in Lakes," Trans. AGU 36, pp. 612-614.

[13] Carnahan, Brice, Luther, H. A., and Wilkes, James O. (1969). Applied Numerical Methods, John Wiley and Sons, Inc., New York.

[14] Carpenter, J. H. (1960). "Tracer for Circulation and Mixing in Natural Waters," Public Works, 91, pp. 110-112.

[15] Carter, H. H. and Okubo, A. (1965). A Study of the Physical Processes of Movement and Dispersion in the Cape Kennedy Area. Final Report under the U. S. Atomic Energy Commission, Report NYO-2973-1, Chesapeake Bay Institute, The John Hopkins University.

[16] Carter, William J. (1962). Theory of Machine Design, Hemphill's Book Store, Austin, Texas.

[17] Chen, Carl W. (1970). "Concepts and Utilities of Ecologic Model," J. San. Engr. Div. Amer. Soc. Civil Engrs., 96, (SA5), pp. 1085-1097.

[18] Chow, Ven Te. (1959). Open-Channel Hydraulics, McGraw-Hill Book Company, New York.

[19] Churchill, M. A. (1957). "Effects of Storage Impoundments on Water Quality," J. San. Engrg. Div. Amer. Soc. Civil Engrs., 83, (SA1), pp. 1171-1 to 1171-48.

[20] Collings, M. R. (1968). "Selection of Dye-Injection and Measuring Sites for Time-of-Travel Studies," Selected Techniques in Water Resources Investigations, 1966-1967, Geol. Survey Water Suppl., Paper 1892, U. S. Govt. Printing Office, Washington, D. C., pp. 23-29.

[21] Crandall, Stephen H. (1956). Engineering Analysis - A Survey of Numerical Procedures, McGraw-Hill Book Company, New York.

[22] Crank, J., and Nicolson, P. (1947). "A Practical Method for Numerical Evaluation of Solutions of Partial Differential Equations of the Heat Conduction Type," Proc. Camb. Phil. Soc., 43, pp. 50-67.

[23] Csanady, G. T. (1966). "Accelerated Diffusion in Skewed Shear Flow of Lake Current," J. Geophys. Res., 72(2), pp. 411-420.

[24] Daily, James W., and Harleman, Donald R. F. (1966). Fluid Dynamics, Addison-Wesley Publishing Co., Inc., Reading, Mass.

[25] Delfino, J. J. (1968). "Aqueous Environmental Chemistry of Managanese," Ph.D. Thesis, Water Chemistry, Univ. of Wisconsin, Madison.

[26] Diachishin, Alex N. (1963 A). "Dye Dispersion Studies," J. San. Engr. Div. Amer. Soc. Civil Engrs., 89, (SA1), pp. 29-50.

[27] Dischishin, Alex N. (1963 B). "Waste Disposal in Tidal Waters," J. San. Engr. Div. Amer. Soc. Civil Engrs., 89, (SA4), pp. 23-43.

[28] Douglas, J., Jr. (1955). "On the Numerical Integration of $\partial^2 u/\partial x^2 - \partial^2 u/\partial y^2 = \partial u/\partial t$ by Implicit Methods, J. Soc. Industrial Applications Math., 3, pp. 42-65.

[29] Douglas, J., Jr., and Rachford, H. H., Jr. (1956). "On the Numerical Solution of Heat Conduction Problems in Two and Three Space Variables," Trans. Amer. Math. Soc., 82, pp. 421-439.

[30] Dunn, Bernard. (1968). "Nomographs for Determining Amount of Rhodamine B Dye for Time-of-Travel Studies," Selected Techniques in Water Resources Investigation, 1966-1967, Geol. Surv. Water-Supply Paper, 1892, U. S. Govt. Printing Office, Washington, D. C.

[31] Einstein, A. (1905). "Investigations on the Theory of the Brownian Movement," An. Physik, 17, pp. 549-560. Translation Reprinted by Dover Press, New York, 1956.

[32] Elder, J. W. (1959). "The Dispersion of Marked Fluid in Turbulent Shear Flow," J. Fluid Mech., 5, pp. 544-560.

[33] Elder, Rex A., Krenkel, Peter A., and Thackston, Edward L., (eds.). (1968). Proceedings of the Specialty Conference on Current Research into the Effects of Reservoirs on Water Quality, (Jan. 1968), Technical Report No. 17, Dept. of Envir. and Water Res. Engrg., Vanderbilt Univ., Nashville, Tenn.

[34] Elder, Rex A. and Wunderlich, Walter. (1968). "Evaluation of Fontana Reservoir Field Measurements," Proceedings of the Specialty Conference on Current Research into the Effects of Reservoirs on Water Quality, (Jan. 1968), Technical Report No. 17, Dept. of Envir. and Water Res. Engrg., Vanderbilt Univ., Nashville, Tenn.

[35] Entz, B. (1969). "Limnological Conditions in Volta Lake, The Greatest Man-Made Lake in Africa," Nature and Resources, Bull. of the International Hydr. Decade, V. (4), UNESCO, pp. 9-16.

[36] Estes, John E., and Golomb, Berl (1970). "Oil Spills: Method for Measuring Their Extent on the Sea Surface," Science, 169 (3946), Aug. 1970, pp. 676-678.

[37] Fair, Gordon, M., Geyer, John C., and Okun, Daniel A. (1966). Water and Wastewater Engineering, Vol. 1, John Wiley and Sons, Inc., New York.

[38] Fair, Gordon M., Geyer, John C., and Okun, Daniel A. (1968). Water and Wastewater Engineering, Vol. 2, John Wiley and Sons, Inc., New York.

[39] Falk, L. L. (1961). "Some Modes of Waste Dilution in Receiving Waters," 16th Indiana Waste Conference, (May 1961), Purdue Univ., Lafayette, Indiana.

[40] Feuerstein, D. L., and Selleck, R. E. (1963). "Fluorescent Tracers for Dispersion Measurements," J. San. Engr. Div. Amer. Soc. Civil Engrs., 89, (SA4), Part 1, pp. 1-21.

[41] Fietz, Trevor, R., and Wood, Ian R. (1967). "Three-Dimensional Density Current," J. Hydraulics Div. Amer. Soc. Civil Engrs., 93, (HY6), pp. 1-23.

[42] Fischer, Hugo B. (1966). Longitudinal Dispersion in Laboratory and Natural Streams, Report KH-R-12, June 1966, W. M. Keck Laboratory of Hydraulics and Water Resources, California Institute of Technology, Pasadena, California.

[43] Fischer, Hugo B. (1967 A). "Flow Measurements with Fluorescent Tracers," J. Hydraulics Div. Amer. Soc. Civil Engrs., 93, (HY 1), pp. 139-140.

[44] Fischer, Hugo B. (1967B). "The Mechanics of Dispersion in Natural Streams," J. Hydraulics Div. Amer. Soc. Civil Engrs., 93, (HY 6), pp. 187-216.

[45] Fischer, Hugo B. (1968). Methods for Predicting Dispersion Coefficients in Natural Streams with Applications to Lower Reaches of the Green and Duwamish Rivers, Washington - Dispersion in Surface Water, Geological Survey Professional Paper 582-A, U. S. Geol. Survey, Washington, D. C.

[46] Fomin, L. M. (1964). The Dynamic Method in Oceanography, Elseview Publishing Company, New York.

[47] Forel, F. A. (1892-1894). LeLéman, 3 Voll., Lausanne, Switzerland.

[48] Forel, F. A. (1901). Handbuch der Seenkunde, Englehorn, Stuttgart.

[49] Forsythe, G. E., and Wasow, W. R. (1960). Finite Difference Methods for Partial Differential Equations, John Wiley and Sons, Inc., New York.

[50] Foxworthy, J. E., Tibby, R. B., and Barsom, G. M. (1966). "Dispersion of a Surface Waste Field in the Sea," J. Water Poll. Control Fed., 38(7), pp. 1170-1193.

[51] Foxworthy, J. E., and Kneeling, H. R. (1969). Eddy Diffusion and Bacterial Reduction in Waste Fields in the Oceans, Alan Hancock Foundation, Report 69-1, Univ. of Southern Calif.

[52] Frenkiel, F. N. (1953). "Turbulent Diffusion," Advanced Application Mechanics, 3, pp. 61-107.

[53] Fruh, E. Gus (1970). Selective Withdrawal at Lake Livingston - Preliminary Evaluations, 1969, CRWR Rept. 57, Center for Research in Water Resources, The Univ. of Texas at Austin.

[54] Gebhard, Thomas C., and Masch, Frank D. (1969). Evaluation of Micro-Models for Near Surface Dispersion in Reservoirs, Technical Report HYD 10-6902, Hydraulic Engineering Lab, The Univ. of Texas, Austin, Texas.

[55] Gifford, F. (1955). "Atmospheric Diffusion from Volume Sources," J. Meteorol., 12, pp. 245.

[56] Gifford, F. (1957). "Relative Atmospheric Diffusion of Smoke Puffs," J. Meteorol., 14, pp. 410-414.

[57] Gifford, Frank, Jr. (1959). "Statistical Properties of a Fluctuating Plume Dispersion Model," Adv. Geophs., 6, pp. 117-137.

[58] Glover, R. E. (1964). Dispersion of Dissolved or Suspended Materials in Flowing Streams, Geological Survey Professional Paper 411B, U. S. Geol. Survey, Washington, D. C.

[59] Guizerix, J., Grandclement, F. and Hours, R. (1963). "Les Mesures de Debits Effectuees en France a L'Aide de Traceurs Radioactifs Par la Methode d'Integrations," Radioistopes in Hydrology, Proceedings Symp. on the Appl. of Radioisotopes in Hydrology, Int. Atomic Energy Commission, Vienna, pp. 255-281.

[60] Harleman, D. R. F. (1966). "Diffusion Processes in Stratified Flow," Chapter 12, Estuary and Coastline Hydrodynamics, (A. T. Ippen, Ed.), McGraw-Hill Book Company, New York, pp. 575-597.

[61] Hays, James R., Krenkel, Peter A., and Schnelle, Karl B., Jr. (1966). Mass Transport Mechanisms in Open-Channel Flow, Tech. Rep. No. 8, San. and Water Res. Engrg., Dept. Civil Engrg., Vanderbilt Univ., Nashville, Tenn.

[134] Walker, R. F. (1958). "Disposal of Industrial Wastes at Maitland, Ontario, Works of DuPont of Canada," 13th Indiana Waste Conference, May (1958), Purdue Univ., Lafayette, Indiana, pp. 720-729.

[135] Water Resources Engineers, Inc. (1968). Prediction of Thermal Energy Distribution in Streams and Reservoirs, (Final Report). Prepared for Dept. of Fish and Game, State of California, Water Resources Engineers, Inc., Walnut Creek, Calif.

[136] White, Allen, and Gloyna, Earnest F. (1970). Radioactivity Transport in Water - Mathematical Simulation Technical Report 19 to the U. S. Atomic Energy Commission, Center for Research in Water Resources, Univ. of Texas, Austin, Texas.

[137] Wiegel, Robert L. (1961). "Some Engineering Aspects of Wave Spectra," Ocean Wave Spectra, Proceedings of a Conference, National Academy of Sciences, Easton, Maryland, May 1-4, 1961, Prentice-Hall, Inc., Englewoods Cliffs, New Jersey, pp. 309-321.

[138] Williams, J. R. (1967). "Movement and Dispersion of Fluoresent Dye in the Duwamish River Estuary," Geol. Survey Research 1967, Chap. B, Geol. Survey Professional Paper 575-B, U. S. Print. Office, Washington, D. C., pp. B245-B249.

[139] Wilson, Joe R., and Masch, Frank D. (1967). Field Investigations of Mixing and Dispersion in a Deep Reservoir, Tech. Report HYD 10-6701, Hydraulics Engineering Lab, Univ. of Texas, Austin, Texas.

[140] Wunderlich, Walter O., and Elder, Rex A. (1968). "Reservoir Modeling for Thermal Stratification Conditions," Water - 1968, Symposium Series 90, Vol. 64, Amer. Inst. of Chem. Engrs., New York.

[141] Yotsukura, Nobuhiro, and Fiering, Myron B. (1964). "Numerical Solution to a Dispersion Equation," J. Hydraulics Div. Amer. Soc. Civil Engrs., 90 (HY 5), Part 1, pp. 83-104.

[142] Zumberge, James H., and Ayers, John C. (1964). "Hydrology of Lakes and Swamps," Handbook of Applied Hydrology, Chapter 23, (ed. Ven Te Chow), McGraw-Hill Publishing Company, New York.

[62] Holley, E. R. (1969). "Unified View of Diffusion and Dispersion," J. Hydraulics Div. Amer. Soc. Civil Engrs., 95 (HY 2), pp. 621-631.

[63] Hull, D. E. (1962). "Dispersion and Persistence of Tracer in River Flow Measurement," Int. J. Applied Radiation and Isotopes, 13, p. 63.

[64] Hutchinson, G. E. (1957). A Treatise on Limnology, Vol. I, Geography, Physics and Chemistry, John Wiley and Sons, Inc., New York.

[65] Ichiye, T. (1959). "A Note on Horizontal Diffusion of Dye in the Ocean," J. Oceanogr. Soc. in Japan, 15, pp. 171-176.

[66] Ichiye, T., and Plutchak, N. B. (1966). "Photodensimetric Measurement of Dye Concentrations in the Ocean," Limnology and Oceanography, 11, pp. 364-370.

[67] Joseph, J., and Sendner, H. (1958). "Horizontal Diffusion in the Sea, Dtsch. Hydrogy. Z, 11 (2), pp. 47-77.

[68] Kato, Masao, Sato, Otomaru, Morita, Yoshiku, Kohama, Minoru and Hayachi, Nobuo (1963). "A Study in River Engineering Based on the Results of Field Measurements of Flow Velocities with Radioisotopes in the Sorachi River, Japan," Radioisotopes in Hydrology, Proceedings Symp. on the Appl. of Radioisotopes in Hydrology, Int. Atomic Energy Commission, Vienna, pp. 89-110.

[69] Kent, R. (1960). "Diffusion in a Sectionally Homogeneous Estuary," J. San. Engr. Div. Amer. Soc. Civil Engrs., 86 (SA 2), pp. 15-47.

[70] Kisiel, Chester C. (1969). "Time Series Analysis of Hydrologic Data," Advances in Hydroscience, Vol. 5, 1969, (Ed. - Chow, VenTe), Academic Press, New York.

[71] Kolmogorov, A. N. (1941). "The Local Structure of Turbulence in Incompressible Viscous Fluid for Very Large Reynolds Numbers," Comptes Rendus Acad. Sci. U.S.S.R., 30, pp. 301-305.

[72] Kullenberg, G. (1967). "In Situ Measurements of Horizontal and Vertical Diffusion in the Thermocline in Swedish Coastal Waters," Symposium on Diffusion, Int. Assoc. Physical Oceanography, IUGG, Sept. 25 - Oct. 7, 1967, held at Berne, Switzerland, (Abstract only).

[73] Kunz, K. S. (1957). Numerical Analysis, McGraw-Hill Book Company, New York.

[74] Lee, G. Fred. (1970). Factors Affecting the Transfer of Materials Between Water and Sediments Literature Review No. 1, Eutrophication Information Program, Water Res. Ctr., Univ. of Wisconsin, Madison.

[75] Lee, Chin-Yuan, and Masch, Frank D. (1969). Macro-Turbulence from Wind Waves, Technical Report HYD 10-6903, Hydraulics Engineering Laboratory, University of Texas, Austin, Texas.

[76] Le Méhauté, Bernard (1962). "Philosophy of Hydraulics," J. Hydraulics Div. Amer. Soc. Civil Engrs., 88 (HY 1), pp. 45-66.

[77] Levich, Veniamin G. (1962). Physico chemical Hydrodynamics, Prentice-Hall, Inc., Englewood Cliffs, New Jersey.

[78] Liggett, James A., and Hadjitheodoru, Christos (1969). "Circulation in Shallow Homogeneous Lakes," J. Hydraulics Div. Amer. Soc. Civil Engrs., 95 (HY 4), pp. 1273-1288.

[79] Liggett, James A. (1970). "Cell Method for Computing Lake Circulation," J. Hydraulics Civ. Amer. Soc. Civil Engrs., 96 (HY 3), pp. 725-743.

[80] Masch, Frank D. (1964). "Mixing and Dispersion of Wastes by Wind and Wave Action," Advances in Water Poll. Res., Vol 3, (E. A. Pearson-Ed.), The MacMillan Company, New York, pp. 145-175.

[81] Masch, Frank D. and others (1968A). Suggestions for the Development of Numerical Models for the Temperature Structure in Inland Cooling Waters, (Communication from Dr. Frank D. Masch, Oct. 31, 1968).

[82] Masch, Frank D., and Shankar, Nilankatan J. (1968B). "Mathematical Simulation of Two-Dimensional Horizontal Convective-Dispersion in Well-Mixed Estuaries," Int. Assoc. Hydraulic Res., pp. C32-1 - C32-9.

[83] Masch, Frank D. and others (1969). A Numerical Model for the Simulation of Tidal Hydrodynamics in Shallow Irregular Estuaries, Technical Report HYD 12-6901, The University of Texas, Austin, Texas.

[84] Masch, Frank D. and others (1970). "Research Needs on Thermal and Sedimentary Pollution in Tidal Waters - By the Committee on Tidal Hydraulics Division," J. Hydraulics Div. Amer. Soc. Civ. Engrs., 96 (HY 7), pp. 1539 - 1548.

[85] Mickelsen, W. R. (1960). "Measurements of the Effect of the Molecular Diffusivity - Turbulent Diffusion," J. Fluid Mech., 7 pt. 3, pp. 397-400.

[86] Munk, W. H., Ewing, G. C., and Revelle, R. R. (1949). "Diffusion in Bikini Lagoon," Trans. Amer. Geophys. Union, 30, pp. 59-66.

[87] Okubo, Akira, Hasegawa, S., Amano, M., and Takeda, I. (1957). "Report of the Observation Concerning the Diffusion of Dye Patch in the Sea off the Coast of Tokai-Mura," Research Papers of Japan Atomic Energy Institute, No. 2, pp. 17-21.

[88] Okubo, Akira (1962 A). "A Review of Theoretical Models of Turbulent Diffusion in the Sea," J. Oceanogr. Soc. of Japan, 29 annv. vol., pp. 286-319.

[89] Okubo, Akira (1962 B). Horizontal Diffusion from an Instantaneous Point Source Due to Oceanic Turbulence, Report No. 32, Chesapeake Bay Institute, The John Hopkins Univ.

[90] Okubo, Akira (1965). "A Note of Horizontal Diffusion from an Instantaneous Source in a Non-uniform Flow," J. Oceanogr. Soc. of Japan, 22, pp. 35-40.

[91] Okubo, Akira (1968 A). A New Set of Oceanic Diffusion Diagrams, Technical Report 38, Reference 68-6 (June 1968), Chesapeake Bay Institute, The John Hopkins Univ.

[92] Okubo, Akira, and Karweit, Michael J. (1968). Diffusion from a Continuous Source in a Uniform Shear Flow Contribution No. 139, Chesapeake Bay Institute and Dept. of Earth and Planetary Sciences, The John Hopkins Univ., pp. 514-520.

[93] Orlob, Gerald T. (1959). "Eddy Diffusion in Homogeneous Turbulence," J. Hydraulics Div. Amer. Soc. Civil Engrs., 8s (HY 9), pp. 75-101.

[94] Orlob, Gerald T. (1961). "Eddy Diffusion in Homogeneous Turbulence," Amer. Soc. of Civil Engrs. Trans., Vol. 126 (pt. 1), pp. 397-438.

[95] Parker, Frank L. (1961). "Eddy Diffusion in Reservoir and Pipelines," J. Hydraulics Div. Amer. Soc. Civil Engrs., 87 (HY 3), pp. 151-171.

[96] Parker, Frank L., and Krenkel, Peter A. (Eds.) (1969). Engineering Aspects of Thermal Pollution, Vanderbilt Univ. Press, Nashville, Tenn.

[97] Patterson, C. C., and Gloyna, E. F. (1963). Radioactivity Transport in Water - The Dispersion of Radionuclides in Open Channel Flow, Tech. Report 2, Environmental Health Engrg. Lab, The Univ. of Texas, Austin, Texas.

[98] Patterson, C. C., and Gloyna, E. F. (1963). Radioactivity Transport in Water - The Dispersion of Radionuclides in Open Channel Flow, The Univ. of Texas Environmental Health Engrg. Research Lab. Tech. Report of U. S. Atomic Energy Commission.

[99] Peaceman, D. W., and Rachford, H. H., Jr. (1955). The Numerical Solution of Parabolic and Elliptic Differential Equations," J. Soc. Indust. Appl. Math., 3, (No. 1), pp. 28-41.

[100] Pearson, E. A. (1956). "An Investigation of the Efficacy of Submarine Outfall Disposal of Sewage and Sludge," California State Water Pollution Control Board Publ. 14, Sacramento, California.

[101] Pearson, E. A. (1959). "Marine Waste Disposal Considerations Paper Presented at Annual Meeting of Federation of Sewage and Industrial Wastes Ass'n, Dallas, Texas, Oct. (1959)," Manual of Disposal of Refining Wastes, Amer. Petr. Inst., New York.

[102] Pritchard, D. W., and Carpenter, J. H. (1960). "Measurement of Turbulent Diffusion in Estuarine and Inshore Waters," Bull. Int. Assoc. Sci. Hydrol., No. 20, pp. 37-50.

[103] Replogle, John A., Meyers, Lloyd E., and Brust, Kenneth J. (1966). "Flow Measurements with Fluorescent Tracers," J. Hydraulics Div. Amer. Soc. Civil Engrs., 92, (HY 5), pp. 1-15.

[104] Reynolds, John Z. (1966). Some Water Quality Considerations of Pumped Storage Reservoirs, Dissertation, University of Michigan.

[105] Richardson, L. F. (1962). "Atmospheric Diffusion Shown on a Distance - Neighbour Graph," Proc. Roy. Soc. London, A 110, pp. 709-773.

[106] Richtmyer, R. C. (1957). Difference Methods for Initial Value Problems, Interscience, New York.

[107] Rouse, Hunter (1938). Fluid Mechanics for Hydraulic Engineers, McGraw-Hill Book Company, New York.

[108] Sauer, Stanley P., and Masch, Frank D. (1969). Methods for Evaluating the Effects of Upstream Control Measures on Watershed Yield, Tech. Rep. HYD 13-6901, Hyd. Engrg. Lab, Dept. of Civ. Engrg., The Univ. of Texas, Austin, Texas.

[109] Sayre, W. W., and Chamberlain, A. R. (1964). "Exploratory Laboratory Study on Lateral Turbulent Diffusion at the Surface of an Alluvial Channel," U. S. Geological Survey Circ. 484, U. S. Geol. Survey, Washington, D. C.

[110] Sayre, W. W., and Chang, F. M. (1968). A Laboratory Investigation of Open-Channel Dispersion Processes for Dissolved, Suspended and Floating Dispersants, Geological Survey Professional Paper 433-E, U. S. Geol. Survey, Washington, D. C.

[111] Schlichting, H. (1961). "Boundary Layer Theory," Handbook of Fluid Dynamics, Section 9, (Streeter, Victor L., Editor-in-Chief), McGraw-Hill Book Company, Inc., New York.

[112] Schonfeld, J. C. (1959). Diffusion by Homogeneous Isotropic Turbulence, Report FA-1959-1, Rijkswaterstaat, The Netherlands.

[113] Shankar, Nilakantan Jothi (1970). Influence of Tidal Inlets on Salinity and Related Phenomena in Estuaries, Dissertation for degree of Doctor of Philosophy, The Univ. of Texas, Austin, Texas, May 1970.

[114] Shull, Roger D., and Gloyna, Earnest F. (1968). Radioactivity Transport in Water - Simulation of Sustained Releases to Selected River Environments, Tech. Report to the U. S. Atomic Energy Commission, Center for Research in Water Resources, The Univ. of Texas, Austin, Texas.

[115] Slotta, Larry S., and others (1969). Stratified Reservoir Currents, Bulletin No. 44, Oct. 1969, Engineering Experiment Station, Oregon State Univ., Corvallis, Oregon.

[116] Smith, G. D. (1965). Numerical Solution of Partial Differential Equations, Oxford University Press, New York.

[117] Smith, Winchell (1969). Feasibility Study of the Use of the Acoustic Meter for Measurement of Net Outflow from the Sacramento - San Joaquin Delta in California, Geological Survey Water Supply Paper, 1877, U. S. Dept. of the Interior, Washington, D. C.

[118] Southwood, Raymond W., and Deleeuw, Samuel L. (1965). Digital Computation and Numerical Methods, McGraw-Hill Book Company, New York.

[119] Stall, John B., and Hiestand, Douglas W. (1969). Provisional Time-of-Travel for Illinois Streams, Rept. of Investigation 63, Illinois State Water Survey, Urbana, Ill.

[120] Stefan, Heinz (1970). "Stratification of Flow from Channel into Deep Lake," J. Hydraulics Div. Amer. Soc. Civil Engrs., 96 (HY 7), pp. 1417-1434.

[121] Stone, H. L., and Brian, P. L. T. (1963). "Numerical Solution of Convective Transport Problems," A. I. Ch. E. Journal 9, pp. 681-688.

[122] Sverdrup, H. U., Johnson, M. W., and Fleming, R. H. (1942). The Oceans, Prentice-Hall, New York.

[123] Taylor, G. I. (1954). "The Dispersion of Matter in Turbulent Flow Through a Pipe," Proc. of the Royal Society, A, Vol. CCXXIII (1954), pp. 446-468. (Reprint appearing in The Scientific Papers of Sir Geoffrey Ingram Taylor, Vol. II, (Edited by G. K. Batchelor), Univ. Press, Cambridge, Mass, 1960, pp. 466-488.

[124] Taylor, G. I. (1959). "The Present Position in the Theory of Turbulent Diffusion," (Landsberg H. E. ed.), Advances in Geophysics, 6, Academic Press, New York, pp. 101-111.

[125] Thackston, Edward L., and Krenkel, Peter A. (1966). Longitudinal Mixing and Reaeration in Natural Streams, Tech. Report no. 7, Sanitary Engineering, Vanderbilt Univ., Nashville, Tenn.

[126] Thermo-Systems, Inc. (1970). Hot Film and Hot Wire Anemometry - Theory and Application, Bulletin TB 5, Thermo-Systems, Inc., St. Paul, Minnesota.

[127] Townsend, A. A. (1961). "Turbulence," Handbook of Fluid Dynamics (Streeter, Victor L.), McGraw-Hill Book Company, Inc., New York, pp. 10-21.

[128] Timblin, L. O., and Peterka, A. J. (1963). "Open Channel Flow Measurements," Radioisotopes in Hydrology, Proc. Symp. on Appl. of Radioisotopes in Hydrology, Int. Atomic Energy Commission, Vienna, pp. 25-57.

[129] U. S. Geological Survey (1954). Water Loss Investigation: Lake Hefner Studies, Technical Report, Geol. Survey Prof. Paper 269, U. S. Gov't. Print. Off., Washington, D. C.

[130] U. S. Geological Survey (1968). Selected Techniques in Water Resources Investigations, 1966-1967, Water Supply Paper 1892, (Compiled by: Chase, E. B., and Payne, F. N.), U. S. Gov't. Print. Off., Washington, D. C.

[131] Van Dorn, W. (1953). "Wind Stress on an Artifical Pond," J. Marine Research, Vol. 12 (No. 3), p. 953.

[132] Velz, C. J., and Gannon, J. J. (1960). "Forecasting Heat Loss in Ponds and Streams," J. Water Poll. Contr. Fed., 32 (4), pp. 392-417.

[133] Vercelli, Francesco (1951). Il Mare - L Laghi - I Ghiacciai, Stamperia Artistica Nazionale, Torino, Italy.